Cellular Roles for Proteins Linked to Phosphatidylinositol (3,5)-bisphosphate Metabolism

Jane Whittingham

Thesis submitted in accordance with the requirements of the University of Liverpool for the degree of Doctor of Philosophy

September 2008

Cellular Roles for Proteins Linked to Phosphatidylinositol (3,5)-bisphosphate Metabolism

Jane Whittingham

Abstract

The phosphoinositide lipids PtdIns(3)*P* and PtdIns(3,5)P_2 play important roles on the endocytic pathway. PtdIns(3)*P* localises to early endosomes and multivesicular bodies (MVBs) and is proposed to recruit proteins involved in fusion of early endosomes and internalisation of ubiquitinated receptors. PtdIns(3,5)P_2 is proposed to be involved in terminal maturation of lysosomes and endosome to Golgi transport, but the precise role of this lipid in mammalian cells remains unclear. Studies in yeast have identified various proteins associated with PtdIns(3,5)P_2 metabolism, for which mammalian homologues have been found. These are the PtdIns(3)*P*-5-kinase Fab1/PIKfyve, Fig4 a 5-phosphatase that dephosphorylates PtdIns(3,5)P_2, Vac14 which has been shown to act as an upstream activator of PIKfyve, and WIPI-2/Svp1 a putative downstream effector of PtdIns(3,5)P_2.

In this study I have further characterised three of these proteins and examined the cellular roles of all four with respect to a variety of trafficking pathways in which PtdIns(3,5)P_2 has been implicated. siRNA was used to examine the knockdown phenotypes of each of these proteins. Furthermore, I directly compared for the first time the effects of knockdown of PIKfyve, with acute pharmacological inhibition of its enzymatic activity. Loss of PIKfyve

activity caused a failure in the retrieval of a variety of different cargos to the trans-Golgi network (TGN), including mannose-6-phosphate receptors, responsible for efficient delivery of lysosomal enzymes, and the TGN resident protein TGN46, leading to their accumulation in dispersed punctae. A failure in tyrosine kinase receptor downregulation was also observed following combined knockdown of PIKfyve with either Vac14 or Fig4 or following pharmacological inhibition of PIKfyve. PIKfyve knockdown alone had no effect, suggesting a low threshold of PtdIns(3,5)P_2 is necessary and sufficient for this pathway.

Svp1 is the best characterised PtdIns(3,5)P_2 effector in yeast and is also an autophagy-related gene (Atg18), thereby implicating PtdIns(3,5)P_2 in this process. A family of putative mammalian Svp1 homologues have been identified, known as the WIPI family. I investigated the role of PtdIns(3,5)P_2 and WIPI-2 in mammalian autophagy. By monitoring formation of the autophagosome marker GFP-LC3 II, PIKfyve and WIPI-2 were found to have opposite effects. Furthermore, WIPI-2 redistributes to punctate structures upon induction of autophagy, which partially colocalise with autophagosome markers, in a manner dependent not on PIKfyve but on PI(3)-kinase activity.

The evidence presented suggests that PtdIns(3,5)P_2 may play a role in mediating the maturation of a subset of MVBs, leading to swelling of endosomal compartments and rendering the MVB/late endosome or autophagosomes refractory to fusion with the lysosome in cells depleted of PIKfyve.

Table of Contents

Chapter Two: Materials and Methods

List of Figures

List of tables

Abbreviations

3-AT	3-amino-1,2,4-triazole
AP-1	Adaptor protein complex 1
Atg	Autophagy related gene
BAR	Bin1, Amphiphysin, Rvs167 domain
BSA	Bovine serum albumin
CCV	Clathrin-coated vesicle
CD8	Cluster of differentiation 8
cdM6PR	Cation-dependent mannose-6-phosphate receptor
cDNA	Complementary DNA
CGN	*cis*-Golgi network
CHMP	Charged multivesicular body protein
ciM6PR	Cation-independent mannose-6-phosphate receptor
CMT	Charcot Marie Tooth disorder
CURL	Compartment of uncoupling receptor and ligand
Cvt	Cytoplasm to vacuole targeting
DAB	Diaminobenzidine
DAG	Diacylglycerol
DAMP	3-(2,4-dinitroanilino)-3'-amino-N-methyldipropylamine
DEP	Dishevelled, Egl-10, Pleckstrin domain
DMEM	Dulbecco's modified eagle's medium
DMSO	Dimethyl sulphate
DNA	Deoxyribonucleic acid
DNP	Dinitrophenol
dNTP	Deoxynucleotide triphosphates
DTT	Dithiothreitol
EBSS	Earl's buffered saline solution
EEA-1	Early endosomal antigen-1
ECL	Enhanced chemical luminescence
ECV	Endosomal carrier vesicle
EDTA	Ethylenediaminetetraacetic acid
EM	Electron microscopy

ENTH	Epsin N-terminal homology domain
ER	Endoplasmic reticulum
ERC	Endosomal recycling complex
FBS	Foetal bovine serum
FCA	Freund's complete adjuvant
FERM	Band 4.1, Ezrin, Radixin, Moeisin domain
FIA	Freund's incomplete adjuvant
FYVE	Fab1, Yotb, Vac1, EEA-1 domain
GFP	Green fluorescent protein
GGA	Golgi-associated gamma-ear containing ARF-binding proteins
GRAM	Glucosyltransferase Rab-like GTPase activator and myotubularin
HGF	Hepatocyte growth factor
HRP	Horseradish peroxidase
Hrs	Hepatocyte growth factor regulated tyrosine kinase substrate
IF	Immunofluorescence
ILV	Intralumenal vesicle
IP_3	Inositol triphosphate
IPTG	Isopropyl-β-galactopyranosidase
kb	kilobase
kDa	kiloDalton
KDRES	siRNA resistant
KLH	Keyhole limpet haemocyanin
LAMP-1/2	Lysosomally-associated membrane protein 1/2
LB	Luria-Bertani
LBPA	Lysobisphosphatidic acid
LDL	Low density lipoprotein
LDM	Low density microsomal fraction
LiOAc	Lithium acetate
MAPK	Mitogen activated protein kinase
MOI	Multiplicity of infection

MTM	Myotubularin
MVB	Multivesicular body
NCBI	National Centre for Biotechnology Information
NP40	Nonidet P40
NSF	N-ethylmaleimide sensitive factor
OD	Optical density
ORF	Open reading frame
OsO_4	Osmium tetroxide
PAS	Pre-autophagosomal structure
PBS	Phosphate buffered saline
PCA	Protein fragment complementation analysis
PCR	Polymerase chain reaction
PDGF	Platelet derived growth factor receptor
PE	Phosphatidylethanolamine
PEG	Polyethylene glycol
PFA	Paraformaldehyde
PH	Pleckstrin homology domain
PIKfyve	Phosphoinositide kinase for five position containing a FYVE domain
PLC	Phospholipase C
PROPPINs	Beta-propeller proteins that interact with phosphoinositides
PtdIns	Phosphatidylinositol
PX	Phox homology domain
qPCR	Quantitative PCR
RNA	Ribonucleic acid
RNAi/siRNA	RNA interference/short interfering RNA
RT-PCR	Reverse transcription PCR
SD	Synthetic defined medium
SDS-PAGE	Sodium dodecyl sulphate polyacrylamide gel electrophoresis
SNAP	Soluble NSF attachment protein
SNARE	SNAP receptor

STAM	Signal transducing adaptor molecule
Svp1	Swollen vacuole phenotype 1
TAE	Tris-acetate-EDTA
TCP	T-complex protein
TEMED	N,N,N',N'-tetramethylethylenediamine
Tf	Transferrin
TGN	Trans-Golgi network
TIP-47	Tail-interacting protein of 47kDa
TLR	Toll-like receptor
TOR	Target of Rapamycin
TSG101	Tumour suppressor gene 101
TX-100	Triton X-100
VAMP	Vesicle-associated membrane protein
VHS	Vps27, Hrs and STAM domain
Vps	Vacuolar protein sorting
Vti1B	Vps10 tail interactor 1B
WB	Western blotting
WIPI	WD repeat-containing proteins that interact with phosphoinositides
Y2H	Yeast two-hybrid

Acknowledgements

My sincere thanks go first to my supervisors Michael Clague and Sylvie Urbé for guiding me through my PhD and providing an extremely high quality and stimulating working environment and for their continual support, technical and personal advice. Thanks also to Ian Prior, Chris Sanderson and Francis Barr for helping out at various stages of my research with their expertise and a friendly ear.

Thanks to all members of the lab and department past and present who helped to create a happy working and socialising environment, in particular, to Alex Laude, Dean Hammond and Ricky Buus, and more recently Chris Thorne, for creating a happy office environment. Also to Mark Sherwood for being a fantastic housemate and friend.

Thanks also to my Leeds festival buddy Beck Welchman, for all her help with last minute technical questions and for lots of laughs in and out of the lab. To Seb Hayes for checking up on me and making sure I hadn't fallen into a PhD abyss, and for many laughs and stimulating conversation topics. Special thanks to Zehra Akerman for all her technical help in the lab and always having a smile for me, I miss her a lot! And thanks to Monica Faronato, Monika Chojnowska, and Han Liu for invariably looking after cells, sharing lunch and coffee breaks and creating a friendly work atmosphere.

I also owe a huge debt of gratitude to Hannah Polson with whom I spent a month collaborating in London, to whom I owe my newfound 'expertise' in autophagy techniques, and for making my stay there thoroughly

enjoyable. Also to Julie Charabolous and Alison Beckett for their expertise in all things yeast and EM, for their unwavering help and technical expertise.

I am also indebted to the Wellcome Trust for their financial support over the course of my PhD.

And most importantly, my most heartfelt thanks go to all my family and friends who have helped me through the good times and the bad. Particularly to my wonderful parents whose love and support is an invaluable source of encouragement and above all, to my fantastic husband-to-be, who has put up with it all over the course of our time together and always without complaint, who always believed in me even when I wasn't so sure of myself, and most importantly, provided a never ending supply of hugs!

CHAPTER ONE

Introduction

1.1 Phosphatidylinositol lipids

1.1.1 Phosphatidylinositol

Anderson and Roberts first identified inositol as a lipid constituent in mycobacterium in 1930 (Hawthorne, 1960). The term phosphoinositide came from Folch, to describe a brain phospholipid containing inositol (Folch, 1949). The most widely distributed phosphoinositide is phosphatidylinositol (PtdIns) in which a phosphatidic acid residue is attached to the 1-hydroxyl of inositol. PtdIns makes up less than 10% of membrane lipid in eukaryotic cells, approximately 20% in yeast, and 5% in Protozoa. It is rarely found in bacteria, mycobacteria being the exception. It is an acidic phospholipid that, in essence, consists of a phosphatidic acid backbone, linked via the phosphate group to inositol (hexahydroxycyclohexane). The structure of PtdIns is shown in figure 1.1. Of the possible stereoisomers, only myo-inositol has been found in naturally occurring phosphoinositides, with one axial hydroxyl in position two, and the remainder equatorial. The fatty acid composition can be as much as 80% 1-stearoyl 2-arachidonoyl (18:0, 20:4), with much smaller quantities of other species (Hawthorne and White, 1975). The biosynthetic route for the synthesis of PtdIns is shown in figure 1.1, as first identified by Agranoff and expanded upon by the work of Paulus and Kennedy (Agranoff *et al.*, 1958; Paulus and Kennedy, 1960).

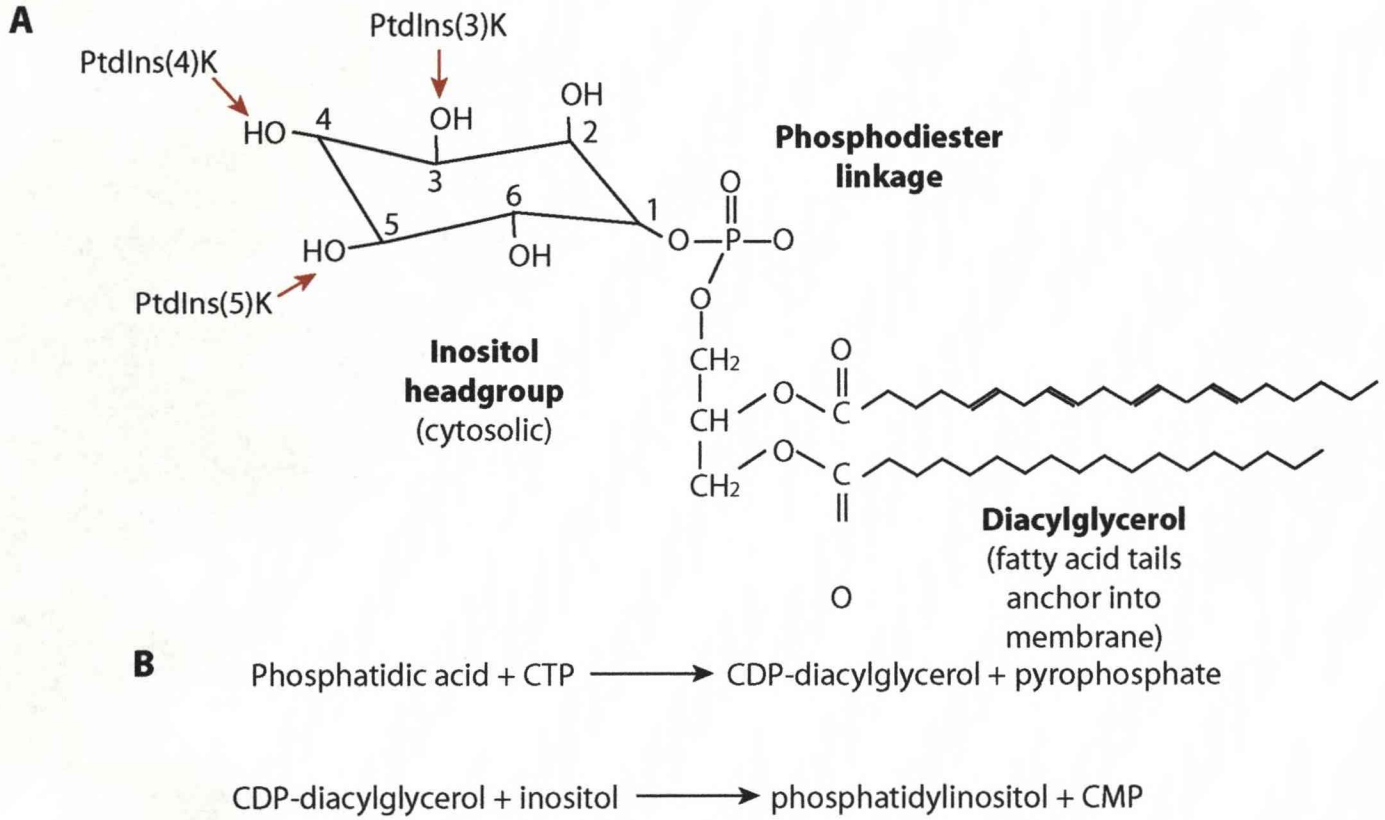

Figure 1.1. Structure of phosphatidylinositol and biosynthetic pathway for its generation
A) The structure of PtdIns and the site of action of the kinases that use it as a substrate. Adapted from Handbook of Lipid Research, Bell, 1996. B) The biosynthetic route for generation of PtdIns established by Paulus and Kennedy, 1960. CTP = cytidine triphosphate, CDP = cytidine diphosphate, CMP = cytidine monophosphate. The second reaction is catalysed by the enzyme CDP-diacylglycerol 3-phosphatidylinositol transferase, and is activated by either Mg^{2+} or Mn^{2+}.

1.1.2 Di and triphosphoinositides

In the 1950's and 60's Mabel and Lowell Hokin, two of the key players in early phosphoinositide research, made a series of vital discoveries to this field. Using a method for analysis of individual phospholipids introduced by Rex Dawson (Dawson, 1954), they extracted lipids from pancreatic slices incubated with [2-^{3}H]inositol and identified seven phospholipids (Hokin and Hokin, 1958, 1964a). Much later it became clear that PtdIns could be differentially phosphorylated at the 3, 4 and 5 positions of its inositol ring to generate seven distinct di and triphosphoinositides. These are found on the cytoplasmic face of cell membranes and act as substrates for a number of enzymes, including phospholipase C (PLC) and the phosphoinositide phosphatases and kinases that catalyse the conversion of phosphoinositides from one form to another (Martin, 1998). The seven mammalian phosphoinositides and their metabolising enzymes are shown in figure 1.2.

Hokin and Hokin also demonstrated that muscarinic cholinergic stimulation of pancreatic fragments increased the turnover of cellular PtdIns (Hokin and Hokin, 1955, 1958). This subsequently came to be known as the 'PI effect' and was the focus of much research not just by the Hokins but numerous other groups. It soon became obvious that PtdIns turnover was a reaction associated with a wide variety of receptors linked to diverse biological processes. In 1964, the Hokins suggested that PLC-catalysed PtdIns hydrolysis might initiate the PI effect, as they observed an increase in phosphatidic acid, which they hypothesised would be formed from the diacylglycerol (DAG) product of PtdIns breakdown (Hokin and Hokin, 1964b). It was not until the 1980's, following a series of controversial discoveries,

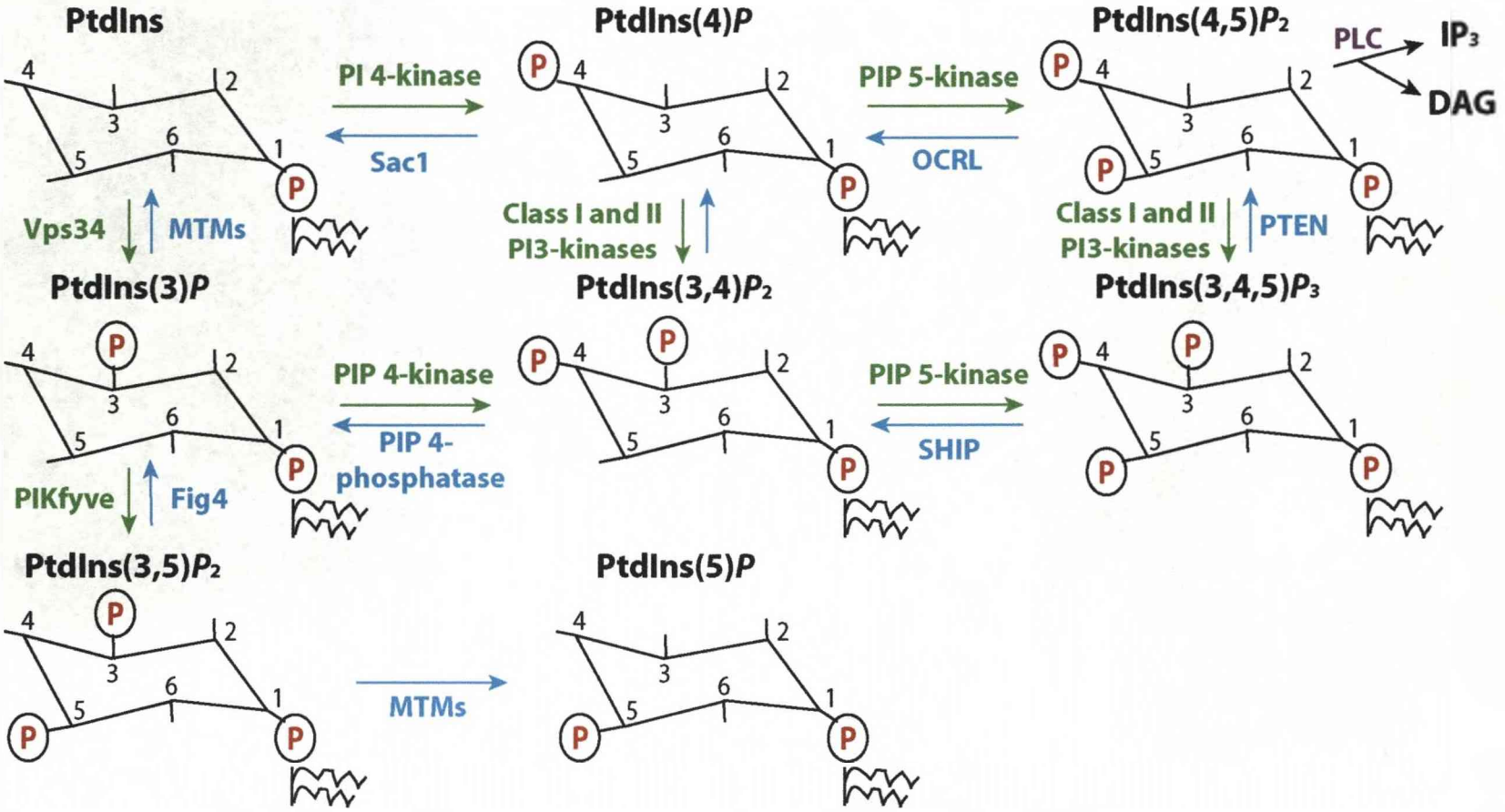

Figure 1.2. The seven mammalian phosphoinositides and their metabolising enzymes.
An illustration of the seven phosphoinositides and the kinases (green), phosphatases (blue) and phospholipases (brown) involved in their metabolism. DAG - diacylglycerol, IP3 - inositol(1,4,5)triphosphate, OCRL - oculocerebrorenal syndrome of Lowe, SHIP - SH2 domain containing inositol 5-phosphatase, PTEN - phosphatase and tensin homologue, PLC - phospholipase C.

that experimental evidence began to indicate that this initial reaction in stimulated PtdIns turnover was not the breakdown of PtdIns itself, but of one of its phosphorylated derivatives Phosphatidylinositol(4,5)bisphosphate (PtdIns(4,5)P_2) (Abdel-Latif *et al.*, 1977; Kirk *et al.*, 1981).

Phosphoinositides have since been shown to play a role in a vast range of vital cellular processes such as cell growth, cell survival, and calcium signalling. The hydrolysis of PtdIns(4,5)P_2 by PLC, for example, was subsequently shown to generate inositol(1,4,5)triphosphate (IP_3) and DAG (Berridge, 1983). IP_3 liberates intracellular stores of calcium and thereby has a key function in calcium signalling (Berridge and Irvine, 1989), whereas DAG activates Protein kinase C (PKC), initiating a multitude of cell specific downstream pathways of this kinase (Bell, 1986). The first evidence for the role of phosphoinositides in cell growth and transformation stems from the observation that PtdIns(3,4)P_2 and PtdIns(3,4,5)P_3 can only be found after stimulation with platelet-derived growth factor receptor (PDGFR) (Auger *et al.*, 1989), but that in NIH3T3 cells transformed with polyoma virus, the levels of these phosphoinositides is elevated, even in the absence of serum (Serunian *et al.*, 1990).

1.1.3 Phosphoinositide binding domains

Phosphoinositides are able to orchestrate this wide range of cellular functions through the recruitment of a vast array of different proteins to a target membrane via specific phosphoinositide binding domains. The PH (pleckstrin homology) domain was the first binding domain reported and has been shown to be the eleventh most common domain in the human

proteome, in over 250 proteins (Harlan *et al.*, 1994; Lemmon and Ferguson, 2000). But over the years a range of others have been identified, including ENTH (Epsin N-terminal homology) (Itoh *et al.*, 2001), PX (phox homology) (Cheever *et al.*, 2001; Kanai *et al.*, 2001; Xu *et al.*, 2001), FYVE (Fab1, YOTB, Vac1, EEA-1) (Stenmark *et al.*, 1996; Gaullier *et al.*, 1998; Patki *et al.*, 1998), FERM (Band 4.1, Ezrin, Radixin, Moeisin) (Niggli *et al.*, 1995; Hirao *et al.*, 1996), BAR (Bin1, Amphiphysin, Rvs167) (Zhang and Zelhof, 2002), GRAM (glucosyltransferase Rab-like GTPase activator and myotubularin) (Berger *et al.*, 2003; Tsujita *et al.*, 2004) and C2 domains (Davletov and Sudhof, 1993). These domains are frequently found in combination with additional modules that are involved in the formation of protein-protein or protein-lipid interaction networks. Some of them show specific and high affinity binding to a particular phosphoinositide as outlined in figure 1.3. These domains act to recruit their host proteins to particular sites on the plasma or other intracellular membranes. Furthermore, they provide valuable tools to assess the localisation of phosphoinositides in the cell. A number of phosphoinositides, including PtdIns(3,5)P_2, have been found to play a role in membrane trafficking events. These trafficking pathways are reviewed in section 1.2.

1.2 Compartmentalisation of cells and membrane trafficking pathways

1.2.1 Intracellular trafficking pathways

A key feature of eukaryotic cells is the presence of internal membrane-bound organelles that are in continual exchange with one another

Domain	Protein (eg.)	Target lipid
PH	PLC1ð	PtdIns(4,5)P_2
	GRP1	PtdIns(3,4,5)P_3
	FAPP1	PtdIns(4)P
PX	Akt/PKB	PtdIns(3,4)P_2, PtdIns(3,4,5)P_3
	p40phox	PtdIns(3)P
	p47phox	PtdIns(3,4)P_2
	SNX-1	PtdIns(3)P, PtdIns(3,5)P_2
	SNX-2	PtdIns(3)P
	SNX-3	PtdIns(3)P
FYVE	EEA-1	PtdIns(3)P
	Hrs	PtdIns(3)P
	Fab1/PIKfyve	PtdIns(3)P
ENTH	Epsin 1	PtdIns(4,5)P_2
	EpsinR	PtdIns(4)P
GRAM	MTM1	PtdIns(3,5)P_2
	MTMR3	PtdIns(5)P
	MTMR6	PtdIns(5)P
	MTMR2	PtdIns(3,5)P_2, PtdIns(5)P
WD40	WIPI family	PtdIns(3,5)P_2

Figure 1.3. Phosphoinositide binding domains.
Key phosphoinositide binding domains, examples of proteins that possess them and their lipid binding specificity. Adapted from Takenawa and Itoh, 2006.

and the plasma membrane. Most of these organelles are elements of the exo- and endocytic pathways; inward and outward-directed pathways whereby material passes through the organelles in an orderly and sequential fashion by means of specific transport vesicles and membrane fission and fusion reactions. Development of high-resolution electron microscopy and ultracentrifugation techniques in the 1950's permitted the visualisation of this subcellular compartmentalisation of cells and their biochemical pathways for the first time (Dalton and Felix, 1954; Baudhuin *et al.*, 1965; De Duve, 1965). Subsequently, autoradiographic electron microscopy studies of the secretory pathway in pancreatic acinar cells demonstrated that newly synthesised proteins are transported to the cell surface through distinct secretory compartments and small membrane-bound organelles (Jamieson and Palade, 1967). This lead to the development of the intracellular vesicular transport hypothesis, whereby transport vesicles continually bud off from one membrane and fuse with another, carrying membrane components and soluble molecules that are collectively termed 'cargo' (Palade, 1975). Mechanisms for membrane retrieval are also in place to ensure balance in membrane flow.

Intracellular trafficking events can be broadly divided into two pathways. The internalisation of extracellular material at the plasma membrane is termed the endocytic pathway, and the opposing traffic of newly synthesised proteins from the cell interior to the plasma membrane occurs via the biosynthetic pathway.

1.2.2 The endocytic pathway

Endocytosis is the general term used for the internalisation of extracellular material by invagination and pinching off of membrane-bound vesicles at the plasma membrane. Reknowned cytologist Christian de Duve first proposed the term endocytosis at a CIBA foundation meeting in 1963. It is a broad term that encapsulates various processes such as phagocytosis, pinocytosis, clathrin-dependent receptor-mediated endocytosis, and clathrin-independent endocytosis. It occurs in all animal cell types, can result in the uptake of a huge variety of different materials, and plays essential roles in a number of physiological processes in both individual cells and whole organisms. These include nutrient uptake, removal of activated signalling receptors, antigen presentation and maintenance of cell polarity (Mukherjee et al., 1997). The best-characterised form of endocytosis is clathrin-dependent receptor-mediated endocytosis. This is dependent upon the coat protein clathrin, which assembles into a polyhedron to coat a new vesicle as it forms, and coordinates vesicle formation and protein sorting. The membrane invagination subsequently buds off to form a clathrin-coated vesicle (CCV). In general, material that enters the endocytic pathway has several potential fates: recycling to the plasma membrane, degradation in the lysosome, or delivery onto the biosynthetic pathway through a series of membrane-bound compartments that are identified by a range of established markers (van Meel and Klumperman, 2008). An overview of the endocytic and biosynthetic pathways is shown in figure 1.4.

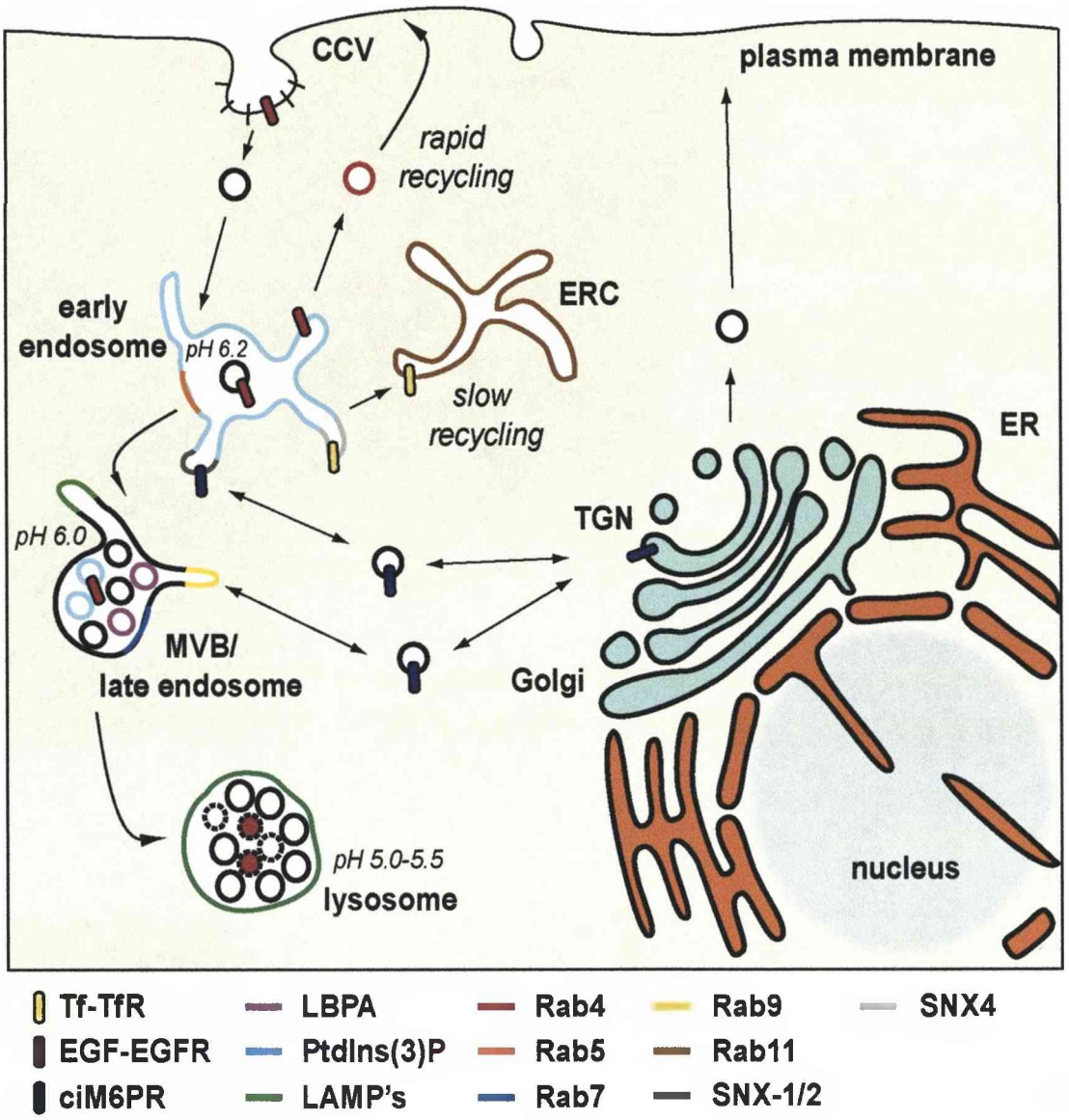

Figure 1.4. Trafficking on the endocytic and biosynthetic pathways. Summary of the current understanding of the compartmentalisation of the endocytic and biosynthetic pathways, the membrane proteins that define each compartment and the trafficking itineraries of exemplary cargoes. Clathrin-mediated endocytosis is shown as the best understood example. Cargo enters the early endosome when uncoated CCV's fuse. The tubulovesicular early endosome mediates the sorting of different cargos to the lysosome or into recycling pathways. Biosynthetic cargo also joins the endocytic pathway at the early and late endosome and likewise cargo can be retrieved from these locations.

1.2.3 Early endosomes

After entering the cytoplasm, CCV's rapidly lose their clathrin coat and fuse with early endosomes scattered throughout the periphery. Cargo accumulates here within two to five minutes after internalisation (Besterman *et al.*, 1981; Griffiths *et al.*, 1989). They are pleiomorphic structures of mildly acidic pH (5.9-6.0), composed of vacuolar and tubular domains that exhibit extensive connectivity but maintain their identity at least in part by virtue of their complement of Rab GTP-ases (Hopkins, 1983; Mellman *et al.*, 1986; Chavrier *et al.*, 1990). Their acidic nature is maintained by the presence of vacuolar H^+ ATPase pumps in the limiting membrane (Mellman *et al.*, 1986). Originally described as the CURL (compartment of uncoupling receptor and ligand) in 1983 by Geuze and Slot (Geuze *et al.*, 1983), they are also often referred to as sorting endosomes as they represent major sorting stations on the endocytic pathway. From here, internalised cargo can be recycled back to the plasma membrane, passed on to the degradative or biosynthetic pathways or in certain cells sorted into regulated secretory vesicles.

For most receptor-ligand complexes, their ultimate fate is to be directed to the proteolytic machinery in the lysosome, at this site, either or both of the components are degraded. In the case of Epidermal Growth Factor (EGF), both it and its receptor are targeted for destruction. However, in the case of Low-Density Lipoprotein (LDL), whilst the ligand is destined for lysosomal degradation, the receptor is dissociated from the ligand and recycled back to the plasma membrane. Alternatively, as in the case of Transferrin (Tf) and its receptor, both ligand and receptor are recycled back to the plasma membrane together. The use of specific membrane

permeable vacuolar ATP-ase inhibitors, showed that the acidic environment of endosomes is crucial for the dissociation of some ligands from their receptors at this stage (Presley *et al.*, 1997).

1.2.3.1 Geometric sorting

The mechanism through which these different receptor-ligand complexes are sorted has been a subject of much interest over the years and has lead to a number of proposed theories. The 'geometric sorting' model suggests that recycling back to the plasma membrane is a default pathway, as no specific sorting motifs for this pathway have been identified as yet. Instead, the geometry of the endosome regulates separation of membrane-bound receptors into tubular extensions of the early endosome, with a high surface to volume ratio that is well suited to carrying membrane protein cargo from one compartment to another, whilst acid-releasable ligands are distributed throughout the volume of the vesicular endosome and follow the bulk flow to the degradation pathway (Mayor *et al.*, 1993).

Despite the lack of identified sorting motifs, sorting of proteins into recycling endosomes could still occur by a regulated mechanism. Conserved sorting motifs occur in proteins on other trafficking pathways, such as the DXXLL motif to which the GGA (Golgi-associated γ-ear containing ARF-binding) proteins bind, directing specific cargo proteins into CCV's at the trans-Golgi network (TGN) (Hirst *et al.*, 2007). Recent evidence has also identified a highly conserved tripeptide motif in the cytoplasmic tail of the cation-independent mannose-6-phosphate receptor (ciM6PR), necessary for its retrieval from endosomes to the TGN (as discussed in section 1.2.7),

which lends support to the selectivity of a variety of sorting events (Seaman, 2007). Furthemore, different cargos have been found in distinct tubules. For example, ciM6PR are retrieved to the TGN in tubules formed by the action of the retromer coat complex (Mari *et al.*, 2008), whereas late endosomal proteins LAMP-1 and LAMP-2 (lysosomally associated membrane proteins), to be delivered to the lysosomal limiting membrane, are found in tubules associated with the adaptor protein complex AP-3 (Peden *et al.*, 2004), and Tf receptors are found in yet more distinct tubules, recently shown to be associated with the sorting nexin protein, SNX4 (Traer *et al.*, 2007). Together these results suggest that a range of morphologically distinct transport intermediates arise from the early endosome. Whether or not this segregation is selective remains to be determined.

1.2.3.2 Sorting-by-retention

The 'sorting-by-retention' model (Sachse *et al.*, 2002) proposes that receptor-ligand complexes targeted for lysosomal degradation are concentrated in bilayered coated areas of the endosomal membrane in a manner dependent on clathrin, for subsequent inclusion into the intralumenal vesicles (ILVs) by the endosomal sorting apparatus that governs this process (described in detail in section 1.2.4.1; see also figure 1.5). The fate of receptor-ligand complexes may also be dependent on the intracellular concentration of ligand, and in fact internalised receptors could also actively promote the remodelling of this compartment to suit their needs; there is evidence that EGFR itself increases the number of ILVs upon internalisation (White *et al.*, 2006).

A recent study of in depth examination of early endosome dynamics has found that there are seemingly two populations, a static fraction, and a rapidly maturing, motile fraction. CCV's bearing cargo destined for lysosomal degradation are proposed to be 'fast-tracked' into the degradation pathway by delivery to the motile fraction. For example, around 80% of EGF was found to be associated with the motile fraction, whilst 65% of recycling Tf receptor was associated with the static population. Furthermore, this study suggested that the sorting of receptors could begin at an even earlier stage and that their fate could also be governed by entry into different sub-classes of CCV at the plasma membrane and delivery to distinct endosomes (Lakadamyali *et al.*, 2006).

1.2.3.4 Recycling to the plasma membrane

After leaving early endosomes, recycling can occur by a direct, fast route through transport intermediates, mediated by the Rab GTP-ase Rab4, or a slow route through recycling endosomes, sometimes referred to as endosomal recycling compartments (ERC's), which are morphologically and functionally distinct from the early/sorting endosome (Sheff *et al.*, 1999; Sonnichsen *et al.*, 2000). ERC's are characterised by the acquisition of the Rab GTP-ase Rab11, in contrast to the Rab5 complement on early endosomes, and they do not contain ligands and receptors destined for degradation (ie. LDL), and are less acidic. Transport along the recycling pathway is dependent on the actin cytoskeleton and unconventional myosin motors, and it is possible that these may play a role in the biogenesis of the prerequisite tubules (Huber *et al.*, 2000; Apodaca, 2001). As the early

endosome matures it gradually acquires intralumenal vesicles of 40-90nm diameter, into which cargo targeted for lysosomal degradation is sorted. The number of ILVs often represents another means for classification of different compartments on the endocytic pathway, early endosomes are described as compartments having between 1 and 8 ILVs (van Meel and Klumperman, 2008).

1.2.4 Multivesicular bodies

Multivesicular bodies (MVBs) were described by electron microscopists over 30 years ago (Gorden *et al.*, 1978; Haigler *et al.*, 1979). They are classified as containing more than 8 ILVs, contain molecules that have been internalised through endocytosis or biosynthetic material received from the TGN (Woodman and Futter, 2008), and possess a different complement of proteins on their limiting membrane, such as the Rab GTP-ases Rab7 and Rab9 and the lysosomal associated proteins LAMP-1 and 2. Once formed they are thought to rapidly acidify and move towards the lysosome in a microtubule and motor-dependent fashion, and fuse with the lysosome in a manner dependent on conventional docking and fusion machinery. In specialised cell types MVBs serve as intermediates in the formation of secretory lysosomes, which under the appropriate stimulus, fuse with the plasma membrane and shed the ILVs into the extracellular space (ie. melanosomes, MHC II compartments and lytic granules) (Blott and Griffiths, 2002). In the majority of mammalian cell types they constitute endosomal intermediates formed from the early endosome.

1.2.4.1 Formation of intralumenal vesicles

Much of our knowledge of the sorting of lysosomaly directed cargo into ILVs has come from studying the internalisation of EGFR. Endocytosed receptors are able to signal from the limiting membrane of endosomes and MVBs, thus internalisation represents a means to terminate the signal by separating the receptor from the cytosol. Indeed, impairment of MVB formation has been found to attenuate EGFR signalling (Lloyd *et al.*, 2002). Sorting of many proteins for lysosomal degradation requires the post-translation modification ubiquitin, a group of proteins known as the ESCRT (endosomal sorting complex required for transport) and the AAA ATPase Vps4.

The ESCRT complexes were identified from a screen of yeast vacuolar protein sorting (Vps) mutants, which identified a class of mutants dubbed the class E mutants (Banta *et al.*, 1988; Raymond *et al.*, 1992). Each of these mutants is characterised by an absence of ILVs and the formation of a multilamellar cup-shaped compartment known as the class E compartment (Rieder *et al.*, 1996; Babst *et al.*, 1997). These class E mutants are found in all of the ESCRT complexes, of which there are three, and are evolutionarily conserved with each yeast protein having a mammalian homologue (Babst, 2005; Winter and Hauser, 2006). ESCRT I is composed of the proteins Vps28, TSG101 (tumour suppressor gene 101), and Vps37. ESCRT II is made up of ELL (RNA polymerase II elongation factor complex)-associated proteins EAP30, EAP25 and EAP45, is recruited transiently to the endosomal membrane, and is required for the subsequent recruitment of ESCRT III. ESCRT III is the most recently characterised

complex, made up of a group of charged MVB associated proteins or CHMPs (2A and B, 3, 4A, B and C and 6). It has also been suggested that another complex of proteins represents an ESCRT 0 complex, that functions prior to ESCRT I. This is the Hrs (Hepatocyte growth factor regulated tyrosine kinase substrate) and STAM (signal transducing adaptor molecule) complex.

The ESCRT complexes form a network that sequentially recruits monoubiquitinated proteins to the surface of MVBs and drives their internalisation into ILVs, potentially through direct involvement in the formation of the ILVs. Current models suggest that ESCRT 0 binds to ubiquitinated cargo proteins and recruits ESCRT I, which in turn recruits ESCRT II and ESCRT III. Cargo is deubiquitinated and the ESCRT complexes are removed, allowing the cargo to be sorted into the inward budding vesicle (Babst, 2005; Winter and Hauser, 2006). The ESCRT machinery is detailed in figure 1.5.

Direct evidence for a role in ILV formation remains elusive, but recent structural data suggests that the ESCRT III proteins can multimerise to form a flat lattice on the endosomal membrane, which could drive ILV formation in one of two ways (Muziol *et al.*, 2006; Shim *et al.*, 2007). Either by modifying the lipid composition of the underlying membrane to induce budding, or by bridging the gap over invaginating buds to promote fusion (Hanson *et al.*, 2008).

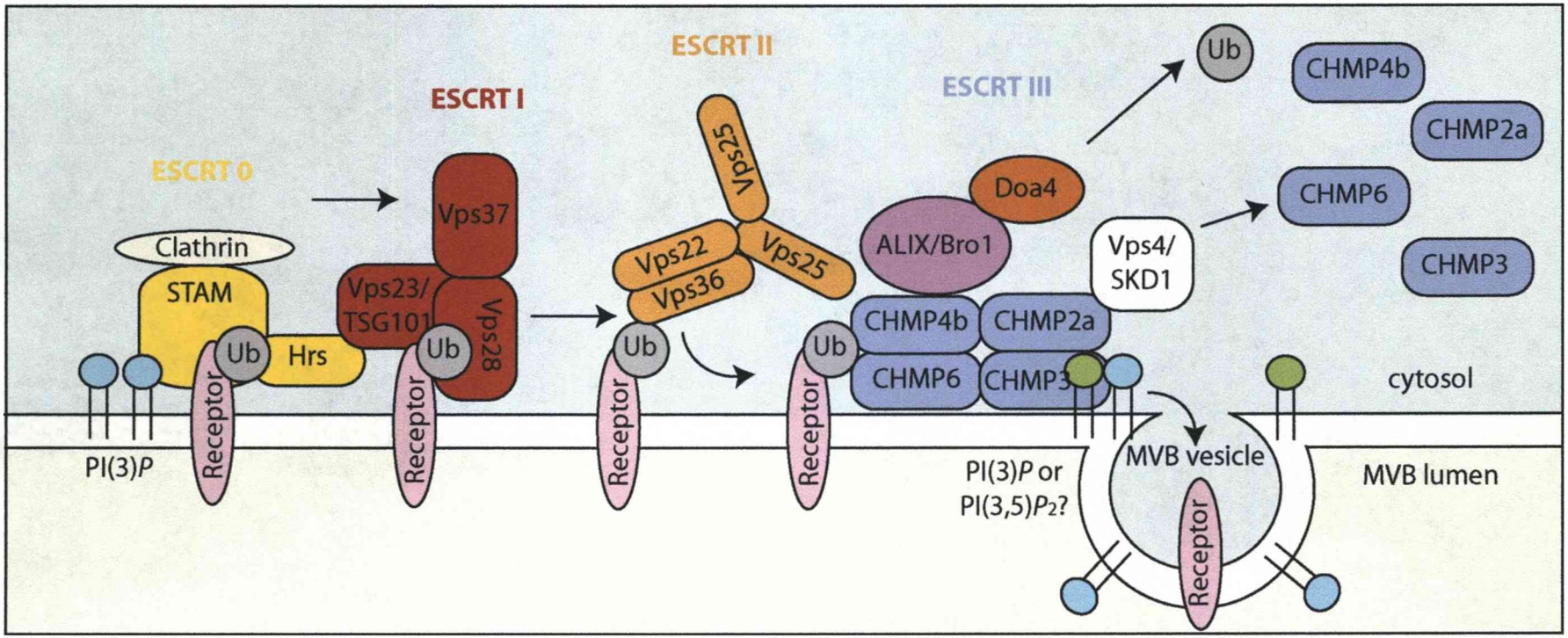

Figure 1.5 The MVB sorting machinery.
The ESCRT 0 complex Hrs/STAM is the first engagement point for ubiquitinated receptors (yellow), STAM binds ubiquitin through its UIM domain. Hrs recruits the ESCRT I complex (red) through interaction with TSG101, and ubiquitinated cargo is transferred to Vps28. ESCRT I binds to the Y-shaped ESCRT II complex (brown), which binds ubiquitinated cargo through Vps36. The Vp36 'arm' of the complex is proposed to swing across and transfer cargo ESCRT III (purple). ESCRT III associates with the AAA-ATPase Vps4, which disassembles it for further rounds of sorting. It also associates with ALIX (Bro1 in yeast), thought to recruit the deubiquitinating enzyme Doa4, for which the mammalian homologue is unclear, to deubiquitinate the receptor prior to internalisation. ESCRT 0 binds to membranes through its FYVE domain association with PtdIns(3)*P*. PtdIns(3,5)P_2 may be involved through binding of ESCRT III Vps24/CHMP3, and may play a role in MVB vesicle budding.

1.2.4.2 Different populations of ILVs

MVBs can appear to be either mutlilamellar (onion-like) or multivesicular (pomegranate-like), and this together with the finding that different ILVs often have different protein and lipid compositions, has lead to the suggestion that not all ILVs are functionally equivalent (White *et al.*, 2006). In fact, accumulating evidence suggests that different populations of ILVs or different lipid microdomains on their surface could be involved in regulating multiple fates of ILVs and their internalised cargos. ILVs display lysobisphosphatidic acid (LBPA) or PtdIns(3)*P* on their limiting membrane (Kobayashi *et al.*, 1999; Gillooly *et al.*, 2000). LBPA is thought to be involved in sphingolipid hydrolysis and transport of cholesterol. It is also proposed to be relatively resistant to intracellular lipases, and thus seems a strange choice for ILVs that are to be degraded in the lysosome. ILVs are also known to be rich in tetraspannins (such as CD63) and GPI-linked proteins, both of which associate with sphingolipid and cholesterol-rich rafts (Kobayashi *et al.*, 2000). These findings have lead to the suggestion that clustering of proteins within lipid rafts once inside ILVs may lead to further protein sorting and recycling. This is further reinforced by the fact that ciM6PRs have been found on the limiting membrane of ILVs, and antibodies against LBPA impair their retrieval from the late endosome (Corvera *et al.*, 1999), these receptors are therefore also thought to recycle from the later stages of the endocytic pathway.

1.2.5 Lysosomal degradation

The mature MVB/late endosome contains some lysosomal enzymes, has a similar pH to the lysosome and the same glycoproteins on its limiting membrane. Lysosomes can only be identified by virtue of their physical properties on gradients, and their electron dense appearance by EM, and the fact that they lack various proteins such as ciM6PR, Rab7 and Rab9 and phosphorylated hydrolase precursors (Luzio *et al.*, 2000). Christian de Duve first introduced the term lysosome in 1955, following his studies of the intracellular distribution of enzymes using centrifugal fractionation (de Duve, 1983). By 1959, the concept of the lysosome as a membrane-bound organelle that contains acid hydrolases involved in digestion of substances that enter the cell by endocytosis, was born. EM analysis found that they constitute up to 5% of the intracellular volume, and are of heterogeneous size and morphology. As with earlier stages of the endocytic pathway they possess proton-pumping vacuolar ATP-ases that maintain the lumenal environment at a pH of 4.6-5.0, essential for lysosomal degradation functions (Mellman *et al.*, 1986).

1.2.6 Theories of endolysosomal progression

There is still much debate about how the different endocytic compartments form, and how cargo is passed from one compartment to another. Theories of endolysosomal progression are summarised in figure 1.6. The endosomal maturation model suggests that early endosomes are formed *de novo*, and that they progressively mature into MVBs/late endosomes as the formation of tubular recycling/sorting compartments is

exhausted, and the compartment becomes refractory to fusion with incoming material and is instead able to fuse with the lysosome (Murphy, 1991; Dunn and Maxfield, 1992).

The second model proposes that the early endosome is a stable compartment, maintained by the balance of incoming and outgoing material and that transport between compartments is mediated not by fusion or maturation, but by endosomal carrier vesicles (ECV's) that form from the early endosome and fuse with the MVB/late endosome (Griffiths and Gruenberg, 1991). It remains to be conclusively demonstrated which hypothesis is correct, and indeed the two may not be mutually exclusive. In fact, recent live cell imaging studies have reconciled mechanistic aspects of both models. Marino Zerial's group explored the dynamics of Rab proteins during intracellular transport and described a model of the conversion of Rab proteins as a mechanism of progression. It's proposed that degradative cargo becomes highly enriched in progressively fewer and larger endosomes, which are removed from the tubular endosomal network and undergo a conversion in which they lose Rab5 and gain Rab7 (Rink *et al.*, 2005).

There are several other theories to suggest how the MVB/late endosome fuses with the lysosome. The 'kiss-and-run' model (a continuous cycle of transient contacts between late endosomes and lysosomes during which material is transferred), and the hybrid organelle theory (a direct fusion of late endosomes and lysosomes to form a distinct hybrid organelle) (Luzio *et al.*, 2000). Recent time-lapse and electron microscopy experiments have lead to the general belief that progression from late endosome to lysosome is

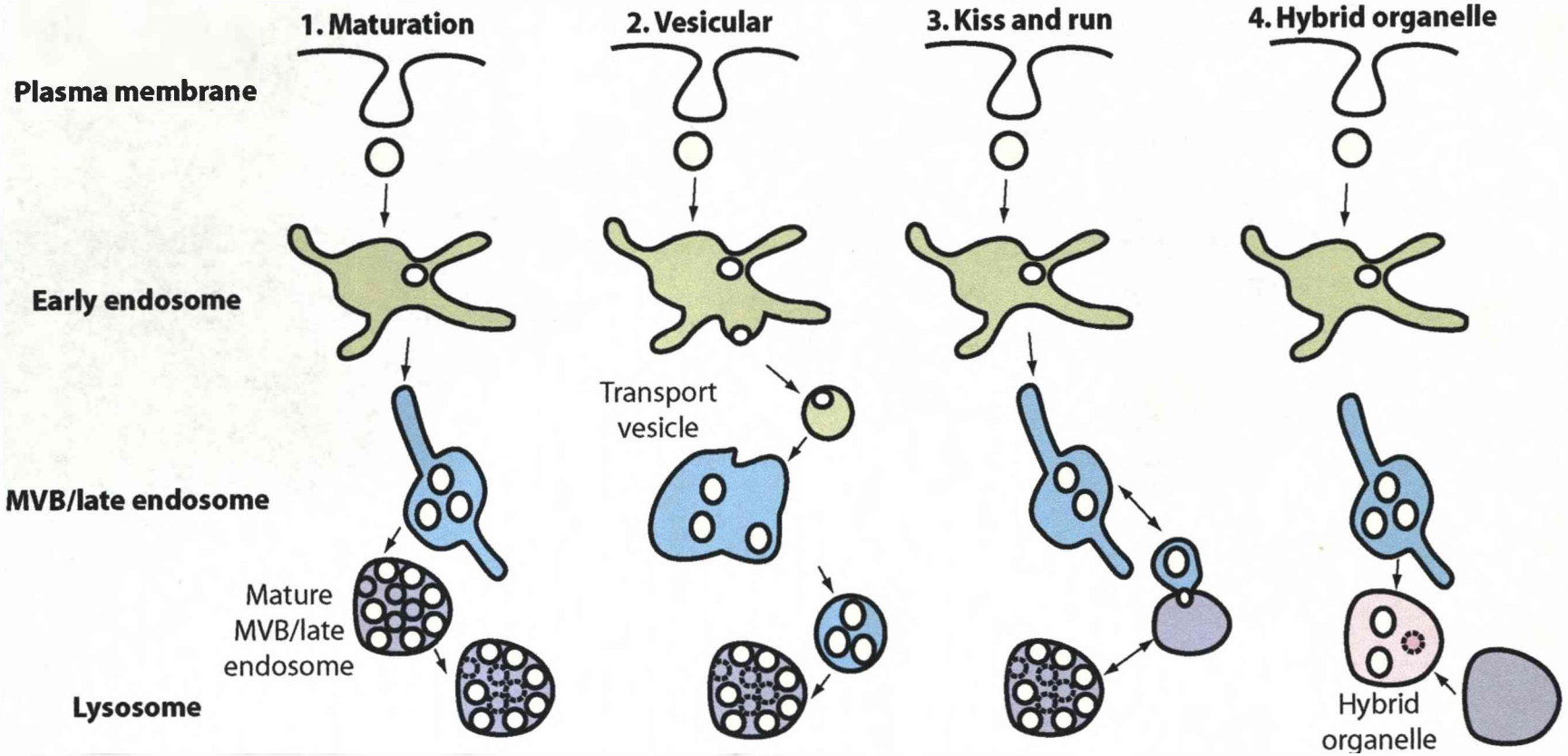

Figure 1.6. Theories of endolysosomal pathway progression.
Adapted from Luzio, 2007. Various theories of progression between endosomal compartments have been proposed and these are not necessarily mutually exclusive. 1. the early endosome forms *de novo* and progressively matures into an MVB/late endosome that acquires the capacity to fuse with the lysosome. 2. each compartment is stable, maintained by a balance of incoming and outgoing material that is transferred by means of ECV's. 3. a contiunous cycle of transient contacts occurs between compartments, during which material is transferred. 4. Compartments directly fuse with one another to form a hybrid organelle, from which the respective compartments are then reformed.

most likely a combination of direct fusion and kiss and run events resulting in a transient hybrid organelle from which lysosomes reform (Storrie and Desjardins, 1996; Luzio *et al.*, 2000; Mullins and Bonifacino, 2001; Luzio *et al.*, 2003).

1.2.7 The biosynthetic pathway

The biosynthetic pathway involves the trafficking of newly synthesised proteins from the Endoplasmic Reticulum (ER) through the Golgi apparatus, to various intracellular destinations (Palade, 1975). The Golgi complex is composed of polarised stacks of flattened membrane bound compartments called cisternae (Rambourg and Clermont, 1990), which have a *cis* (entry) face and a *trans* (exit) face. The stacks are made up of 5 regions, the *cis*-Golgi network (CGN), the *cis*, *medial* and *trans* cisternae, and the *trans*-Golgi network (Dunphy and Rothman, 1985). The CGN is a collection of fused tubulovesicular clusters that receives vesicles containing proteins from the ER. As they pass through the Golgi cisternae these proteins undergo various post-translational modifications, such as ordered remodelling of their N-linked oligosaccharide side chains, performed by a range of transmembrane processing enzymes associated with each cisterna (Dunphy and Rothman, 1985). They then pass to the TGN, a major cellular protein sorting station (Griffiths and Simons, 1986; Mellman and Simons, 1992). At least four post-golgi anterograde transport pathways exist in most cell types: two pathways to the plasma membrane (constitutive and regulated secretion), one pathway direct to the lysosome, and at least one pathway to the lysosome via endosomes. Constitutive secretion pathways to the plasma

membrane are thought to be the default pathway, as no specific signal for transport on this pathway has yet been identified. Regulated secretion involves the packaging of proteins into secretory vesicles that then release their contents at the plasma membrane in response to a certain stimulus.

1.2.7.1 TGN to endosome anterograde transport

Probably the best understood sorting mechanism at the TGN is for proteins destined for transport to the lysosome. A subset of the oligosaccharide modifications added to proteins as they pass through the Golgi complex serve as tags to direct these proteins to the lysosome. The hydrolytic enzymes that perform the degradative function of the lysosome are synthesised in the ER and modified in the Golgi by the addition of mannose-6-phosphate groups. These groups are recognised by the mannose-6-phosphate receptors (M6PRs) resident in the TGN membrane (Kornfeld and Mellman, 1989; Kornfeld, 1992). There are two distinct M6PRs in mammalian cells, the 46kDa cation-dependent M6PR (cdM6PR) and the 300kDa cation-independent M6PR (ciM6PR), both of which are type I transmembrane proteins that share some sequence homology in their lumenal domains (Kornfeld, 1992).

M6PRs are sorted into CCV's at the TGN along with their cargo. This process was initially thought to involve the adaptor protein complex 1 (AP-1), part of a family of heterotetrameric proteins consisting of two large subunits termed adaptins (γ and β_1 in the case of AP-1), a medium-sized subunit (μ_1) and a small subunit (σ_1). This structure is highlighted in figure 1.7. These adaptor protein complexes bind to clathrin and select cargo proteins and

regulate the formation of CCV's (Gallusser and Kirchhausen, 1993; Traub *et al.*, 1995). However, AP-1 does not directly bind the acidic-cluster-dileucine residues in M6PRs (Honing *et al.*, 1997; Zhu *et al.*, 2001).

Recent evidence suggests that Golgi-to-endosome trafficking is mediated by the GGA proteins, of which there are three in mammalian cells (GGA1, 2 and 3). GGA proteins are monomeric proteins with a modular structure consisting of a VHS (Vps27, Hrs and STAM) domain, which recognises the acidic-cluster-dileucine signals in M6PRs, a GAT domain, which interacts with the GTP-bound form of ADP ribosylation factor (ARF), a hinge domain, which binds clathrin, and a GAE domain, which interacts with γ-synergin and other potential regulators of coat assembly (Dell'Angelica *et al.*, 2000; Hirst *et al.*, 2000). The domain structure of GGA-1 is shown in figure 1.7. In fact, GGA proteins have also recently been shown to bind AP-1 (Doray *et al.*, 2002), suggesting that the two may cooperate to mediate packaging of cargo into CCV's at the Golgi.

1.2.7.2 Endosome to TGN retrograde transport

Certain proteins that are transported onto the endocytic pathway require retrieval to the TGN for recycling, and this occurs via retrograde transport pathways. For example, to maintain the efficient transport of acid hydrolases to the lysosome, the M6PRs need to be recycled to the TGN to avoid degradation in the lysosome and for use in subsequent rounds of transport. Until recently, this recycling process had remained relatively poorly characterised, and only a few putative candidates for mediating it had been identified. The best characterised of these were the small GTP-ase

Rab9, its effector protein p40, and the protein TIP-47 (tail interacting protein 47). As the name suggests TIP-47 can interact with the cytoplasmic tail of M6PRs, and this complex has been shown to regulate the retrograde transport of these receptors (Riederer *et al.*, 1994; Diaz and Pfeffer, 1998).

It has now become widely accepted that multiple parallel pathways exist to regulate endosome-to-TGN transport. A number of cargoes, such as the B-subunit of the Shiga toxin (an AB_5 type toxin produced by *Escherichia coli* that is thought to hijack endosome to TGN transport pathways) and TGN46 (a TGN resident protein that is thought to cycle to the plasma membrane and return via the endocytic pathway) have been found to traffic to the TGN via early/recycling endosomes, bypassing the late endocytic pathway and therefore independently of the Rab9/TIP47 complex (Ghosh *et al.*, 1998; Mallard *et al.*, 1998). Analysis of Vps mutants in *S. cerevisiae* identified three mutants with phenotypes that were basically the same as the yeast protein Vps10 (Seaman *et al.*, 1997), a protein that performs an identical function to the mammalian M6PRs. These proteins were subsequently found to be components of a vesicle coat complex known as retromer, that mediates retrieval of Vps10 to the TGN. Subsequently, the mammalian homologues of yeast retromer were identified. It is composed of the Vps proteins Vps35, Vps29 and Vps26, which are involved in cargo recognition, and two members of the sorting nexin family SNX-1 and SNX-2, which are thought to regulate membrane binding through their phosphoinositide-binding PX domain, and membrane curvature through their BAR domain (Haft *et al.*, 2000; Arighi *et al.*, 2004). The structure of the mammalian retromer complex is outlined in figure 1.7.

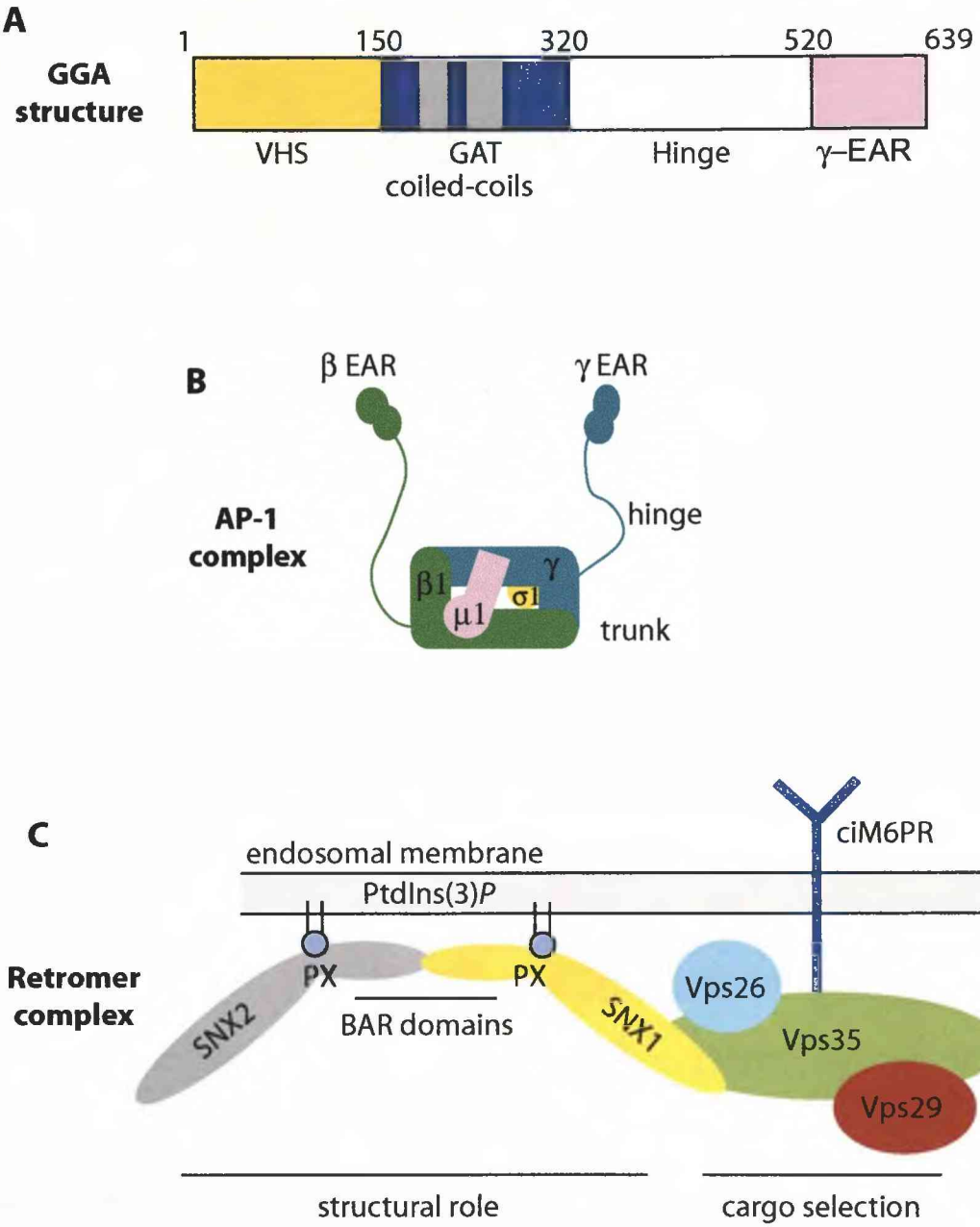

Figure 1.7 Structure of proteins involved in transport pathways between the TGN and endocytic pathway.
A) Domain structure layout of the GGA proteins (numbering from GGA-1).
B) Structure of the Adaptor protein complex 1 (AP-1).
C) Structure of the mammalian retromer complex. Vps35 interacts with cargo such as the ciM6PR and also with Vps26 and Vps35 through its N and C terminus respectively. SNX-1 is able to bind to the Vps35-29-26 complex. SNX1 and SNX2 have PX domains through which they bind PtdIns(3)*P* and BAR domains that are proposed to regulate membrane curvature.

1.3 Phosphoinositides and membrane trafficking

Whilst PtdIns(3,4)P_2, PtdIns(4,5)P_2 and PtdIns(3,4,5)P_3 are localised predominantly to the plasma membrane (Gray *et al.*, 1999; Watt *et al.*, 2002), the other phosphoinositides, PtdIns(3)*P*, PtdIns(4)*P* and PtdIns(3,5)P_2 are enriched in intracellular organelle membranes, where they play a role in intracellular membrane trafficking. The localisation of the key phosphoinositides involved in membrane trafficking and examples of their effector proteins is illustrated in figure 1.8.

1.3.1 PI(3)-kinases

The first indication that phosphoinositides played a role in membrane trafficking came from genetic studies of transport to the yeast vacuole. Examination of mutants of the Vps genes required for transport from the Golgi to the vacuole identified a gene that encoded a PI(3)-kinase, Vps34. Subsequent cloning of this gene and sequence comparison revealed that Vps34p was 37% identical in its primary sequence to a mammalian PI(3)-kinase p110α (Herman and Emr, 1990; Hiles *et al.*, 1992; Schu *et al.*, 1993). Vps34 specifically phosphorylates PtdIns at the 3 position on its inositol ring to produce PtdIns(3)*P* (Schu *et al.*, 1993). In *S. cerevisiae*, temperature sensitive *Vps34* mutant cells exhibited a defect in protein sorting to the vacuole and PI(3)-kinase activity when shifted to a non-permissive temperature (Stack *et al.*, 1995). It was subsequently shown to be the sole PI(3)-kinase in *S. cerevisiae* (Stack and Emr, 1994).

In contrast multiple mammalian PI(3)-kinases (8 catalytic subunits in total) have been identified and classified according to their substrate

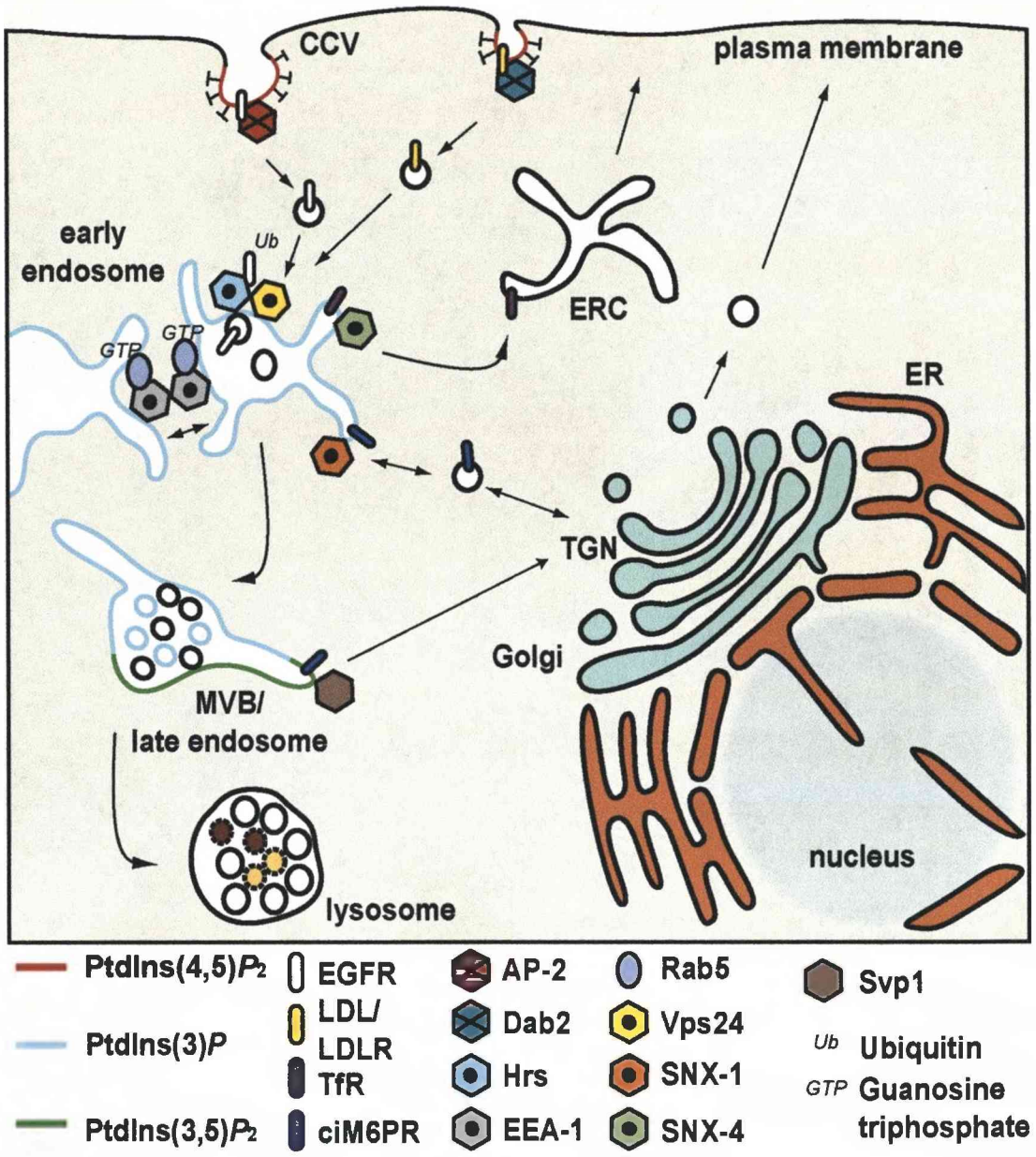

Figure 1.8 Localisation of phosphoinositides and selected effectors on the endocytic pathway.

PtdIns(4,5)P_2 is highly enriched at the plasma membrane where it recruits the adaptor complex AP-2 to promote CCV formation and internalisation of cell surface receptors, such as Tf receptor. It has also been implicated in AP-2 independent internalisation of LDL receptor probably through the effector protein DAB2. PtdIns(3)P and PtdIns(3,5)P_2 play key roles in regulating endo-lysosomal compartments. EEA-1 is recruited to early endosomes by PtdIns(3)P and GTP-bound Rab5, where it regulates homotypic fusion. PtdIns(3)P also binds components of the ESCRT machinery, such as Hrs, to coordinate internalisation of ubiquitinated receptors, as well as components of the Retromer complex, including SNX-1, involved in retrograde transport of ciM6PRs. PtdIns(3,5)P_2 binds Svp1/Atg18, which may regulate endosome to TGN transport.

specificities (Zvelebil *et al.*, 1996). These multiple isoforms can be divided into three classes, but all share a homologous region consisting of a catalytic core domain, a PtdIns-kinase domain, and a C2 domain. Class I PI(3)-kinases are heterodimeric molecules composed of a 100kDa catalytic subunit (p110) and a regulatory subunit (p85, p55, p50 or p101), of which there are multiple isoforms. They are further subdivided into class IA and class IB, which are activated by receptor tyrosine kinases and heterotrimeric G-protein coupled receptors respectively. Class I primarily use PtdIns(4,5)P_2 as their substrate *in vivo* (Fry, 1994; Vanhaesebroeck and Waterfield, 1999).

Class II PI(3)-kinases comprise three catalytic subunits, C2α, C2β and C2γ. They possess a C-terminal C2 domain, which allows phospholipids to bind in a Ca^{2+}-independent manner (MacDougall *et al.*, 1995), and they exhibit a substrate specificity for PtdIns, PtdIns(4)*P* and PtdIns(4,5)P_2 *in vitro* (Vanhaesebroeck and Waterfield, 1999).

Finally, the sole class III PI(3)-kinase is hVps34, a ubiquitously expressed kinase that specifically phosphorylates PtdIns to produce PtdIns(3)*P*. In both humans and yeast Vps34 associates with the N-terminally myristoylated serine/threonine kinase Vps15/p150, which recruits Vps34 to cell membranes and enhances its lipid kinase activity (Stack *et al.*, 1993; Murray *et al.*, 2002; Stein *et al.*, 2005).

A role for mammalian PI(3)-kinases in membrane trafficking was identified through the use of PI(3)-kinase inhibitor Wortmannin, an anti-fungal compound (Brian, 1957). Wortmannin completely inhibits the class I, II β and γ and class III PI(3)-kinases at doses below 100nM (Fruman *et al.*, 1998). Wortmannin treatment was found to inhibit the fusion of early endosomes

(Jones and Clague, 1995; Li *et al.*, 1995), reduce the rate of recycling of internalised Tf receptor (Martys *et al.*, 1996; Spiro *et al.*, 1996), disrupt the lysosomal transport of PDGF receptor (Shpetner *et al.*, 1996), and inhibit the formation of internal vesicles in MVBs (Futter *et al.*, 2001) or the sorting of EGFR (Petiot *et al.*, 2003). However, it was not clear from these studies which isoforms of PI(3)-kinase were responsible for these effects. As a result of this, different experimental techniques such as siRNA treatment, hVps34 inhibitory antibodies and overexpression studies, all of which have their individual caveats, have lead to different assignments of hVps34 function in mammalian cells. To date, small specific inhibitors of hVps34 have yet to be identified.

1.3.2. PtdIns(3)P

Despite the lack of specific hVps34 inhibitors, PtdIns(3)*P* has been shown to play a vital role in endocytic membrane trafficking. In the 1990's early endosomal antigen-1 (EEA-1) protein was identified as a wortmannin-sensitive component of endocytic vesicles (Patki *et al.*, 1998). This lead to the identification of the FYVE domain as a specific PtdIns(3)*P* binding domain that directed EEA-1 to the early endosomal membrane, where it was subsequently shown to be involved in early endosome homotypic fusion (Mills *et al.*, 1998; Simonsen *et al.*, 1998). Since then more than 70 proteins have been shown to possess PtdIns(3)*P* binding domains, including PX, GRAM, and FYVE domains, implicating this lipid in a range of membrane trafficking functions, such as the internalisation of ubiquitinated receptors into

MVBs through recruitment of components of the ESCRT machinery (Urbe *et al.*, 2000; Raiborg *et al.*, 2001).

1.3.3 Other phosphoinositides involved in membrane trafficking

Other phosphoinositides have been shown to play a role on the endocytic pathway. PtdIns(4,5)P_2 is localised predominantly to the plasma membrane, and here it has been shown to regulate the internalisation of CCV's. Clathrin coats of internalised endocytic vesicles are rapidly removed through dephosphorylation of PtdIns(4,5)P_2 by the 5-phosphatase synaptojanin, rendering them competent to fuse with the early endosome (Jost *et al.*, 1998). PtdIns(4)*P* has been found to localise to the Golgi membrane by visualisation of a GFP-tagged PH domain from the PtdIns(4)*P* binding protein FAPP1. At the Golgi it is proposed to be involved in regulating transport pathways to the cell surface (Godi *et al.*, 2004).

1.4 PtdIns(3,5)P_2

A relatively novel phosphoinositide, PtdIns(3,5)P_2, is also proposed to be involved in endocytic membrane trafficking, as discussed in section 1.9. The presence of this phosphoinositide was confirmed independently in mouse fibroblasts and *S. cerevisiae* in 1997 (Dove *et al.*, 1997). It constitutes a small proportion of the total phospholipid in a cell, typically 0.1% or less. However, cellular levels increase dramatically in response to hyperosmotic stress, 30-fold in yeast, 2 to 6-fold in plants and in some animal cells also, and in other mammalian cells in response to other stresses, such as UV radiation, interleukin-2 and fibrinogen in platelets (Dove *et al.*, 1997;

Banfic *et al.*, 1998; Cooke *et al.*, 1998; Jones *et al.*, 1999; Sbrissa and Shisheva, 2005). It is present in all eukaryotic cells examined thus far, including yeast, plants, protozoa and mammalian cells (Dove *et al.*, 1997; Whiteford *et al.*, 1997; Odorizzi *et al.*, 2000; Shisheva, 2001; Cooke, 2002; Efe *et al.*, 2005; Leondaritis *et al.*, 2005). In the years since PtdIns(3,5)P_2 was first described, a variety of key proteins associated with its metabolism have been identified. Four of these proteins are detailed in the following sections.

1.5 PtdIns(3)P 5-kinase

1.5.1 Fab1

PtdIns(3,5)P_2 is made by the consecutive actions of a PI(3)-kinase and the sole PtdIns(3)*P* 5-kinase, Fab1 (Cooke *et al.*, 1998; Gary *et al.*, 1998; Odorizzi *et al.*, 2000; Morishita *et al.*, 2002). Fab1 was originally identified from a screen for abnormal nuclear segregation (hence **f**ormation of **a**ploid and **b**inucleate cells) (Yamamoto *et al.*, 1995). It is part of an evolutionarily ancient gene family, and the protein is the product of a single gene in most species. It is predicted to encode a 257kDa protein in yeast with significant sequence homology to other known phosphoinositide phosphate kinases at its C terminus (Yamamoto *et al.*, 1995).

The majority of our understanding of the cellular localisation and function of PtdIns(3,5)P_2 has come from the study of cells defective in the activity of this kinase. Yeast Fab1 mutant cells produce undetectable levels of PtdIns(3,5)P_2 (Gary *et al.*, 1998) and generate a characteristic grossly enlarged vacuole (the yeast equivalent of the mammalian lysosome) that fills

much of the cell. Further to this, the vacuole is improperly acidified (Yamamoto *et al.*, 1995; Cooke *et al.*, 1998; Gary *et al.*, 1998). Some yeasts also show a sensitivity to certain types of stresses, such as heat, and others inefficient mating, meiosis or sporulation (Rabitsch *et al.*, 2001; Briza *et al.*, 2002), and a failure to properly respond to mating factors (Morishita *et al.*, 2002; Onishi *et al.*, 2003), all of which are proposed to reflect a general slowing of both the endo- and exocytic machinery (Shaw *et al.*, 2003; Osborne *et al.*, 2008). *Candida albicans* yeast demonstrate a failure in hyphal growth on solid media (Zheng *et al.*, 1998; Rabitsch *et al.*, 2001; Augsten *et al.*, 2002; Bidlingmaier and Snyder, 2002; Briza *et al.*, 2002; Morishita *et al.*, 2002; Onishi *et al.*, 2003; Shaw *et al.*, 2003; Osborne *et al.*, 2008).

1.5.2 PIKfyve

The first full-length orthologues of Fab1 were identified in the yeast *Schizosacchoromyces pombe* (SpFab1) (McEwen *et al.*, 1999) and in murine adipocytes (Shisheva *et al.*, 1999). The murine protein was termed p235 or PIKfyve (**P**hosphoinositide **k**inase for **f**ive position containing a **fyve** domain). It was originally cloned from a mouse adipocyte library through a screen for transcripts that are enriched in fat and muscle. The human gene was recently assembled based on a human EST database, and the generated PCR product was found to be 2098 residues (Cabezas *et al.*, 2006), it is located on chromosome 2 (2q34) and comprises 41 exons.

NCBI (National Centre for Biotechnology Information)-Blast analyses and various characterisation in the literature demonstrate that PIKfyve is

evolutionarily conserved, with homologues in *Caenorhabditis elegans*, *Drosophila melanogaster* and a number of other organisms. The mouse homologue is 85% identical to human PIKfyve, that of *D. melanogaster* is 28% identical and *C. elegans* and *S. cerevisiae* sequences show less than 30% identity (Cabezas *et al.*, 2006). All of these proteins have come to be known as type III phosphatidylinositol phosphate (PIP) kinases, to distinguish them from the type I PIP kinases that are PtdIns(4)*P* 5-kinases, and the type II PIP kinases that are PtdIns(5)*P* 4-kinases (Cooke, 2002).

1.5.3 PIKfyve/Fab1 domains

With the possible exception of *Arabidopsis thaliana* (the only genome which encodes more than one potential PtdIns(3)*P* 5-kinase), all of the type III PIP-kinases contain four domains. These domains are highlighted in figure 1.9.

The FYVE domain is a Zinc finger domain found in proteins that bind to PtdIns(3)*P* (Burd and Emr, 1998; Gaullier *et al.*, 1998; Patki *et al.*, 1998). The FYVE domain of Fab1 has been shown to bind to PtdIns(3)*P in vitro*, albeit more weakly than other FYVE domains. However, this lower affinity was thought to be due to the construct used lacking the final 36 amino acids of the FYVE domain (Burd and Emr, 1998). The PIKfyve FYVE domain has also been shown to bind PtdIns(3)*P*. A GST-FYVE fusion protein from PIKfyve, localises to endosomal membranes in a manner dependent on cellular PtdIns(3)*P* levels (Sbrissa *et al.*, 2002b).

The TCP-1 (T complex protein 1)/chaperonin-like domain is homologous to a subunit of the chaperonin domain-containing protein TCP-1,

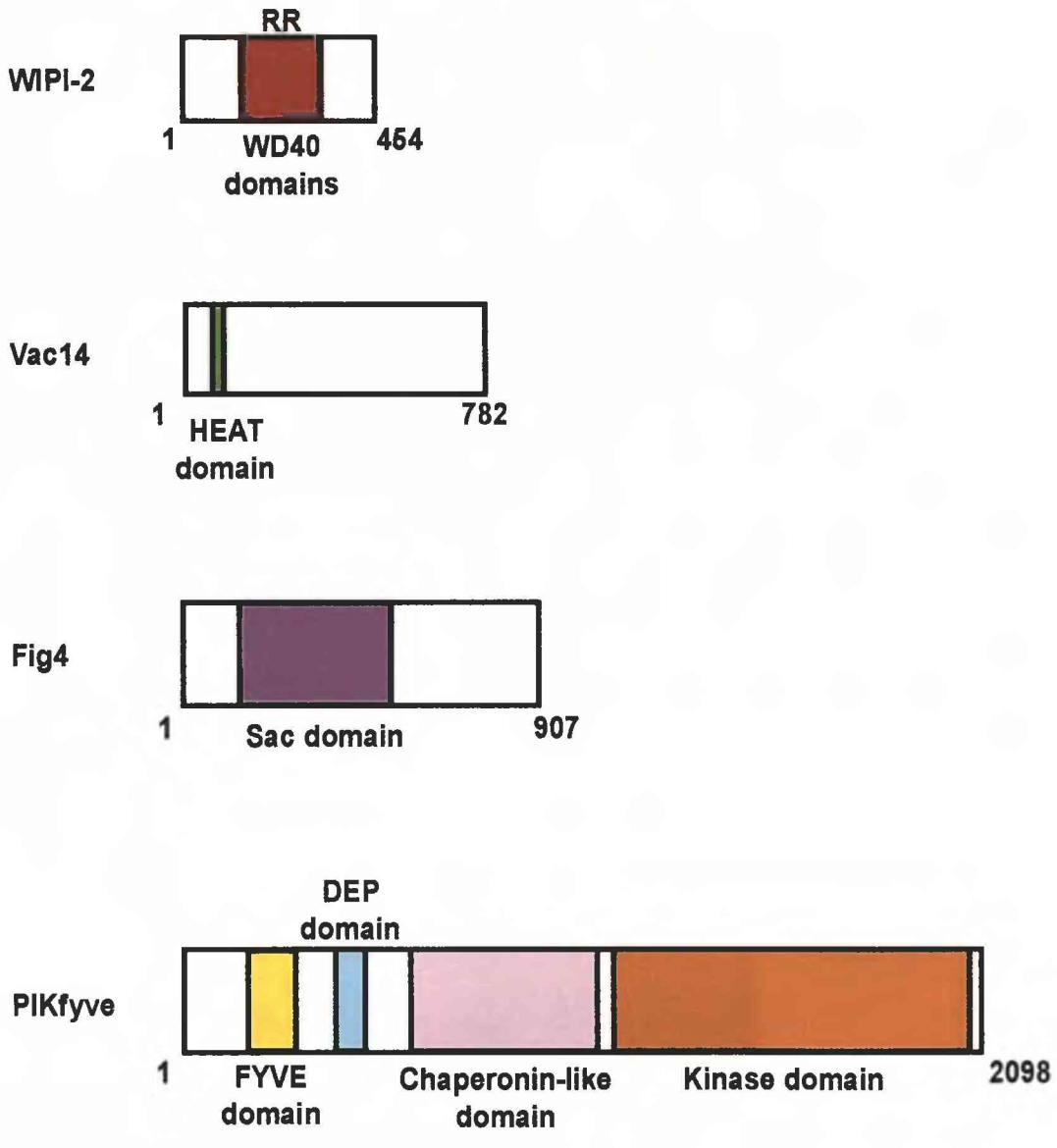

Figure 1.9. Domain structures of mammalian PtdIns(3,5)P_2 associated proteins.

Diagram illustrating the domain structures of the mammalian proteins WIPI-2, Fig4 and Vac14 and PIKfyve as predicted by protein motif analysis with PFAM (http://pfam.sanger.ac.uk/) and detailed in previous studies of PIKfyve. WIPI-2 contains 7 WD40 domains within the indicated area, each of which is found within one blade of the beta-propeller.

an 8 sub-unit chaperone that binds exclusively to actin and tubulin. Although no specific role for this domain has been characterised, a PIKfyve mutant lacking residues 560-1231, which includes this domain, is catalytically inactive (Sbrissa *et al.*, 1999). PIKfyve is also known to be involved in the pathology of Francois Neetens Mouchetee Fleck Corneal Dystrophy, an autosomal dominant human syndrome characterised by the presence of numerous white flecks scattered in all layers of the stroma. Interestingly, most mutations involved in this disease are of the nonsense and frameshift type and are found in and around this domain in PIKfyve (Li *et al.*, 2005).

The cysteine rich domain is unique to the type III PIP-kinases and as yet has no defined role (McEwen *et al.*, 1999; Shisheva *et al.*, 1999) and the PIP-kinase domain is the C-terminal catalytic domain. Mutations in this domain in both Fab1 and PIKfyve abrogate its kinase activity (Sbrissa *et al.*, 2000). Finally, PIKfyve orthologues from *Mus musculus*, *Homo sapiens* and *D. melanogaster* also contain a DEP domain (Shisheva, 2001), named for three of the proteins it was first identified in (Dishevelled, Egl-10 and Pleckstrin) (Ponting and Bork, 1996). Again this has no characterised role, but is not present in lower organisms, and has been identified in a number of signalling molecules and implicated in their membrane targeting (Wong *et al.*, 2000).

1.5.4 Lipid kinase activity

In *S. cerevisiae* Fab1 mutants have undetectable levels of PtdIns(3,5)P_2, even following hyperosmotic stress, a condition that normally provokes a marked increase in the levels of this lipid (Cooke *et al.*, 1998;

Gary *et al.*, 1998). A GST-fusion protein has been shown to exhibit PtdIns(3)*P* 5-kinase activity when assayed *in vitro*, with the following substrate specificity; PtdIns(3)*P* >> PtdIns(4)*P* > PtdIns (Cooke *et al.*, 1998; McEwen *et al.*, 1999). This lipid kinase activity is abrogated by the mutation of an aspartic acid residue to an arginine at position 2134 *in vivo*, and a lysine to a methionine at position 2059 *in vitro* (Gary *et al.*, 1998; McEwen *et al.*, 1999).

All other type III PIP-kinases from other organisms, have also been found to have 5-kinase activity *in vitro*, and display similar substrate specificity to Fab1. Expression of PIKfyve in a Fab1 mutant strain restores PtdIns(3,5)P_2 synthesis and reverts the Fab1 mutant phenotype *in vivo*, suggesting a conserved physiological function of these proteins (Sbrissa *et al.*, 1999). Although *in vitro* PtdIns(3,5)P_2 can be produced by the action of a type I PIP-kinase on PtdIns(3)*P*, non equilibrium labelling experiments have shown that the majority of PtdIns(3,5)P_2 must be synthesised by a PtdIns(3)*P* 5-kinase, and a type I PIP-kinase also does not restore levels of PtdIns(3,5)P_2 or complement the Fab1 mutant phenotype (Dove *et al.*, 1997; Whiteford *et al.*, 1997; McEwen *et al.*, 1999).

PIKfyve has also been proposed to synthesise PtdIns(5)*P*, the most recently identified phosphoinositide (Rameh *et al.*, 1997) *in vitro* and *in vivo* (Shisheva *et al.*, 1999; Shisheva, 2001). The opinion on this matter remains somewhat divided. Some groups believe that the type III PIP-kinases are most likely dedicated to the production of PtdIns(3,5)P_2 and that any production of PtdIns(5)*P* is of limited biological significance (McEwen *et al.*, 1999; Cooke, 2002). Furthermore, they believe that the major route of

PtdIns(5)*P* synthesis in the cell is through hydrolysis of PtdIns(3,5)P_2 (this is discussed in more detail in section 1.6).

Another school of thought suggests that direct phosphorylation of PtdIns by PIKfyve is also a major route of PtdIns(5)*P* synthesis in addition to hydrolysis of PtdIns(3,5)P_2. Indeed, PIKfyve has been shown to readily produce PtdIns(5)*P* *in vitro*, and HEK293 cell lines expressing wildtype or kinase-deficient PIKfyve show 2-fold higher and 2-fold lower mass levels of PtdIns(5)*P* respectively (Shisheva, 2001; Sbrissa *et al.*, 2002a). The counter argument to these findings states that evidence from *in vitro* kinase assays must be treated with caution as these are carried out in non-physiological conditions that can affect binding specificities. Furthermore, the complementation of PtdIns(3,5)P_2 production in Fab1 mutants by overexpression of PIKfyve, does not also lead to an increase in PtdIns(5)*P* (McEwen et al., 1999), and although this has been revised recently, based on more effective expression of PIKfyve (Michell *et al.*, 2006), the debate remains inconclusive. Furthermore, PtdIns(5)*P* is not thought to be present in yeast (Walker *et al.*, 2001; Schaletzky *et al.*, 2003) and the data suggesting that PIKfyve is required for PtdIns(5)*P* synthesis in HEK293 cells does not distinguish between the requirement of PIKfyve activity to directly make PtdIns(5)*P* and the requirement of PIKfyve to make PtdIns(3,5)P_2 as a substrate for PtdIns(5)*P* by its subsequent hydrolysis. Hence, this subject requires further investigation.

1.5.5 Localisation

In *S. cerevisiae* Fab1 localises to the vacuolar and endosomal membranes and the cytosol (Gary *et al.*, 1998). Although the methods used in this study cause osmotic stress and stimulate PtdIns(3,5)P_2 production, subsequent experiments using HA and GFP-tagged fusion proteins found that they did indeed localise to the vacuolar membrane, and HA-Fab1 was shown to colocalise with Vac8, a known vacuolar protein (Gary *et al.*, 1998; Dove *et al.*, 2002).

Despite the production of anti-PIKfyve antibodies by a number of different groups, none of these antibodies proved useful for testing the localisation of endogenous PIKfyve, this has only been examined in 3T3-L1 adipocytes (Shisheva *et al.*, 1999). In both these studies, and in other mammalian cell lines, using overexpression contructs, PIKfyve was found to localise to peripheral vesicular structures and the cytoplasm. Overexpression studies went on to determine that there was no colocalisation with Tf (recycling endosomes), Dextran (late endosomes) or β-COP (Golgi), and that treatment with Brefeldin A, which disrupts the Golgi stacks, did not affect the localisation of PIKfyve (Shisheva *et al.*, 1999; Shisheva *et al.*, 2001).

It was initially reported that the vesicular structures were predominantly MVB/late endosome compartments, as they colocalised with ciM6PR. However, more recent studies in HeLa cells using low expression levels of GFP-PIKfyve, have demonstrated that PIKfyve is predominantly found on EEA-1 labelled tubulovesicular early endosomes (Cabezas *et al.*, 2006; Rutherford *et al.*, 2006). Closer inspection revealed that PIKfyve is

actually localised to microdomains on early endosomes distinct from EEA-1 and Hrs (Cabezas *et al.*, 2006).

1.5.6 PIKfyve functions

The potential fundamental significance of PIKfyve-dependent functions to human physiology is hinted at by the embryonic lethality of *D. melanogaster* and *C. elegans* PIKfyve null mutants (Nicot *et al.*, 2006; Rusten *et al.*, 2006). PIKfyve has been shown to be potentially important in a number of different processes. Its most widely studied function is in the maintenance of endosomal membrane homeostasis. The key feature of Fab1 mutants, as described in section 1.4, is the formation of a massively swollen vacuole (Gary *et al.*, 1998). Various studies have examined the effects of manipulating PIKfyve activity in mammalian cells where the result of overexpression of a kinase-deficient mutant, depletion of PIKfyve through siRNA or treatment with a specific inhibitor of PIKfyve (discussed in section 1.5.7), is a progressive accumulation of dilated endosomes and swollen cytoplasmic vacuoles (Sbrissa *et al.*, 1999; Ikonomov *et al.*, 2003a; Rutherford *et al.*, 2006; Jefferies *et al.*, 2008). However, despite the similar phenotypes, the requirement for PIKfyve activity has been suggested to be at different compartments in yeast and mammalian cells (Ikonomov *et al.*, 2006), whilst Fab1 is proposed to act at the yeast vacuole (Gary *et al.*, 2002; Rudge *et al.*, 2004), PIKfyve function has been placed at both the early endosome and MVB in mammalian cells (Cabezas *et al.*, 2006; Rutherford *et al.*, 2006), and at the late endosome in *C. elegans* (Nicot *et al.*, 2006). The origin of the swollen vacuoles remains an unanswered question of

mammalian PtdIns(3,5)P_2 biology. They are proposed to be the result of reduced ILV internalisation and membrane retrieval to the TGN (Ikonomov *et al.*, 2001; Rutherford *et al.*, 2006). In support of these hypotheses, PIKfyve interacts with components of the endosome-to-TGN retrograde transport machinery. Furthermore, a functional relationship between PIKfyve and the mammalian AAA ATPase Vps4 homologue, SKD1 has been established. Ectopic expression of catalytically inactive SKD1 in Cos7 cells leads to vacuolation, and this can be partially rescued by overexpression of wildtype PIKfyve, suggesting a role for PIKfyve in the final step of ILV formation (Ikonomov *et al.*, 2002b).

A number of proteins have been shown to interact with PIKfyve, which have hinted at a variety of cellular functions. Perhaps the best characterised of these is the interaction with Vac14, also referred to as ArPIKfyve, which serves as an allosteric activator of PIKfyve activity. Vac14 also forms a complex with the proposed PtdIns(3,5)P_2 5-phosphatase Fig4. As such these three proteins may potentially form a ternary complex in both yeast and mammalian cells, which tightly regulates the levels of PtdIns(3,5)P_2. These interactions will be discussed in more detail in the relevant sections for these proteins. PIKfyve has also been shown to interact with the Rab9 effector p40 through its chaperonin domain (Ikonomov *et al.*, 2003b), which forms a complex with TIP-47 to regulate the retrieval of ciM6PR in a retromer-independent manner from the late endosome (Diaz and Pfeffer, 1998). Intriguingly, all of these proteins, including PIKfyve have been shown to be important for HIV viral replication, as this pathway facilitates the late endosome-to-TGN transport of the virus such that HIV Env is sorted into

virions for budding at the plasma membrane (Ikonomov *et al.*, 2003b; Murray *et al.*, 2005).

In addition to its lipid kinase function, PIKfyve also demonstrates a protein kinase function. A key target of this function is autophosphorylation at serine residues, which is thought to regulate the lipid kinase activity, as it caused a 70% decrease in the lipid product and is largely abrogated by lipid substrates *in vitro*. The lipid and protein kinase activity are mediated by the same residues, including lysine 1831, which is thought to contribute to the ATP-binding pocket. PIKfyve is also proposed to transphosphorylate other proteins; the only example demonstrated thus far is p40. PIKfyve is found to be principally a phosphoprotein *in vivo* although the role of this phosphorylation has yet to be clearly established (Sbrissa *et al.*, 2000; Ikonomov *et al.*, 2003b).

1.5.7 Specific inhibitor of PIKfyve

Recent work has characterised a novel specific inhibitor of PIKfyve; compound YM201636, from a drug discovery programme directed at PI(3)-kinase (Hayakawa *et al.*, 2006). Previously, the overexpression of a kinase-inactive PIKfyve and siRNA knockdown, were the only tools available to study PIKfyve. These methods have a variety of limitations, not least of which is side effects of a gradual onset of PtdIns(3,5)P_2 depletion. An inhibitor of PIKfyve allows a more acute, immediate loss of PIKfyve kinase activity and PtdIns(3,5)P_2. This inhibitor is a pyridofuropyrimidine compound shown to specifically inhibit PIKfyve *in vitro* with a half-maximal inhibitory concentration (IC_{50}) of 33nM. Under cell culture conditions, in NIH3T3 cells

stimulated with serum, YM201636 inhibits the production of PtdIns(3,5)P_2 by 80% at a concentration of 800nM (Jefferies *et al.*, 2008). The PIKfyve inhibitor used in this study (MF4) is identical to YM201636, save for an amino group on the back-end of the molecule. The structures of MF4 and its inactive analogue MF2, which lacks an oxygen molecule on the morpholine ring, are shown in figure 1.10 and were synthesized and tested by Dr Kevan Shokat (University of California, San Francisco, USA). MF4 inhibits PIKfyve with an IC_{50} of 23nM, whereas MF2 shows no activity even at 5μM. Corresponding MF4 values for class I PtdIns 3-kinases are 0.25μM (p110α), 1μM (p110ß), 0.9μM (p110γ), 0.8μM (p110δ).

1.6 Fig4 and other phosphatases

1.6.1 Phosphoinositide 5-phosphatases

In yeast there is evidence that the turnover of PtdIns(3,5)P_2 is principally mediated by the protein Fig4. It was originally identified as a pheromone-induced gene in a screen for enhanced or reduced beta-galactosidase activity in response to α-mating factor pheromone (Erdman *et al.*, 1998). A role in PtdIns(3,5)P_2 regulation was first proposed upon the discovery that Fig4 mutations suppressed the vacuole size defects and temperature sensitivity associated with mutants of the Fab1 activator Vac7 (see section 1.7), and restored PtdIns(3,5)P_2 levels (Gary *et al.*, 2002). It is one of four genes (Sac1, Sjl2, and Sjl3) in *S. cerevisiae* whose gene products contain a sac domain, named after the protein in which it was first identified, Sac1 (Hughes *et al.*, 2000). *In vitro* the sac domains of Sac1, Sjl2, and Sjl3 dephosphorylate PtdIns(3)*P*, PtdIns(4)*P* and PtdIns(3,5)P_2 (Guo *et*

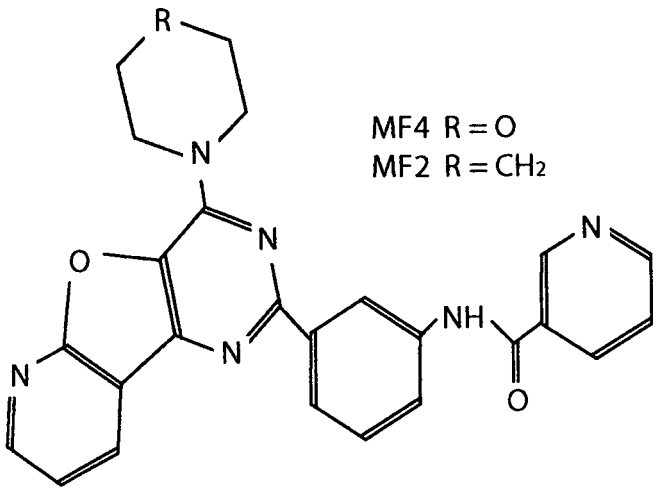

Figure 1.10. Structure of PIKfyve inhibitor.
Structure of PIKfyve inhibitor (MF4) and inactive analogue (MF2). These compounds were obtained from Kevan Shokat at UCSF following independent testing of activity and specificity *in vitro*. MF4 IC_{50} against PIKfyve is 23nM. The generation of MF4 and MF2 is outlined in materials and methods.

al., 1999). Sjl2 and Sjl3 also possess a C-terminal type II 5-phosphatase domain (Srinivasan *et al.*, 1997; Stolz *et al.*, 1998).

There are two types of mammalian 5-phosphatases that share a conserved $CX_5R(T/S)$ catalytic domain. Only the type II 5-phosphatases hydrolyse phosphoinositide phosphates (type I are protein and inositol polyphosphate 5-phosphatases) and they have an extended region N-terminal to the catalytic domain that is characterised by further regulatory domains, including the sac domain. The first mammalian sac-domain containing protein identified was Synaptojanin (McPherson *et al.*, 1996). It has since become clear that there are two types of mammalian sac-domain containing proteins, those like Synaptojanin and those more like the yeast Sac1. The sac domain is able to hydrolyse the phosphate from any position on the inositol ring, but is unable to dephosphorylate adjacent phosphates, thus it cannot hydrolyse PtdIns(4,5)P_2 to PtdIns, for example. Synaptojanin-like mammalian 5-phosphatases, as with the yeast proteins Sjl2 and Sjl3, also possess a 5-phosphatase domain that overcomes the inability of the sac domain to dephosphorylate adjacent phosphates (Hughes *et al.*, 2000).

The sac domain is composed of seven conserved motifs that define phosphoinositide phosphatase enzymatic activity (Guo *et al.*, 1999). The sixth of these motifs contains the $CX_5R(T/S)$ sequence that is thought to represent the catalytic residues, although the activity of this motif has only been examined in any great detail in the type I 5-phosphatases. The structure of the sac domain and the conserved residues in each motif are illustrated in figure 1.11.

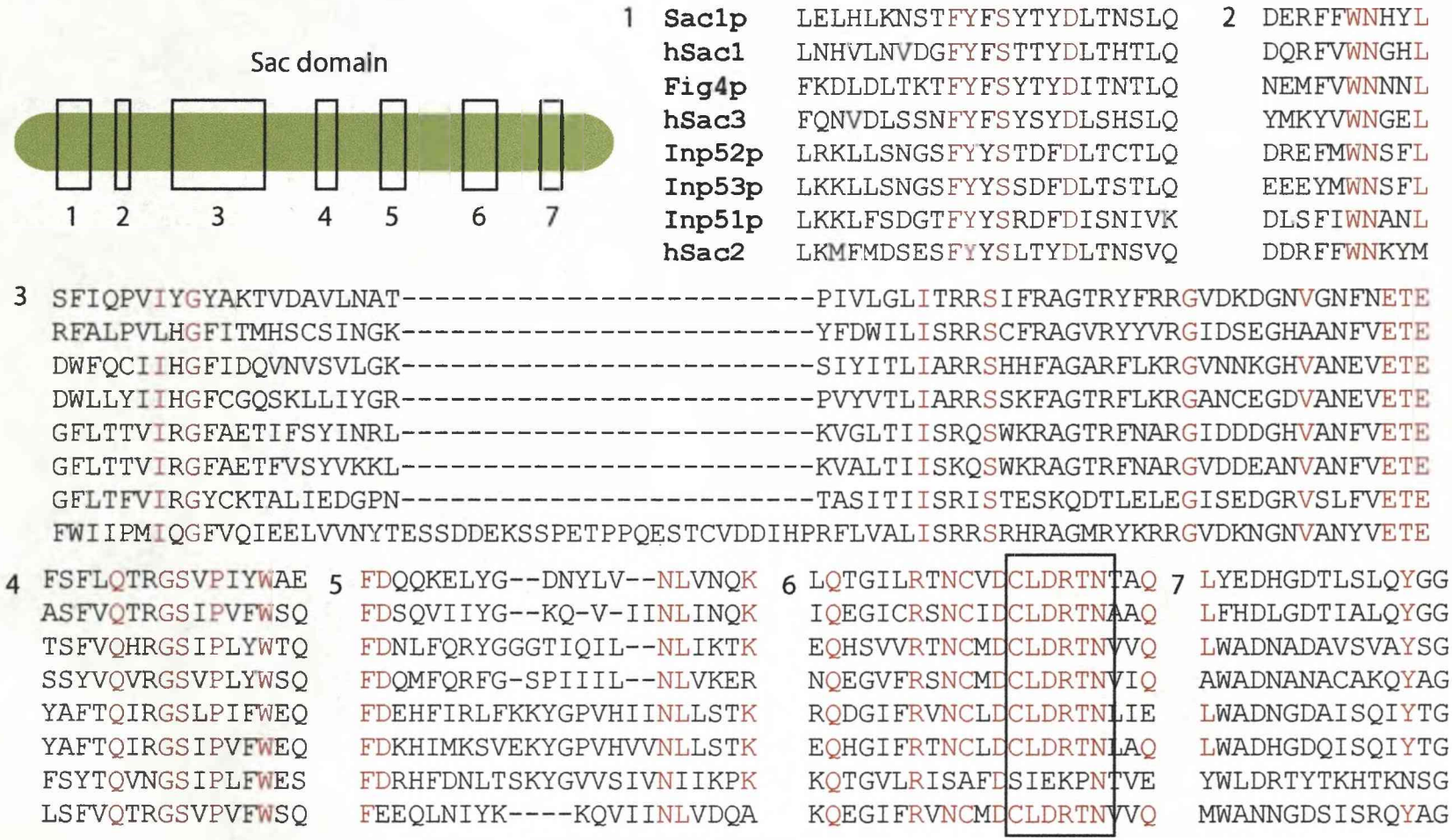

Figure 1.11. The Sac domain (adapted from Hughes *et al*, 2000).
The sac domain contains 7 highly conserved motifs. The catalytic Cx5R(T/S) motif is highlighted in motif 6. Shown are the sac domains of the yeast and mammalian SCIP's. Inp51 does not contain several of the residues that are highly conserved in the other proteins, which may account for the lack of phosphatase activity it displays.

1.6.2 Fig4/Sac3

There are three mammalian proteins with homology to the yeast Sac1, hSac1, hSac2 and hSac3. hSac3 (referred to as hFig4 in this study) has 40%/58% identity/similarity respectively to *S. cerevisiae* Fig4, and is therefore thought to represent the mammalian homologue of this protein. Neither the yeast protein nor its mammalian homologue possesses the transmembrane domain found within the other Sac1 like proteins, which could reflect the proposed recruitment of Fig4 to the membrane by its interaction with the Fab1/PIKfyve activator Vac14 (as discussed later). Database searches (ie. PFAM) suggest that hFig4/Sac3 possesses multiple phosphorylation sites for serine/threonine kinases, indicating that this protein may be regulated by phosphorylation. It also possesses several putative motifs known to interact with the endocytic machinery, such as the FxDxF motif found in Epsin, Eps15 and synaptojanin, which binds the alpha subunit of the AP-2 adaptor complex, and a clathrin box (LVIID), which binds the beta-propeller structure of clathrin heavy chain (Sbrissa *et al.*, 2007). The domain structure of Fig4 is shown in figure 1.9.

Fig4 was first confirmed to be a phosphoinositide 5-phosphatase in *S. cerevisiae* by Rudge and colleagues, who showed that it is a magnesium-activated PtdIns(3,5)P_2-specific phosphatase, which localises to the yeast vacuole membrane (Rudge *et al.*, 2004). More recently, phosphatase activity was demonstrated for the mammalian protein *in vitro*, with different phosphoinositide specificity demonstrated for different overexpression constructs. Although a preference for PtdIns(4,5)P_2 was displayed for myc-Sac3, at least a portion of this can be attributed to the activity of

phosphatases associated with myc-Sac3 coimmunoprecipitates, as a preference for PtdIns(3,5)P_2 was demonstrated with GFP-Sac3 and PtdIns(4,5)P_2 hydrolysis was not detected in intact cells (Sbrissa *et al.*, 2007). It is therefore most likely that the role of hFig4/Sac3 as a PtdIns(3,5)P_2 specific 5-phosphatase, is conserved in higher organisms.

1.6.3 Dual role of Fig4

In *S. cerevisiae* Fig4 has been shown to be the major phosphatase *in vivo* required for the rapid turnover of PtdIns(3,5)P_2 during hyperosmotic stress. Following hyperosmotic shock there is a rapid and transient increase in PtdIns(3,5)P_2 levels, which reach a maximum 20-fold increase after 5 minutes that then persists for 10 minutes. However, this subsequently returns to basal levels after 30 minutes of hyperosmotic shock, suggesting that the PtdIns(3,5)P_2 is being rapidly turned over. In Fig4 mutants this return to basal levels is delayed until 60 minutes, suggesting that turnover of PtdIns(3,5)P_2 is defective in these cells. However, the fact that turnover is delayed and not blocked completely, and that under basal conditions Fig4 mutants show no change in PtdIns(3,5)P_2 levels or in vacuole size, suggests that there may be other pathways for degrading PtdIns(3,5)P_2 (Duex *et al.*, 2006a; Duex *et al.*, 2006b). Indeed, although knockdown of other sac domain containing proteins alone does not affect the levels of PtdIns(3,5)P_2, a combined knockdown of multiple genes does cause elevated PtdIns(3,5)P_2 levels under basal conditions (Duex *et al.*, 2006a).

Fig4 has since been shown to play a more complex role in the regulation of PtdIns(3,5)P_2 levels than first thought. Intriguingly, it interacts

with Vac14, an activator of Fab1/PIKfyve kinase activity, and therefore plays a role in regulating both synthesis and turnover of PtdIns(3,5)P_2. Indeed, in *S. cerevisiae* maximal elevation of PtdIns(3,5)P_2 following hyperosmotic stress requires both Vac14 and Fig4, and Fig4 mutants synthesise only 25% of wildtype PtdIns(3,5)P_2 (Duex *et al.*, 2006b). The localisation of each protein may be dependent on the other; therefore this may simply represent an indirect effect of Vac14 mislocalisation. However, even in Fig4 mutants that do not affect Vac14 localisation there is still a defect in PtdIns(3,5)P_2 synthesis, suggesting that Fig4 plays a more direct role in both synthesis and turnover of this lipid (Duex *et al.*, 2006a).

Recent evidence suggests that Fab1 may regulate the vacuolar localisation of both Vac14 and Fig4 through its chaperonin domain, leading to the suggestion that all three proteins form part of a common lipid kinase complex that is recruited to the vacuolar membrane through the interaction of the Fab1 FYVE domain with PtdIns(3)*P* (Botelho *et al.*, 2008). This has also been suggested in mammalian cells where a direct interaction between Vac14 and PIKfyve as well as Vac14 and Fig4 has been demonstrated, with the three proteins forming a proposed ternary complex (Sbrissa *et al.*, 2007).

1.7 Vac14

1.7.1 Identification of Vac14 and Vac7 as upstream activators of Fab1

The fact that overexpression of Fab1 in *S. cerevisiae* does not result in a significant increase in PtdIns(3,5)P_2 levels (Gary *et al.*, 1998) suggests that there must be limiting regulatory factors. Indeed, various different screens in *S. cerevisiae* have subsequently identified two upstream

activators of Fab1 kinase activity. Vac7 and Vac14 were identified from yeast genetic screens, to uncover vacuole inheritance mutants distinct from the Vps mutants which also often display defects in vacuolar segregation (Gomes de Mesquita *et al.*, 1996; Wang *et al.*, 1996). Three classes of so-called vacuolar (Vac) mutants were identified. Vac14 and Vac7 were classified as class III Vac mutants, sharing an unlobed, enlarged vacuole that fills nearly the entire cytoplasm. Subsequently, they were also identified from a screening of the Eurofan II panel of yeast deletion mutants, for mutants with a swollen vacuole phenotype similar to that observed in Fab1 mutants (Dove *et al.*, 2002).

Both Vac14 and Vac7 have been shown to act as upstream activators of Fab1 kinase activity (Bonangelino *et al.*, 1997; Bonangelino *et al.*, 2002). All three mutants share similar phenotypes, overexpression of Fab1 is able to rescue both Vac14 and Vac7 mutants, and simultaneous overexpression of Fab1 and Vac14 results in 48% more PtdIns(3,5)P_2 production than Fab1 overexpression alone (Bonangelino *et al.*, 2002), consistent with the notion that the two act in concert and that Vac14 acts upstream of Fab1 as an activator of its kinase activity, rather than a negative regulator of phosphatase activity, despite the fact that it also interacts with the 5-phosphatase Fig4, as discussed in section 1.6.

1.7.2 Role in hyperosmotic stress

Vac14 and Vac7 both localise to the yeast vacuole, and in the case of Vac14 this association with the membrane is stabilised by its interaction with Fig4 (Rudge *et al.*, 2004), and more recently it has been suggested that both

Vac14 and Fig4 are recruited to the vacuole membrane through their interaction with Fab1 (Botelho *et al.*, 2008). Vac14 is required for the maximal response to hyperosmotic shock, although overexpression of Fab1 is able to restore basal levels of PtdIns(3,5)P_2 back to near normal levels in Vac14 mutant cells, it does not restore the response to hyperosmotic stress (Bonangelino *et al.*, 2002). This and the fact that Fab1 retains partial activity in the absence of Vac14 suggest that Vac14 activates Fab1 kinase activity for maximal PtdIns(3,5)P_2 production under certain stimuli. Indeed, subsequent studies showed that both Vac14 in a complex with the phosphatase Fig4, and Vac7, were all required for this response, and the subsequent turnover of PtdIns(3,5)P_2 (Duex *et al.*, 2006a; Duex *et al.*, 2006b). Although no direct interaction has been demonstrated between Vac14 and Fab1 (Dove *et al.*, 2002), a recent study has shown that Fab1 does most likely bind to both Vac14 and Fig4 through its chaperonin domain to form a common lipid kinase complex (Botelho *et al.*, 2008). *S. cerevisiae* Vac14 possesses a putative transmembrane domain and motifs that suggest involvement in membrane trafficking such as the HEAT repeats found in many membrane trafficking proteins including Vps15, which regulates its interaction with the PI(3)-kinase Vps34 (Bonangelino *et al.*, 2002). The domain structure is shown in figure 1.9.

1.7.3 Mammalian Vac14

Vac7 homologues have yet to be discovered in any other organisms, however Vac14 has homologues in the genome of every eukaryote sequenced to date. In mammalian cells Vac14 is a widespread but relatively

low abundance protein. Its role in mammalian cells mimics that in *S. cerevisiae*, it acts as an upstream activator of the kinase PIKfyve, and mammalian Vac14 and PIKfyve have been shown to coimmunoprecipitate with one another and partially colocalise on MVB/late endosome membranes. In fact, Vac14 coimmunoprecipitates can catalyse the formation of PtdIns(3,5)P_2 and PtdIns(5)P, further demonstrating that the two proteins have a strong and stable interaction in mammalian cells.

Knockdown of Vac14, in mammalian cells does not cause the vacuolation seen in PIKfyve knockdown cells; instead it renders cells prone to vacuolation following treatment with ammonium chloride. The same is true of knockdown of Fig4 in mammalian cells (Sbrissa *et al.*, 2007). Knockdown of Vac14 also leads to a marked decrease in PIKfyve kinase activity, but not in the levels of the protein itself, and also to a reduction in both PtdIns(3,5)P_2 and PtdIns(5)P levels (Sbrissa *et al.*, 2004).

1.7.4 Neurodegeneration

In a whole animal context, mutations in Fig4 and loss of Vac14 have recently been found to be a cause of neurodegeneration. A mutation in Fig4 has been found in the pale tremor mouse and human patients with the Charcot Marie Tooth disorder CMT4J. Cultured fibroblast from pale tremor mice were found to have a 3-fold reduction in PtdIns(3,5)P_2 and enlarged cytoplasmic vacuoles in approximately 40% of cells. Recent studies in Vac14 knockout mice found that homozygotes died 1-2 days after birth. Cells cultured from these mice developed cytoplasmic vacuoles, had normal

levels of PIKfyve, but reduced PtdIns(3,5)P_2 levels, indicating that Vac14 acts as an activator of PIKfyve *in vivo* (Zhang *et al.*, 2007).

Recent evidence from mammalian cells suggests that PtdIns(3,5)P_2 can also be hydrolysed by the PtdIns(3)-phosphatases known as the myotubularins, mutations in several of which also cause variations of the neurodegenerative disorder Charcot Marie Tooth disease, as with Fig4 (Wishart and Dixon, 2002; Pendaries *et al.*, 2003). There are 12 mammalian myotubularins, only some of which are catalytically active. These are proposed to hydrolyse PtdIns(3,5)P_2 at the D-3 position of its inositol ring to form PtdIns(5)P, although this remains somewhat controversial.

1.8 PtdIns(3,5)P_2 effectors

Limited knowledge of the binding domains that specifically target this lipid have lead to limited identification of PtdIns(3,5)P_2 effectors. Various groups have reportedly elucidated novel binding partners with different levels of specificity for this lipid and these are described in the following sections.

1.8.1 PROPPINs

Probably the best characterised PtdIns(3,5)P_2 effector in *S. cerevisiae* is the protein Svp1 (**s**wollen **v**acuole **p**henotype), which was identified in a screen for mutants that phenocopy the enlarged vacuole of Fab1 mutant cells (Dove *et al.*, 2004). Svp1 has also been identified as Aut10, Atg18 and Cvt18 reflecting its roles in the autophagy and cytoplasm-to-vacuole (cvt) targeting pathways (Barth *et al.*, 2001; Guan *et al.*, 2001), this is discussed in further detail in section 1.9.4.

Interestingly, Svp1 is separated from Fab1 on chromosome VII by only one open-reading frame. In a similar manner to Fab1, Fig4 and Vac14, Svp1 also localises to the yeast vacuole membrane, in a Fab1 kinase-dependent manner, but in addition it also localises to an as yet uncharacterised punctate compartment. Overexpression of Fab1 does not rescue the Svp1 mutant phenotype, however overexpression of low levels of GFP-Svp1 does, suggesting that the defect is caused by a loss of Svp1 and not an indirect loss of Fab1, and that Svp1 is downstream of PtdIns(3,5)P_2 production. The *S. cerevisiae* genome encodes two other Svp1-like proteins, HSV1 (also called Mai1 or Atg21) and HSV2, which do not cause vacuole enlargement, localise to a non-vacuolar compartment and do not require Fab1 for their localisation. GST-Svp1 has been shown through several different methods to bind to PtdIns(3,5)P_2 with high specificity (an apparent K_D of approximately 180nM), 10-fold greater than the binding of the FYVE domain of Hrs to PtdIns(3)*P*. It also weakly binds to PtdIns(3)*P* and requires Magnesium for the specificity of binding. Svp1 mutant cells produce 5-10 times more PtdIns(3,5)P_2 than normal but still have an aberrant vacuole morphology, suggesting that these cells must not be correctly responding to PtdIns(3,5)P_2 (Dove *et al.*, 2004). Svp1 has also been shown to bind Fab1 by yeast two-hybrid analysis, suggesting that it may also negatively regulate the kinase activity of Fab1 (Georgakopoulos *et al.*, 2001). Whilst the vacuole morphology phenotype of Fab1 mutant cells is reiterated by Svp1 mutant cells, they do not display the heat tolerance, vacuole acidification or MVB sorting defects of Fab1 mutants, thus Svp1 is clearly not involved in all PtdIns(3,5)P_2 cellular functions (Dove *et al.*, 2004).

Svp1-like proteins are widespread in all eukaryotes. According to Dove and Colleagues, the most Svp1-like human homologue is encoded by the DKFZp434J154 gene, which they term hSvp1a and which corresponds to WIPI-2 (Dove *et al.*, 2004). In fact, there are four human Svp1-like homologues, which have become known as the WIPI family, for **W**D-repeat containing proteins that **i**nteract with **p**hosphoinositides (Jeffries *et al.*, 2004; Proikas-Cezanne *et al.*, 2004). As illustrated in figure 1.12, the mammalian proteins are phylogenetically divided into two distinct groups: WIPI-1/WIPI-2 and WIPI-3/WIPI-4. There is some suggestion in the literature that WIPI-1 represents the yeast protein Atg18 and WIPI-2 represents Atg21. However, a reciprocal blast analysis tells us that both WIPI proteins are actually both slightly more Atg18-like than Atg21-like, which is reflected in the relative identities of the different proteins, see Table 1.1 below. This is further supported by genome exploration studies, which have shown that Atg18 is always present but that Atg21 is restricted to yeast (personal communication Daniel Ridgen, University of Liverpool). What is clear from phylogenetic analyses is that WIPI-3 and WIPI-4 group more closely with the yeast protein HSV2.

Table 1.1 Shared identity of WIPI family with yeast Svp1-like proteins

Identity/similarity	Atg18	Atg21	HSV2
WIPI-1	21.76/20.23%	14.65/17.82%	17.32/18.14%
WIPI-2	22.89/16.7%	14.72/18.15%	18.18/18.39%
WIPI-3	19.44/13.49%	16.67/13.29%	22.77/14.73%
WIPI-4	21.17/17.28%	15.87/17.06%	23.79/17.4%

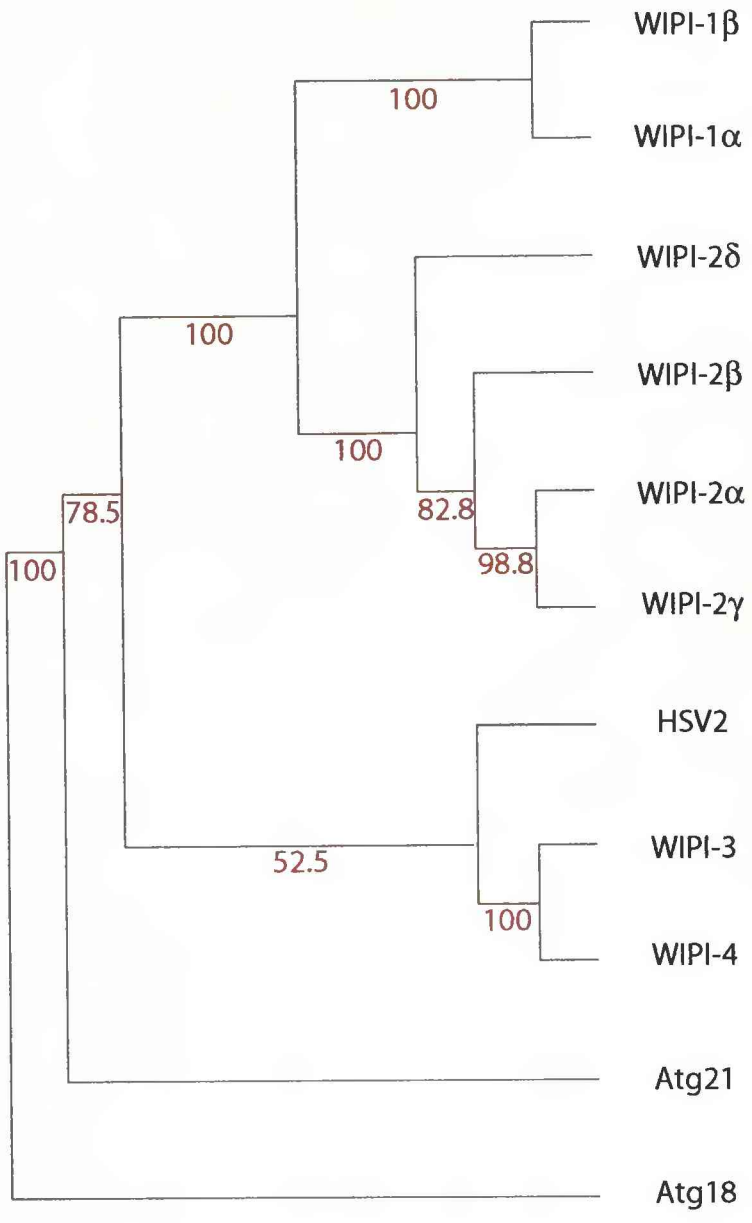

Figure 1.12. Phylogenetic analysis of the PROPPIN's
Parsimonious tree illustrating the relationships between the mammalian and yeast PROPPIN's, created by PHYLIP phylogenetic analysis software (Felsenstein, J. 1993. PHYLIP (Phylogeny Inference Package) version 3.5c. Distributed by the author. Department of Genetics, University of Washington, Seattle). The mammalian WIPI family forms two groups. WIPI-1 and WIPI-2 are more closely related to the yeast protein Atg18, whereas WIPI-3 and WIPI-4 are more closely related to the yeast protein HSV2. Numbers in red indicate bootstrap values.

The term PROPPIN has also been proposed to encompass this entire family of proteins in all organisms, for beta-**prop**eller **p**roteins that interact with **p**hospho**in**ositide (Michell *et al.*, 2006). This is in reference to the fact that the key feature of all these proteins is that they are predicted to fold into beta-propellers. Beta-propellers are a diverse group of proteins built of between 4 and 8 blades packed in a circular array. Each blade consists of a 4-stranded antiparallel beta sheet (Neer *et al.*, 1994; Yu *et al.*, 2000). The PROPPIN's are part of a superfamily of proteins within the beta-propeller fold, that are characterised by the possession of highly conserved repeating units composed of around 40 amino acids and typically ending with Try-Asp residues (hence WD repeat proteins). The domain structure of WIPI-2 is shown in figure 1.9. Their common function is to regulate the assembly of multiprotein complexes by presenting a stable attachment platform (Fong *et al.*, 1986; Garcia-Higuera *et al.*, 1996).

Svp1 possesses a widely conserved basic region between blades 5 and 6. Mutation of a pair of arginine residues within this region reduced the binding to PtdIns(3,5)P_2 40-fold, and an overexpression construct with these residues mutated does not rescue the enlarged vacuole phenotype, suggesting that Svp1 binds PtdIns(3,5)P_2 through these residues and that it requires this binding to perform its vacuole functions (Dove *et al.*, 2004). These basic residues are conserved in higher eukaryotes, suggesting that phospholipid binding is likely to be an ancestral, evolutionarily conserved property.

All of the human WIPI genes are ubiquitously expressed, with particularly high expression in skeletal and heart muscle and testis. WIPI-1

and WIPI-2 give rise to alternative splice variants, WIPI-1 α and β and WIPI-2 α, β, δ and γ. To date only WIPI-1 α and β (WIPI-49) have been examined in the literature. In this study WIPI-2 α is characterised. WIPI-1β/WIPI-49 has been shown to bind phosphoinositides with higher specificity for PtdIns(3)*P* than for PtdIns(3,5)P_2 through a liposome binding assay (Jeffries *et al.*, 2004), thus it remains unclear which lipid the mammalian proteins bind. A summary of the four key PtdIns(3,5)P_2 proteins and their proposed functions is shown in figure 1.13.

1.8.2 Other effectors

Other effectors that have been identified include the ENTH domain containing Epsins, Ent3 and Ent5. Some groups report specific binding to PtdIns(3,5)P_2 by qualitative lipid overlay assays (Friant *et al.*, 2003; Eugster *et al.*, 2004), whilst others report no specific binding to any phosphoinositides through surface plasma resonance (SPR) analysis on phosphoinositide-doped phospholipids (Michell *et al.*, 2006). The ESCRT III complex protein Vps24/CHMP3 was identified from phage-display based screen for proteins that bind PtdIns(3,5)P_2 (Whitley *et al.*, 2003). However, this protein displays no recognised phosphoinositide-binding domain, and subsequent SPR studies again demonstrated no specificity for any phosphoinositide (Michell *et al.*, 2006). The ability of these proteins to bind PtdIns(3,5)P_2 and act as effectors remains to be clarified, but they are proposed to act in MVB sorting.

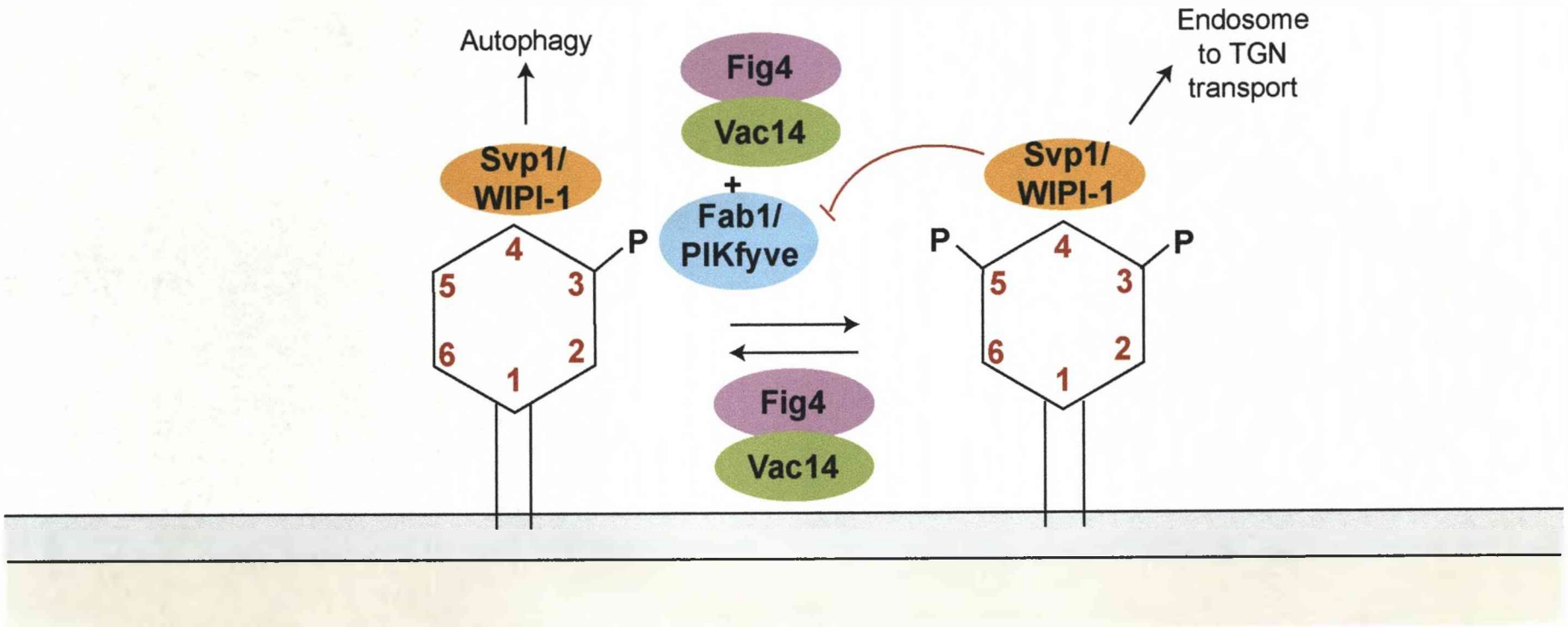

Figure 1.13. Proteins associated with PtdIns(3,5)P_2 metabolism
PtdIns(3,5)P_2 is formed from the action of the sole PtdIns(3)P 5-kinase Fab1 (PIKfyve in mammalian cells). PIKfyve activity is enhanced by its upstream activator Vac14, which interacts directly with PIKfyve. Vac14 also interacts with the propsed PtdIns(3,5)P_2 5-phosphatase, Fig4, which hydrolyses PtdIns(3,5)P_2, forming PtdIns(3)P. It is suggested that these three proteins form a common complex which tightly regulates the synthesis and turnover of PtdIns(3,5)P_2 and is recruited to endosomal membranes through the PtdIns(3)P binding FYVE domain of PIKfyve/Fab1. The downstream effector Svp1 (yeast) and one member of the mammalian family, WIPI-1, are proposed to bind both PtdIns(3,5)P_2 and to a lesser extent PtdIns(3)P, to regulate membrane retrieval pathways in autophagy and endosome to TGN trafficking pathways.

Other proteins that have been reported to bind PtdIns(3,5)P_2, but for which a function has yet to be ascribed are α-tocopherol-binding protein (ATTP) (Krugmann *et al.*, 2002), two Sec14 domain-containing proteins in plants (Kearns *et al.*, 1998), the sorting nexin SNX1 (Cozier *et al.*, 2002) and trafficking protein Ivy1p (Lazar *et al.*, 2002).

1.9 Cellular role of PtdIns(3,5)P_2

Given the diverse nature of functional outputs of PIKfyve activity it is possible that PtdIns(3,5)P_2 controls a range of cellular processes, several of these are discussed in the following sections.

1.9.1 Endomembrane homeostasis and terminal maturation of the lysosome

In PtdIns(3,5)P_2 deficient yeast cells the terminal compartment of the endocytic pathway, the vacuole, is grossly enlarged (Yamamoto *et al.*, 1995; Gary *et al.*, 1998; Odorizzi *et al.*, 1998). There is also a failure in the trafficking of certain cargoes to the vacuole (Odorizzi *et al.*, 1998). Importantly, a variety of different studies have documented remarkably similar enlargement of endosomal compartments in *Drosophila*, *C. elegans* and all mammalian cell lines tested, suggesting that PtdIns(3,5)P_2 is important in the homeostasis of endosomal membranes and that this is an evolutionarily conserved function (Sbrissa *et al.*, 1999; Nicot *et al.*, 2006; Rusten *et al.*, 2006; Rutherford *et al.*, 2006). This was shown to be dependent on PtdIns(3,5)P_2 synthesis by Shisheva and colleagues, who demonstrated that a point mutant defective in PtdIns(5)-*P*, but synthesising near normal levels of PtdIns(3,5)P_2, did not cause vacuolation (Ikonomov *et*

al., 2002a). Furthermore, it is not only loss of the kinase PIKfyve/Fab1 that elicits these effects, but other PtdIns(3,5)P_2-associated proteins as well (Chow *et al.*, 2007; Zhang *et al.*, 2007). The precise molecular mechanisms underlying the role of PtdIns(3,5)P_2 in endomembrane homeostasis have yet to be elucidated. It has previously been hypothesised that PtdIns(3,5)P_2 regulates ILV formation, fission of transport intermediates from early endosomes (Ikonomov *et al.*, 2006), or the retrieval of membrane to the TGN (Rutherford *et al.*, 2006).

Studies from a variety of different organisms show that the swollen compartment labels with late endosomal/lysosomal markers and is not acidified (Nicot *et al.*, 2006; Rutherford *et al.*, 2006). Although *S. cerevisiae* show a defect in the trafficking of certain cargoes to the vacuole, in mammalian cells and *C. elegans* there is no defect in receptor internalisation, recycling or transport to the lysosome or subsequent protein degradation (Ikonomov *et al.*, 2003a; Nicot *et al.*, 2006; Rutherford *et al.*, 2006). It was suggested that PtdIns(3,5)P_2 therefore controls the maturation of the lysosome. However, studies in *Drosophila* demonstrated a role for PtdIns(3,5)P_2 in downregulation of wingless and notch receptors (Rusten *et al.*, 2006). Thus, the literature from different organisms remains to be consolidated and the precise nature of the role of PtdIns(3,5)P_2 in endolysosomal trafficking pathways is yet to be defined.

1.9.2 Endosome to TGN trafficking

PtdIns(3,5)P_2 has been implicated in retrograde transport pathways to the TGN through a number of different lines of evidence, and a failure in

retrieval of membrane from endosomal compartments in PtdIns(3,5)P_2 deficient cells is proposed to contribute to the membrane swelling. In *S. cerevisiae* the Fab1 activator Vac7 and the PtdIns(3,5)P_2 downstream effector Svp1/Atg18 have been shown to be involved in retrograde transport of cargo from the yeast vacuole to the TGN (Bonangelino *et al.*, 1997; Dove *et al.*, 2004). Vac14 binds to the yeast orthologue of the γ–adaptin subunit of the AP-1 complex (Alp4). This complex is thought to be involved in both anterograde and retrograde TGN transport pathways, as detailed in section 1.2.7. Furthermore, AP-1 was subsequently shown to be required for the activation of Fab1 in PtdIns(3,5)P_2 dependent processes at the vacuole (Phelan *et al.*, 2006). Vac14 has also been shown to bind to the yeast protein Vps5, the yeast equivalent of the retromer component SNX-2 (Gavin *et al.*, 2006).

In mammalian cells siRNA mediated ablation of PIKfyve lead to a change in the steady state distribution of ciM6PR to more early endosomal structures, partial degradation of ciM6PR, and a delay in the retrieval of chimeric CD8-ciM6PR and sortilin constructs, suggesting that retrieval of cargo to the TGN was perturbed and increasingly diverted towards the lysosome (Rutherford *et al.*, 2006). It was proposed that PtdIns(3,5)P_2 may regulate retromer-dependent retrieval of ciM6PR, a hypothesis that is consistent with evidence that shows that PtdIns(3,5)P_2 may bind to the retromer component SNX-1 (Cozier *et al.*, 2002). In addition, overexpression of the mammalian PtdIns(3,5)P_2 binding protein WIPI-1 affects the distribution of both AP-1 and ciM6PR (Jeffries *et al.*, 2004).

However, as mentioned previously, PIKfyve has also been shown to bind to the Rab9 effector p40 and to play a role in the trafficking of cargo from the late endosome to the TGN through regulation of the membrane association of the Rab9/p40/TIP47 complex (Ikonomov *et al.*, 2003b; Sbrissa *et al.*, 2005). Given that retromer-dependent retrieval is proposed to occur at the early endosome and yet the nature of the swollen compartment appears to be late endosomal or lysosomal, it seems likely that PtdIns(3,5)P_2 may regulate membrane retrieval from both of these compartments.

1.9.3 Autophagy

Autophagy, literally self-eating, is a ubiquitous process of cellular protein degradation in eukaryotic cells. Its main function is to restore the levels of amino acids and eliminate damaged organelles in response to stress conditions, allowing the cell to adapt to environmental and/or developmental changes. It differs from apoptosis in that it forms a normal part of a cell's physiological processes, however under abnormal circumstances it can initiate autophagic cell death or type II programmed cell death (Schweichel and Merker, 1973). The amount of research in the autophagy field has seen a rapid expansion in recent years (Klionsky, 2007), and it has been implicated in a range of different cellular processes such as cancer (a number of genes required for autophagy are also tumour suppressors) (Gozuacik and Kimchi, 2004), ageing (involved in the clearance of protein aggregates that accumulate during neurodegenerative diseases such as Huntington's and Parkinson's) (Rajawat and Bossis, 2008) and the immune response (pathogens are encapsulated into autophagosomes during

infection, and autophagy has been linked to the toll-like receptor (TLR) response to infection) (Seay and Dinesh-Kumar, 2007; Xu *et al.*, 2007).

Although Christian de Duve first described autophagy more than 40 years ago, our molecular understanding of this process has only just begun. There are three types of autophagy: chaperone-mediated autophagy is a mechanism that allows the degradation of cytosolic proteins that possess a particular consensus pentapeptide motif (Majeski and Dice, 2004), microautophagy is the direct engulfment of the cytoplasm by protrusions from the surface of the degradative organelle (Kunz *et al.*, 2004), and macroautophagy (Klionsky, 2005; Yorimitsu and Klionsky, 2005) (henceforth referred to as autophagy).

Autophagy begins with the formation of a phagophore or limiting membrane, the source of which is unknown, and continues with the extension of the phagophore to surround a portion of the cytosol. The ends of the phagophore fuse, forming a double membrane bound organelle called the autophagosome. This fuses with endocytic organelles to form either an amphisome (through fusion with early endosomes) or an autolysosome (through fusion directly with the lysosome). The contents are subsequently degraded and the resulting amino acids are exported into the cytosol and recycled (Arstila and Trump, 1968; Gordon and Seglen, 1988; Stromhaug and Seglen, 1993).

1.9.3.1 Induction of autophagy

Autophagy is conducted by a complex array of so-called Atg (autophagy related) genes that function at different stages of this process.

To date 30 Atg genes have been identified in yeast involved in various forms of autophagy. The autophagic machinery in other model eukaryotic organisms such as *Dictyostellium discoideum*, *Arabiodopsis thaliana*, *D. melanogaster* and *C. elegans* overlap considerably with that in yeast, but non display the complete convergence of yeast and mammals (Klionsky, 2007).

Autophagy occurs at a basal rate in normal growing cells, but is dramatically induced in response to certain types of environmental stress, such as nutrient starvation and inhibition of the target of rapamycin (TOR) protein (Schworer and Mortimore, 1979; Mortimore and Poso, 1987). Under nutrient rich conditions autophagy is inhibited by the serine/threonine protein kinase TOR, which either directly or indirectly phosphorylates Atg13. Atg13 forms part of the autophagy-inducing complex, also composed of Atg17 and the serine/threonine kinase Atg1. Following nutrient deprivation or following treatment with rapamycin (an inhibitor of TOR), Atg13 is rapidly and partially dephosphorylated and has an increased affinity for binding to Atg1. These changes correlate with an increase in autophagic activity (Kamada *et al.*, 2000).

Autophagy is also activated by nutrient deprivation in mammalian cells, which may act through repression of the mammalian TOR protein (mTOR) or other as yet undefined mechanisms, thus far the only component of the autophagy-inducing complex to have been identified in mammalian cells is the Atg1 orthologue ULK-1 (Chan *et al.*, 2007). In mammalian cells, the negative regulatory cascade upstream of mTOR includes a class I PI(3)-kinase, PDK1, and Akt/PKB (O'Reilly *et al.*, 2006). Concordantly, the phosphatase PTEN acts antagonistically to the PI(3)-kinase to induce

autophagy (Arico *et al.*, 2001; Ueno *et al.*, 2008). Autophagy can also be induced by deprivation of insulin and other growth factors which signal through the PI(3)-kinase/AKT pathway (Wagner, 2005). Figure 1.14 outlines the stages of autophagy and the Atg genes required in yeast and mammalian cells.

1.9.3.2 Role of PtdIns(3)P in autophagy

Following induction of autophagy, the initial stages of vesicle nucleation occur. This has been shown to be dependent, both in yeast and mammals, on the activation of the class III PI(3)-kinase Vps34 and generation of PtdIns(3)*P*. This activation depends on the formation of a multiprotein complex that includes, in yeast, Atg6/Beclin 1, Vps15, and Atg14, and in mammals, Atg6/Beclin 1, Vps15, UVRAG, Bif-1 (also known as endophillin B1) and Ambra 1 (Kametaka *et al.*, 1998; Kihara *et al.*, 2001). In mammals, Beclin 1 interacts with Bcl-2 or its close homologue Bcl-X_L, and the activation of the complex requires the dissociation of these two proteins (Liang *et al.*, 1998).

1.9.3.3 Vesicle elongation

The process of elongation and completion of the autophagosome are conducted by two evolutionarily conserved ubiquitin-like conjugation systems in both yeast and mammals (Ohsumi and Mizushima, 2004). Ubiquitin is conjugated to target proteins via the action of a cascade of enzymes known as E1 activating enzymes, E2 conjugating enzymes and E3 ligases (Hershko and Ciechanover, 1992; Jentsch, 1992; Varshavsky, 1992). The first system

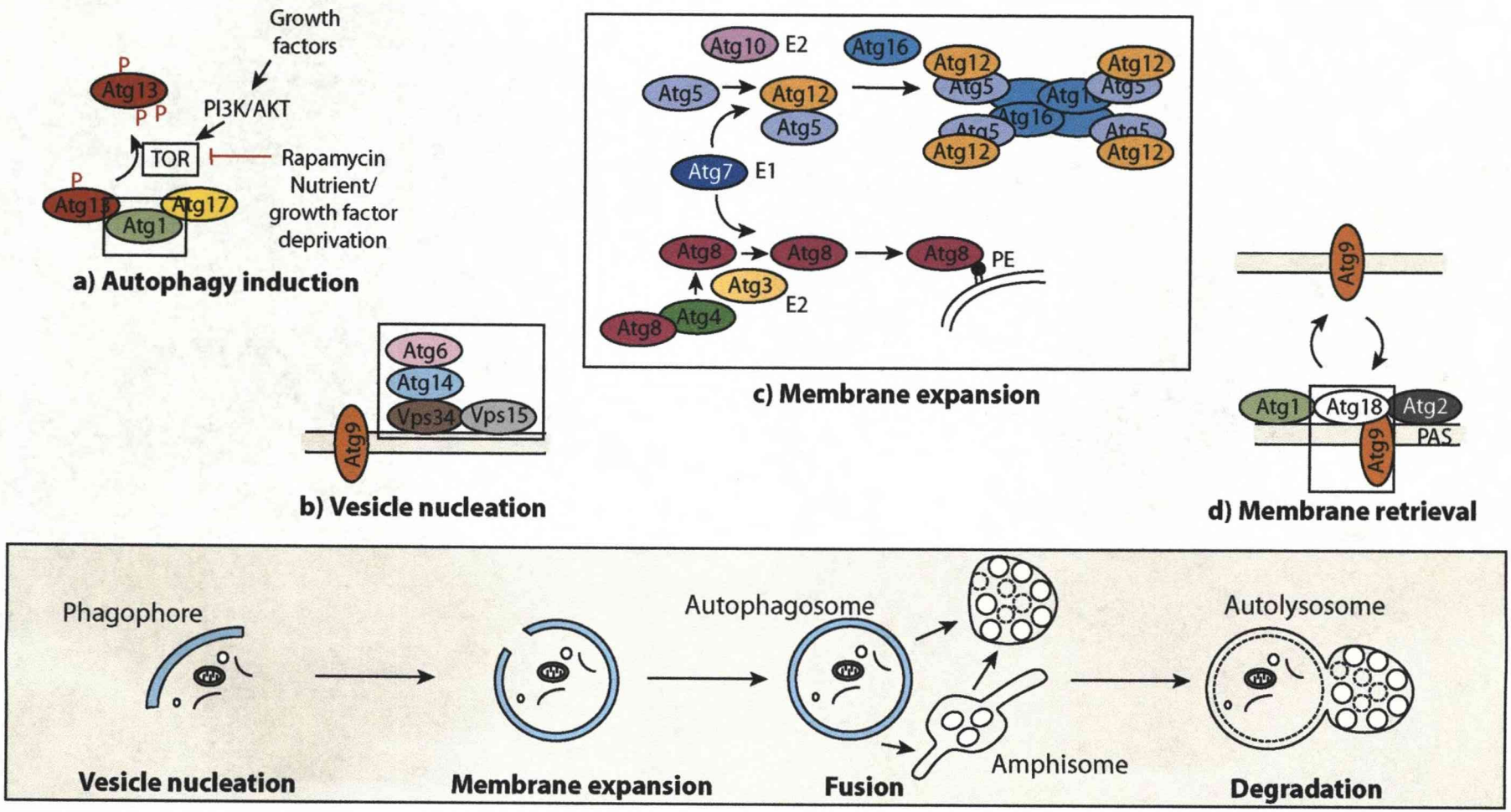

Figure 1.14. The molecular machinery of autophagy.
The stages in the autophagic pathway and the molecular machinery involved in each step in *Sacchoromyces cerevisiae*. See main text for further description of the proteins involved. Proteins with conserved function in mammalian cells are highlighted with a black box.

in autophagy involves the conjugation of Atg12 to Atg5, via an E1-like enzyme Atg7 and an E2-like enzyme Atg10. The resulting conjugate is organised into a complex by associating with Atg16, to form the Atg16-Atg5-Atg12 complex.

The second pathway involves the conjugation of the lipid phosphatidlyethanolamine (PE) to a glycine residue of Atg8 (Ohsumi and Mizushima, 2004). The mammalian homologue of Atg8 is LC3, originally identified as microtubule associated protein 1 light chain 3 (Kabeya *et al.*, 2000). This conjugation occurs by the sequential action of the protease Atg4, the E1-like enzyme Atg7, and the E2-like enzyme Atg3. It leads to the conversion of Atg8/LC3 from a soluble, cytoplasmic form to a membrane-associated form; the membranes that it associates with are predominantly those of the forming autophagosome. Yeast Atg8 mediates tethering and fusion of liposomes containing Atg8-PE *in vitro*, leading to the suggestion that this recruitment of Atg8/LC3 to the autophagosome membrane is responsible for the phagophore membrane expansion (Kabeya *et al.*, 2000; Xie *et al.*, 2008).

1.9.3.4 Proposed role of PtdIns(3,5)P_2 in autophagy

In yeast the integral membrane protein Atg9 is localised to the PAS (pre-autophagosomal structure; the proposed site of initiation of autophagosome formation) and an as yet uncharacterised punctate localisation, but is excluded from the completed autophagosome (Noda *et al.*, 2000; Suzuki *et al.*, 2001; Kim *et al.*, 2002). Given that Atg9 is a transmembrane protein, it must be retrieved from the PAS by vesicular

transport, prior to autophagosome completion. It has subsequently been shown that Atg2, Atg18 and the PI(3)-kinase complex are all required for the retrieval of Atg9 (under these mutant backgrounds Atg9 localises solely to the PAS) and Atg9 has been shown to bind Atg18 in a manner dependent on Atg1 and Atg2 (Reggiori *et al.*, 2004). Precisely how the Atg1-Atg13 complex mediates Atg9 retrieval is still unclear. The current hypothesis is that the Atg1-Atg13 complex (involved in the initiation of autophagy) induces a simultaneous interaction between Atg18, Atg9 and Atg2 at the PAS. The formation of this complex mediates the retrieval of Atg9 from the PAS once its function is completed. An *S. cerevisiae* Atg18 mutant displayed an accumulation of autophagosomes, and was suggested to possess a defect in the fusion of autophagosomal structures with the yeast vacuole (Barth *et al.*, 2001).

Atg18 is also known as Svp1 and has been shown to bind both PtdIns(3)*P* and PtdIns(3,5)P_2 (see section 1.8). The nature of the proposed role of Atg18 as part of an Atg9 retrieval complex is somewhat reminiscent of its role in retrieval from the yeast vacuole to the TGN under vegetative conditions, suggesting that PtdIns(3,5)P_2 may have a dual role in this process under different cellular conditions. However, some data has shown that the role of Atg18/Svp1 in autophagy is independent of its capacity to bind PtdIns(3,5)P_2 (Dove *et al.*, 2004).

A second member of the Svp-1 like protein family in yeast, Atg21/HSV2, plays a role in the Cvt pathway, in the recruitment of Atg8 to the PAS (pre-autophagosomal structure) or expanding phagophore under vegetative conditions (Meiling-Wesse *et al.*, 2004). Although a mammalian

Svp1 homologue WIPI-1 has been shown to be involved in autophagy, it's relationship with Atg9 and the importance of its lipid-binding capabilities in autophagy have yet to be determined.

The role of the kinase Fab1/PIKfyve in autophagy has also been recently assessed. In Fab1 mutant *Drosophila*, there was an accumulation of amphisomes (Rusten *et al.*, 2007), in *C. elegans pkk-3* mutants an accumulation of LC3 was observed (Nicot *et al.*, 2006), and in mammalian cells treated with a specific inhibitor of PIKfyve (YM201636) there was a decrease in protein degradation (Jefferies *et al.*, 2008), following starvation induced autophagy. These data suggest that Fab1/PIKfyve and possibly the effector protein Atg18 play a role in the later stages of the autophagy pathway. However, the precise role of PtdIns(3,5)P_2 in autophagy, and how this relates to Atg18 as an effector protein, remains to be clarified.

1.10 Current work

A number of key questions remain to be resolved in respect to PtdIns(3,5)P_2 metabolism in mammalian cells, that may provide further insight into the role of this lipid in endocytic membrane trafficking pathways. The aim of the current work was to examine four mammalian proteins associated with PtdIns(3,5)P_2 metabolism: PIKfyve, Vac14, Fig4 and WIPI-2, and to:

1) produce and characterise various tools to permit further study of these proteins

2) analyse their cellular localisation

3) produce purified protein

4) examine the interactions between these proteins (in particular, focusing on the Vac14-Fig4 interaction)

5) assess the knockdown phenotypes of each protein in mammalian cells to assess the roles of each protein in common endocytic trafficking pathways, and in starvation-induced autophagy

6) directly compare the phenotypes associated with both PIKfyve siRNA treatment and pharmacological inhibition

CHAPTER TWO

Materials and Methods

2.1 Molecular biology

2.1.1 Reagents

Mouse full-length PIKfyve and human full-length Fig4 cDNA were obtained from the Kazuso Institute, Japan (clone names mib04069 and ha06690). Mouse full-length Vac14 was obtained from the Mammalian Gene Collection I.M.A.G.E Consortium (clone # IRAKp961N24109Q). Human full-length WIPI-2 was obtained from the RZPD German Resource Centre for Genome Research (clone # DKFZp434J154Q). XL1-Blue supercompetent cells (#200236), *Pfu*Ultra™ and *Pfu*Turbo™ DNA Polymerase were all obtained from Stratagene (La Jolla, CA, USA). DH5α subcloning efficiency chemically competent cells (#18265-017), One Shot BL21 (DE3)pLysE competent cells (#C6060-03), electrophoresis grade agarose and all custom made primers for PCR were obtained from Invitrogen (Paisley, UK). Luria-Bertani broth (#LAB191) was obtained from Lab M (Bury, UK). TAE (#EC-872) was obtained from National Diagnostics (Hull, UK). Quick-load 1kb DNA ladder (#N0468S), T4 DNA polymerase (#M0252S), T4 DNA ligase (#M0205S), Calf Intestinal Alkaline Phosphatase (#M0209S) and all restriction endonucleases were obtained from New England Biolabs (Hertfordshire, UK). Mini-prep (#27106), HiSpeed Maxi-prep (#12633), gel extraction (#28604) and PCR purification (#28704) kits were all obtained from QIAgen (Crawley, UK). A complete list of plasmids used is outlined in

Table 2.4. All other chemicals were from Sigma Aldrich (Poole, UK) unless otherwise stated.

2.1.2 Preparation of competent E. Coli for transformation

Luria-Bertani (LB) broth and agar were made up with distilled water and used for all culture of *E. coli*. 100ml LB broth was inoculated with 5ml of log-phase *E. coli* and incubated at 37°C with shaking at 250rpm in a Lab-Therm shaker (Kühner, Switzerland). Once cells had reached an optical density $(OD)_{550}$ of 0.48 they were chilled on ice for 15 minutes. Cells were pelleted (5min, 2500rpm, 4°C) and pellets resuspended in 30ml ice-cold TfBI buffer (100mM $RbCl_2$, 50mM $MnCl_2$, 30mM KOAc, 10mM $CaCl_2$, 15% (v/v) glycerol, pH adjusted to 5.8 with HOAc, sterile filtered). Cells were then chilled on ice for 20-30 minutes, pelleted again, and resuspended in 4ml ice-cold TfBII buffer (10mM MOPS pH 7.0, 10mM $RbCl_2$, 75mM $CaCl_2$ and 15% (v/v) glycerol, sterile filtered). Cells were dispensed in 50µl aliquots on dry ice and stored at -80°C. Competent *E. coli* DH5α were prepared for DNA production and commercially purchased DH5α and XL1-Blue supercompetent cells were also used for this purpose.

Larger DNA constructs, which proved more difficult to transform into bacteria, were often transformed using electrocompetent *E. coli*. In this case 500ml LB broth was innoculated with a 2.5ml suspension of log-phase *E. coli* and incubated at 37°C with shaking at 300rpm to an OD_{600} of 0.5-0.6. Cells were chilled on ice for 15 minutes, pelleted (3000rpm, 10 minutes, 4°C) and resuspended in 50ml ice-cold 10% glycerol. Cells then underwent a series of pelleting and resuspension steps in 25ml ice-cold 10% glycerol, followed by

4ml ice-cold 10% glycerol, followed by 1.5ml ice-cold 10% glycerol, and then dispensed in 50µl aliquots on dry ice and stored at -80°C.

2.1.3 Transformation of competent E. coli

Typically 50µl DH5α or XL1-Blue *E. coli* were thawed on ice. Approximately 50ng (plasmid DNA) or 5µl (ligation) was added to the thawed cells and incubated for 30 minutes on ice. Cells were heat-shocked (42°C for 45 seconds for XL1Blue or 37°C for 20 seconds for DH5α) in a water bath and then immediately returned to ice for 2 minutes. 250µl LB was added to the cells and they were incubated at 37°C for 1 hour with shaking at 250-300rpm. 200µl of this culture was plated onto pre-warmed LB agar plates supplemented with 100µg/ml Ampicillin or 25µg/ml Kanamycin or other appropriate antibiotics, determined by the resistance of the plasmid. For larger plasmids, a lower ampicilin concentration was used to encourage growth.

For electrocompetent transformation of larger plasmids, 40µl electrocompetent *E. coli* were thawed on ice, and 1-2µl DNA was added. Cells were incubated on ice for 10 minutes and, subsequently the mixture was transferred to an electroporation cuvette. The sides of the cuvette were dried, the cuvette was placed in between the contacts of a micropulser (Bio-Rad), set to Ec2, and pulsed. The cuvette was placed immediately back on ice and 250µl LB added. The cell culture was then incubated for 1 hour at 37°C with shaking at 235rpm and then 50µl of this culture was plated onto an LB agar plate supplemented with the appropriate antibiotic.

For subsequent purification of DNA from transformants, a single colony was picked and incubated overnight in LB broth (5ml for mini-preps and protein purification cultures, 150ml for maxi-preps) supplemented with appropriate antibiotic. Bacteria were then pelleted by centrifugation (4500rpm, 15 minutes, 4°C), the supernatant removed and DNA purified using mini or maxi-prep kits according to the manufacturer's protocol. The concentration of maxi-prep DNA was estimated by measurement of the OD_{260} of the DNA and also by agarose gel electrophoresis and comparison to a 1kb DNA ladder. The purity of DNA for transfection purposes was also assessed by measurement of the ratio of OD_{260} to the OD_{280} of the DNA.

2.1.4 Agarose gel electrophoresis

An agarose gel (between 0.8 and 1.2%) was prepared by adding electrophoresis grade agarose to TAE buffer. The mixture was heated in a microwave until the agarose had completely dissolved and then cooled at room temperature. Ethidium bromide was then added to a final concentration of 0.5µg/ml, the gel was poured and then left at room temperature to set. DNA samples were made up in sample buffer (5% w/v glycerol, 0.1mM EDTA, 0.04% bromophenol blue) and resolved in TAE in a Fisherbrand horizontal midi electrophoresis tank (Fisher Scientific, Loughborough, UK) along with 10µl (per lane) of 1kb Quickload DNA ladder, at 100V. DNA bands were then visualised using an ultraviolet light source.

2.1.5 Restriction endonuclease analysis

Restriction digests were set up using enzymes and buffers from New England Biolabs and using reaction conditions specified by the manufacturer. Typically digests were performed for 1 hour, using 1µg DNA in a total volume of 10µl. For subcloning, approximately 4-6µg of DNA were digested in a total volume of 50µl for at least 4 hours (see Table 2.1). For each digest an excess of enzyme was added with the volume not exceeding 10% of the total mixture.

Products were analysed by agarose gel electrophoresis. For sub-cloning, gel fragments were excised using a sterile knife and DNA purified using a gel extraction kit. To ensure optimal activity of enzymes and production of DNA, double digests were sometimes carried out sequentially. After the first digest, 10% of the incubation mixture was run on an agarose gel to determine its success, whilst the remainder was run through a PCR purification column prior to the second digest.

Table 2.1. Reaction mixture for a typical restriction digest

Reagent	Volume
Nuclease-free water	Variable
10x restriction enzyme buffer	1µl
DNA sample	1µg
Restriction enzyme	1µl
Final volume	10µl

Reagent	Volume
Nuclease-free water	Variable
10x restriction enzyme buffer	5µl
DNA sample	4-6µg
Restriction enzyme	2-3µl
Final volume	50µl

2.1.6 Polymerase chain reaction (PCR)

Each of the plasmids made as part of this study underwent a PCR amplification using primers designed to add restriction sites, to enable sub-cloning into a range of different vectors. DNA was PCR amplified using *PfuUltra*™ or *Turbo*™ enzymes. PCR reactions were set up at 4ºC. A typical PCR reaction mixture is shown in table 2.2. The first step in the reaction consisted of a single cycle of 2 minutes at 95ºC. This was followed by thermal cycling which typically consisted of a denaturation period of 30 seconds at 95°C, followed by 30 seconds at the annealing temperature (dependent on primer size and base content; typically the highest Tm of both primers - 5°C) and an extension time of 1-2 minutes per kilobase (kb) of the target DNA sequence. 25 cycles were performed, culminating in a polishing stage of 10 minutes at 72°C. PCR products were analysed by gel electrophoresis and the correct size gel fragment excised and run through a QIAquick PCR purification column. A 'no template' control was always run alongside each PCR reaction. PCR conditions were occasionally altered to increase PCR product yield, for example, the number of cycles was increased to 30 or the extension time was increased to 2kb/minute.

Table 2.2. Reaction mixture for a typical PCR amplification

Reagent	Volume
Nuclease free water	Variable
10x Pfu buffer	5µl
dNTPs (25mM each)	0.5µl
Primer 1 (100ng/µl)	2.5µl
Primer 2 (100ng/µl)	2.5µl
Template DNA	50ng
Pfu Turbo	1µl
Total	50µl

Table 2.3 Primers used for PCR and site-directed mutagenesis

Name	Use	Sequence (5' to 3')
JW-WIPI-2 F	PCR	aaggatccccatgaacctggcgagcc
JW-WIPI-2 R	PCR	ccgtcgactcagtcagcagtcgaagaatc
JW-Fig4 F	PCR	aatgatcatgcccacggccgccgccccca
JW-Fig4 R	PCR	ggctcgagtcacaggtagcggttcctgatg
JW-Fig4-F2*	PCR	aattggatccaaatgcccacggccgccg
JW-Fig4 R2*	PCR	gcctcgagcccgaggaacctttctgtc
JW-Fig4sf	Seq	tcatgggttctgtgggcagt
JW-Fig4sr	Seq	ctctggtgtccaccagtaag
JW-Vac14 F	PCR	ccagatctccatgaacccagagaaggattttg
JW-Vac14 R	PCR	aactcgagtcagaggataactctgcggtc
JW-Vac14sf	Seq	cagctggcgggccgggtaat
JW-Vac14sr	Seq	agctggaagagctcggtgga
WIPI-2 KDRES F	PCR	ctcacgacagcccttggcagcgctggcctttg
WIPI-2 KDRES R	PCR	caaaggccagcgctgccaaggggctgtcgtgag
WIPI-2 RR mutant F	SDM	ctctttgaattcacgacaggagtaaagagg
WIPI-2 RR mutant R	SDM	cctctttactcctgtcgtgaattcaaagag

Note: Initial pCRTOPO-Fig4 construct 5' end incorrect when sequenced. F2 and R2 (*) primers designed to address this. SDM – site directed mutagenesis, seq – sequencing.

For sub-cloning, PCR products were purified using a PCR purification kit and ligated into pCR4Blunt-TOPO according to the manufacturer's protocol, as outlined in table 2.4.

Table 2.4. pCR4Blunt-TOPO cloning reaction

Reagant	Volume
Fresh PCR product	1µl
Salt solution	1µl
Sterile Water	Add to a final volume of 5µl
TOPO® vector	1µl
Final volume	6µl

2µl of this cloning reaction was then used to transform chemically competent MACH1™-T1® *E. coli* cells and grown overnight on LB agar plates supplemented with 100µg/ml ampicillin. DNA was purified from transformants by mini and maxi-prep and DNA was subsequently analysed by restriction endonuclease digest and agarose gel electrophoresis, to check for full-length and correctly orientated insert. Correct pCR4Blunt-TOPO constructs were sent for automated fluorescent DNA sequencing at the DNA Sequencing Service (University of Dundee) using the internal M13F and M13R priming sites within the pCR4Blunt-TOPO vector and specifically designed insert specific primers if needed.

2.1.7 Ligations and sub-cloning

DNA was sub-cloned into a variety of different expression vectors:

Table 2.5. Plasmids generated for this project

Plasmid name	Origin	Use
pSPORT1-hSvp1a	RZPD	Subcloning
pCRTOPO-WIPI-2	JW	Subcloning
pEGFPC2-WIPI2	JW	Overexpressed protein IF, WB
pCMVmyc-WIPI2	JW	Overexpressed protein IF, WB
pTrcHisC-WIPI2	JW	Bacterial protein production (His tag)
pAcHis-WIPI2	JW	Baculovirus protein production
pACT2-WIPI2	JW	Y2H (prey)
pFBT9-WIPI2	JW	Y2H (bait)
pCRTOPO-WIPI-2 KDRES	JW	Subcloning (RNAi resistant clone)
pCMVmyc-WIPI-2 KDRES	JW	Overexpressed protein RNAi resistant. Rescue experiments
pSPORT6.1-mVac14	I.M.A.G.E consortium	Subcloning
pCRTOPO-mVac14	JW	Subcloning
pTrcHisC-mVac14	JW	Bacterial protein production
pAcG2T-mVac14	JW	Baculovirus protein production
pCMVHA-mVac14	JW	Overexpressed protein WB, IF, IP
pEGFPC2-mVac14	JW	Overexpressed protein WB, IF, IP
pACT2-mVac14	JW	Y2H (prey)
pFBT9-mVac14	JW	Y2H (bait)
pSPORT1-hFig4	KI	Subcloning
pCRTOPO-hFig4	JW	Subcloning
pAcHis-hFig4	JW	Baculovirus protein production
pEGFPC2-hFig4	JW	Overexpressed protein WB, IF, IP
pCMVmyc-hFig4	JW	Overexpressed protein WB, IF, IP
pACT2/pFBT9-hFig4	JW	Y2H bait and prey

Note: hSvp1a = WIPI2. Abbreviations: KI – Kazuso Institute, Japan; RZPD - German Resource Center for Genome Research, I.M.A.G.E – The I.M.A.G.E Consortium; FC – Frank Cooke, UCL; HS – Harald Stenmark, Oslo, HP – Hannah Polson, CRUK; IF-immunofluorescence; WB – Western blotting.

Vector and insert were prepared by restriction digest agarose gel electrophoresis. The correct sized bands were extracted from the agarose using a gel extraction kit. Vector and insert were then combined in a ligation reaction (see Table 2.6 below). Typically 50-100ng of vector DNA was used and an equimolar ratio of insert DNA calculated using the following formula:

$$\text{Insert DNA (ng)} = \frac{\text{Vector DNA (ng) x size insert (kb)}}{\text{size vector (kb)}}$$

A vector to insert ratio of 1:1, 1:3 or 1:5 was used depending on the type of ligation (blunt or sticky end) and the possibility of multiple inserts being ligated into vector DNA. The mixture was incubated either at room temperature for 3 hours or overnight at 4°C. Between 2 and 5µl ligation reaction was used to transform chemically or electrocompetent *E. coli* and then plated on selective agar plates. DNA was purified from transformants using miniprep kits. Mini-prep DNA was verified using restriction endonuclease digest and agarose gel electrophoresis. Once the correct ligated product was obtained a DNA maxi-prep and glycerol stock of each construct were also made and stored appropriately.

Table 2.6. Subcloning ligation reaction using T4 DNA ligase

	1:1	1:3	Insert alone	Vector alone
Vector	Calculated volume	Calculated volume	-	Calculated volume
Insert	Calculated volume	Calculated volume x 3	Calculated volume	-
10 x T4	1µl	1µl	1µl	1µl
T4 Ligase	1µl	1µl	1µl	1µl
Sterile water	Make up to final volume	Make up to final volume	Make up to final volume	Make up to final volume
Total	10µl	10µl	10µl	10µl

It was occasionally necessary to design a cloning strategy incorporating blunt ended ligation if, for example, vector and insert were in different frames. For blunt end ligations 3' overhangs were removed or 5' overhangs filled in using a T4 DNA polymerase enzyme (see table 2.7 below).

Table 2.7. T4 polymerase reaction

Reagent	Volume
DNA	Variable
T4 buffer	5µl
dNTPs	4µl of 5mM mix (100mM each final)
T4 polymerase	3µl (1-3U/µg)
Water	Variable

Abbreviations: dNTPs (deoxynucleotide triphosphates – four derivatives: adenosine, guanine, cytosine and thymine)

The mixture was incubated at 12°C for 15 minutes and then the enzyme was heat inactivated for 10 minutes at 75°C in the presence of EDTA to a final volume of 10mM.

In many cases vectors were dephosphorylated using Calf Intestinal Alkaline Phosphatase to prevent vector self-ligation and reduce background; this was done by adding 0.5µl CIP to the 50µl digest volume and incubating the mixture at 37°C for 20 minutes.

pCR4Blunt-TOPO and pTrcHisC vectors were obtained from Invitrogen (Paisley, UK). pEGFPC2, pCMV-HA and pCMV-myc were from Clontech (Saint-Germain-en-Laye, France). pAcG2T was from BDBiosciences (Oxford, UK) and pCMVFlag2c from Stratagene (La Jolla, USA). pACT2, pFBT9 (derived from pGBT9) and pAcHis (derived from pAcSG2) were from Francis Barr (University of Liverpool, UK).

2.1.8 Site-directed mutagenesis

In order to generate RNAi resistant WIPI-2 constructs, specific amino acids were mutated using an overlapping PCR method (see Figure 2.1), using pCRTOPO-WIPI-2 as a template. The final product was transformed into pCR4BluntTOPO and sequenced as described previously to ensure the correct amino acid changes.

2.1.9 RNA extraction, reverse transcription and quantitative PCR

Due to the unavailability of a Fig4 antibody, it was necessary to assess the knockdown of Fig4 by RT-PCR. HeLa cells were seeded onto 6-well plates and transfected twice with 40nM Fig4 siRNA oligos over a 72 hour

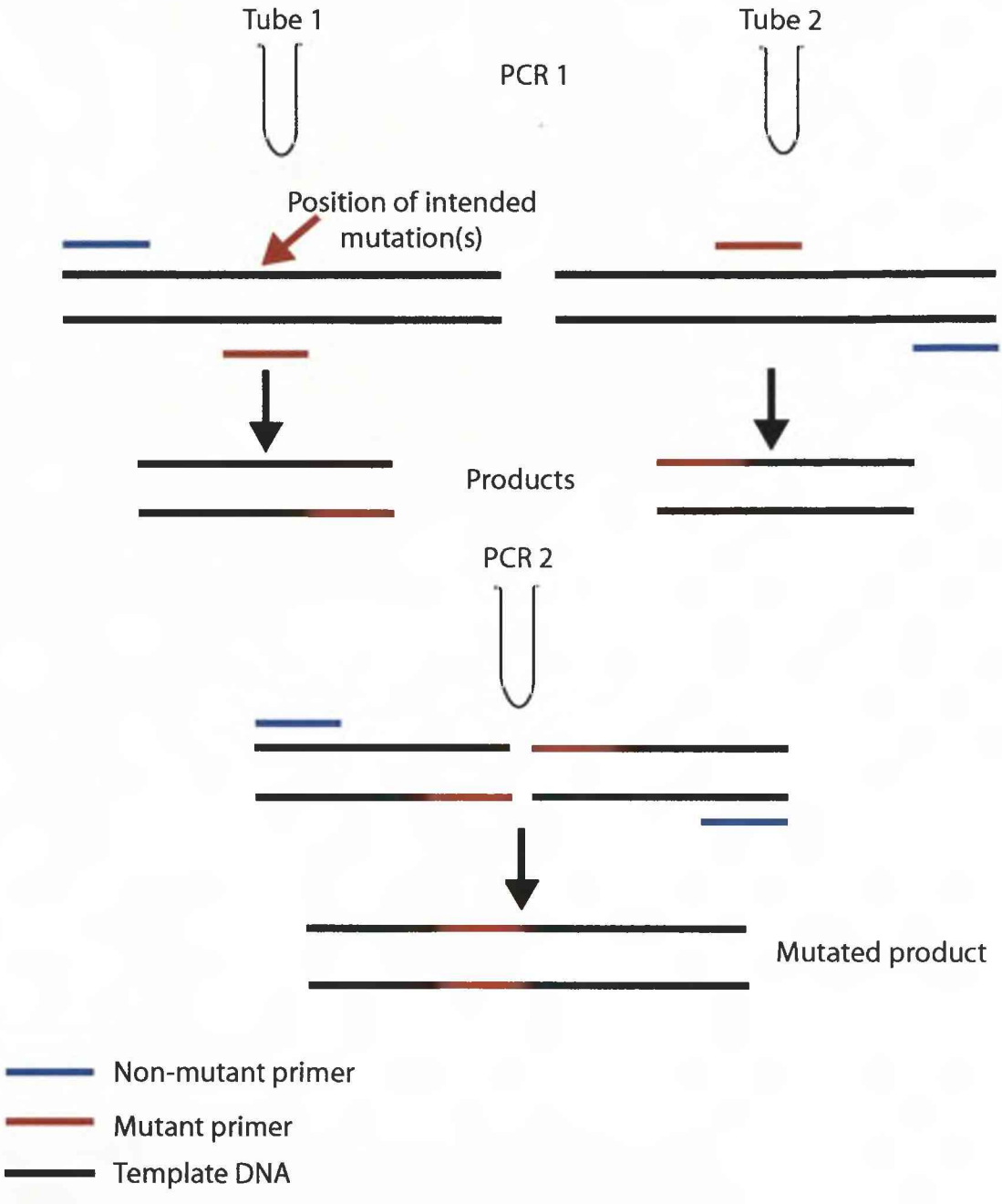

Figure 2.1. Overlapping PCR to create siRNA resistant WIPI-2. pCRTOPO-WIPI-2 template was incubated in two separate PCR reactions with complimentary forward and reverse primers containing the necessary mutations , and a forward or reverse primer complimentary to the beginning or end of the template sequence. The products from the first PCR reaction were then incubated in a second PCR reaction with the same non-mutant primers complimentary to the beginning and end of the sequence. In this reaction a full-length product is created that incorporates mutated forward and reverse strands.

period, as described in section 2.3.7. Cells were subsequently trypsinised from the dish and centrifuged in an eppendorf tube. RNA was extracted from the resultant cell pellet using the RNAeasy® mini kit (Qiagen) and the QIAshredder for homogenisation, according to the manufacturer's instructions. RNA was quantified in a spectrophotometer at Abs_{260} and the purity of RNA assessed by measuring the ratio of absorbance at 260 and 280. 1µg of RNA was reverse transcribed into cDNA using the QuantiTect Reverse Transcription kit (Qiagen) according to the manufacturer's instructions. Genomic DNA contamination was minimised by first treating with the gDNA wipeout buffer provided with the kit. cDNA was quantified by qPCR using the DyNAmo™ HS SYBR® Green qPCR kit (Finnzymes, Finland) according to the manufacturer's instructions. Both a no template control and an actin housekeeping gene control were used. A typical qPCR reaction is shown below in table 2.8.

Table 2.8. Typical qPCR reaction

	Template	NTC
Mastermix*	7.5µl	7.5µl
F primer (1µg/µl)	0.3µl	0.3µl
R primer (1µg/µl)	0.3µl	0.3µl
RNAase free H2O	6.4µl	6.4µl
cDNA	1.5µl	-

*Mastermix contains hot start version of modified *Thermus brokianus* DNA polymerase, SYBR® Green I, optimised PCR buffer, 5mM $MgCl_2$, and dNTP mix.

The qPCR reaction was cycled in an iQ5 Multicolor Real-Time PCR Detection System (Biorad, Hemel Hempstead, UK) for the following times and temperatures.

95°C for 2 minutes

95°C for 30 seconds

60°C for 30 seconds } 35 cycles

72°C for 30 seconds

72°C for 10 minutes

cDNA levels were quantified using the accompanying BioRad software.

2.2 Protein Biochemistry

2.2.1 Reagents

Chemicals were obtained from Sigma unless otherwise stated. ProtoGel- 30% Acrylamide/Bisacrylamide solution (37.5:1 w/v ratio) (#EC-890), AccuGel_ 30% Acrylamide/Bisacrylamide solution (19:1 w/v ratio) (#EC-849), ProtoGel resolving buffer (#EC-892), ProtoGel stacking buffer (#EC-893), N,N,N',N'-Tetramethylethylenediamine (TEMED) (#EC-503) and Tris-Glycine-SDS PAGE buffer (#EC-870) were all obtained from National Diagnostics. Ammonium persulphate (APS) (#A3678), 2-mercaptoethanol (#M6250) and Ponceau S (#P7170) were obtained from Sigma. Pre-stained broad range (#P7708S) and unstained broad range (#P7702S) SDS-PAGE molecular weight standards were from New England Biolabs (NEB). PROTRAN nitrocellulose 0.45µm pore-size (BA 83, #10401465) was purchased from Schleicher & Schuell, GmbH, Dassel, Germany. Marvel skimmed milk powder was from Premier Brands, UK and bovine serum

albumin (BSA) (#40-00-410) was from First Link UK Ltd. SuperSignal West Pico enhanced chemiluminescence (ECL) substrate was obtained from Pierce, Rockford, IL, USA (#34080). Isopropyl-ß-thiogalactopyranoside (IPTG) was obtained from Melford Laboratories Ltd. Suffolk, UK (#MB1008). Mammalian protease inhibitors (#P8340) and bacterial protease inhibitors (#P8465) were obtained from Sigma. NuPAGE Antioxidant (#NP0005) and MOPS SDS running buffer (#NP0002-02) were from Invitrogen.

2.2.2 SDS polyacrylamide gel electrophoresis (SDS-PAGE)

The resolution of proteins in polyacrylamide gels was performed using the denaturing, discontinuous system described by Laemmli (Laemmli, 1970). Gels were set up in BioRad Mini-Protean® 3 cell apparatus according to the manufacturer's instructions. Samples were resuspended in 5 x SDS-PAGE sample buffer containing ß-mercaptoethanol. Recipes for gels and sample buffer are given in tables 2.9 and 2.10. Samples were boiled for 5 minutes at 98°C prior to loading onto a gel alongside standard molecular weight markers. Typically, gels were run for 15mins at 90V and 80mins at 135V in 1x electrophoresis running buffer (containing 50mM Tris, 0.1% SDS and 380mM glycine). Gels were then incubated for 1 hour with Coomassie Blue Stain (1mg/ml Coomassie Brilliant Blue (Gibco), 10% acetic acid, 50% methanol) or processed for Western blotting (see section 2.2.3). Gels were destained at room temperature for 1 hour (5% acetic acid, 35% methanol) and dried at 80°C for 2 hours under a vacuum with a BioRad gel drier. Alternatively, pre-cast NuPAGE Bis-Tris SDS-PAGE 4-12% gradient gels were used for greater resolution of a range of different molecular weight

proteins (#NP0321, Invitrogen). Gels were run in the XCell *SureLock* Mini-Cell system (Invitrogen). Typically gels were run in NuPAGE MOPS SDS buffer containing NuPAGE Antioxidant at 200V for 60 minutes.

Table 2.9. Recipes for SDS-PAGE gels

Ingredient	Resolving gel			
	6%	8%	10%	12%
30% acrylamide (ml)	4	5.34	6.66	8
4X Resolving Buffer (ml)	5.2	5	5	5
Distilled water (ml)	10.58	9.24	7.92	6.58
TEMED (µl)	20	20	20	20
10% APS (µl)	200	200	200	200
Total volume (ml)	20	20	20	20

Ingredient	Stacking gel
	4%
30% acrylamide (ml)	1.35
4X Resolving Buffer (ml)	2.5
Distilled water (ml)	6.1
TEMED (µl)	10
10% APS (µl)	50
Total volume (ml)	10

Table 2.10 Recipe for sample buffer

Sample buffer (100ml)	5x	1x	Final concentration
0.5mM Tris-Cl pH 8.0	31.25ml	12.5ml	62.5mM
SDS	3g	15g	3%
10% Glycerol	50g	10g	10%
3.3% 2-mecaptoethanol*	6.25ml	1.25ml	3.3%
Bromophenol blue	0.05g	0.01g	0.01%

*Alternatively DTT was added to sample buffer at a final concentration of 1mM before use.

2.2.3 Western Blotting

Following SDS-PAGE proteins were transferred to nitrocellulose for 60 minutes at 24V in a Genie blotter (Research Products International Corp., Ill, USA). Membranes were stained with Ponceau S in order to monitor the efficiency of transfer, then incubated in 5% milk in phosphate-buffered saline (PBS) for at least 1 hour (at room temperature) or overnight (at 4°C) in order to block non-specific binding. Membranes were then incubated in blocking buffer containing specific primary antibodies for at least 1 hour (at room temperature) or overnight (at 4°C). Unbound antibodies were removed by repeated rinsing in PBS and then membranes incubated for 1 hour at room temperature in solutions containing fluorescent or horseradish peroxidase (HRP)-conjugated secondary antibodies. Proteins were detected either via enhanced chemiluminescence (ECL) or using a LI-COR Odyssey® infrared imaging system according to the manufacturer's protocol.

Table 2.11 Primary and secondary antibodies used in this study

Antibody	Species	Source	Use
Anti-Beclin	Mouse	BD Trans. Labs	WB
Anti-ULK-1	Mouse	Santa Cruz	WB
Anti-CIMPR	Rabbit	Paul Luzio	IF
Anti-CIMPR (STO52)	Rabbit	Sharon Tooze	WB
Anti-SNX1	Rabbit	Matthew Seaman/ AbCam	IF WB
Anti-Vps26	Rabbit	Matthew Seaman/ AbCam	IF WB
Anti-WIPI2	Rabbit	JW	WB/IF
Anti-Vac14	Rabbit	JW	WB/IF
Anti-PIKfyve	Rabbit	Lois Weisman	WB/IF
Anti-WIPI1	Rabbit	Sharon Tooze	WB
Anti-EGFR-R1	Mouse	CRUK	IF
Anti-EGFR (1005) sc-03	Goat	Santa Cruz	WB
Anti-LAMP1	Mouse	NIHCD	IF
Anti-EEA1	Rabbit	Ian Mills	IF
Anti-EEA1	Mouse	BD Trans. Labs	IF
Anti-LC3	Mouse	Nanotools	WB/IF
Anti-TGN46	Sheep	Vas Ponnambalam	IF
Anti-GM130	Sheep	Francis Barr	IF
Anti-Golgin 245	Mouse	Santa Cruz	IF
Anti-Met	Mouse	Cell Signalling	WB
Anti-CD8	Mouse	Matthew Seaman	IF/WB
Anti-HA	Mouse	Clontech	IF/WB
Anti-His	Mouse	Qiagen	WB
Anti-myc	Mouse	Upstate	WB
Anti-GFP	Sheep	Ian Prior	IF/WB
Anti-phospho-Akt	Rabbit	Cell Signalling	WB
Anti-phospho-MAPK	Mouse	Cell Signalling	WB
Anti-α tubulin	Mouse	Sigma	IF
Anti-Transferrin receptor	Mouse	Boehringer	IF

Antibody	Source	Catalogue Number	Use
Anti-mouse IgG-HRP	Sigma	A4416	WB
Anti-mouse IgM-HRP	Sigma	A8786	WB
Anti-rabbit IgG-HRP	Sigma	A9169	WB
Donkey anti-mouse IRDye® 800CW	Licor Biosciences	926-32212	WB
Donkey anti-mouse IRDye® 680	Licor Biosciences	926-32222	WB
Donkey anti-rabbit IRDye® 800CW	Licor Biosciences	926-32213	WB
Donkey anti-rabbit IRDye® 680	Licor Biosciences	926-32223	WB
Donkey anti-goat IRDye® 800CW	Licor Biosciences	926-32214	WB
Anti-mouse IgG-AF 594	Molecular Probes	A11005	IF
Anti-mouse IgM-AF 594	Molecular Probes	A21044	IF
Anti-rabbit IgG-AF 594	Molecular Probes	A11012	IF
Anti-mouse IgG-OG 488	Molecular Probes	O6380	IF
Anti-rabbit-IgG-OG 488	Molecular Probes	O6381	IF

Table 2.11 gives details of all primary and secondary antibodies used for both western blotting and immunofluorescence.

2.2.4 Stripping Western Blots

Western blots were briefly washed in PBS to remove residual ECL reagent and then incubated in stripping buffer (62.5mM Tris-HCl pH6.7, 2% SDS (w/v), 100mM 2-mercaptoethanol) at 50°C for 30 minutes with occasional agitation. Membranes were then given two 10 minute washes in

PBS containing 0.1% (w/v) Tween-20. The membranes were then blocked and re-probed as described in section 2.2.3.

2.2.5 Protein Assay

The protein concentration of cell lysates was determined by the Bradford method using the BIO-RAD protein assay kit (#500-0006). Bovine immunoglobulin (#I9640, Sigma) was used to create a standard curve each time the assay was performed. Cells lysates prepared in buffers containing SDS were quantified using the BCA protein assay kit (Pierce, UK) according to the manufacturer's instructions.

2.2.6 Recombinant protein production from E.coli

Constructs to be expressed were sub-cloned into pTrcHisC bacterial expression vectors. One Shot BL21(DE3)pLysE competent cells were transformed with the relevant constructs according to manufacturer's instructions. Transformed cells were grown overnight, then diluted 1:20 into 500ml LB to an OD_{550} of 0.8. Protein production was induced with the addition of IPTG and grown for 4 hours at 37°C. Bacteria were harvested by centrifugation for 15 minutes at 4°C in a Jouan centrifuge (CR412, #29404191, Jouan, Saint Herblain, France) at 3,500 x *g* followed by resuspension in PBS, another round of centrifugation and the pellet snap frozen in liquid nitrogen.

2.2.7 Purification of His_6-tagged recombinant proteins

Bacterial pellets were resuspended in 15ml IMAC 5 buffer (20MM Tris-

HCl pH 8.0, 300mM NaCl, 5mM imidazole) supplemented with lysozyme (0.5mg/ml) and bacterial protease inhibitors. The resultant supernatant was rotated end-over-end at 4°C for 30 minutes followed by sonication on ice 6x 30 seconds with the MICROSON XL2000 ultrasonic sell disrupter. This lysate was pelleted by centrifugation in a Beckman Coulter Optima MAX ultracentrifuge (MLA-80 rotor) at 100, 000 x *g* for 30 minutes. The recovered supernatant was rotated end-over-end for 2 hours at 4°C with 0.5ml pre-washed nickel-nitrilotriacetic acid (Ni-NTA) beads. Beads were spun for 5 minutes at 700 x *g* and washed 4x in IMAC 20 buffer (20MM Tris-HCl pH 8.0, 300mM NaCl, 20mM imidazole). Purified His_6-tagged proteins were eluted from Ni-NTA beads with IMAC 200 buffer (20mM Tris-HCl pH 8.0, 300mM NaCl, 200mM imidazole) and dialysed against 50mM Tris/HCl pH 7.2, 100mM NaCl, 1mM DTT. Purified proteins were aliquotted, snap frozen and stored at –80°C.

2.2.8 Generation of recombinant baculovirus

Sf9 cells were cultured in IPL-41 medium (Sigma) supplemented with 10% foetal bovine serum (FBS), 2% yeastolate, 1% fungizone (250µg/ml), and 50mg/ml Gentamicin (all from Invitrogen). Cells were maintained in 175cm^2 flasks at 27°C, and split 1:3 when confluent. The BD BaculoGold™ Baculovirus Expression Vector System was purchased from BD Biosciences (Oxford,UK). Recombinant baculovirus was obtained by cotransfection of Sf9 cells with the protein of interest (in a His-tagged baculovirus vector) and BaculoGold DNA. 60mm diameter dishes were seeded with 2 x 10^6 cells, which were then allowed to adhere for 5 minutes. In an eppendorf tube

0.5µg of BaculoGold DNA was combined with 4.5µg of maxiprep DNA of interest, mixed gently and incubated at room temperature for 5 minutes. Subsequently 1ml Transfection Buffer B was added to the DNA mixture and 1ml Transfection Buffer A was added to the cells to replace the growth medium. The DNA/buffer mix was then added dropwise to the plates with gentle rocking. The plates were incubated at 27°C for 4 hours and the medium was then replaced with fresh growth medium. The level of infection was assessed after 4 days and the supernatant harvested after 5 days. The viral stock was then amplified by seeding 2 x 10^7 Sf9 cells in a 175cm^2 flask, adding 200µl viral stock and incubating the cells at 27°C for 4-5 days. The supernatant was then harvested into 50ml tubes and the amplified viral stock was titrated to assess protein production and determine the amount of virus required for optimal protein production. For titration of the virus, 5 x 10^4 cells were seeded per well of a 96 well plate. The cells were allowed to adhere for 15 minutes. 100µl of amplified stock was added to the first well, and then serially diluted over the next 11 wells to create a titration of the viral stock. The dish was then sealed with parafilm and incubated for 2.5 to 3 days at 27°C. Subsequently cells were washed with 1 x PBS and then lysed in 50µl sample buffer. Samples were boiled for 10min prior to loading 30µl of each sample onto a coomassie gel alongside 15µl control uninfected sample.

2.2.9 Production of recombinant protein from baculovirus

6 175cm^2 flasks were each seeded with 2 x 10^7 cells. Cells were allowed to adhere for 5-10 minutes prior to the addition of 170µl (optimum amount as determined by titration – see chapter 3) of amplified baculovirus

protein. Cells were incubated at 27°C for 2 days and the supernatant was harvested into 50ml tubes (one 50ml tube per 2 flasks). 500µl of supernatant was removed to a 1.5ml eppendorf tube, spun for 3 minutes at full 4,500rpm, rinsed in PBS, spun again and then resuspended in 100µl sample buffer for analysis on Coomassie gel. The remaining supernatant was then spun for 10 minutes at 2,000rpm at room temperature. The supernatant was discarded and the pellet was snap frozen in liquid nitrogen and stored at -80°C until purification. All baculovirus waste was mixed with 2% Trigene and then discarded after 24 hours, whilst plasticware was autoclaved immediately after use.

2.2.10 Purification of His-tagged proteins from baculovirus infected cells

Each cell pellet prepared as described in section 2.2.9 was resuspended in 3ml lysis buffer (10mM Tris pH 7.5, 100mM NaCl, 1mM DTT, protease inhibitor cocktail). Cells were then lysed by sonication with a large sonicator probe in short bursts. Lysed material was pelleted at 45, 000 rpm at 4°C for 15 minutes. Nickel-NTA beads were washed 3 times in IMAC5 buffer (see section 2.2.7 for details of IMAC buffers) and Sf9 supenatant was subsequently incubated with the beads at 4°C for 2 hours. 50µl samples of sonicated material and supernatant were removed for analysis on a coomassie gel. The pellet was resuspended in 2ml 1X sample buffer and 50µl removed for analysis on a gel. Beads were pelleted at 1500rpm for 2 minutes, 50µl of unbound material kept for analysis and then beads were washed 4 times with IMAC20 and then eluted in 3 times in 1ml IMAC200 each time. 50µl samples of the eluate and beads were removed and then

the eluate was dialysed overnight at 4°C against 50mM Tris/HCl pH 7.2, 100mM NaCl, 1mM DTT. The various stages of the prep were analysed by SDS-PAGE gel electrophoresis and coomassie stain and the dialysed protein stock was aliquotted, snap frozen and stored at -80°C.

2.3 Cell Biology

2.3.1 Reagents

All cell culture reagents were obtained from Invitrogen unless otherwise stated. All plasticware used was from Corning Inc, Corning, NY, USA. All chemicals were from Sigma unless otherwise stated. Purified active heterodimeric human hepatocyte growth factor (HGF) was obtained from Genentech Inc. (San Francisco, CA, USA). Purified mouse EGF was obtained from J. Smith, Liverpool, UK.

The protease inhibitor Leupeptin was obtained from Sigma Aldrich and the vacuolar ATPase proton pump inhibitor Concanamycin (#344085) was obtained from Merck Biosciences, Whitehouse Station, NJ, USA. PIKfyve inhibitor was a kind gift of Kevin Shokat (UCSF, USA). GST-2xFYVE (Hrs) vector was a gift from Harald Stenmark (Gillooly *et al.*, 2000) and was produced in bacteria and isolated with Glutathione Sepharose then biotinylated with Sulfo-NHS-LC-Biotin (Pierce, UK).

2.3.2 Cell culture

HeLa, HEK293A, and HEK293T were cultured in a humidified 5% CO_2 atmosphere at 37°C in Dulbecco's Modified Eagle's Medium (DMEM), supplemented with 10% FBS, 1% non-essential amino acids, and 1%

penicillin/streptomycin sulphate. Cells were maintained by growing to confluence in 100mm dishes before being split at 1:5 dilution every 2-3 days as appropriate.

For most biochemical assays and transfections, cells were seeded in either 100mm or 60mm diameter dishes, or in 6-well plates at a density such that they would be approximately 80% confluent at the onset of the experiment. For immunofluorescence studies cells were seeded at a lower density in 6-well plates on 22mm x 22mm coverslips or in 12-well plates on 19mm diameter coverslips (Scientific Laboratory Supplies, Nottingham, UK).

2.3.3 Culture of HeLaM CD8-ciM6PR and CD8-Furin cell lines

CD8-ciM6PR-HeLaM and CD8-Furin HeLaM cells (a generous gift of Dr Matthew Seaman, Cambridge Research Institute) are a stably transfected cell line expressing chimeras of the luminal domain of CD8 fused to the with the cytoplasmic tail of the CIMPR and Furin (Seaman, 2004). For maintenance, cells were grown in HeLa medium supplemented with 0.5mg/ml G418.

2.3.4 Transfection of tissue culture cells

Cells were usually seeded at a density such that they would be approximately 50% confluent at the time of transfection. Cells were routinely transfected with GeneJuice (#70967, Merck Biosciences) at a ratio of 3µl transfection reagent to 1µg DNA according to the manufacturer's instructions.

2.3.5 Immunofluorescence

Cells grown on coverslips were fixed immediately after each experiment (or following a 5 minute incubation in 0.05% Saponin in PBS to remove cytosolic staining) by a 15-minute incubation in 3% paraformaldehyde (PFA) (TAAB, UK) in PBS. Residual PFA was quenched by a 20 minute incubation in 50mM NH_4Cl in PBS and then cells were permeabilised by a 5 minute incubation in 0.2% Triton-X-100 in PBS (except where cells were treated with saponin prior to fixation). Alternatively, cells were fixed in 100% methanol for 10 minutes at -20°C. Cells were then blocked by incubation in 10% goat serum/PBS or 0.2% fish skin gelatin/PBS for at least 30 minutes. Coverslips were incubated for 20 minutes with specific primary antibodies diluted in 5% goat serum/PBS or 0.2% gelatin/PBS. Following extensive washing, coverslips were then incubated for 20 minutes with secondary antibodies diluted in 5% goat serum/PBS or 0.2% gelatin/PBS. After further washing coverslips were mounted on glass microscope slides (Scientific laboratory supplies, Nottingham, UK) using a mounting medium containing Mowiol® 4-88 (#475904, Merck Biosciences) and where necessary a DAPI stain. Cells were then observed on a SP2 AOBS (Leica; HCX PL APO CS 63.0 x 1.4 oil objective) confocal microscope. For experiments using Biotinylated GST-2xFYVE protein, cells were permeabilised in 20μM digitonin in 80mM Pipes pH 6.7, 1mM MgCl2, 5mM EGTA, and blocked in 10% BSA/20μM digitonin-Pipes. Subsequent antibody incubations were in 5% BSA/20μM digitonin-Pipes, and washes in Pipes buffer.

2.3.6 Growth factor stimulation and cell lysis

Cells were serum-starved for 16 hours in serum-free DMEM and subsequently stimulated for the required time periods with approximately 100ng/ml HGF/SF or 100ng/ml EGF. Where used, PIKfyve inhibitor was also present throughout the period of growth factor stimulation. Following this, the cells underwent three washes with ice-cold PBS and were then lysed for 10 minutes on ice in lysis buffer (0.5% Nonidet P40 (NP-40, Merck Biosciences), 25mM Tris-HCl pH7.5, 100mM NaCl, 50mM NaF) supplemented with mammalian protease inhibitor cocktail (#P8340, Sigma) and phosphatase inhibitor cocktail II (#P8340, Sigma). Lysates were pre-cleared by centrifugation at 21000 x g and the protein yield determined as described in section 2.2.5. Alternatively, cells were lysed in 1X sample buffer containing 2-mecaptoethanol or DTT, or in hot SDS lysis buffer (1% SDS, 50mM NaF, 1mM EDTA) at 110°C for 10 minutes with intermittent vortexing.

2.3.7 RNA interference

Cells were seeded at 5.88 x 10^5 per 60mm diameter dish in full HeLa medium and allowed to adhere overnight. Immediately before transfection, the HeLa medium was replaced with DMEM containing no serum and no antibiotics. Cells were then transfected with short interfering RNA (siRNA) oligonucleotides using the oligofectamine transfection reagent (#12252-01, Invitrogen) according to the manufacturer's protocol. On-Target Plus SMARTpool and deconvoluted duplex siRNA oligonucleotides (oligos) were obtained from Dharmacon Inc., Lafayette, CO, USA. For each knockdown 40nM oligos were used. Initially, pooled oligos were used for knockdown, but

once knockdown efficiency had been determined oligo pools were deconvoluted and individual specific oligos were used for each protein. For details of the specific siRNA oligos used for each protein see table 2.12. A non-specific control VII (# D-001206-07020) RNA duplex was also purchased from Dharmacon (sense 5'-ACUCUAUCGCCAGCGUGACUU-3'; antisense 5'-PGUCACGCUGGCGAUAGAGUUU-3'). Four hours after transfection serum was added to the medium to a final concentration of 10%. A two-hit protocol was used in each case, in which, after 24h transfection, cells were trypsinised and reseeded, allowed to adhere overnight and then transfected for a further 24h with a second hit of 40nM oligos. For 10cm diameter dishes and 6-well plates the number of cells and amount of siRNA used was scaled up or down appropriately.

Table 2.12. Pooled and individual deconvoluted oligos used in this study

Protein target	Accession number	Pooled oligo number
PIKfyve	NM_015040	#L-005058-00-0005
Vac14	NM_018052	#L-015729-00-0005
WIPI-2	NM_015610	#L-020521-01-0005
WIPI-1	NM_017983	#L-018205-01-0005
Fig4	NM_014845	#L-019141-00-0005

Protein target (Oligo number)	Sense	Antisense
PIKfyve (J-005058-13)	5'-GGCACAAGCUAUAGCAAUUUU-3'	5'-PAAUUGCUAUAGCUUGUGCCUU-3'
Vac14 (J-015729-08)	5'-GGUCAGAGGCCCUUUCAUCUU-3'	5'-PGAUGAAAGGGCCUCUGACCUU-3'
WIPI-1 siGenome (D-018205-03-0005)	5'-CCUAUAAUCUUGUGCCGUG-3'	
WIPI-2 (J-020521-09)	5'-CGACAGUCCUUUAGCGGCAUU-3'	5'-PUGCCGCUAAAGGACUGUCGUU-3'
WIPI-2 (J-020521-12)	5'-GGACCGGGUACUUCGGGAAUU-3'	5'-PUUCCCGAAGUACCCGGUCCUU-3'
ULK-1 siGenome (D-005049-01-0005)	5'-CCUAAAACGUGUCUUAUUU-3'	
Beclin (specially designed)	5'-GACGUGGAAAAGAACCGCAUU-3'	5'-UGCGGUUCUUUUCCACGUCUU-3'

2.3.8 Immunoprecipitation

Immunoprecipitation was performed by incubating 750µg lysed protein with end-over-end rotation with 5µl GFP or HA antibody and 30µl protein G-agarose (#P4691, Sigma) for 2 hours at 4°C. Resultant immunoprecipitates were washed three times in wash buffer containing 0.1% NP-40, 25mM Tris-HCl pH7.5 and 150mM NaCl and then once in 10mM Tris pH7.5 to remove detergent, before preparation for SDS-PAGE by adding 30µl 1.5x sample buffer.

2.3.9 Transmission Electron Microscopy

Cells were washed three times with ice-cold PBS^{++} (supplemented with 0.1M $CaCl_2$ and $MgCl_2$) and then fixed in 4% PFA/2.5% glutaraldehyde for 30 minutes on ice. Cells were then washed again in PBS and then post-fixed in 1% Osmium tetroxide (OsO_4) in distilled water on ice in the dark for 1 hour. Subsequently, the cells were washed three times in PBS, and then twice in distilled water for 30 minutes each time, followed by incubation in 5% Uranly acetate in 30% ethanol for 1 hour. Samples were dehydrated by sequential 10 minute ethanol washes in 30%, 60%, 70%, 80% and then twice in 100% ethanol, then infiltrated with a 1:1 ratio of resin to 100% ethanol for 30 minutes. The infiltration resin was completely removed and 100% resin added to the samples. 100% resin was added to several resin moulds, which were placed face down on top the cell sample. Samples were polymerised at 60°C for 2-3 days.

2.3.10 HRP uptake experiments

Cells were incubated in 10mg/ml HRP (#P8375 Biozyme, South Wales, UK) in serum-free medium at 37°C for 10 minutes, 1 hour or 4 hours. Subsequently, cells were washed 3 times in ice-cold PBS^{++} and then fixed in 0.5% glutaraldehyde for 30 minutes. At room temperature cells were then washed 3 times in 0.1M Tris-Cl pH 7.6. Following this cells were incubated for 10 minutes in 0.1% diaminobenzidine (DAB, Sigma) in Tris buffer and then for 10 minutes in 0.1% DAB and 0.01% H_20_2 in Tris buffer at room temperature in the dark. The reaction was terminated by washing 3 times, for 5 minutes each, in Tris buffer, and then 2 times, for 5 minutes each, in

PBS. Cells were post-fixed in 1% OsO4 in 0.1M phosphate buffer pH 7.4 for 1 hour in the dark on ice and then processed for EPON embedding and EM as described from the post-fixation stage in section 2.3.9.

2.3.11 CD8 uptake assay

CD8-CIMPR or CD8-Furin cells were seeded onto coverslips and treated with siRNA as described in section 2.3.7 or with 800nM PIKfyve inhibitor for 4 hours. Subsequently coverslips were transferred to a well containing 3ml ice-cold DHB (serum-free DMEM containing 25mM Hepes and 0.2% fatty-acid free BSA (Fraction V, Sigma) for 15 minutes on ice. They were then incubated face down on a 100µl spot of DHB containing 1µg/µl monoclonal anti-CD8 antibody (courtesy of Matthew Seaman, Cambridge Research Institute) for 1 hour on ice in the dark. Following this the coverslips were washed twice in ice cold PBS and transferred back into pre-warmed growth medium for the required time period. Cells were then fixed and processed for immunofluorescence as described in section 2.3.5.

2.3.12 Shiga toxin assay

Cy3-STxB was a kind gift from Francis Barr, University of Liverpool. HeLa cells were seeded onto coverslips and treated with siRNA as described in section 2.3.7 or with 800nM PIKfyve inhibitor for 4 hours. Subsequently coverslips were incubated on ice for 30 minutes with 2µg/ml Cy3-STxB in uptake medium (DHB - as described in section 2.3.11). Coverslips were then washed in 1X PBS and transferred to normal growth medium for the required

timepoints at 37°C, 5% CO_2. Subsequently, cells were fixed and processed for immunofluorescence as described in section 2.3.5.

2.3.13 Acidification assays

Acridine Orange was added to cells in full growth medium at a concentration of 5µg/µl for 10 minutes. Cells were subsequently washed in 1X PBS and mounted onto slides in PBS for live imaging. As a control cells were treated with 100nM concanamycin for 1 hour prior to treatment with Acridine Orange. Lysotracker red was added to medium at 100nM for 120 minutes prior to fixation and processing for immunofluorescence.

2.4 Yeast two-hybrid assay

2.4.1 Reagents

pACT2 and pFBT9 vectors were kind gifts from Francis Barr (University of Liverpool, UK). The yeast two-hybrid host strain PJ69-4A (MATa trp1-901 leu2-3, 112 ura3-52, his3-200 gal4Δ gal80Δ LYS2::GAL1-HIS3 GAL2-ADE2 met2::GAL7-lacZ) was used as the bait strain for all Y2H experiments (provided by Phil James, University of Wisconsin, USA). PJ69-4A carries three independent GAL4-responsive reporter genes (GAL1-HIS3, GAL2-ADE2 and GAL7-lacZ). The PJ69-4A strain was developed to provide a suitable mating partner with identical genotype to PJ69-4A resulting in the yeast strain PJ69-4_ (provided by Phil James). PJ69-4_ was used as the prey strain for all Y2H experiments. *Taq* polymerase, Yeast Extract and Peptone 140 (#30392-021) were from Invitrogen/Gibco (Paisley, UK).

Lithium acetate (LiOAc), PEG3350, Sodium hydroxide, salmon testes DNA and all amino acids were from Sigma Aldrich (Poole, UK). Glucose (#GLU03) and yeast nitrogen base (#CYN0410 without amino acids) were from Formedium (Hunstanton, UK). Agar (#400-050) was from Biogene (Cambridge, UK). Casamino acids (#228-830) were from DIFCO (Voigt Global Distribution, Kansas, USA).

2.4.2 Yeast transformations

Vac14, WIPI-2 and Fig4 were subcloned into pACT2 (prey vector – DNA activation domain) and pFBT9 (bait vector - DNA binding domain). 2ml YPAD medium (for recipes see Table 2.15) was inoculated with PJ69-4A Mat-a (bait) or complimentary mating-type switched Mat-α (prey) yeast cells and grown overnight at 30°C with shaking at 200rpm. The following morning 8ml of YPAD medium was added to the cells and they continued to be incubated for a further 5 hours. The cell culture was spun at 2,300 rpm for 5 minutes and the supernatant discarded. The cell pellet was resuspended in 5ml 100mM LiOAc. 1.5ml of this resuspension was removed and centrifuged at 2,300rpm for 5 minutes. The supernatant was discarded once again and then the pellet was resuspended in the mixture in table 2.13.

Table 2.13. Typical reaction for transformation of yeast with miniprep DNA

Ingredient	Volume
50% (v/v) PEG3350	185µl
1M LiOAc	28µl
Distilled H_20	36µl
Denatured salmon testes DNA	7µl
Miniprep DNA of interest	1µl
Total	350µl

The samples were cycled in a PCR machine as follows:

30°C for 30 minutes

42°C for 25 minutes

30°C for 1 minute

The resulting mixture was plated onto SD (synthetic defined) agar plates lacking in tryptophan and low in adenine (for bait constructs) and in leucine (for prey constructs) and grown for 3 days at 30°C. Colonies were checked by PCR using primers specific to the insert. A typical yeast colony PCR is outlined in table 2.14.

Table 2.14. Yeast colony PCR (reaction mixture per colony)

Ingredient	Volume
F primer (10mM)	0.75µl
R primer (10mM)	0.75µl
dNTPs	0.45µl
Taq polymerase buffer	1.5µl
$MgCl_2$	0.75µl
Taq polymerase	0.15µl
DMSO	0.3µl
H_20	7.35µl
Total	12µl

Yeast colonies were resuspended in 3µl 0.02M sodium hydroxide for lysis and then added to 12µl of PCR mastermix. PCR reactions were cycled as follows:

95°C for 5 minutes

95°C for 1 minute

Annealing temperature of primer -5°C for 1 minute } 35 cycles

72°C for 3 minutes 30 seconds

72°C for 5 minutes

The same yeast colony was also added to 20µl of water and subsequently spotted onto selective agar plates and grown at 30°C for 5 days to test the autoactivation of the constructs. A pool of glycerol stocks of colonies that do not autoactivate was made

Table 2.15. Recipes for yeast media

YPAD (500ml)	SD-X (500ml)
10g Glucose 10g Peptone 5g Yeast Extract 0.05g Adenine 10g Agar (For solid medium)	10g Glucose 3.35g Yeast Nitrogen Base Appropriate amount of amino acid X 10g Agar (For solid medium)

SD + Casamino acids + ura + high ade
10g Glucose 3.35g Yeast Nitrogen Base 7g Casamino acids 0.01g Uracil 0.05g Adenine

Table 2.16. Selective media/agar

Name	Description	Use
YPAD	Nutrient rich yeast medium/agar	Growth of yeast
SD-W	**S**ynthetic **d**efined medium deficient in Tryptophan	Bait selection
SD-L	Deficient in Leucine	Prey selection
SD-WH	Deficient in Tryptophan and Histidine	Testing for autoactivation of bait constructs (Increased stringency)
SD-LH	Deficient in Leucine and Histidine	Testing for autoactivation of prey constructs (Increased stringency)
SD-WHAT	Deficient in Tryptophan and Histidine 3-amino-1,2,4-triazole (3-AT)	Testing for autoactivation of bait constructs (increased stringency)
SD-LHAT	Deficient in Leucine and Histidine 3-AT	Testing for autoactivation of prey constructs (Increased stringency)
SD-WA	Deficient in Tryptophan and Adenine	Testing for autoactivation of bait constructs (most stringent)
SD-LA	Deficient in Leucine and Adenine	Testing for autoactivation of prey constructs (most stringent)
SD-WL	Deficient in Tryptophan and Leucine	Double selection, used to select diploids after mating
SD-WLHAT	Deficient in Tryptophan and Leucine and Histidine 3-AT	Triple selection (less stringent), used for selecting interacting partners
SD-WAL	Deficient in Tryptophan, Adenine and Leucine	Triple selection, used for selecting interacting partners (most stringent)

2.4.3 Yeast mating

Yeast glycerol stocks were spotted onto appropriate selective media and allowed to grow for 3 days at 30°C. Colonies were then resuspended in 20µl water and 2µl of both bait and prey were spotted onto a YPAD plate on top of one another and allowed to grow overnight at 30°C. The following day growth was transferred onto selective media (-WL followed by –WLHAT and –WAL) using a sterilised velvet cloth. Plates were incubated at 30°C for 5 days.

2.4.4 Beta-gal assay

As an alternative assay for interacting partners, this assay was used to assay the level of reporter construct transcription. To transfer diploid yeast growth onto filter paper it was laid on top of the growth and rubbed gently. The filter paper was then submerged in liquid nitrogen for 10 seconds to lyse the cells. After thawing the filter paper for 30 seconds, it was covered with ß-gal reagent (6mls Z buffer (60mM Na_2HPO_4, 40mM $Na_2H_2PO_4$, 10mM KCl, 1mM $MgSO_4$) 1.6mg/ml X-Gal reagent, 11µl ß-mercaptoethanol), and checked for air bubbles. This was covered over and left at 37°C for approximately 5 hours; with colour change (white to blue indicating production of ß-Gal) monitored and recorded every hour.

The theory underlying yeast two-hybrid assays is outlined in figure 2.2.

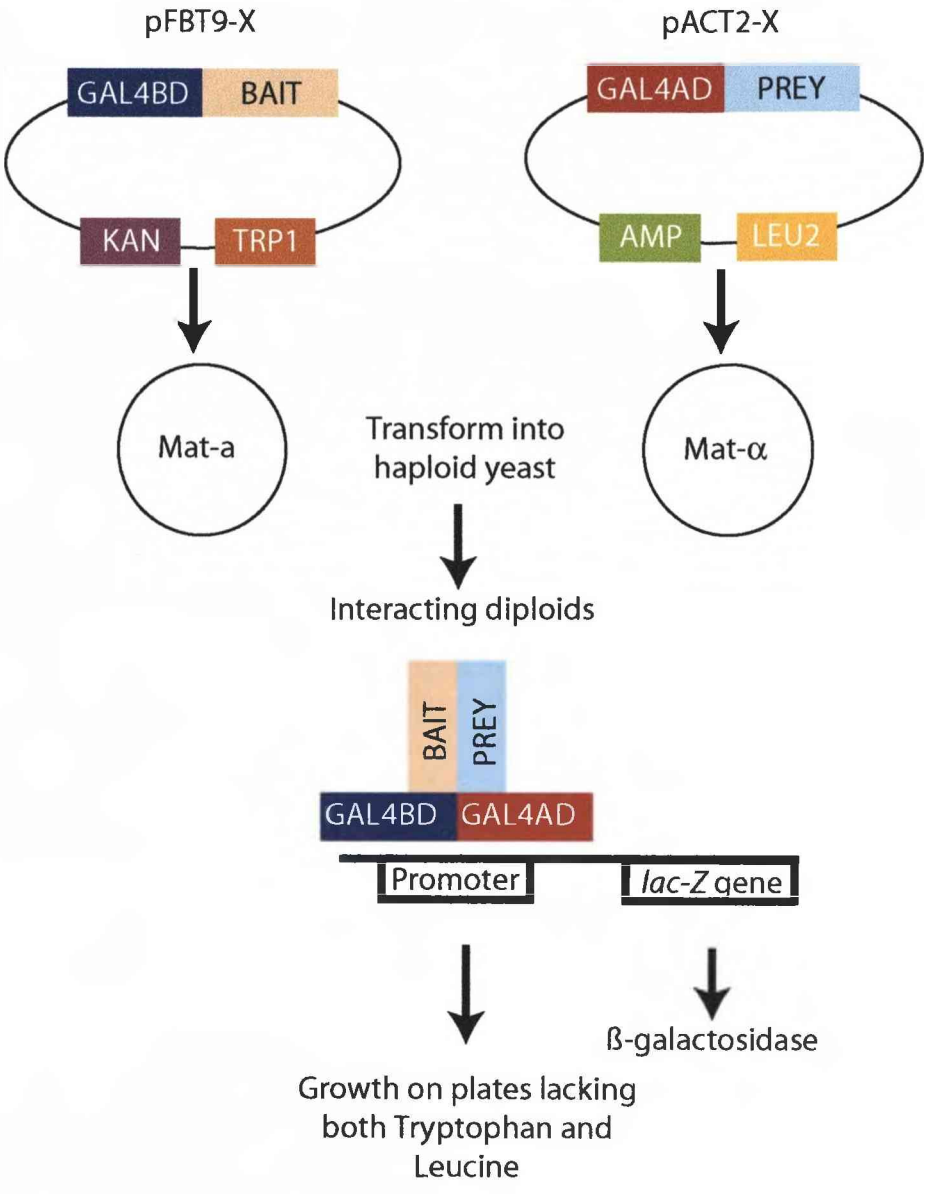

Figure 2.2. Yeast two-hybrid assay.
The yeast two hybrid method developed by Fields and Song to detect protein-protein interactions. Genes of interest are cloned into bait and prey vectors which possess either a DNA binding domain or an activating domain, and the yeast genes for Tryptophan and Leucine, to confer growth on drop out medium. These are then transformed into living haploid yeast of two different mating types. The yeast are then mated and diploids are selected by growth on medium deficient in both Leucine and Tryptophan. If bait and prey proteins interact then the DNA and activating domain wil be brought into close proximity and bind the promoter of a reporter gene, thus driving its transcription. Interacting partners are selected by growth on a triple drop out medium also deficient in Adenine.

2.5 Autophagy assays

2.5.1 LC3 lipidation assay

2GL9 cells (HEK293A cells stably transfected with GFP-LC3) were treated with siRNA as described in section 2.3.7 (except that 80nM oligos were used for each transfection), or with 800nM PIKfyve inhibitor for 4 hours. Cells were subsequently either 'fed' in normal growth medium, or starved in Earl's Buffered Saline Solution (EBSS) for 2 hours. Cells were then lysed in 80µl (for each well of a 12-well dish) 1X sample buffer. Prior to running on a gel 1mM DTT and 0.01% bromophenol blue was added to the samples. 10µg each sample was run on a 12% 1.5mm Bis-Tris gel by SDS-PAGE. Proteins were transferred to nitrocellulose. Following transfer the membrane was incubated in Ponceau S for 5 minutes to monitor protein transfer, and then processed by Western blotting as described in section 2.2.3. GFP-LC3 lipidation was examined using a polyclonal sheep GFP antibody (Ian Prior, University of Liverpool), and protein loading monitored using polyclonal anti-tubulin antibody (Sigma, Poole, UK). The extent of lipidation was quantified using Odyssey software or Image J (Rasband, W.S., ImageJ, U. S. National Institutes of Health, Bethesda, _Maryland, USA, http://rsb.info.nih.gov/ij/, 1997-2007) and a ratio of GFP-LC3II to total GFP-LC3 levels was determined.

2.5.2 LC3 II spot formation assay

2GL9 cells were seeded onto coverslips pre-treated with 0.1mg/ml poly-D-Lysine, and at the end of an experiment, cells were fed in normal growth medium or starved in EBSS for 2 hours prior to fixation in 3%

PFA/PBS and processing for immunofluorescence as described in section 2.3.5. For detection of endogenous LC3 cells were fixed in ice-cold methanol for 10 minutes at -20°C and incubated with a monoclonal anti-LC3 antibody (Nanotools, Germany). Where used Wortmannin (Sigma, #W1628) was added to medium for 30 minutes at 100nM and Leupeptin (Millipore, UK) was added to cells with starvation medium at a concentration of 0.25mg/ml.

2.6 Antibody production

2.6.1 Antibody production

A custom antibody service provided by Covance was used to produce rabbit polyclonal antibodies against mVac14, hFig4 and hWIPI-2. mVac14 (762 -782), hFig4 (891-907) and hWIPI-2 (430-454) (see Figure 3.1 for more details) were conjugated to Keyhole Limpet Haemocyanin (KLH) using M-Maleimideobenzoic acid N-hydroxy succinimide ester (MBS). MBS conjugates the amine group within lysine residues in KLH to the sulfhydryl group within cysteine residues of the target peptide. These were then used as antigens to immunise two New Zealand White Rabbits per peptide (UL_003 to UL_008) to account for biological variation. Immunogen was emulsified with Freund's Complete Adjuvant (FCA) for initial injections. Freund's Incomplete Adjuvant (FIA) was used for all subsequent injections (boosts). The immunisation schedule is shown in table 2.17, it followed a three-week cycle of boosts with test bleeds taken approximately 10 days after the boosts. The schedule was concluded with a terminal bleed yielding 55-65ml. Upon arrival antibody bleeds were aliquotted under sterile conditions and stored at -20°C until required.

Table 2.17. Covance immunisation schedule

Day	Procedure
Day 0	**Pre-bleed** (PI) and 1st immunisation (ID/SC) (500μg with FCA)
Day 21	Boost (SC) (500μg with FIA)
Day 42	Boost (SC) (250μg with FIA)
Day 52	**Test bleed** (TB)
Day 63	Boost (SC) (250μg with FIA)
Day 73	**Production bleed 1** (PB1)
Day 84	Boost (SC) (250μg with FIA)
Day 94	**Production bleed 2** (PB2)
Day 105	Boost (SC) (250μg with FIA)
Day 115	**Production bleed 3** (PB3)
Day 118	**Terminal bleed** (EX)

2.6.2 SDS-PAGE modifications

HeLa cells were either transfected with GFP-hFig4, GFP-mVac14 or GFP-hWIPI-2, or were left untransfected, and then lysed 24 hours later. In order to test a single sample with different antisera, a single 8% gel was prepared with transfected protein and untransfected protein from the same samples loaded in alternate lanes. The concentration of the lysates was determined by protein assay as described in materials and methods, and then 30μg was loaded onto an 8% SDS-PAGE gel. The material was

subsequently transferred to nitrocellulose blot, cut into strips and each strip was probed with pre-immune serum and bleeds from each rabbit. The predicted molecular weight of each over-expressed and endogenous protein is shown in table 2.18.

Table 2.18. Predicted molecular weights of over-expressed and endogenous proteins (determined by ExPasy (http://us.expasy.org/cgi-bin/peptide-mass.pl).

Protein	Over-expressed	*Endogenous*
hFig4	130kDa	106.3kDa
hWIPI-2	76kDa	50kDa
mVac14	115kDa	88kDa

2.6.3 Affinity purification of Vac14 and WIPI-2 antibodies

Antibodies were affinity purified using a SulfoLink® Immobilization Kit for Peptides (Thermo Scientific, USA) according to the manufacturer's instructions. 1mg peptide was used, and 2ml of the final bleeds of rabbits UL_003 and UL_008 were used.

CHAPTER THREE

Characterisation of proteins associated with PtdIns(3,5)P_2 metabolism

3.1 Introduction

Proteins that bind or synthesise phosphoinositides are key regulators of membrane traffic and signalling in eukaryotic cells. The precise function and localisation of one of the most recently discovered phosphoinositides, PtdIns(3,5)P_2, in mammalian cells is still poorly understood. Studies in *S. cerevisiae* identified four proteins associated with the metabolism of this lipid, for which mammalian homologues have been identified. As discussed in chapter one, these are the PtdIns(3)*P* 5-kinase PIKfyve/Fab1 (Yamamoto *et al.*, 1995; Shisheva *et al.*, 1999), the PIKfyve activator Vac14 (Bonangelino *et al.*, 2002; Sbrissa *et al.*, 2004), the 5-phosphatase Fig4/Sac3 (Rudge *et al.*, 2004; Sbrissa *et al.*, 2007), and a family of downstream effectors, dubbed the WIPI family (Atg18/Svp1 in yeast) (Dove *et al.*, 2004; Jeffries *et al.*, 2004; Proikas-Cezanne *et al.*, 2004).

The vast majority of the mammalian literature has focused on the kinase PIKfyve, as its loss produces a similar dramatic phenotype to the yeast mutant; swollen cytoplasmic vacuoles (Rutherford *et al.*, 2006). Much remains to be discovered about the other proteins Vac14, Fig4 and the WIPI family, in mammalian cells; their precise function, regulation, and relationship with one another and with the lipid. Previous studies have focused on a specific member of the mammalian WIPI family, WIPI-49 (also known as WIPI-1). For the purposes of this study WIPI-2 was chosen to complement

the pre-existing literature on WIPI-1 (Jeffries *et al.*, 2004; Proikas-Cezanne *et al.*, 2004). As illustrated in section 1.8.1 the mammalian WIPI family is phylogenetically divided into two similar groups composed of WIPI-1 with WIPI-2, and WIPI-3 with WIPI-4 (Proikas-Cezanne *et al.*, 2004). Both WIPI-1 and WIPI-2 are equally closely related to the yeast protein Atg18/Svp1, whereas WIPI-3 and WIPI-4 are more closely related to the yeast protein HSV2. Thus, the development of tools and reagents to study WIPI-2 are particularly important, to assess any functional redundancy of these two proteins.

The aim of the work laid out in this chapter was to prepare an extensive range of tools and reagents in order to better study these proteins in the following ways: 1) To clone the open-reading frame for each protein into a range of different expression vectors. 2) To develop antibodies against each protein. 3) To determine the cellular localisation of each protein through examination of both overexpressed and endogenous protein. 4) To produce recombinant protein for all three proteins. 5) To examine any interactions between the mammalian proteins and determine novel interacting partners.

3.2 Results

3.2.1 Generation of expression constructs

cDNA constructs for Vac14, WIPI-2 and Fig4 were generated as described in the materials and methods chapter. Each ORF was cloned into a range of expression constructs to enable study of these proteins in a

variety of different contexts. Table 3.1 provides a summary of the constructs that were made and for what purpose.

Table 3.1 Summary of the cDNA constructs made from this study.

Plasmid name	Use	Expression tested by WB	Comments
pEGFPC2-WIPI2	GFP tag WB, IF	Yes (76kDa)	30-40% (t.e)*
pCMVmyc-WIPI2	myc tag WB, IF	Yes (52.6kDa)	10%
pTrcHisC-WIPI2	Bacterial recombinant protein	Yes (52.6kDa)	Not expressed
pAcHis-WIPI2	Baculovirus recombinant protein	Yes (51.4kDa)	Insoluble
pACT2-WIPI2	Directed Y2H screen (prey)	No	
pFBT9-WIPI2	Directed Y2H screen (bait)	No	
pCMVmyc-WIPI-2 KDRES	Rescue siRNA phenotype	Yes (52.6kDa)	Not affected by siRNA
pTrcHisC-mVac14	Bacterial recombinant protein	Yes (91.6kDa)	Produces protein
pAcG3X-mVac14	Baculovirus recombinant protein	Yes (114kDa)	Not expressed
pCMVHA-mVac14	HA tag WB, IF, IP	Yes (90.3kDa)	40-50%
pEGFPC2-mVac14	GFP tag WB, IF	Yes (115kDa)	40-50%
pACT2-mVac14	Directed Y2H screen	No	
pFBT9-mVac14	Directed Y2H screen	No	
pAcHis-hFig4	Baculovirus recombinant protein	Yes (105kDa)	Not expressed
pEGFPC2-hFig4	GFP tag WB, IF, IP	Yes (130kDa)	5-10%
pCMVmyc-hFig4	myc tag WB, IF	Yes (106.2kDa)	5%
pACT2-hFig4	Directed Y2H screen	No	
pFBT9-hFig4	Directed Y2H screen	No	

* t.e - transfection efficiency (assessed by immunofluorescence)

3.2.2 Characterisation of antibodies against Fig4 by Western blotting

Antibodies were produced from two New Zealand White rabbits (as described in Materials and Methods) from the peptides shown in Figure 3.1, conjugated to KLH. In order for these antibodies to become useful tools they needed to be characterised for use in various methods and for their specificity against the target protein. Each bleed from the two rabbits for all three antibodies was characterised first by Western blotting, at a dilution of 1:100 and compared to the pre-immune serum which should not contain any specific antibodies. A frozen aliquot of antibody was also tested to determine if freeze-thawing affected serum activity.

Fig4 serum from both rabbits was unable to detect overexpressed GFP-Fig4, which has a predicted molecular weight of approximately 130kDa (Figure 3.2; solid arrow), the expression of which was previously tested by Western blotting. Table 3.1 lists the overexpression constructs generated for this study; Western blotting and immunofluorescence were used to test the correct expression of full-length proteins and assess their transfection efficiency.

HEK293T cells were used to test Fig4 antibodies, to eliminate the possibility that transfection efficiency of overexpressed Fig4 or levels of endogenous protein were below the detection sensitivity of the antibody in HeLa cells. Some proteins are detected by this serum (Figure 3.2), and it is possible that one of these represents a low level of endogenous protein, as there are proteins at the correct molecular weight (106kDa; dashed arrow),

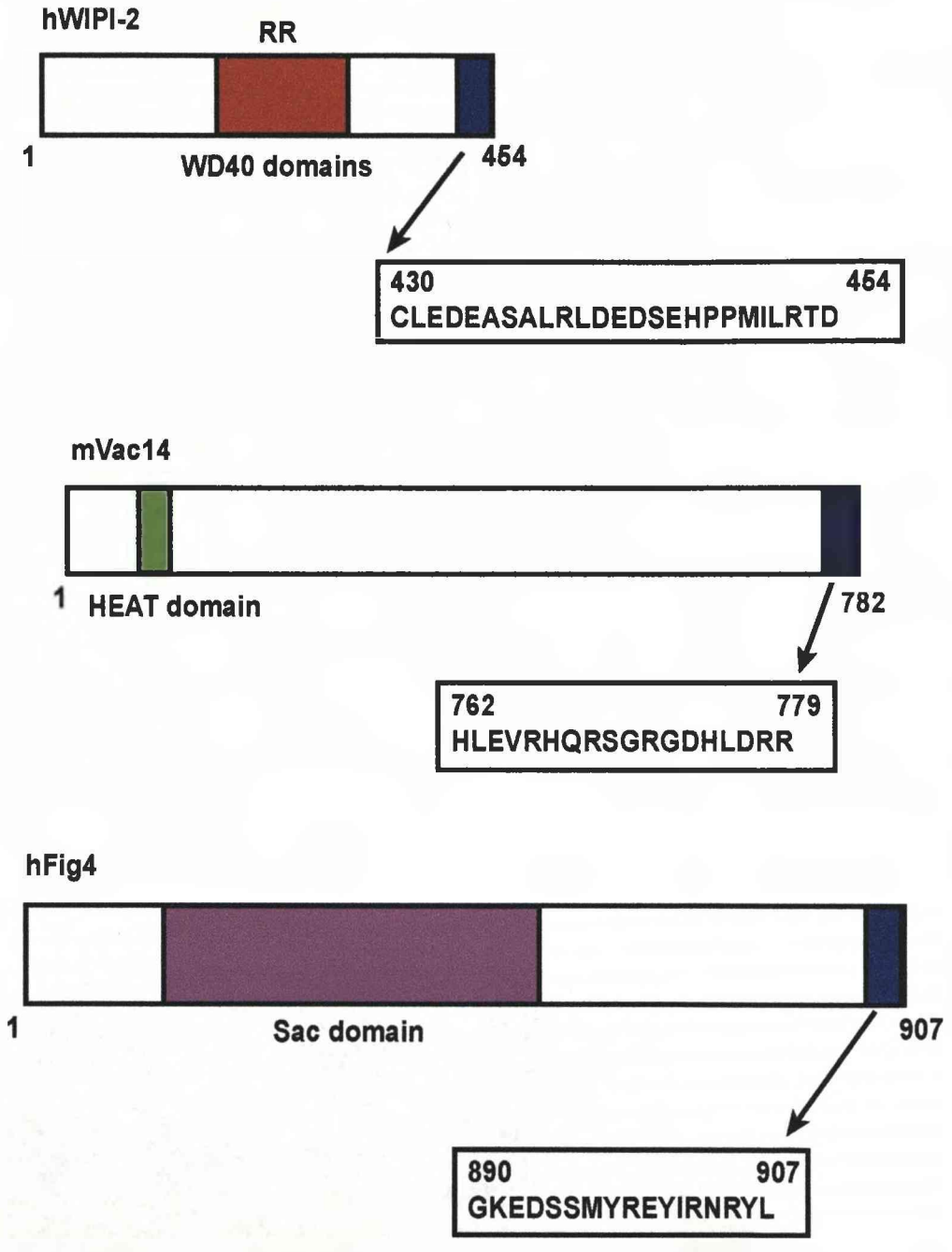

Figure 3.1. Peptides used in the production of antisera.
Diagram illustrating the domain structures of hWIPI-2, hFig4 and mVac14 and the relative position of the peptide used for the production of antibodies. Each peptide is C terminal in location. The sequences are less than 30 amino acids in length; hence their conjugation to KLH facilitates immunisation.

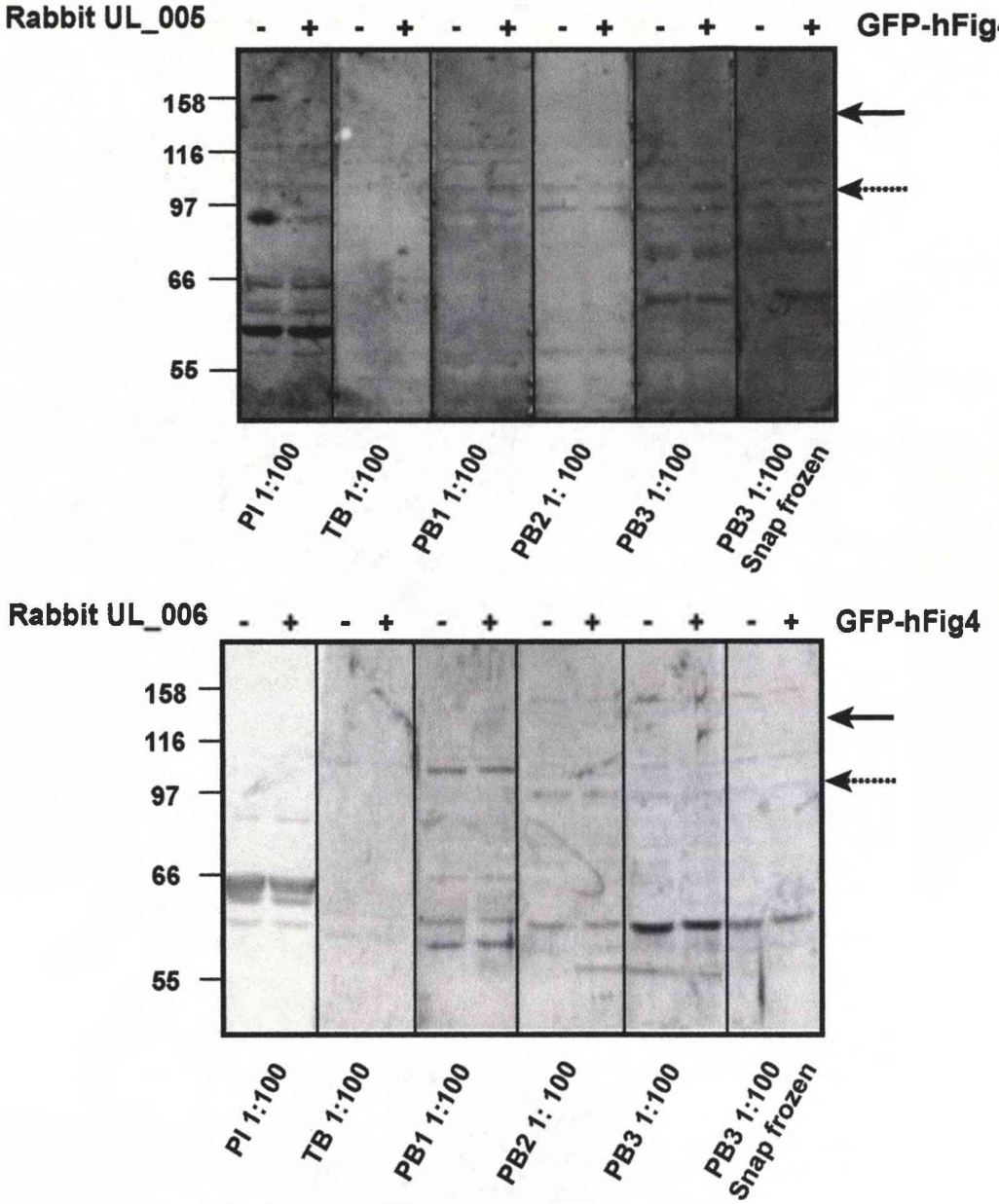

Figure 3.2. Determining the utility of an anti-Fig4 antibody by Western blotting.

HEK293T cells were either transfected with pEGFPC2-hFig4 (+) or left untransfected (-), lysed with hot lysis buffer after 24h, and 30μg lysates resolved on an 8% SDS-PAGE gel. Material was transferred to a nitrocellulose blot and probed with each bleed (PI = Pre-immune, TB = Test bleed, PB = Production bleed) from both rabbits (UL_005 and UL_006). An aliquot was snap frozen in liquid nitrogen and then thawed before use to ensure this did not adversely affect the activity of the serum. Serum from both rabbits does not detect overexpressed Fig4 (130kDa; solid arrow). It is unclear whether endogenous protein is detected or not (103.6kDa; dashed arrow)

detected by several bleeds and not by the pre-immune serum.

In order to test the ability of this antibody to detect endogenous protein, pooled siRNA oligos designed to target Fig4 were used, to determine if any of these bands were ablated by knockdown of the protein. None of the proteins detected by Fig4 serum is suppressed by the siRNA oligos (figure 3.3). It is possible, however, that the Fig4 oligos are ineffective in suppressing Fig4 protein. As such, RT-PCR was performed on HeLa cell lysates treated with Fig4 siRNA oligos, to establish that the messenger RNA levels were depleted. It is clear that these oligos are able to suppress Fig4 messenger RNA levels (figure 3.4). Although this does not always correspond to a loss in protein, the evidence suggests that this antibody is unable to detect Fig4 protein.

3.2.3 Characterisation of antibodies against Vac14 by Western blotting

All bleeds for both rabbits of Vac14 serum were able to detect overexpressed Vac14 protein (GFP-Vac14; 115kDa; solid arrow) and the serum is still active following snap freezing (Figure 3.5). Rabbit UL_008 appears to be more sensitive and detects several bands at approximately the correct molecular weight (88kDa; dashed arrow) for endogenous Vac14. To be certain that these proteins correspond to endogenous Vac14, pooled Vac14 siRNA oligos were used (Figure 3.6). A protein of the correct molecular weight is substantially suppressed by Vac14 siRNA oligos at both 48 and 72 hours of transfection and a range of oligo concentrations.

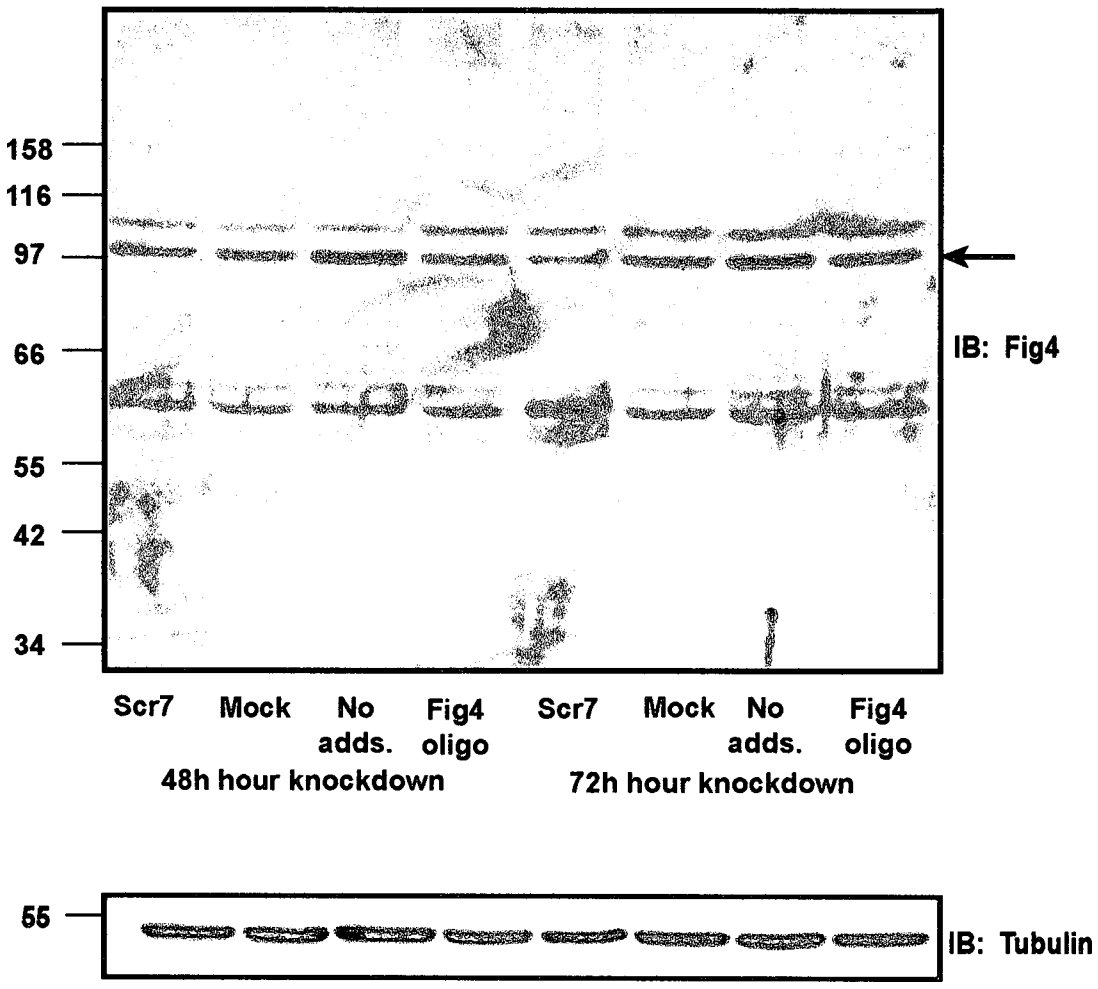

Figure 3.3. Fig4 serum is unable to detect endogenous Fig4 protein. HeLa cells were seeded onto 6-well plates and transfected with 100nM Dharmacon On-Target Plus SMARTpool™ Fig4 oligos for 48 and 72h. Cells were lysed in NP40 lysis buffer and 60μg lysates resolved on an 8% SDS-PAGE gel. Both no treatment (mock), no oligo (no adds.) and scrambled oligo (100nM) (Scr7) controls were also performed. Protein was transferred to nitrocellulose and probed with anti-Fig4 serum (PB3, UL_006, 1:100) and anti-tubulin to control for protein loading. Fig4 oligos do not affect any of the proteins detected by Fig4 serum.

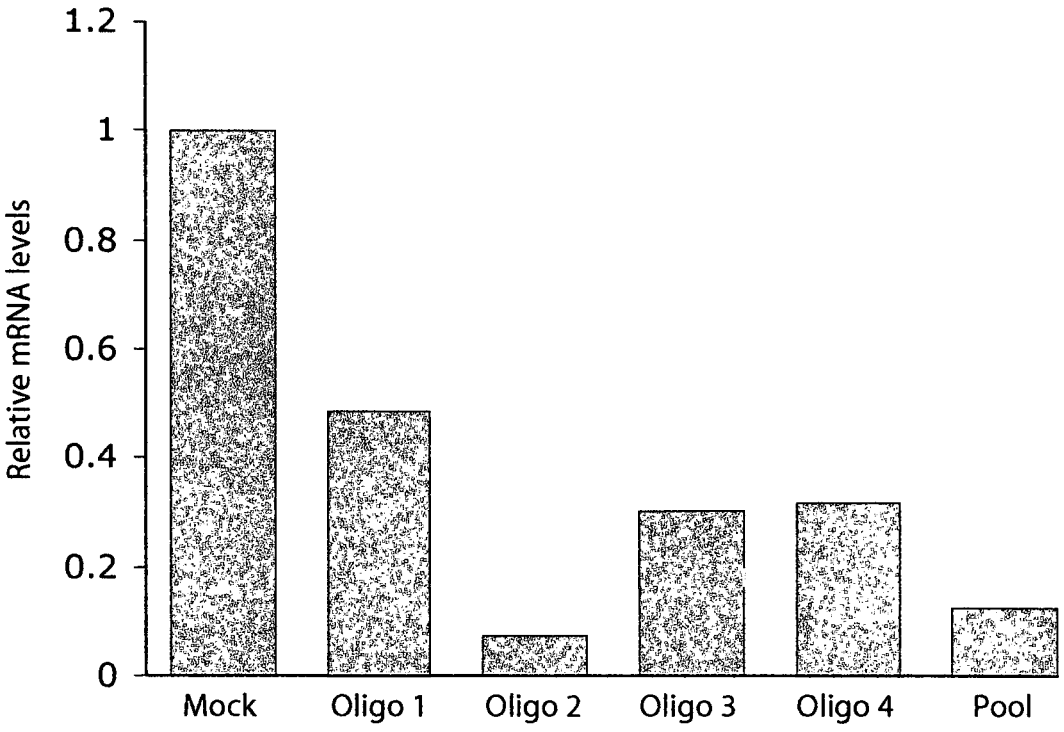

Figure 3.4. Fig4 siRNA oligos effectively reduce mRNA levels of Fig4 . HeLa cells were treated with 40nM individual and pooled siRNA oligos against Fig4 for 72 hours. Cells were then trypsinised, pelleted and RNA was extracted from the cell pellet. The RNA was reverse transcribed into cDNA and this was quantified by qPCR to determine the relative levels of mRNA in each sample compared to control cells. See materials and methods for details. Every oligo affects Fig4 mRNA levels to some extent, both the pooled oligo (used in this study) and oligo 2 give the most significant reduction in mRNA levels.

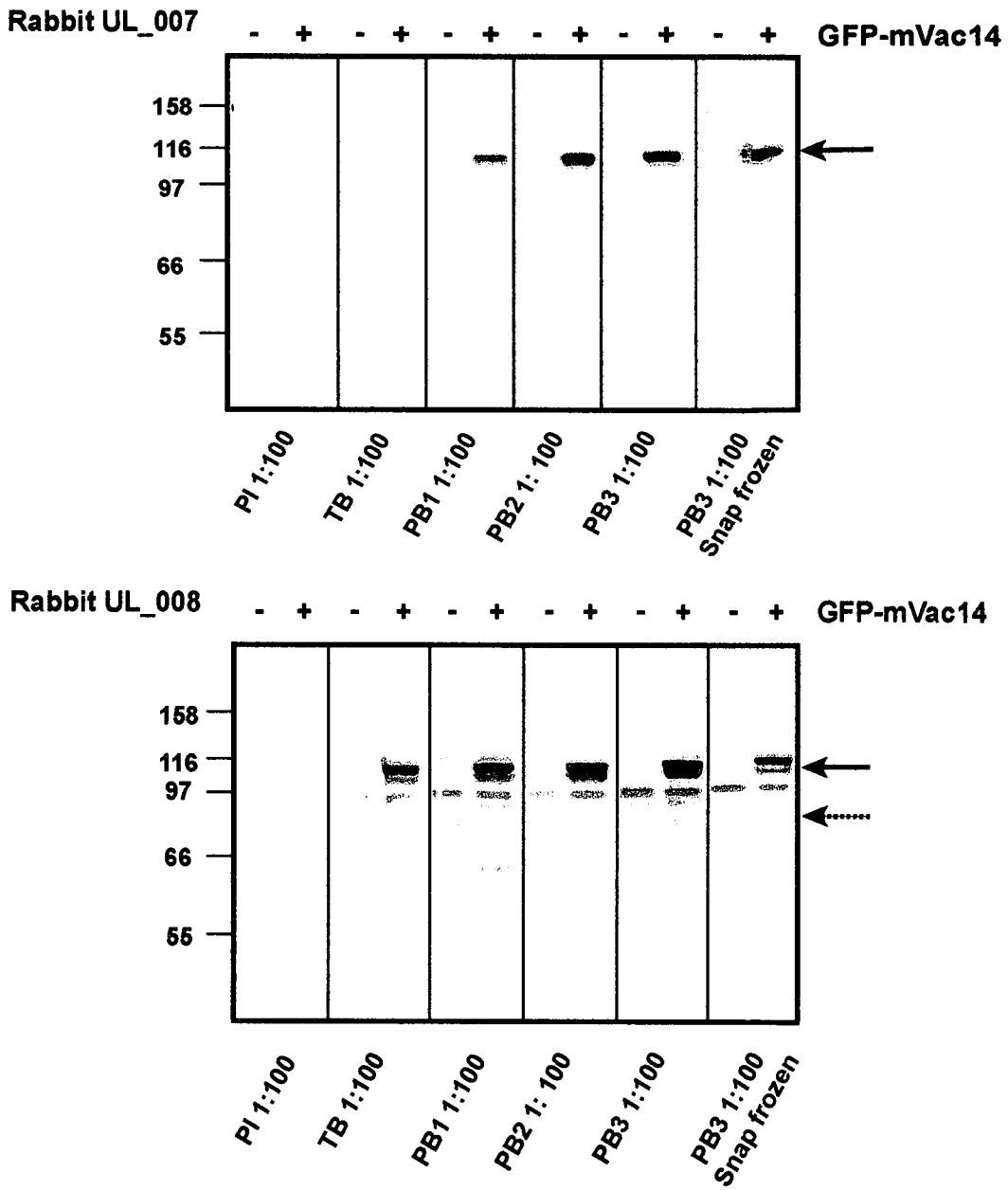

Figure 3.5. Determining the utility of anti-Vac14 antibody by Western blotting.

HeLa cells were either transfected with pEGFPC2-mVac14 (+) or left untransfected (-), lysed with hot lysis buffer after 24h, and 30μg lysates loaded onto an 8% SDS-PAGE gel. Material was transferred to a nitrocellulose blot and probed with each bleed (PI = Pre-immune, TB = Test bleed, PB = Production bleed) from 2 rabbits (UL_007 and UL_008). An aliquot was snap frozen in liquid nitrogen and thawed before use to ensure this did not adversely affect the activity of the serum.

There is a clear band corresponding to the overexpressed protein in each bleed (GFP-Vac14; 115kDa; solid arrow). Rabbit 008 may also detect endogenous protein (88kDa; dashed arrow).

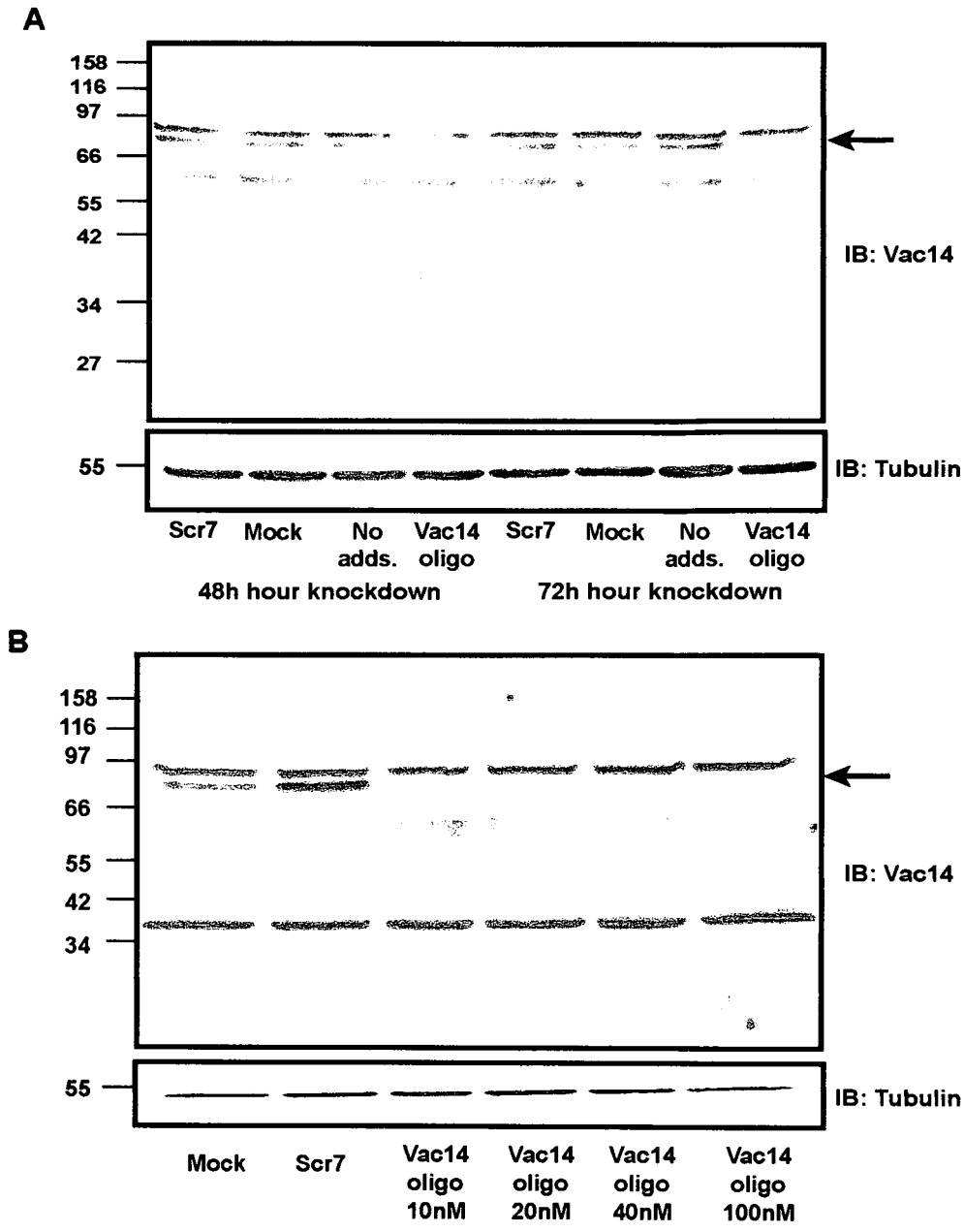

Figure 3.6. Vac14 serum detects endogenous protein by Western blotting.

HeLa cells were seeded onto 6-well plates and transfected with Dharmacon On-Target Plus SMARTpool™ Vac14 oligos for 48 or 72h. Cells were lysed in NP40 lysis buffer and 60μg lysates resolved on a 10% SDS-PAGE gel. Both no treatment (Mock), no oligo (no adds.) and scrambled oligo (Scr7) controls were also performed. Proteins were transferred to nitrocellulose and probed with anti-Vac14 serum (PB3, UL_008, 1:100) and anti-tubulin to control for protein loading.

A) Cells were transfected with 100nM oligos for both 48h and 72h.

B) Cells were transfected with 100nM scrambled and an increasing amount of Vac14 oligo (as indicated) for 72h.

A clear band at the level of endogenous Vac14 (88kDa; solid arrows) is knocked down even after 48h, and to an even greater extent after 72h. Knockdown occurs even at the lowest concentration of oligo.

3.2.4 Characterisation of antibodies against WIPI-2 by Western blotting

For WIPI-2 sera, rabbit UL_003 was able to detect overexpressed protein (GFP-WIPI-2; 76kDa; solid arrow) with increasing sensitivity across the bleeds, and still functioned after freeze-thawing. Rabbit UL_004 appears to detect a much weaker band at the correct molecular weight for overexpressed protein, suggesting that it has much lower sensitivity to rabbit UL_003. Conversely, rabbit UL_004 did detect some proteins at the correct molecular weight for endogenous protein (49kDa; dashed arrow) while rabbit UL_003 did not (Figure 3.7).

The terminal bleeds of each antibody were also tested at two different concentrations (Figure 3.8). These tests demonstrated that for WIPI-2 the terminal bleed of both rabbits were in fact able to detect overexpressed protein (solid arrow) and proteins at the correct molecular weight for endogenous WIPI-2 (dashed arrow), with rabbit UL_003 demonstrating higher sensitivity.

WIPI-2 serum is able to detect endogenous protein (Figure 3.9). A band corresponding to the correct molecular weight for endogenous WIPI-2 is substantially knocked down after both 48 and 72 hours of transfection, and with a range of different oligo concentrations. The molecular weight of this band is slightly higher than expected, with an electrophoretic mobility of 55kDa compared to the predicted 49kDa.

3.2.5 Affinity purification of Vac14 and WIPI-2 antibodies

Although both Vac14 and WIPI-2 antibodies were able to detect endogenous proteins, there were numerous other proteins also detected by

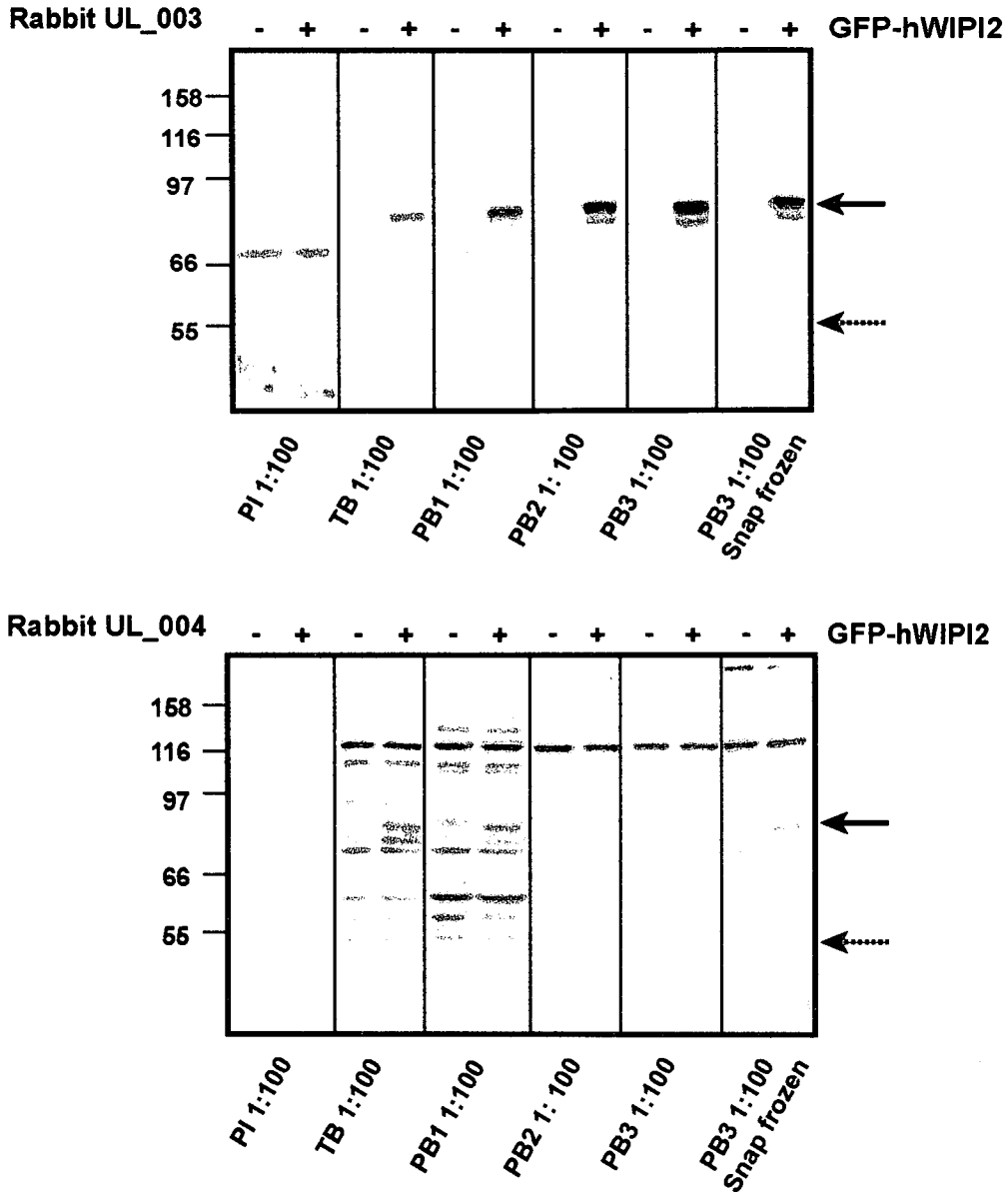

Figure 3.7. Determining the utility of an anti-WIPI-2 antibody by Western blotting.

HeLa cells were either transfected with pEGFPC2-hWIPI2 (+) or left untransfected (-), lysed with hot lysis buffer after 24h, and 30µg lysates were loaded onto an 8% SDS-PAGE gel. Material was transferred to a nitrocellulose blot and probed with each bleed (PI = Pre-immune, TB = Test bleed, PB = Production bleed) from 2 rabbits (UL_003 and UL_004). An aliquot was snap frozen in liquid nitrogen then thawed before use ensure this did not adversely affect the activity of the serum. A band of the correct molecular weight is clearly visible for overexpressed WIPI2 in all bleeds of rabbit 003 (GFP-WIPI-2; 76kDa; solid arrow). Rabbit 004 detects many more non-specific bands and poorly detects overexpressed WIPI-2. It is unclear if either serum detects endogenous protein (49kDa; dashed arrow).

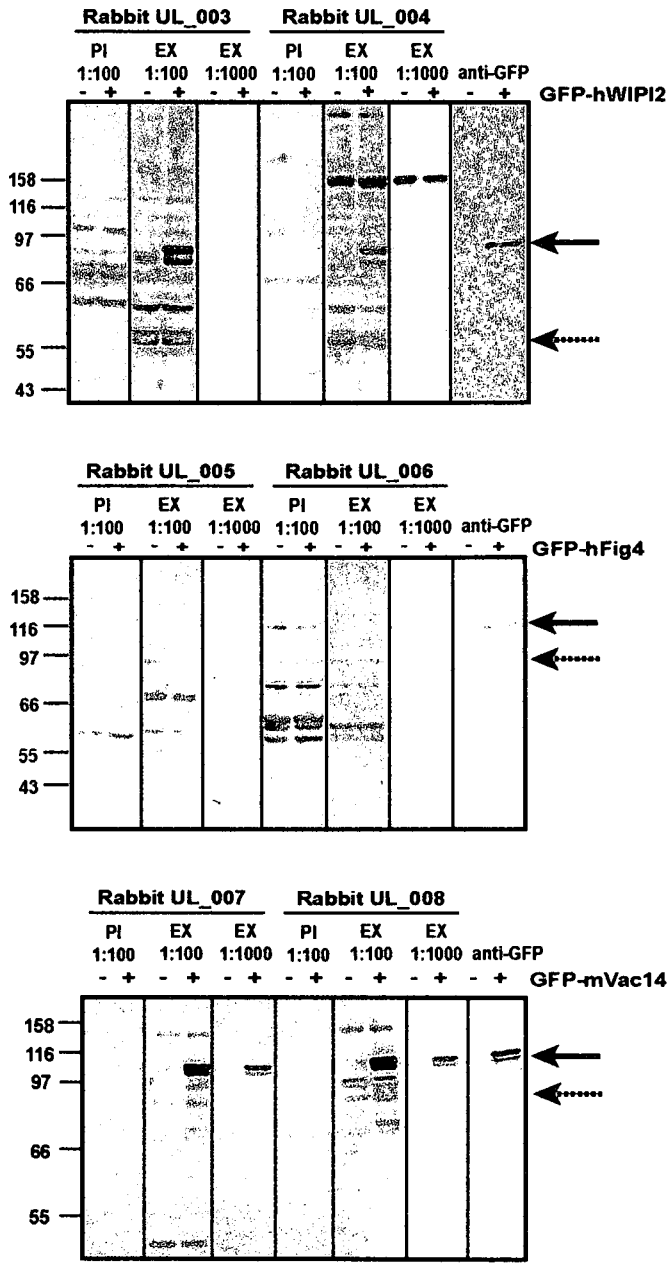

Figure 3.8. Characterisation of the final bleed of each antibody by Western Blotting.

HeLa or HEK293T cells were either transfected with GFP-Vac14, Fig4 or WIPI2 (+) or left untransfected (-), lysed with hot lysis buffer after 24h, and 30μg lysates resolved on an 8% SDS-PAGE gel. Material was transferred to a nitrocellulose blot and probed with final exanguination bleed (EX) and pre-immune (PI) serum from both rabbits. The final lane was probed with an anti-GFP antibody to show the correct molecular weight of overexpressed proteins. All bleeds from both rabbits of WIPI-2 and Vac14 serum detect overexpressed protein (97kDa and 115kDa; solid arrows), and possibly pick up endogenous protein also (49kDa and 88kDa; dashed arrows). Anti-Fig4 serum does not detect either overexpressed (solid arrow) or endogenous (dashed arrow) protein. GFP-Fig4 is correctly expressed as determined by anti-GFP blot (130kDa).

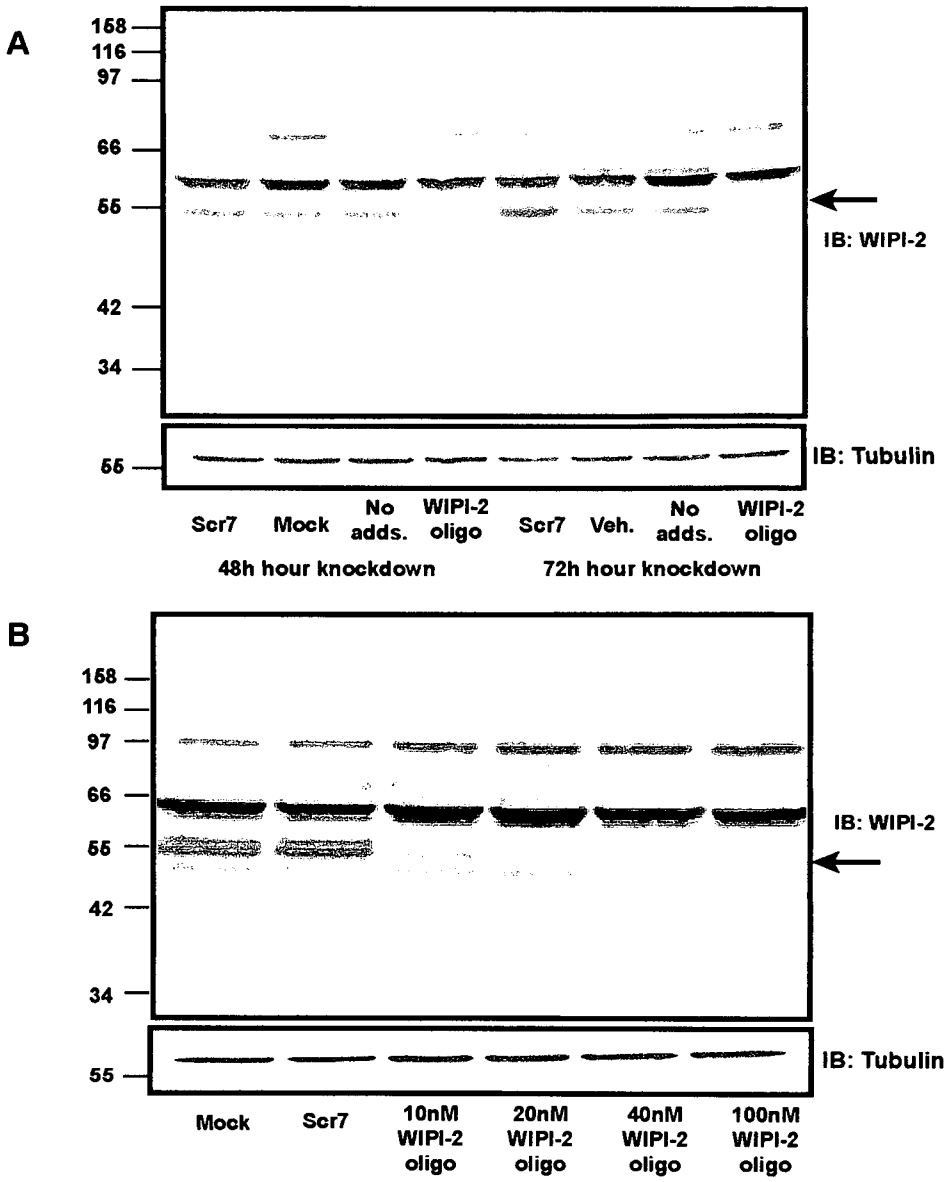

Figure 3.9. WIPI-2 antibodies detect endogenous protein by Western blotting.

HeLa cells were seeded onto 6-well plates and transfected with 100nM Dharmacon On-Target Plus SMARTpool™ WIPI-2 oligos for 48 or 72h. Cells were lysed in NP40 lysis buffer and 60µg lysates loaded onto an 10% SDS-PAGE gel. Both no treatment (Mock), no oligo (no adds.) and scrambled oligo (Scr7) controls were also performed. Protein was transferred to nitrocellulose and probed with anti-WIPI-2 serum (EX, UL_003, 1:100) and anti-tubulin to control for protein loading.

A) Cells were transfected with 100nM oligos for both 48h and 72h.

B) Cells were transfected with 100nM scrambled oligo and an increasing amount of WIPI-2 oligo for 72h.

A band is visible just above the 55kDa marker (solid arrows), which corresponds to endogenous WIPI-2, that is partially knocked down after 48h, but more substantially knocked down after 72h. This band is knocked down to some degree by all oligo concentrations.

these sera. By reducing the concentration of the final bleed, it was possible to reduce the amount of background bands, but it was then difficult to visualise the endogenous protein. To increase the specificity of these antibodies they were affinity purified against the peptides used for immunisation and the resulting affinity purified antibodies were subsequently retested by Western blotting. Both antibodies retain the ability to detect both overexpressed and endogenous protein by Western blotting, and both have a far reduced number of non-specific bands (Figure 3.10). In the case of WIPI-2, the predominant protein detected is now that which is suppressed by treatement with siRNA oligos.

In order to optimise these antibodies for use, and minimise the background to signal ratio, the affinity purified antibodies were tested at a range of different concentrations, to find an optimal working dilution. Affinity purified WIPI-2 is able to detect endogenous WIPI-2 at each concentration to some extent, but with the highest sensitivity at 1:100 and 1:250. Vac14 antibody is able to detect endogenous protein down to a dilution of 1:500 (Figure 3.11). In order to reduce the amount of non-specific background and to conserve antibody stocks WIPI-2 and Vac14 antibodies were typically used at a dilution between 1:250 and 1:500 (see table 3.2 for a summary).

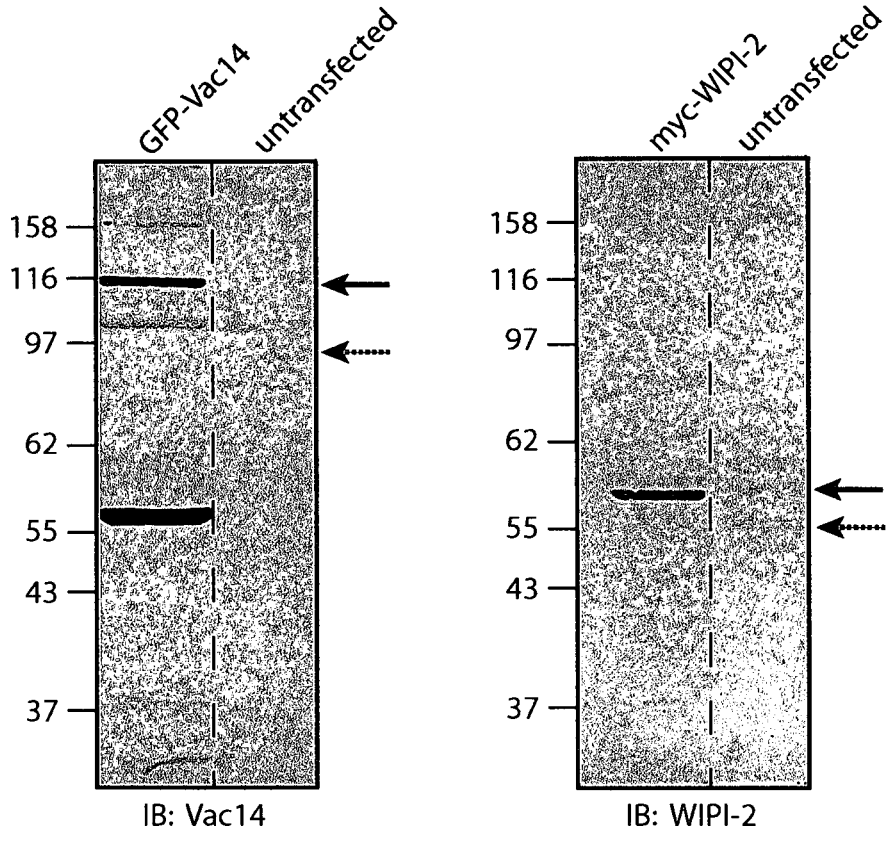

Figure 3.10. Specificity of affinity purified Vac14 and WIPI-2 antibodies for Western blotting.

HeLa cells were transfected with GFP-Vac14 and myc-WIPI-2 and lysates run next to untransfected controls on an SDS-PAGE gel. Proteins were transferred to nitrocellulose and probed with affinity purified antibodies to test their efficacy at specifically detecting endogenous and overexpressed Vac14 and WIPI-2. Both antibodies are still able to detect overexpressed and endogenous protein and detect far fewer non-specific proteins following affinity purification. Arrows mark the position of endogenous (dashed arrow) and overexpressed (solid arrow) proteins.

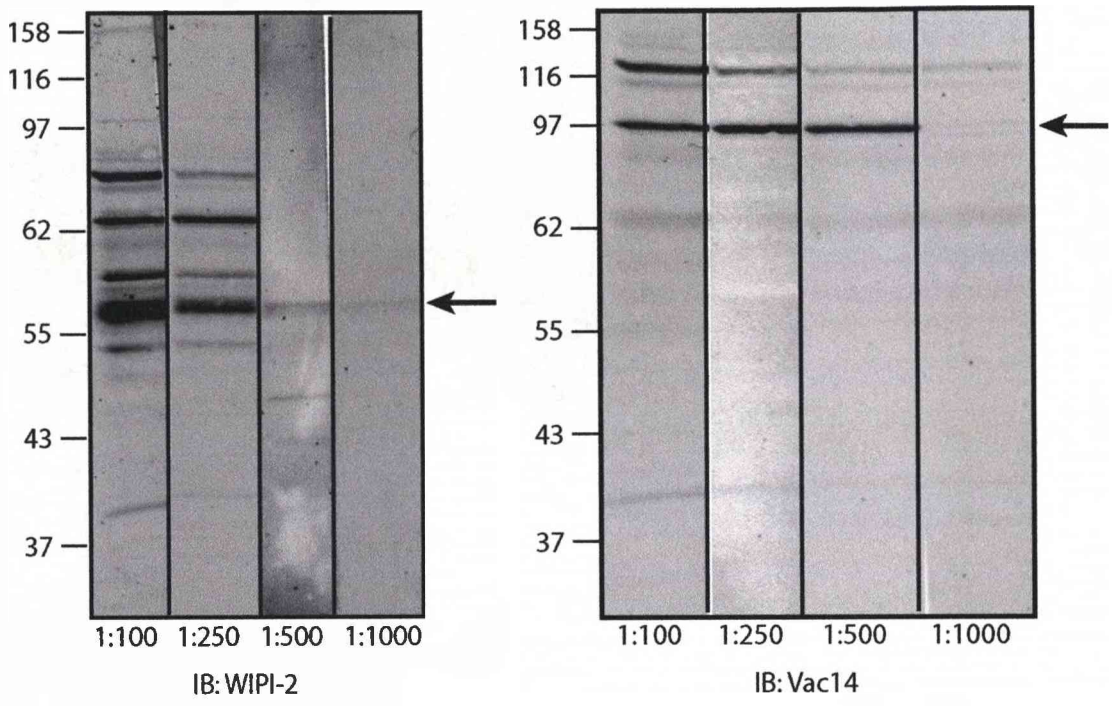

Figure 3.11. Determining the optimal working dilution of affinity purified antibodies for Western blotting.
HeLa cell lysates were resolved on a 10% SDS-PAGE gel. Proteins were transferred to nitrocellulose, and the blot was subsequently cut into one lane strips and probed with different concentrations of WIPI-2 and Vac14 antibodies, to determine the optimal working concentration for Western blotting. Solid arrows mark the position of endogenous protein.

Table 3.2. Summary of conditions for use of characterised antibodies

Antibody	Bleed	Dilution
Rabbit anti-Vac14	Production Bleed 3 UL_008	1:100
	Affinity purified	1:250-1:500 (WB and IF)
Rabbit anti-WIPI-2	Final bleed UL_003	1:100
	Affinity purified	1:250-1:500 (WB and IF)

3.2.6 Localisation of overexpressed proteins

In order to better understand the function of proteins associated with PtdIns(3,5)P_2 metabolism, it is essential to determine their intracellular localisation and thus their most likely sites of action. Each protein was cloned into a GFP tagged vector in order to determine the cellular localisation of the overexpressed protein in HeLa cells. Overexpressed proteins localise predominantly to the cytoplasm (Figure 3.12). However, for both GFP-mVac14 and GFP-hWIPI-2 an underlying punctate stain can be observed in a proportion of cells (approximately 20%). This punctate stain is more clearly revealed upon permeabilisation with saponin prior to fixation.

It has been suggested that Vac14, Fig4 and PIKfyve may all form part of a single protein complex (Sbrissa *et al.*, 2007). In fact Vac14 and Fig4 (Rudge *et al.*, 2004) have been shown to interact with one another, as have Vac14 and PIKfyve (Sbrissa *et al.*, 2004). More recently, an interaction between Vac14 and Svp1/Atg18 has been demonstrated (Tarassov *et al.*, 2008). It is therefore interesting to examine the colocalisation of each of these proteins, to see if they are found at a similar cellular localisation.

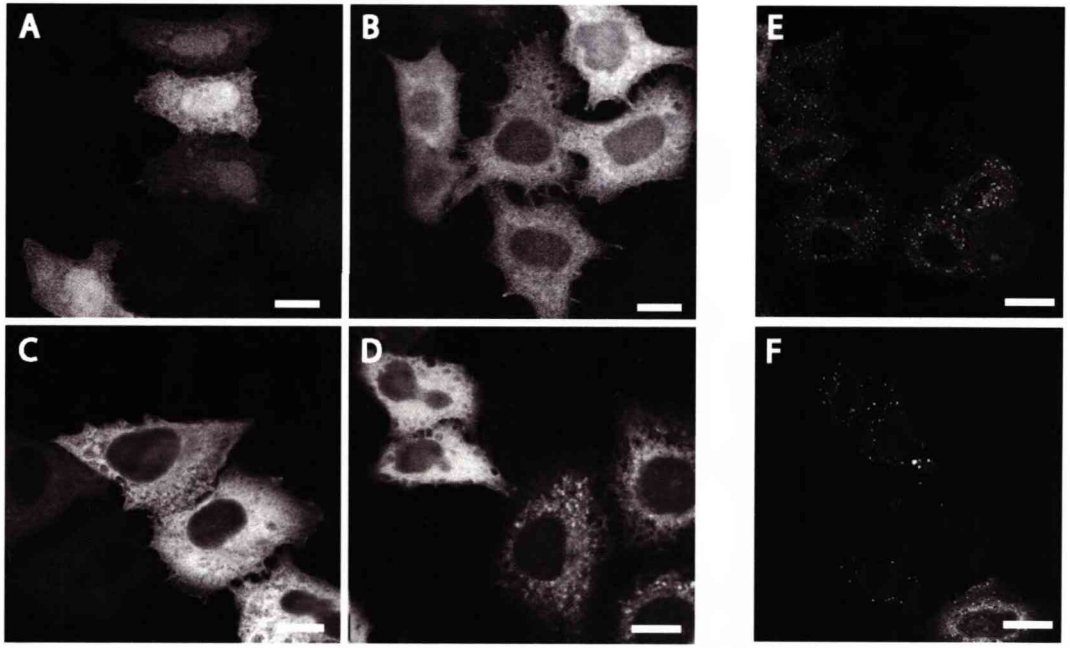

Figure 3.12. The localisation of GFP-tagged Fig4, Vac14 and WIPI-2.
HeLa cells were transfected with A) empty pEGFPC2 vector, B) pEGFPC2-mVac14, C) pEGFPC2-hFig4, and D) pEGFPC2-WIPI-2. 24h later cells were fixed with 3% PFA/PBS and permeabilised with 0.2% Triton/PBS. Each of the overexpressed proteins had a predominantly cytosolic distribution, somewhat reticular in appearance and are excluded from the nucleus. There is an underlying punctate stain in approximately 20% of cells, revealed by saponin permeabilisation for Vac14 and WIPI-2 (E and F respectively) . Confocal sections are shown. Scale bar represents 20μm.

Partial colocalisation of HA-mVac14 with both GFP-hWIPI-2 and GFP-hFig4 was observed (figure 3.13). Although this is somewhat unsurprising given the cytosolic nature of the proteins, the majority of colocalisation between GFP-Vac14 and GFP-Fig4 concentrates at seemingly reticular areas of the cell.

3.2.7 Localisation of endogenous proteins

Due to the caveats of examining overexpressed protein it would also be prudent to examine the localisation of endogenous protein if possible, thus the immunofluorescent staining of WIPI-2 and Vac14 antibodies was studied (Figure 3.14 and 3.15). By examining the colocalisation between overexpressed protein and the staining obtained with the terminal bleed of the two rabbits for each serum, it is clear that both antibodies are able to detect overexpressed protein in HeLa cells by immunofluoresence. Leica image analysis software was used to produce an intensity-scatter plot of the amount of colocalisation in each field of cells. The greater the colocalisation between the two channels the less scatter on both axis. Both sera work well for immunofluorescence at a dilution of 1:100 and 1:1000 and when cells are fixed with paraformaldehyde and permeabilised with Triton X-100. The pre-immune serum generates a much more random scatter plot than the antibodies, showing that it is not specifically detecting the overexpressed protein.

In order to improve the specificity of Vac14 and WIPI-2 antibodies, the sera were affinity purified. The affinity-purified serum was tested by immunofluorescence in HeLa cells, in both control cells and those treated

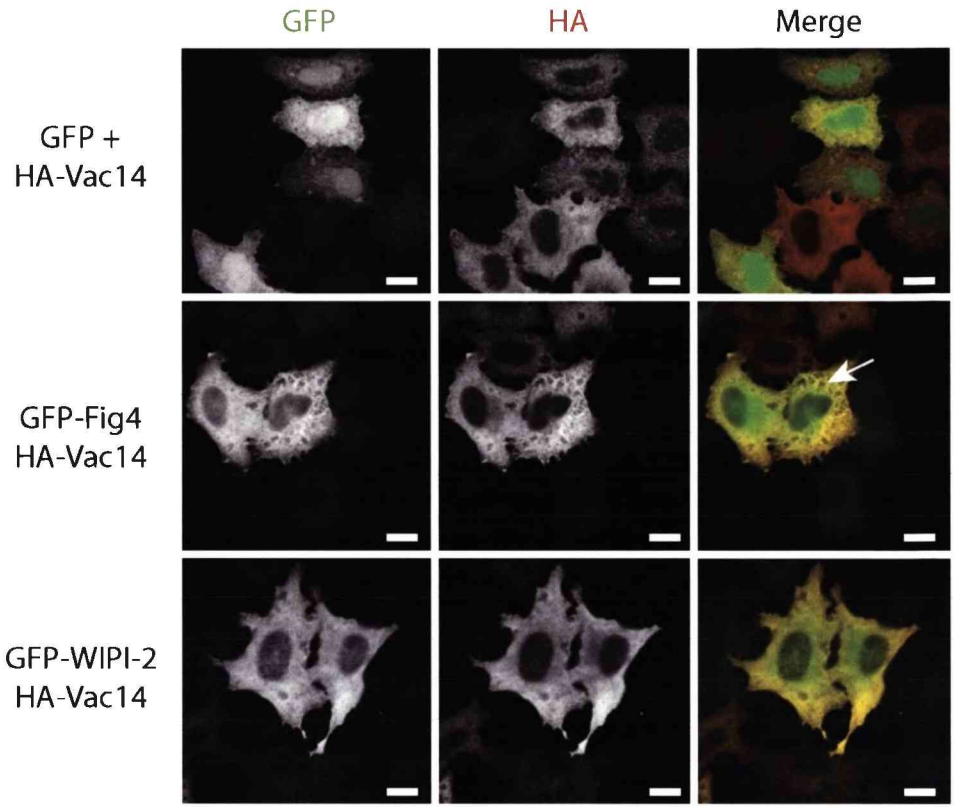

Figure 3.13. Overexpressed GFP-Fig4 and GFP-WIPI-2 partially colocalise with HA-Vac14.
HeLa cells were transfected with combinations of GFP-Fig4, GFP-WIPI-2 and HA-Vac14 for 24h and then fixed in 3% PFA/PBS and permeabilised with 0.2% TX-100. Empty GFP vector was used as a control. Both GFP-WIPI-2 and GFP-Fig4 partially colocalise with HA-Vac14. The colocalisation between GFP-Fig4 and HA-Vac14 is concentrated around areas of reticular stain (as marked with an arrow). Scale bars represent 20μm.

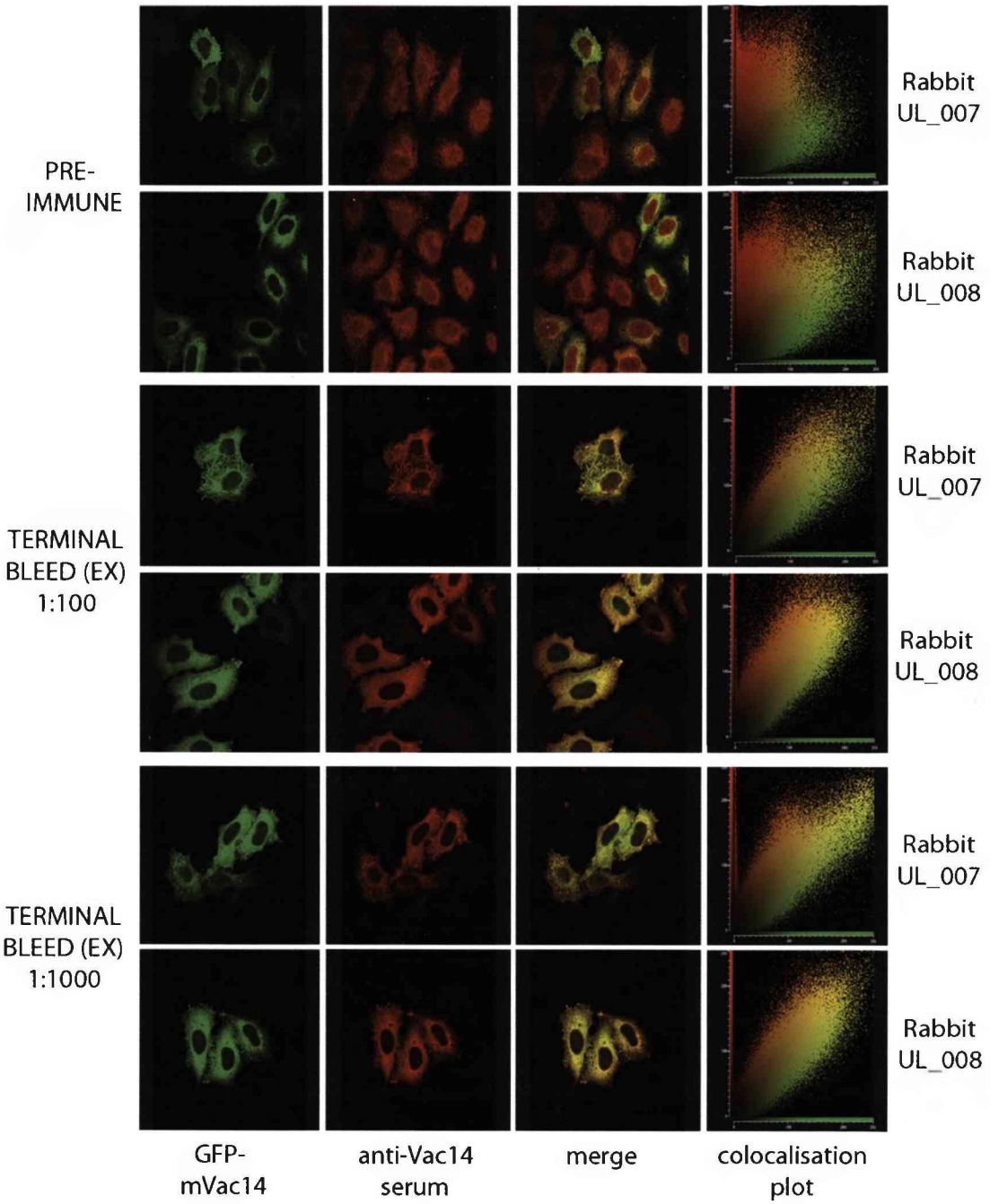

Figure 3.14. Determining the utility of anti-Vac14 antibody for immunofluorescence.

HeLa cells were transfected with a pEGFPC2-mVac14 construct. 24h after transfection cells were fixed with 3%PFA/PBS, permeabilised with 0.2% Triton/PBS and stained with the terminal bleed of anti-Vac14 serum at 1:100 and 1:1000. Secondary antibodies used were AlexaFluor594 donkey anti-rabbit. Cells were visualised on a Leica confocal microscope and a colocalisation scatter plot of each field of cells was produced using leica based software.

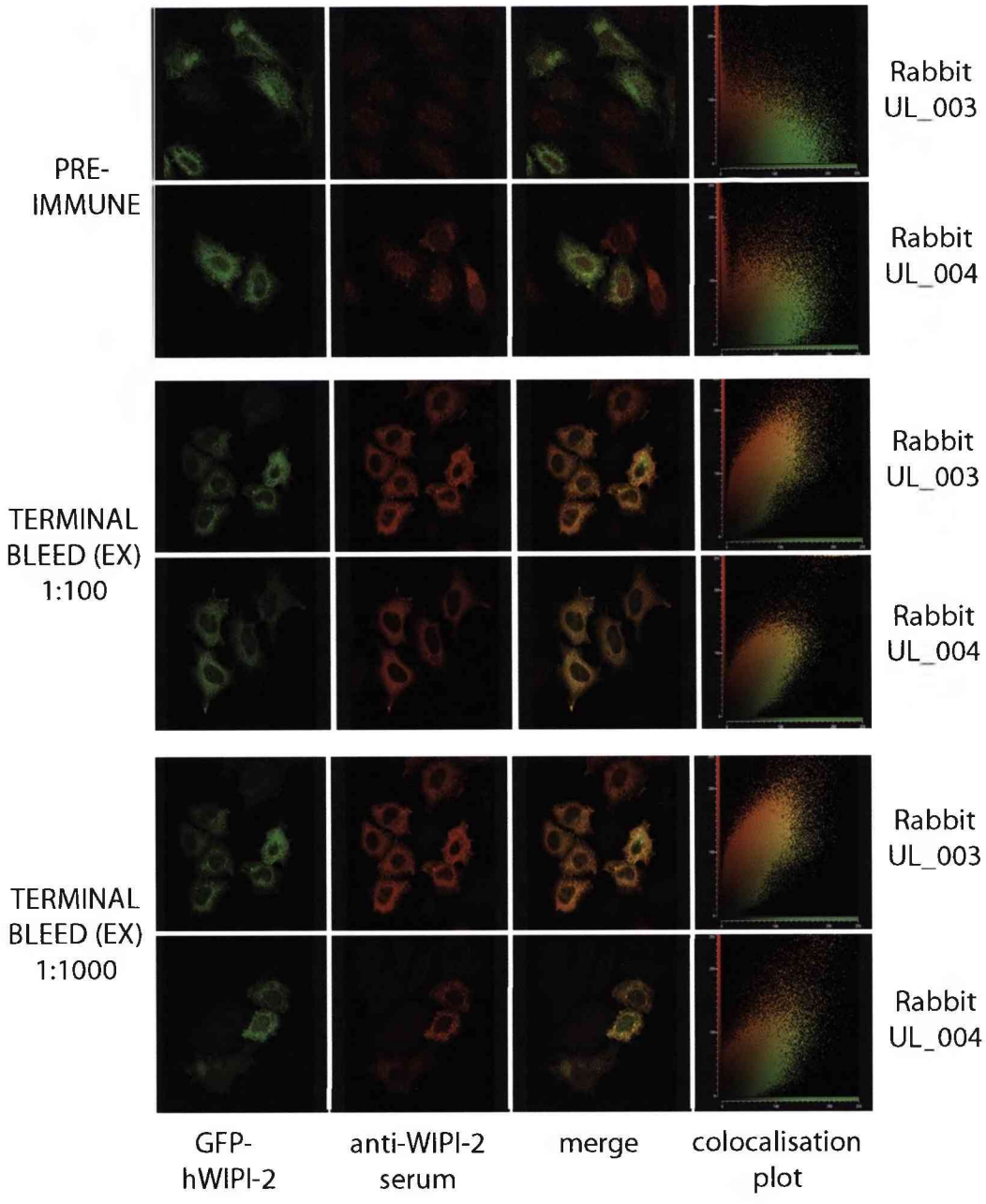

Figure 3.15. Determining the utility of anti-WIPI-2 antibody by immunofluorescence.

HeLa cells were transfected with pEGFPC2-hWIPI-2. 24h after transfection cells were fixed with 3%PFA/PBS, permeabilised with 0.2% Triton/PBS and stained with the terminal bleed of anti-WIPI-2 serum at 1:100 and 1:1000. Secondary antibodies used were AlexaFluor594 donkey anti-rabbit. Cells were visualised on a Leica confocal microscope and a colocalisation scatter plot of each field of cells was produced using leica based software.

with siRNA oligos. The cytosolic staining detected by both Vac14 and WIPI-2 antibodies is lost following siRNA knockdown of these proteins, suggesting that the endogenous protein is being detected, and that the cytosolic stain represents a pool of endogenous protein (Figure 3.16). The punctate structures observed with overexpressed proteins may be an artefact of overexpression, or the sensitivity of the antibodies may not be high enough to detect the endogenous protein on these structures.

3.2.8 Production of purified recombinant Vac14 protein

Another key tool for studying aspects of these proteins is to produce recombinant protein. Both bacterial and baculovirus expression systems were used to attempt to purify His-tagged Vac14, WIPI-2 and Fig4 (see materials and methods for details of expression and purification). Vac14 was purified in bacterial cells. One-shot BL21(DE3)pLysE chemically competent *E. coli* were transformed with pTrcHis-mVac14. Protein production was induced with 0.1mM IPTG for 4 hours at 37°C (the optimum conditions for protein production were determined by testing a variety of temperatures, times and concentrations of IPTG). 50µl samples were taken from each stage of the purification procedure, and 5 or 10µl of each sample resolved on a 10% SDS-PAGE gel. This has been represented as the percentage input from the original sample in a Western blot of the various stages of protein purification, probed with anti-Vac14 antibody (Figure 3.17). It is clear that Vac14 protein production is induced, but there is 'leaky' expression of the protein by the promoter, as it also present in the uninduced sample. Note that less of the induced than uninduced input was loaded on the gel. This

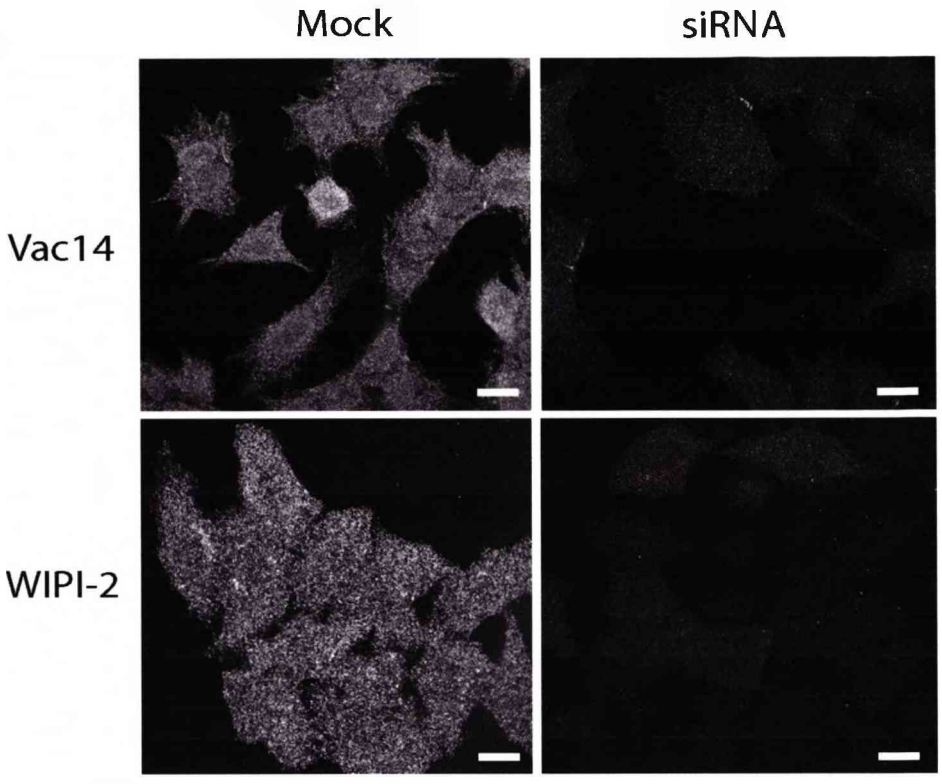

Figure 3.16. Specificity of WIPI-2 and Vac14 antibodies for immunofluorescence.
HeLa cells were fixed, permeabilised and stained with affinity purified antibodies against Vac14 and WIPI-2 in control cells and in cells treated with siRNA against the respective protein, to determine the specificity of immunofluoresent staining of the two antibodies. The majority of immunofluorescent stain is depleted following knockdown of the respective protein, suggesting the cytosolic staining is specific.

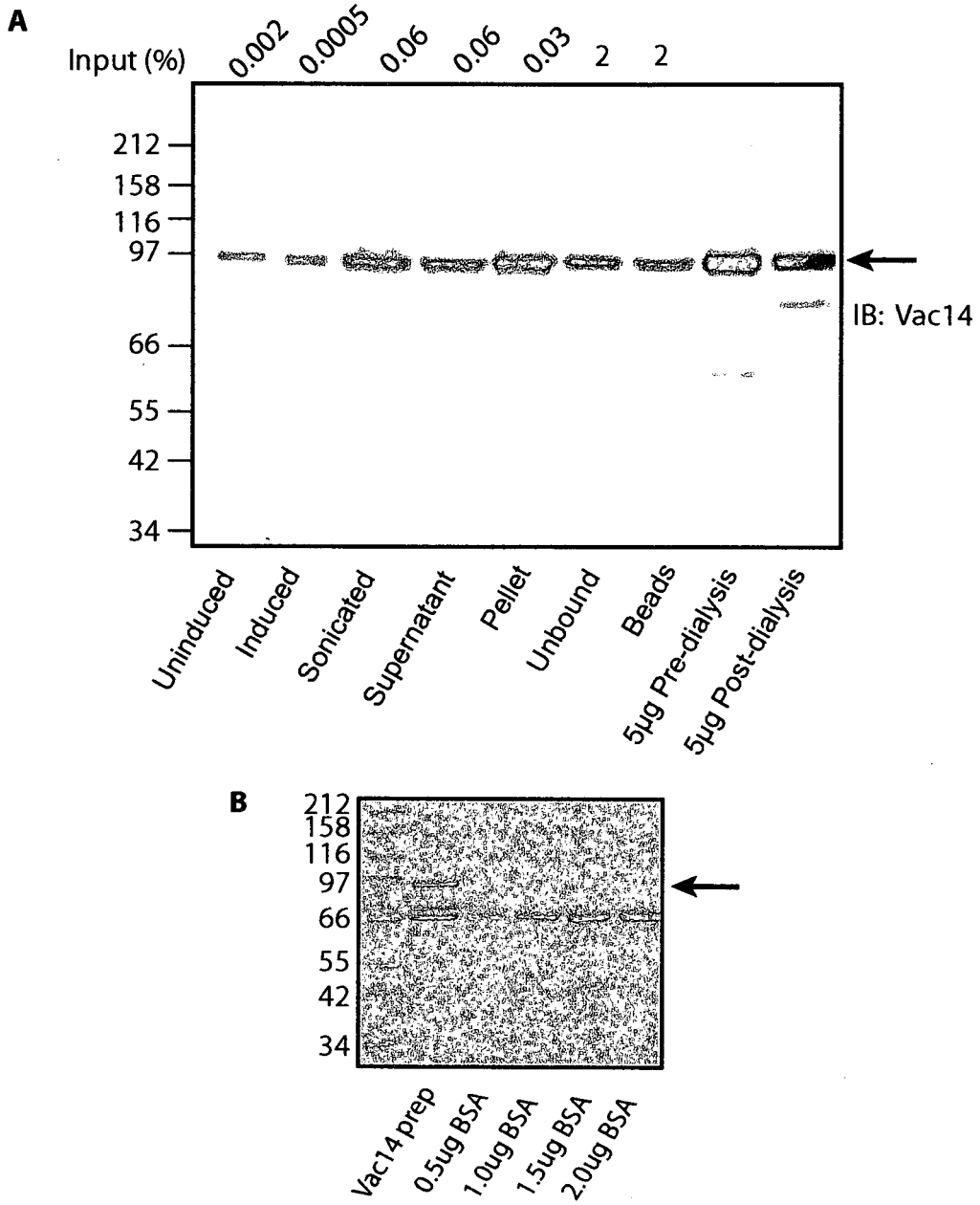

Figure 3.17. Western blot analysis of the expression of His$_6$-mVac14 in BL21 bacterial cells.

His$_6$-Vac14 protein production was induced with 0.1mM IPTG at 37°C for 4 hours and purified on Nickel-NTA beads.

A) Purification samples were analysed by 10% SDS-PAGE, transferred to nitrocellulose and stained with anti-Vac14 antibodies. Molecular weight of His-Vac14 is 91.6kDa.

B) His$_6$-mVac14 protein and a gradient of BSA were run on a 10% SDS-PAGE gel and stained with Coomasie blue. The concentration of full-length His$_6$-mVac14 is between 1 and 1.5µg/µl.

explains why there appears to be no induction of the protein. Protein is lost throughout the course of the purification procedure, with the bulk of protein being insoluble and thus left behind in the pellet fraction. A significant amount also remains bound to the Ni-NTA beads and there are some degradation products detectable after dialysis.

Purified Vac14 protein was compared to a BSA gradient and this shows that the concentration of full-length useable protein was between 1 and 1.5µg/µl. It is interesting to note that degradation/truncation products are present in the final purified protein preparation when examined by Coomassie stain (3.17 B) but not by Western blot (3.17 A). As the antibody used for Western blotting (anti-Vac14) is directed against the C terminus of the protein, it is possible that it does not detect these products as they originate from the His-tagged N terminus, likewise if they represent truncation products. Alternatively, these bands could represent bacterial proteins that have adhered to the beads and are therefore not detected by a Vac14 antibody.

3.2.9 Production of purified recombinant WIPI-2 protein

One of the key goals of obtaining purified proteins would be to examine all three proteins and their interactions with one another. The baculovirus system was used to produce both WIPI-2 and Fig4. Insect cells (Sf9) were transfected with pAcHis-hFig4 or pAcHis-hWIPI-2 along with baculovirus DNA (see materials and methods for details). For optimal production of protein the ratio of virus particles per cell, termed the multiplicity of infection (MOI), must also be optimal. Too low and

asynchronous replication and premature cell lysis can lead to reduced and delayed protein production. Too high and the virus propagates too rapidly, leading to depletion of cellular metabolites before optimum protein production is achieved. It is therefore important to titrate the virus that is produced, to achieve the correct balance. For His_6-WIPI-2 virus, this titration is shown in figure 3.18 A. The virus can be amplified by reinfection of Sf9 cells if necessary, to achieve a higher viral titre.

By coomassie stain the protein of interest was undetectable, thus I transferred the protein to nitrocellulose and probed with the anti-WIPI-2 antibody to determine if protein was produced. From the viral titration it is clear that the lysis or recovery of lysed material was somewhat uneven as the protein levels fluctuate. Previous experience in the lab established that typically between 0.39 and 0.78µl per 5×10^4 cells usually resulted in a high level of protein production. Given that protein levels began to reduce from 0.78µl and above, and that past experience had shown that lower amounts of virus did not produce optimal amounts of protein when scaled up despite indications from the titration, I chose to use 170µl of virus for 2×10^7 cells. This corresponds to 0.425µl of virus per 5×10^4 cells, a range in between the two optimum values.

Protein was purified in a similar manner to bacterial protein. The resultant purification steps for WIPI-2 are shown by Western blot in figure 3.18 B. Although WIPI-2 protein was produced, the majority of protein was insoluble, potentially forming inclusion bodies. And the protein that was not insoluble subsequently dropped out of solution during the dialysis stage. Thus, no useable WIPI-2 protein was produced. Fig4 protein was also not

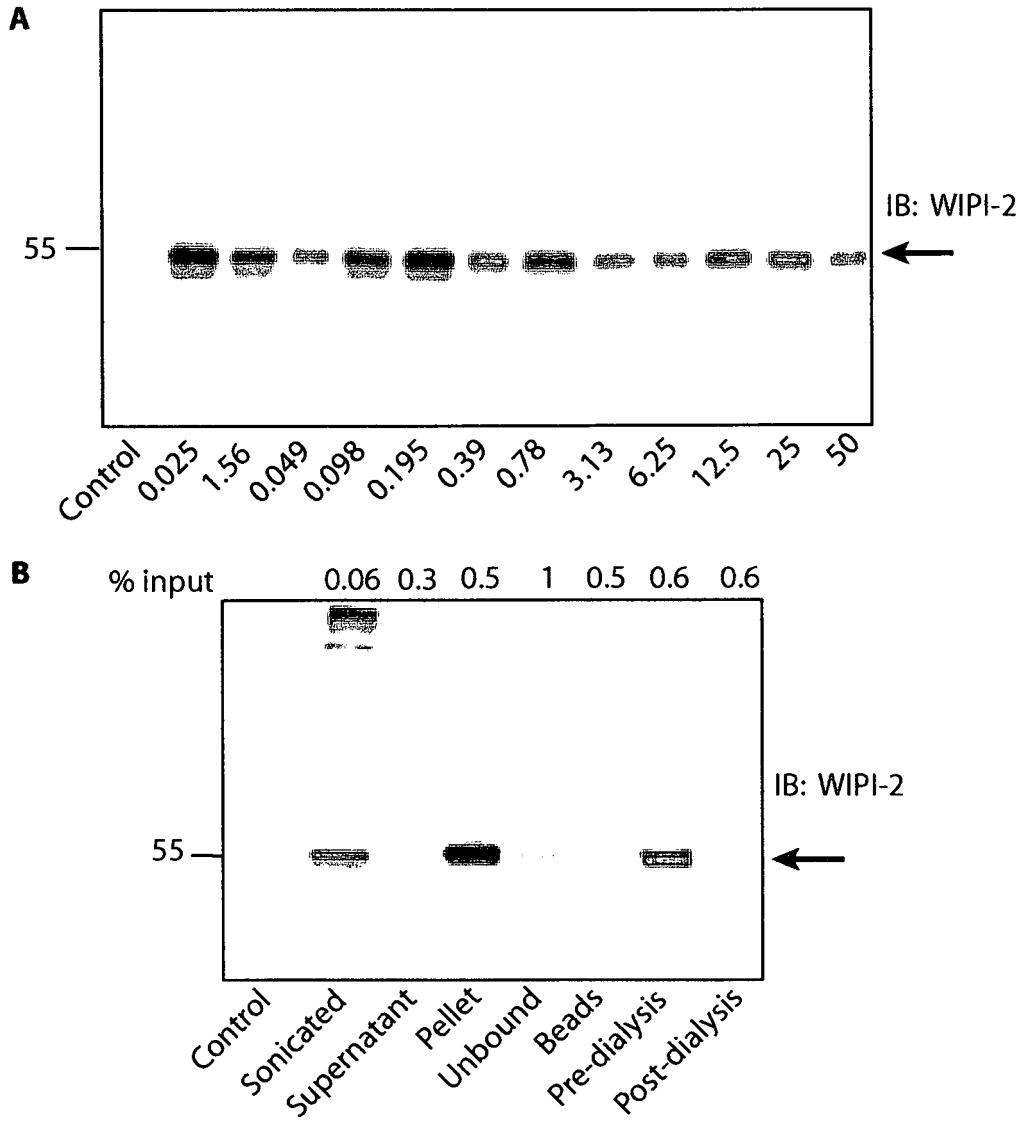

Figure 3.18. His_6-WIPI-2 recombinant protein production using the baculovirus system.

His_6-WIPI-2 protein was produced using the baculovirus system from Sf9 insect cells.

A) Titration of the amplified pAcHis-WIPI-2 virus (see materials and methods for details). The protein was undetectable by Coomasie stain, but once transferred to nitrocellulose and probed with anti-WIPI-2 antibody it could be clearly seen. The titration was used to determine the optimal viral concentration for protein production. Predicted molecular weight of His_6-WIPI-2 is 51.4kDa.

B) Western blot analysis of the stages of His_6-WIPI-2 protein production probed with anti-WIPI-2 antibody. Percentage input represents the amount of total material loaded onto gel. A substantial amount of protein is insoluble. The rest drops out of solution during dialysis.

successfully produced using this system. In this case the initial titration of the virus, showed that recombinant Fig4 virus was not produced, this was judged by Coomassie stain and Western blotting with an anti-His antibody (not shown).

3.2.10 Interaction between Fig4 and Vac14 demonstrated by coimmunoprecipitation of overexpressed proteins

The final stage in characterisation of the three proteins was to examine any possible interactions between them. It had previously been reported that the yeast Vac14 and Fig4 interact with one another (Rudge *et al.*, 2004), and I was able to confirm this finding in mammalian cells, both by coimmunoprecipitation (Figure 3.19), as also described recently in the literature (Sbrissa *et al.*, 2007), and by yeast two-hybrid directed screen (Figure 3.21). It would be useful to also examine the coimmunoprecipitation of the endogenous proteins, however, this was not possible due to the unsuitability of the Fig4 antibody.

3.2.11 Overexpression of Vac14 stabilises Fig4

It was also noted by examining coexpression of HA-Vac14 and GFP-Fig4 by Western blotting, that expression of HA-Vac14 stabilises the expression of GFP-Fig4 (Figure 3.20). Typically, the expression of GFP-Fig4 in HeLa cells is very low, however, upon cotransfection with HA-Vac14 we see a clear band appear that corresponds to the correct molecular weight for GFP-Fig4. Equal protein loading in these two lanes was confirmed by blotting with anti-tubulin antibodies. A similar observation was made in the

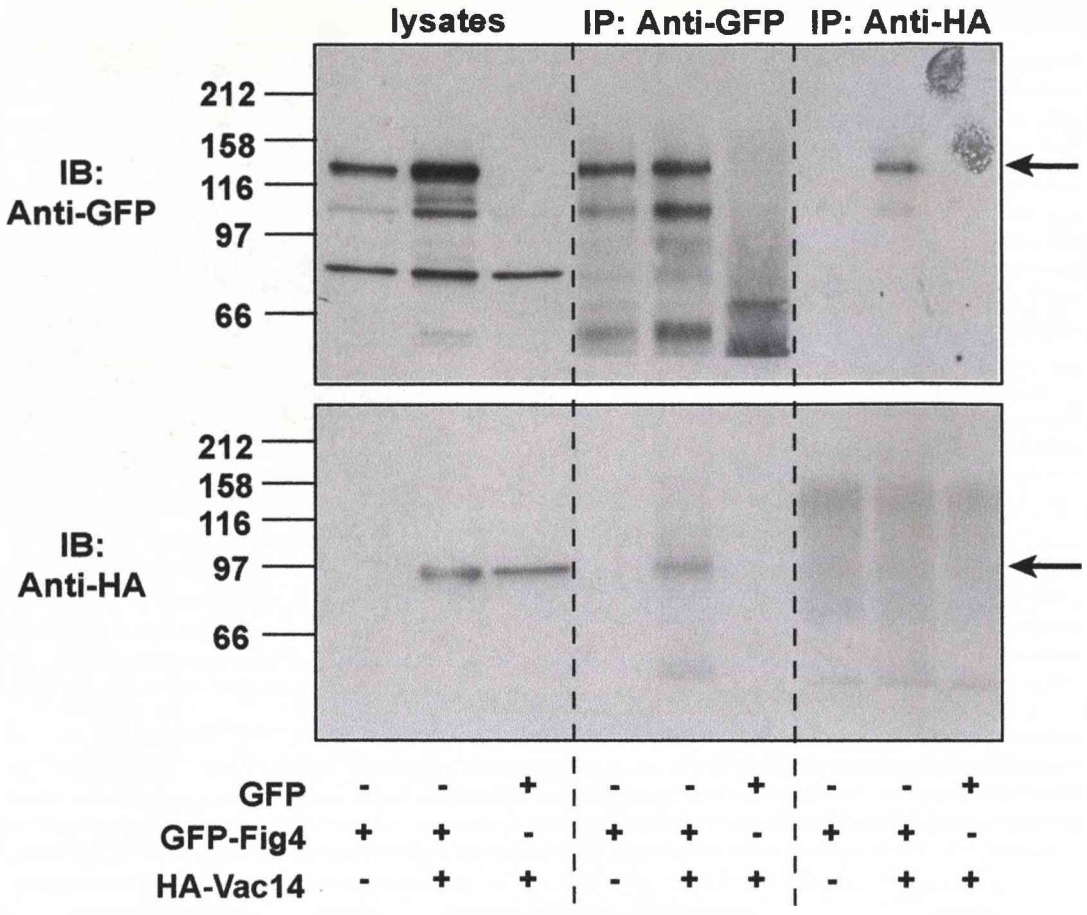

Figure 3.19. Overexpressed GFP-Fig4 and HA-Vac14 coimmunoprecipitate with one another.
HeLa cells were transfected with combinations of GFP-Fig4 and HA-Vac14 for 24h and then lysed in NP40 lysis buffer. 750ug protein was immunoprecipitated with the opposing primary antibody (either sheep polyclonal GFP or mouse monoclonal HA). IP and non-IP lysates were loaded onto an 8% SDS-PAGE gel, proteins were transferred to nitrocellulose and this was subsequently probed with anti-GFP or anti-HA antibodies. GFP-Fig4 is detected by an anti-HA antibody in the IP samples, and vice versa for HA-Vac14, indicating the two overexpressed proteins coimmunoprecipitate with one another.

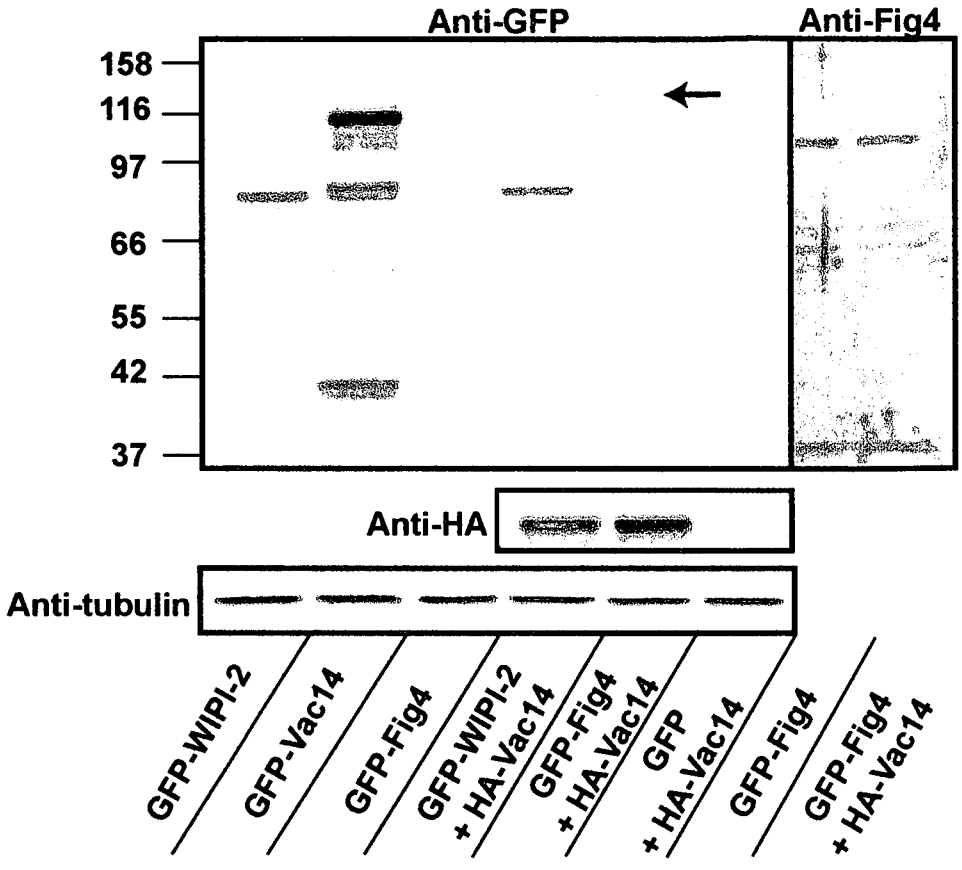

Figure 3.20. HA-Vac14 stabilises GFP-Fig4.
HeLa cells were transfected with the constructs indicated and lysed 24 hours later using NP40 lysis buffer. Cell lysates (60µg) were resolved on an 8% SDS-PAGE gel and electrophoresed material was subsequently transferred to a nitrocellulose blot. The membrane was probed with monoclonal anti-GFP and monoclonal anti-HA antibodies. The final two lanes were separated from the rest of the blot and probed with anti-Fig4 polyclonal serum. Clear bands at the correct molecular weight for each over-expressed protein can be identified, except for GFP-Fig4 where no band is detected. However, upon coexpression with HA-mVac14 a distinct band corresponding to GFP-Fig4 is visible (arrow). This is not the case when the same material is probed with anti-Fig4 serum, no band is detected in either lane.

literature by immunofluorescence of overexpressed Fig4 and Vac14 in Cos-7 cells, the abundance of Fig4 vesicular structures increased when Fig4 and Vac14 were expressed together (Sbrissa *et al.*, 2007). It was hoped that if coexpression with Vac14 could increase the stability of Fig4, then I might be able to see at least overexpressed protein with the anti-Fig4 antibody, and possibly even endogenous protein. This was found not to be the case. Perhaps the levels of overexpressed Fig4 produced are still below the detection threshold of the Fig4 antibody, or the C terminus of the protein, to which the antibody is directed, is degraded.

3.2.12 Interactions demonstrated by directed yeast-two hybrid screen

A directed yeast two-hybrid screen (Figure 3.21) reinforces the interaction between mammalian Fig4 and Vac14. This interaction is found when the proteins are in both bait and prey vectors, although it is stronger when Vac14 is in the prey vector and Fig4 in the bait vector. Interestingly, we also see an interaction between WIPI-1 and WIPI-2. Due to unavailability of the pACT2-WIPI-1 construct, I was unable to test this interaction in both directions. Interestingly, Vac14 is shown to interact with itself, suggesting that this protein may dimerise.

Yeast two-hybrid interactions were confirmed using a beta-galactosidase assay, to examine production of this enzyme. Interacting partners should reconstitute the DNA binding and activation domain of the lacZ gene and expression of beta-galactosidase. If this enzyme is produced then the reagent used in the assay should be turned blue. The interaction between Vac14 and Fig4 is confirmed by beta-galactosidase assay when the

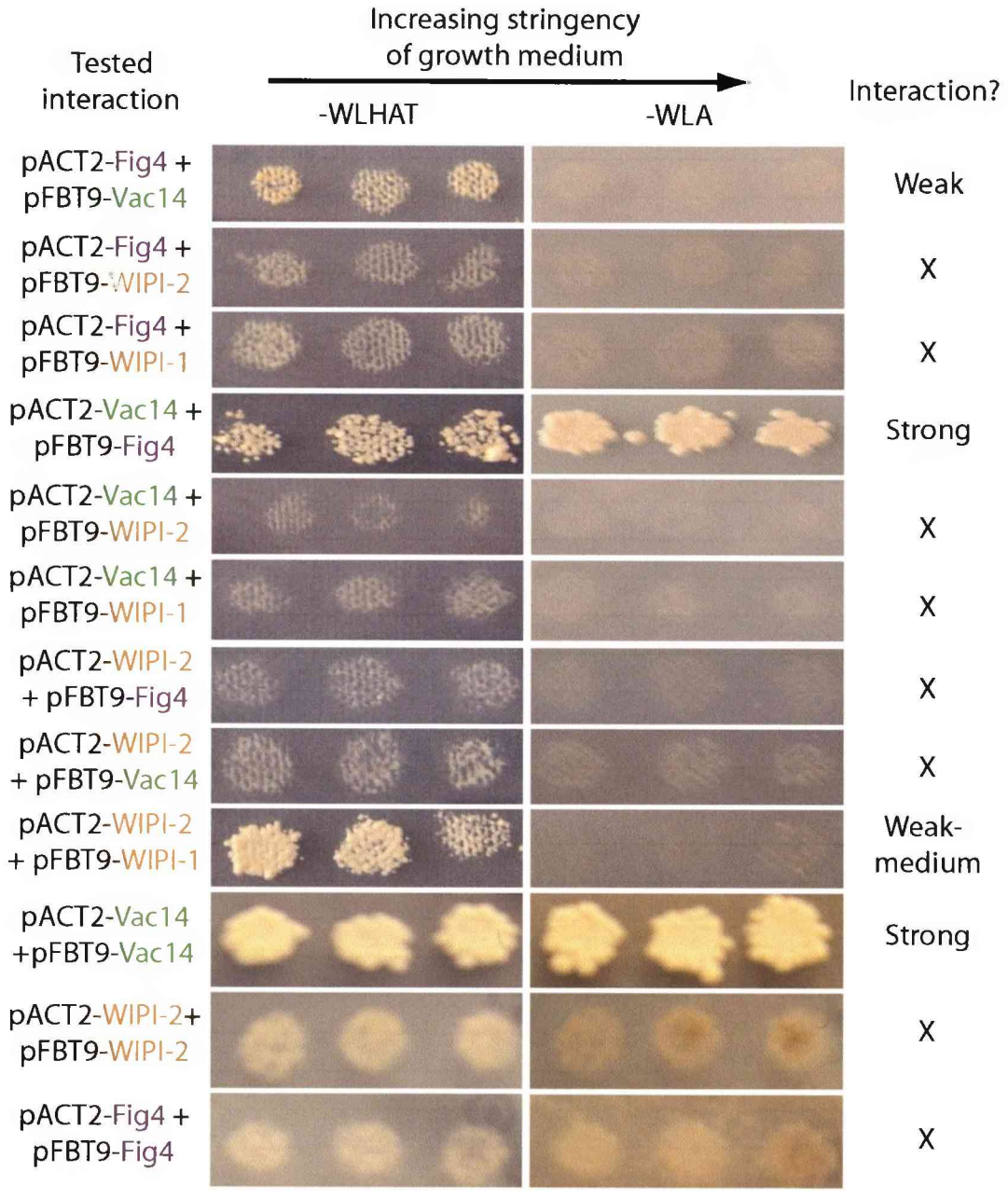

Figure 3.21. Directed yeast two-hybrid screen confirms interaction between mammalian Vac14 and Fig4.
A directed screen employing each protein in both bait and prey vectors was carried out through mating of mat-a and mat-α PJ69-4A yeast. Mated yeast were plated on selection media of increasing stringency and growth was used to score the strength of interaction. Vac14 and Fig4 interact with one another, WIPI-1 and WIPI-2 also interact, and Vac14 interacts with itself.

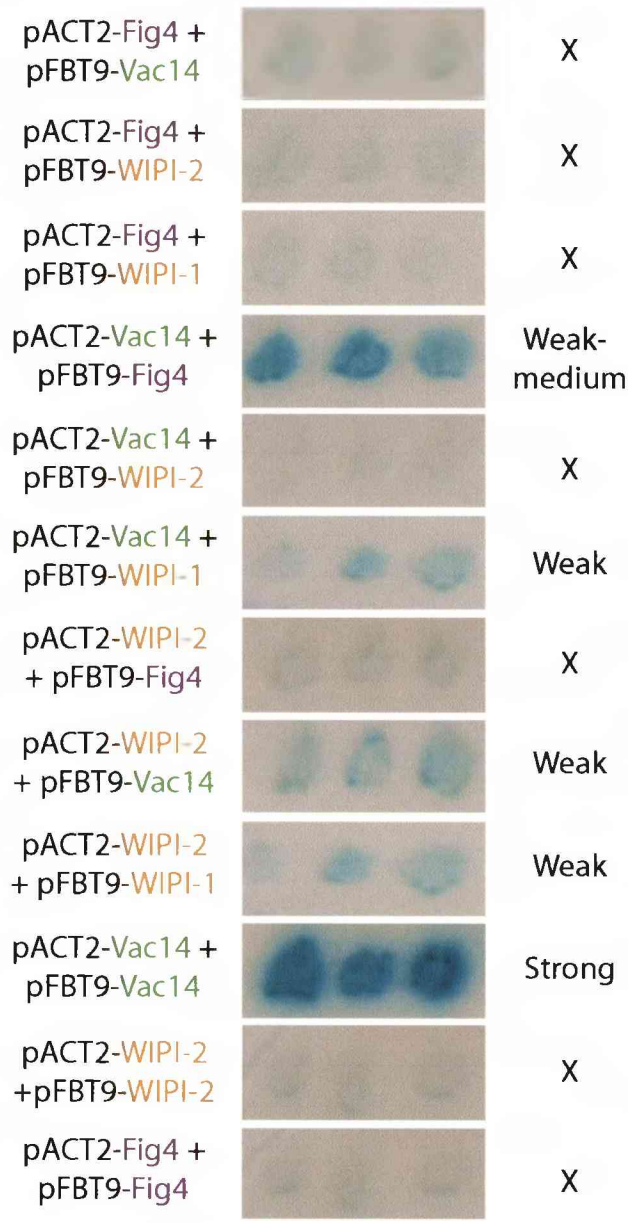

Figure 3.22. Beta-galactosidase assay confirms two-hybrid interactions.

Diploid yeast from the yeast two-hybrid screen were tested for beta-galactosidase enzyme activity. Strong development of blue colour confirms the interaction between Vac14 and Fig4 and Vac14 with itself. There is also weak enzyme activity for WIPI-2 and WIPI-1, and Vac14 with WPI-1 and WIPI-2.

interaction is strong, but not for the weaker interaction when the bait and prey constructs are swapped (Figure 3.22). The interactions between WIPI-1 and WIPI-2 and Vac14 and itself are also confirmed. There is also weak production of this enzyme in the interactions between Vac14 and both WIPI proteins, although this was not detected in the yeast-two hybrid assay itself.

3.3 Discussion

The work presented in this chapter set out to develop key tools to facilitate the study of mammalian PtdIns(3,5)P_2 through analysis of four proteins that regulate its metabolism and cellular functions. A range of mammalian expression vectors and yeast two-hybrid constructs were generated and used in recombinant protein production, localisation studies, and interaction analysis. Functional antibodies against WIPI-2 and Vac14 were generated, that were able to detect both overexpressed and endogenous protein by Western blotting and immunofluorescence, to some extent. Given that there are no antibodies to these proteins commercially available, these are invaluable resources. They were utilised to great extent in this study in order to validate siRNA suppression of proteins (see chapter four), to examine protein localisation (this chapter), and in autophagy studies (see chapter six).

In this chapter I demonstrated that all three overexpressed proteins display a predominantly cytosolic stain, with a reticular pattern in the case of overexpressed Vac14, similar to that seen in Cos-7 cells (Sbrissa *et al.*, 2004), and an underlying punctate stain to some extent in all three. The punctate staining of Fig4 is also reminiscent of that seen in Cos-7 cells

(Sbrissa *et al.*, 2007). None of these proteins are predicted to possess any transmembrane domains, thus the cytosolic staining is unsurprising. However, saponin permeabilisation revealed a weak underlying punctate stain in the case of Vac14 and WIPI-2, which may indicate that these proteins also have a transient association to membranes, potentially to the early endosomes where PIKfyve is found (Rutherford *et al.*, 2006). The nature of the punctate compartments remains somewhat elusive, as the low levels of expression made colocalisation with other markers difficult. The yeast proteins have also been shown to display only weak membrane association (Guan *et al.*, 2001). In the case of Fig4, this membrane association could be through binding of Vac14, as expression of Vac14 has been shown to increase the level of punctate staining of Fig4 (Sbrissa *et al.*, 2007). However, this was not found to be the case in this study when HA-Vac14 and GFP-Fig4 were coexpressed (Figure 3.11), although an accumulation of both proteins was found in areas of reticular staining.

The second important use of the tools generated in this chapter was analysis of direct interaction between Vac14, WIPI-2 and Fig4, producing some confirmatory and some novel data. Table 3.3 and figure 3.23 both illustrate the interactions demonstrated in this study in the context of the current literature. Using both biochemical means, in examining the coimmunoprecipitation of overexpressed Vac14 and Fig4, and the Yeast two-hybrid method, an interaction between Vac14 and Fig4 was confirmed. Our data, along with recently published data (Sbrissa *et al.*, 2007) show clearly that the yeast interaction is conserved in higher organisms, suggesting that this is an important relationship between Vac14 and Fig4.

Data from this study also show that overexpression of Vac14 stabilises Fig4 in HeLa cells, further suggesting that the interaction between these two proteins may be important in a cellular context for the regulation of Fig4 activity. This interaction is particularly interesting because Vac14 has been shown to regulate the activity of the kinase (Rudge *et al.*, 2004), as well as interacting with its counterpart phosphatase Fig4, suggesting that these three proteins may in fact form a single multiprotein complex to tightly regulate the levels of PtdIns(3,5)P_2. Recent data suggests that the yeast proteins may also form part of a common lipid kinase complex, and that Fab1 interacts with both Vac14 and Fig4 through its chaperonin domain and the complex is recruited to the vacuole membrane through the Fab1 FYVE domain, where it regulates both synthesis and turnover of PtdIns(3,5)P_2 (Botelho *et al.*, 2008). It would therefore be interesting to dissect the interaction between the mammalian proteins to determine if the chaperonin domain is also important for this function.

The strongest interaction observed in the screen was between Vac14 and itself. Interestingly, this was also found to be the case for the yeast proteins (Dove *et al.*, 2002), strongly suggesting that this protein may dimerise, and that this has an evolutionarily conserved function for this protein.

Yeast two-hybrid analysis also identified an interaction between WIPI-1 and WIPI-2. Although this may indicate that the WIPI proteins dimerise, and that the similarity between the two proteins allows for heterodimerisation, at least for WIPI-2 no self-interaction was observed. Alternatively, the WIPI

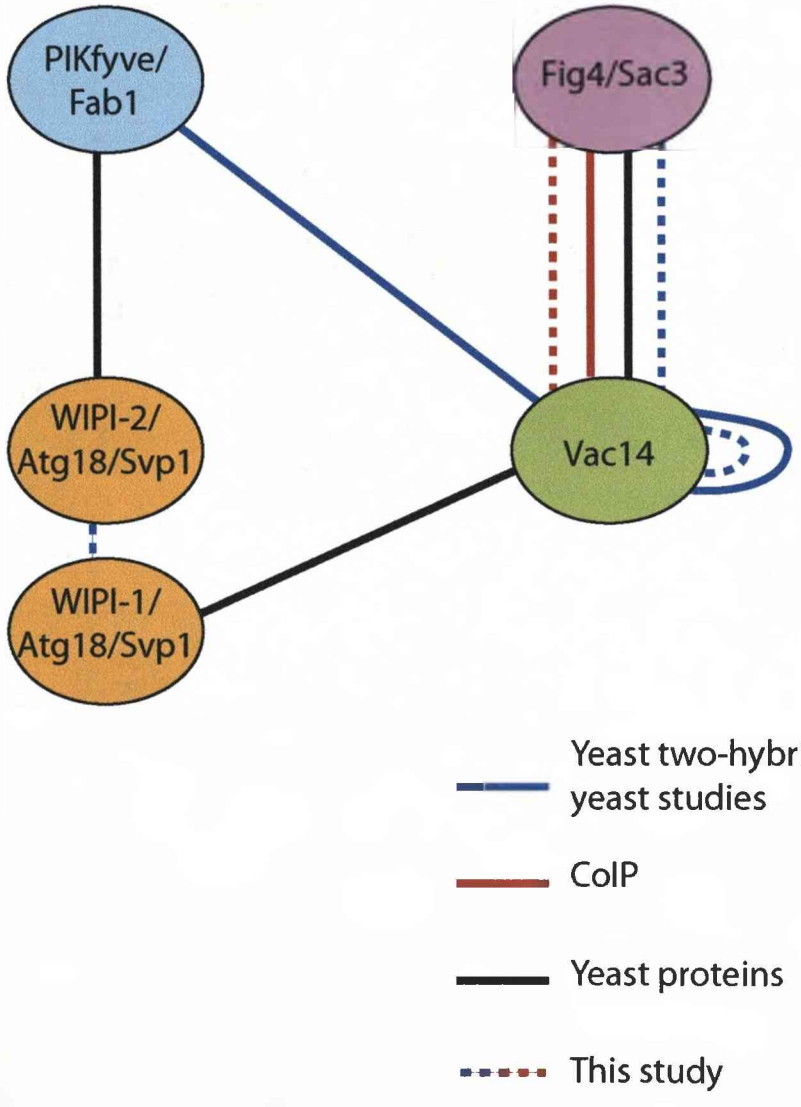

Figure 3.23. Interactions demonstrated in this study in the context of the literature on these proteins.
This diagram illustrates the interactions that have were demonstrated in this study in the context of other previously established data in the literature.

proteins may have some as yet uncharacterised function that requires them to interact with one another. The similarity between the two proteins, and their relationship with the yeast proteins, suggests that there may be some redundancy in the function of these two proteins.

Table 3.3 Summary of known interactions and those demonstrated in this study

Interaction	Protein species	Method	Reference
Vac14 – Fig4	Yeast and mammalian	CoIP Yeast two-hybrid	(Rudge *et al.*, 2004; Sbrissa *et al.*, 2004; Sbrissa *et al.*, 2007) This study
Vac14 – PIKfyve	Mammalian	CoIP	(Sbrissa *et al.*, 2004)
Fab1 – Atg18/Svp1	Yeast	Yeast two-hybrid	(Georgakopoulos *et al.*, 2001)
Vac14 – Atg18/Svp1	Yeast	Protein fragment complementation assay*	(Tarassov *et al.*, 2008)
WIPI-1 – WIPI-2	Mammalian	Yeast two-hybrid	This study
Vac14 – Vac14	Yeast and mammalian	Yeast-two hybrid	This study (Dove *et al.*, 2002)

* Note: In this assay two proteins of interest are fused to complementary fragments of a reporter protein. If the two proteins of interest interact, the reporter fragments are brought together and fold into their native structure, reconstituting the reporter activity of the PCA.

Production of recombinant proteins met with limited success. A useable amount of Vac14 protein was generated, which could therefore be used in future studies to examine the enzymatic activity of Vac14. The production of WIPI-2 could also be reassessed in the future to attempt to increase the solubility of this protein. However, I was unable to obtain any expression of Fig4 protein. Optimising protein production was not prioritised, as I was unable to do the enzymatic studies I had initially set out to do, to address the question of how Vac14 interacts with Fig4 and regulates its function in the cell, and assess the substrate specificity of Fig4.

CHAPTER FOUR

The Role of PIKfyve in Regulating Retrograde Transport Pathways

4.1 Introduction

Despite the fact that much of the machinery that regulates production, turnover and binding of PtdIns(3,5)P_2 has been uncovered, a complete understanding of its precise cellular function remains elusive. Its precursor PtdIns(3)P is localised to the membranes of early endosomes and MVBs (Gillooly *et al.*, 2000), where it plays a role in early endosome fusion by recruitment of EEA-1 (Jones and Clague, 1995; Li *et al.*, 1995; Mills *et al.*, 1998; Simonsen *et al.*, 1998), internalisation of ubiquitinated membrane receptors by recruitment of the ESCRT 0 protein Hrs (Urbe *et al.*, 2000; Raiborg *et al.*, 2001; Raiborg *et al.*, 2002), and formation of intralumenal vesicles (Fernandez-Borja *et al.*, 1999; Futter *et al.*, 2001).

Due to a lack of antibodies or bioreporters for PtdIns(3,5)P_2, its localisation has been inferred from that of the kinase PIKfyve/Fab1. Thus, it is proposed to localise predominantly to the membranes of early endosomes at steady state (Cabezas *et al.*, 2006; Ikonomov *et al.*, 2006; Rutherford *et al.*, 2006), where it has been implicated in a number of endosomal functions. In *S. cerevisiae*, Fab1 mutants, devoid of PtdIns(3,5)P_2, display a range of different phenotypes, including a dramatically swollen vacuole that is improperly acidified (Rudge *et al.*, 2004). Like Fab1, the mammalian kinase PIKfyve, is also essential for endosomal membrane homeostasis, and loss of this enzyme results in the progressive accumulation of cytoplasmic vacuoles

(Ikonomov *et al.*, 2001; Rutherford *et al.*, 2006). One key question that remains to be answered is the origin of these vacuoles.

Given that MVBs in PtdIns(3,5)P_2 depleted cells contain fewer intralumenal vesicles, it has been argued that enlarged vacuoles may result from a defect in inward invagination of the limiting membrane of the MVB (Ikonomov *et al.*, 2003a; Rudge *et al.*, 2004). However, in *S. cerevisiae* Fab1 mutant cells sorting of endocytosed cargo into MVBs is unaffected, and although sorting of biosynthetic cargo to the vacuole is blocked, this can be overcome by irreversible ubiquitination of the cargo (Odorizzi *et al.*, 1998; Dove *et al.*, 2002; Katzmann *et al.*, 2004), suggesting that Fab1 more likely controls the sorting of certain proteins, rather than regulating the process of inward invagination. Likewise, in mammalian cells overexpressing a catalytically inactive mutant PIKfyve, swollen cytoplasmic vacuoles have been described as MVB-like structures with fewer internal vesicles. Although fluid phase endocytosis is perturbed, there is no defect in internalisation or degradation of epidermal growth factor receptor (EGFR) (Ikonomov *et al.*, 2003a). These data suggest that if there is in fact a defect in invagination in MVBs, this is most likely not the predominant mechanism contributing to vacuolation.

A second mechanism has been proposed that implicates PIKfyve in retrograde transport pathways from endosomes to the TGN, such that a defect in membrane retrieval on these pathways could also contribute to endomembrane enlargement (Rutherford *et al.*, 2006). As discussed in detail in section 1.9, knockdown of PIKfyve causes a delay in retrieval of receptors such as ciM6PR and sortilin to the TGN from early endosomes (Rutherford *et*

al., 2006). Furthermore, proteins associated with PtdIns(3,5)P_2 metabolism, such as the yeast protein Atg18/Svp1, one of its mammalian counterparts, WIPI-1, and the PIKfyve activator Vac14, have also been implicated in these trafficking pathways (Dove *et al.*, 2004; Jeffries *et al.*, 2004; Zhang *et al.*, 2007).

In the last chapter, tools for the further analysis of three proteins associated with PtdIns(3,5)P_2 metabolism were generated, and initial characterisation of the proteins performed. Other key methods of cell biology for characterisation of protein function are siRNA-mediated knockdown of the protein of interest, and use of specific small molecule inhibitors. In this chapter we chose to revisit the characterisation of cytoplasmic vacuoles following loss of PIKfyve, and examine the contribution of defective membrane retrieval to the TGN, with the specific aims being to:

1) Characterise the phenotypes induced by knockdown of Vac14, Fig4 and WIPI-2 by fluorescence and electron microscopy.

2) Contrast and compare the effects of PIKfyve knockdown (chronic loss) and loss of PIKfyve activity caused by treatment with PIKfyve inhibitor (acute loss).

3) Examine the effects of knockdown of Vac14, WIPI-2 and Fig4 and inhibition of PIKfyve acitivity on a variety of trafficking pathways between the TGN and the endocytic pathway.

4.2 Results

4.2.1 Demonstrating effective suppression of endogenous proteins

A key aim of this chapter was to assess the knockdown phenotypes of each protein. Therefore, it was important to demonstrate effective knockdown by a range of oligos against each protein. Using previously characterised Vac14 and WIPI-2 antibodies (chapter three), and a generously gifted PIKfyve antibody, pooled oligos were deconvoluted to determine which individual oligos induced a significant level of protein suppression.

Pooled oligos against Vac14 and WIPI-2 were effective in substantially reducing the levels of endogenous protein (Figures 3.6 and 3.9), as were pooled PIKfyve oligos (Figure 4.1). For PIKfyve, oligos 3 and 4 produce substantial knockdown, and this was found to correspond to the oligos that produced cytoplasmic vacuoles. For Vac14, all four oligos gave effective knockdown, and in the case of WIPI-2, oligos 1 and 4 both effectively knocked down endogenous protein.

For all experiments pooled oligos were initially used. Observed phenotypes were then reconfirmed with oligo 4 for WIPI-2 and Vac14 and oligo 3 for PIKfyve. Although Fig4 oligos were deconvoluted by RT-PCR (Figure 3.4), Fig4 pooled oligos were used for all experiments, as the effects on protein levels could not be determined and the pool of oligos gave a substantial reduction in messenger RNA levels.

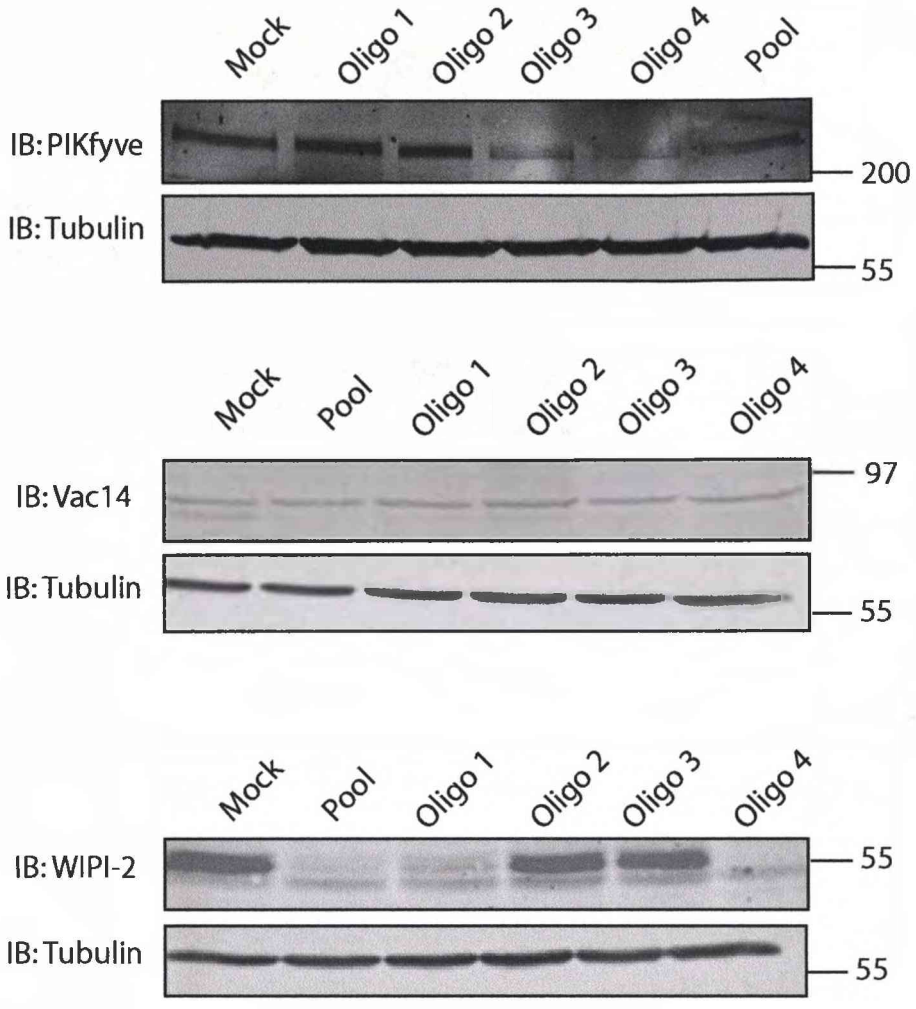

Figure 4.1. Knockdown efficiency of pooled and individual oligos. HeLa cells were treated with 40nM pooled and individual oligos against the indicated proteins for 72h. Cells were lysed in NP40 lysis buffer and run on SDS-PAGE gels, transferred to nitrocellulose and then probed with the indicated antibodies.

4.2.2 Vacuole formation

In yeast, Fab1 mutants display a dramatically swollen vacuole (Rudge *et al.*, 2004). It was previously shown that in mammalian cells, overexpression of a kinase-dead mutant or knockdown of PIKfyve reconstitutes this phenotype, causing an accumulation of swollen cytoplasmic vacuoles of unknown origin (Ikonomov *et al.*, 2002a; Rutherford *et al.*, 2006). This effect was confirmed in HeLa cells with the siRNA oligos used in this study (Figure 4.2 A). It was found that upon treatment of cells with PIKfyve siRNA, approximately 30% of cells developed swollen vacuoles.

When cells were treated with Vac14 siRNA only 3% of cells displayed swollen vacuoles. This is despite its role as an allosteric activator of PIKfyve, and in contrast to the *S. cerevisiae* Vac14 mutant phenotype that mimics that of Fab1, whilst the knockdown of the protein was clearly efficient (Figure 4.1). Interestingly, neither WIPI-2 nor Fig4 displayed any vacuolar phenotype, despite a high degree of knockdown in the case of WIPI-2. A combination of PIKfyve knockdown with knockdown of either Vac14 or Fig4 did not significantly alter the number of cells displaying a vacuolar phenotype. Inhibition of PIKfyve using MF4 also produced the same vacuolar phenotype, in nearly 100% of cells.

4.2.3 Vacuole characterisation

Loss of PIKfyve activity (by both siRNA treatment and inhibition) also caused formation of swollen endosomal compartments (Figure 4.2 B). This is examined in more detail in Figure 4.3. EEA-1 labelled early endosomes

A

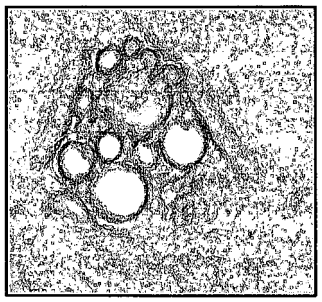

Treatment	% vacuoles
PIKfyve RNAi	30%
Vac14 RNAi	3%
WIPI-2 RNAi	0%
Fig4 RNAi	0%
PIKfyve + Vac14 RNAi	28%
PIKfyve + Fig4 RNAi	27%
Vac14 + Fig4 RNAi	0%
PIKfyve inhibitor	90-100%

B

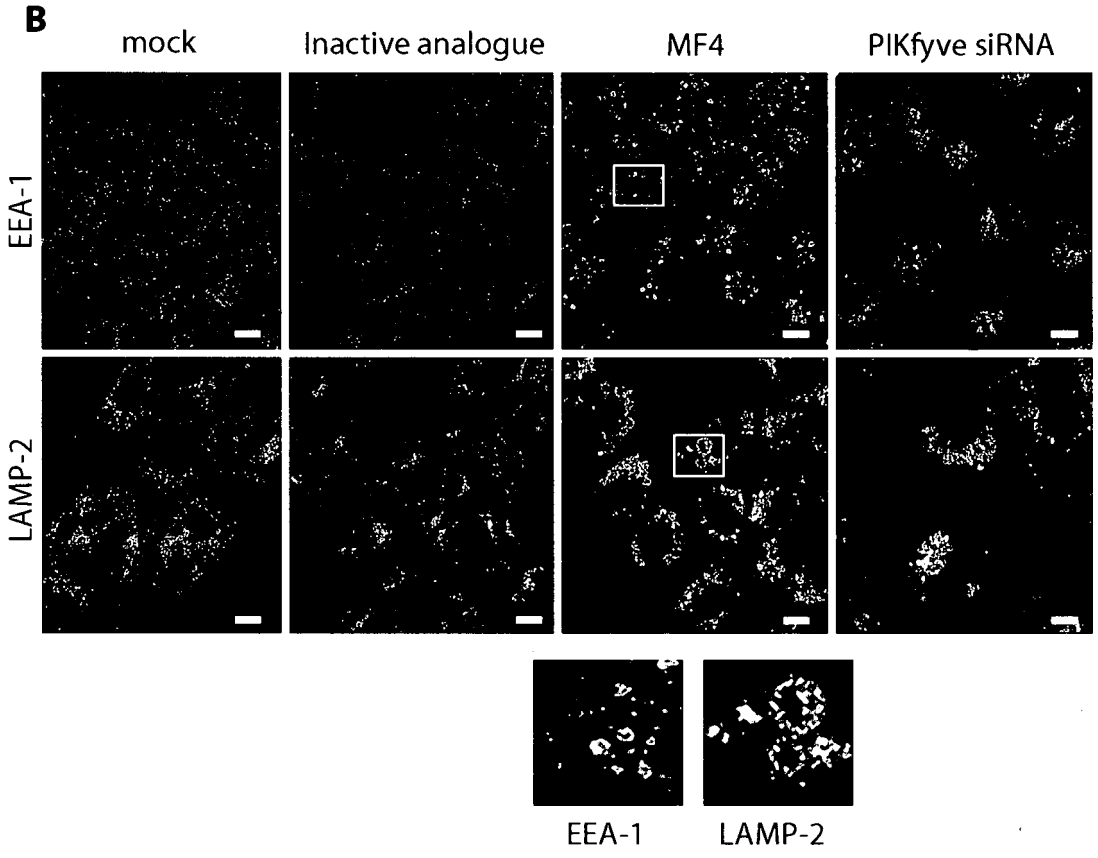

Figure 4.2. PIKfyve knockdown and inhibition induces accumulation of swollen endosomal compartments and large cytoplasmic vacuoles.

HeLa cells were treated with 40nM PIKfyve siRNA oligos for 72h or 800nM MF4 or an inactive analogue for 4h prior to fixation in 3% PFA/PBS, permeabilisation with 0.2% TX-100 and staining with the respective antibodies. A) As with PIKfyve knockdown, its inhibition induces the accumulation of a heterogenous population of swollen cytoplasmic vacuoles. Table of penetrance of vacuole phenotype with different treatments. B) Loss of PIKfyve activity also causes an accumulation of swollen endosomal compartments. Enlgarged images of the boxed areas are displayed underneath the main panel. Scale bars represent 20μm.

are dramatically swollen in comparison to control cells, and often aggregate around the larger cytoplasmic vacuoles from which the early endosomal marker is predominantly excluded. Late endosome/lysosome marker LAMP-2, on the other hand, is associated with the larger cytoplasmic vacuoles, as demonstrated by phase overlay, though it does not appear to uniformly label the limiting membrane, if at all. Initial images suggested that LAMP-2 veicles might be contained within the lumen of the large vacuoles. However, A Z-series taken through individual cells and projected into a 3D image using Leica imaging software demonstrate that LAMP-2 covers the surface of these large vacuoles but is predominantly excluded from the lumen. In fact, the lumen of the large vacuoles is empty for the most part (Figure 4.3 A). Early and late endosome compartments still remain distinct from one another, with very limited colocalisation, mostly at points surrounding the large vacuoles. Staining with anti-tubulin antibodies demonstrated that the microtubule network was intact following loss of PIKfyve activity, and that cytoplasmic vacuoles were sheathed in microtubules (Figure 4.3 B).

Vacuoles were examined by electron microscopy following treatment with PIKfyve inhibitor (Figure 4.3 C). The larger vacuoles are largely unable to take up fluid phase marker HRP even after 4 hours of internalisation, and are mostly empty, although occasionally contain one or two internal vesicles in a cross-section, which most likely correspond to LAMP-2 labelled vesicles observed by immunofluorescence. The vacuoles are surrounded by smaller HRP-labelled swollen compartments, which most likely correspond to the EEA-1 labelled structures observed by IF. Normal MVB compartments and lysosomes were also observed in these cells.

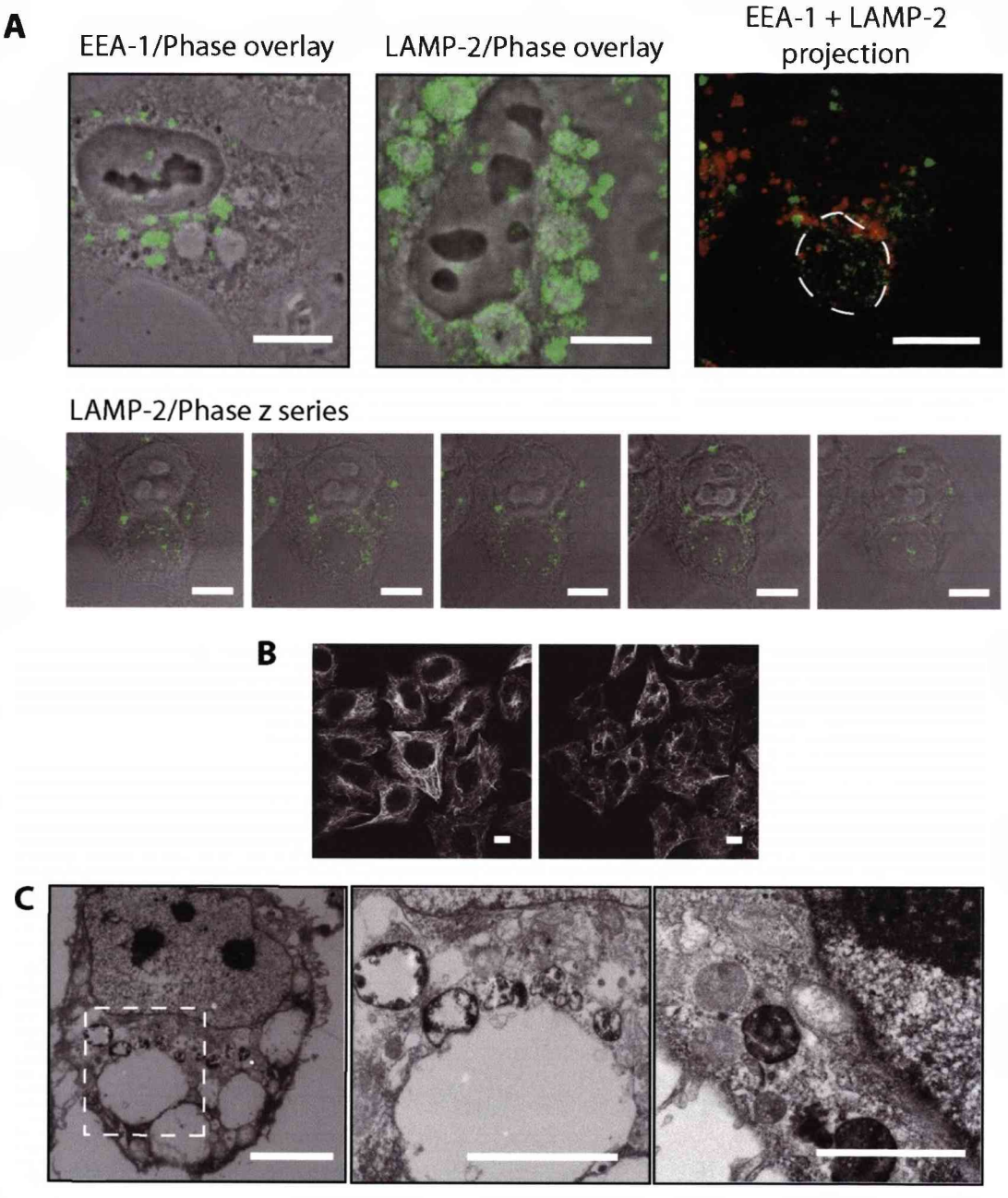

Figure 4.3. Cytoplasmic vacuoles are inaccessible to HRP and endosomal markers.

HeLa cells were treated with 800nM MF4 prior to A) fixation in 3% PFA/PBS, permeabilisation with 0.2% TX-100 and staining with the EEA-1 and LAMP-2 (A) and α–tubulin (B) and C) uptake of HRP for 4 hours and fixation and processing for EM as described in materials and methods. The large vacuoles do not readily take up HRP. Smaller cytoplasmic vacuoles that are positive for HRP and contain some intralumenal vesicles are often found in close proximity to the large vacuoles, as can be seen in both EM and IF pictures. Large swollen vacuoles contain few, if any, internal vesicles. Scale bars represent 10μm.

By inhibiting PIKfyve one mechanism of turnover of PtdIns(3)*P* is prevented, therefore, we might expect to see an increase in the cellular levels of this lipid. However, this was found not to be the case (Jefferies *et al.*, 2008). In order to be certain that MF4 was not also affecting the activity of the 3-kinase Vps34, the localisation of the tandem FYVE domain of Hrs, which binds to PtdIns(3)*P* with high affinity, was examined. As expected, treatment with the PI3-kinase inhibitor wortmannin caused the loss of PtdIns(3)*P* and EEA-1 positive punctae, however, treatment with PIKfyve inhibitor had no effect on either, except that both localised to more swollen compartments as previously demonstrated with EEA-1 (Figure 4.4).

siRNA treated cells were also examined by EM to compare cells treated with PIKfyve siRNA and inhibitor, and to determine if there were any ultrastructural changes following knockdown of WIPI-2, Vac14 and Fig4. In PIKfyve siRNA and to a much lesser extent, some Vac14 siRNA treated cells we can find cytoplasmic vacuoles, that display similar morphology to those seen upon PIKfyve inhibition (Figure 4.5). Once again, normal MVB and lysosome compartments were also observed in the same cells as cytoplasmic vacuoles. Neither Fig4 nor WIPI-2 knockdown produced any significant ultrastructural changes or perturbation in HRP uptake.

4.2.4 Loss of PIKfyve activity affects several endosome to TGN pathways

Previous work has indicated that PtdIns(3,5)P_2 may regulate endosome to TGN trafficking pathways (Ikonomov *et al.*, 2003b; Dove *et al.*, 2004; Jeffries *et al.*, 2004; Rutherford *et al.*, 2006). Therefore, various

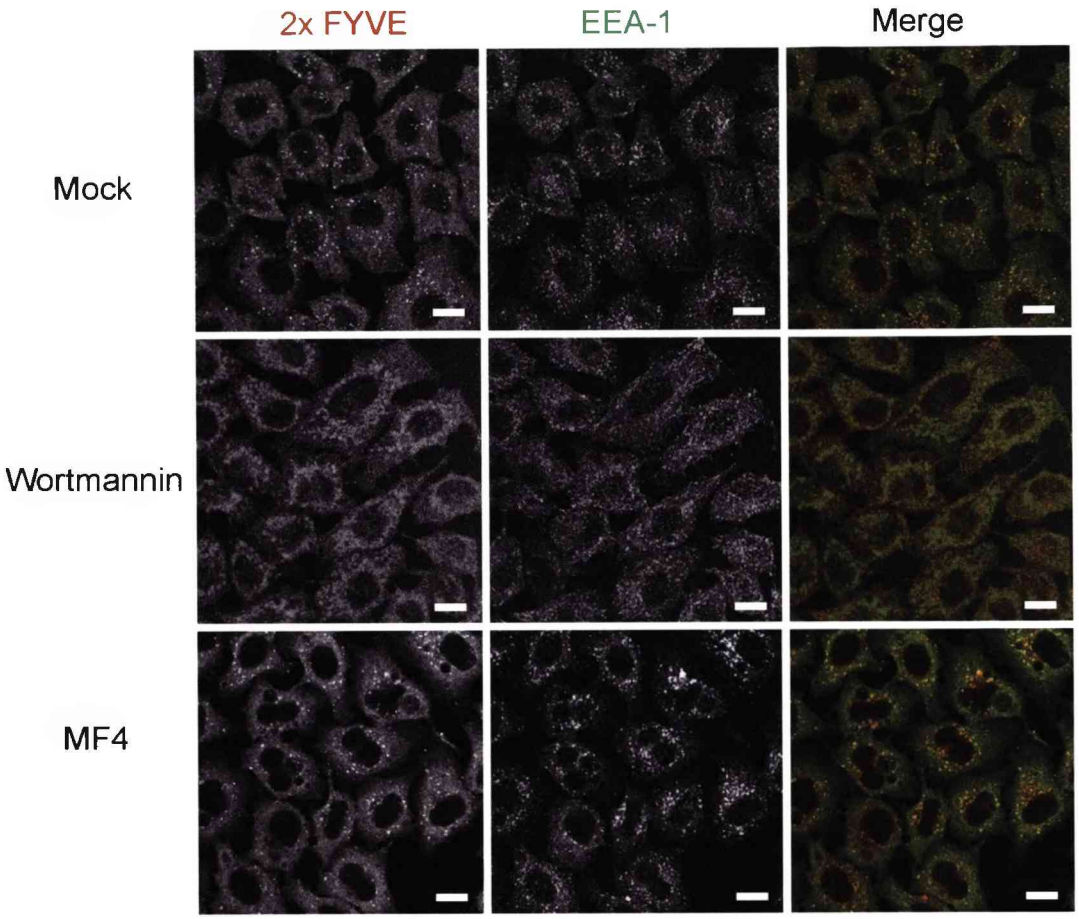

Figure 4.4. PIKfyve inhibitor treatment does not affect the localisation of PtdIns(3)*P* or its subsequent recruitment of EEA-1.
HeLa cells were treated with 800nM MF4 for 4h or 100nM Wortmannin for 30mins prior to fixation in 3% PFA/PBS, permeabilisation with Digitonin in PIPES-MTSB and staining with anti-EEA-1 antibodies and a biotinylated GST-tagged tandem FYVE protein. Unlike wortmannin treatment, inhibition of PIKfyve did not affect the localisation of the tandem FYVE domain protein, nor its colocalisation with EEA-1, suggesting that there is no effect on PtdIns(3)*P* or its recruitment of effector proteins. Scale bars represent 20μm.

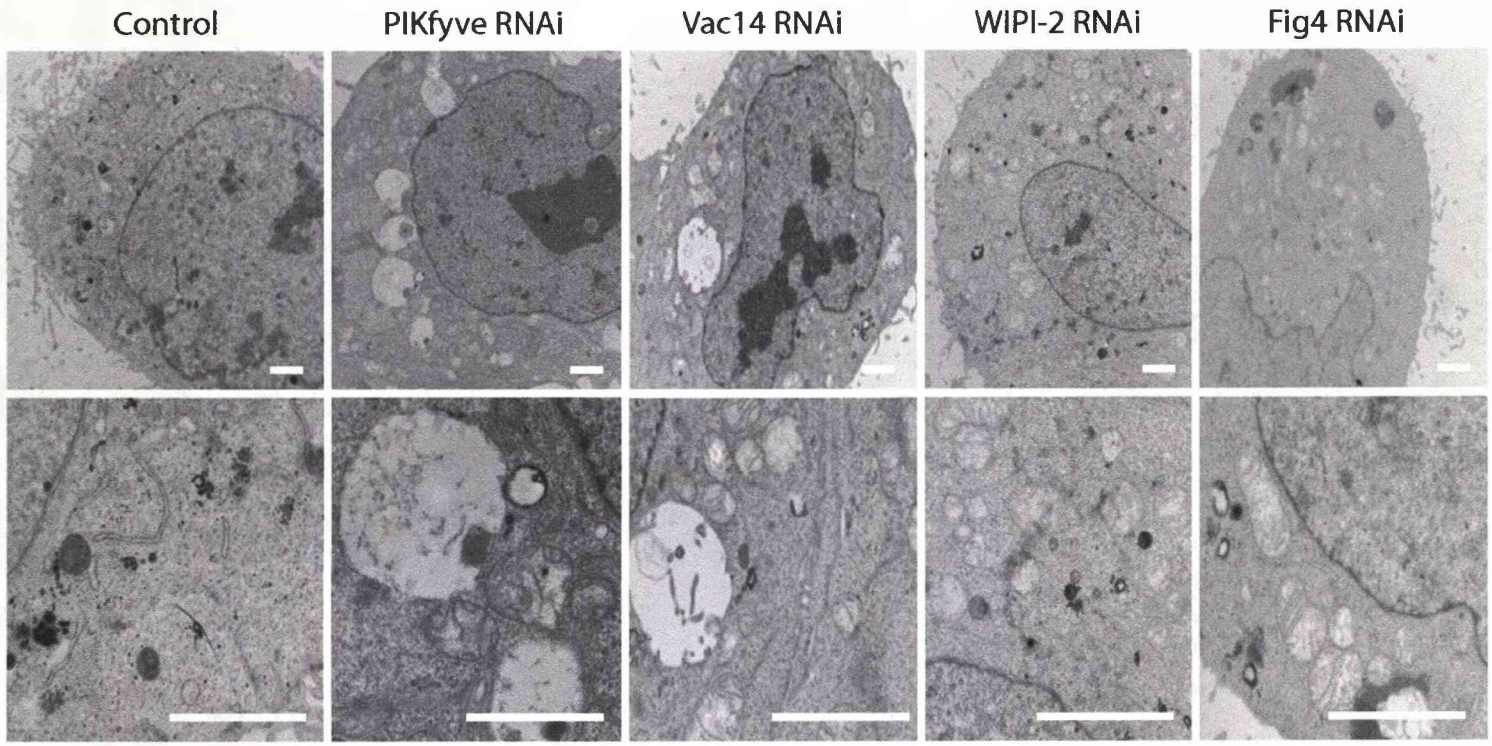

Figure 4.5. siRNA treated cells visualised by electron microscopy.
HeLa cells were treated with 40nM siRNA oligos against the indicated proteins (Vac14, WIPI-2 and PIKfyve individual oligos and Fig4 pooled oligos). After 72h, 10mg/ml HRP was added to the cells for 1h and cells were subsequently processed for EM as described in materials and methods. Cytoplasmic vacuoles are visible in both PIKfyve siRNA treated cells, and to a lesser extent Vac14 siRNA treated cells. These large vacuoles were inaccessible to HRP and were also frequently surrounded by smaller swollen compartments. WIPI-2 and Fig4 siRNA treated cells did not exhibit any dramatically altered phenotype. Scale bars 1μm.

methods were employed to examine this pathway following knockdown of each protein or treatment with the PIKfyve inhibitor.

HeLa cells were treated with siRNA against each protein, and stained for both ciM6PR and a trans-Golgi marker TGN46 (Prescott *et al.*, 1997). ciM6PR bind lysosomal hydrolases (Kyle *et al.*, 1988; Lobel *et al.*, 1989) tagged with mannose-6-phosphate groups at the TGN and assists their carriage to the endocytic pathway, whereupon the hydrolases are delivered to the lysosome, whilst the ciM6PR are retrieved to the TGN for further rounds of transport. I confirmed that siRNA-mediated knockdown of PIKfyve causes a redistribution of ciM6PR, as has previously been shown (Rutherford *et al.*, 2006). In control HeLa cells ciM6PR is typically found in a perinuclear localisation, and displays partial overlap with markers of both the TGN and the endosomal system. Following loss of PIKfyve by siRNA treatment, this marker localises to more swollen compartments and redistributes around the cytoplasmic vacuoles (Figure 4.6). Interestingly, despite a high degree of knockdown of WIPI-2 and Vac14 (Figure 4.1) a loss of these proteins did not affect the distribution of ciM6PR, nor did knockdown of Fig4. Note also that the distribution of the TGN marker TGN46 also appears to be altered following PIKfyve knockdown, this is assessed in more detail in separate figures.

siRNA treatment does not necessarily indicate a specific role for PIKfyve kinase activity, and thus PtdIns(3,5)P_2, on this pathway. As well as taking account for non-specific effects of siRNA oligos, it must also be noted that protein knockdown represents a chronic loss of the protein over time. There is a gradual depletion of cellular levels of the protein of interest, and as

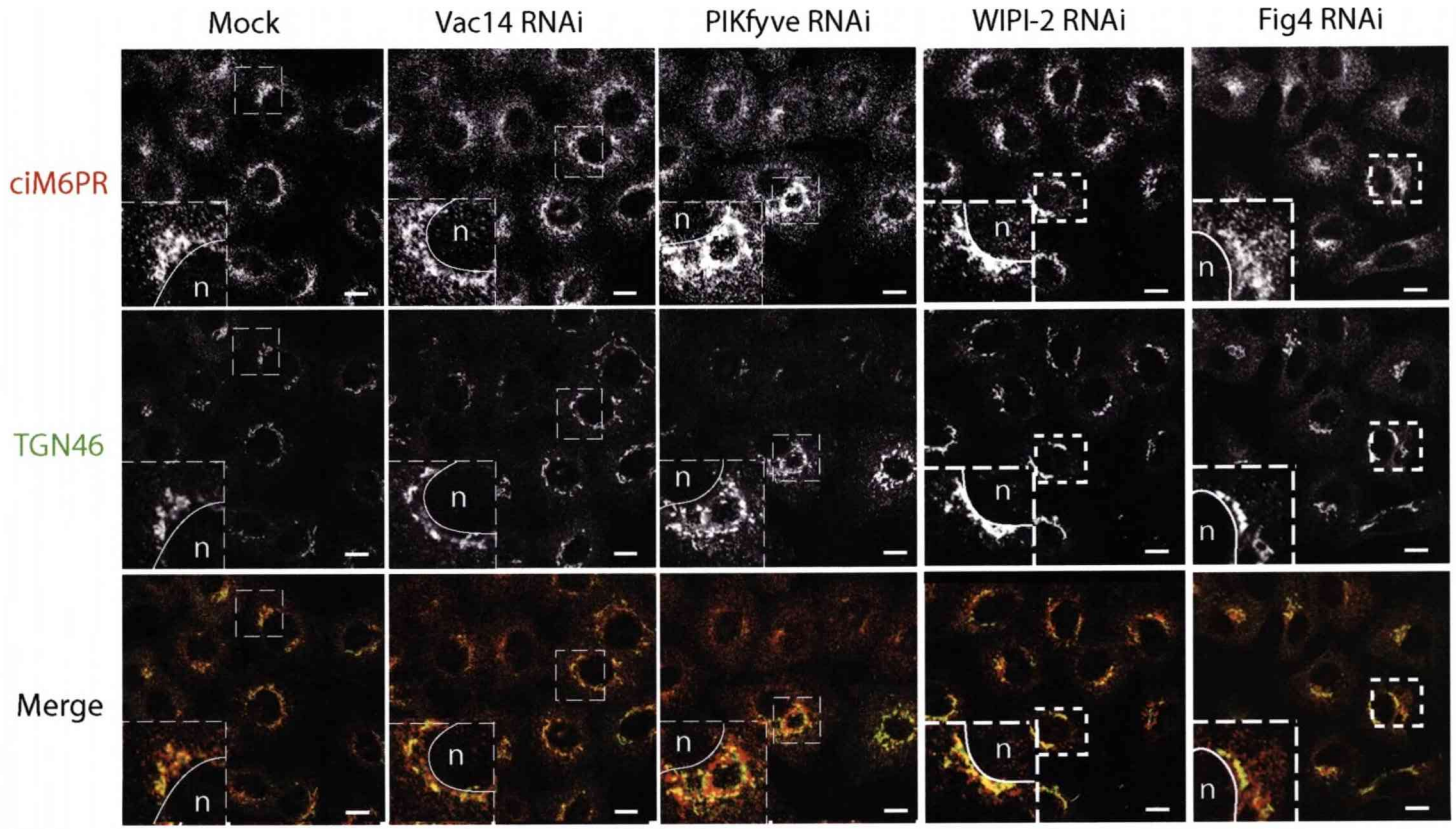

Figure 4.6. PIKfyve knockdown affects the distribution of ciM6PR and TGN46.
HeLa cells were transfected with 40nM oligos against the indicated proteins for 72h and then fixed in 3% PFA/PBS, permeabilised with 0.2% TX-100 and stained with the antibodies against ciM6PR and TGN46. Scale bars represent 20μm. The nucleus (n) is marked on to enlarged insets to distinguish from cytoplasmic vacuoles induced by PIKfyve siRNA. PIKfyve, but not WIPI-2, Vac14 or Fig4 siRNA treatment alters the distribution of both ciM6PR and TGN46 markers.

such compensatory mechanisms can often be employed by the cell, which may be responsible for certain observed effects. Furthermore, siRNA mediated depletion will remove a protein from all of its potential cellular roles, therefore, in the case of PIKfyve, this does not necessarily reflect a loss of the lipid kinase activity and depletion of PtdIns(3,5)P_2. For this reason, a small molecule inhibitor of PIKfyve lipid kinase activity was used to determine the effects of a specific loss of PIKfyve kinase activity. Inhibition of PIKfyve kinase activity gives the same effect on ciM6PR as PIKfyve depletion by siRNA (Figure 4.7). An inactive analogue of the PIKfyve inhibitor (see Figure 1.10 for structure) confirms that this is due specifically to a loss of PIKfyve activity.

It has been suggested that this altered distribution of ciM6PR following loss of PIKfyve is due to failure in their retrieval back to the TGN. One mechanism of retrieval involves the retromer complex, a multimeric coat protein complex that interacts directly with these receptors and facilitates their inclusion into vesicles destined for return to the TGN (Arighi *et al.*, 2004) (see section 1.2.7 for more detail). If the ciM6PR fail to be recycled back to the TGN they may instead be routed to the lysosome and degraded, and a decrease in cellular levels of ciM6PR might be observed. The levels of ciM6PR, and two components of the retromer complex, were assessed by Western blotting. There was no effect on the cellular levels of any of these proteins following either siRNA treatment of any of the proteins investigated, or inhibition of PIKfyve (Figure 4.8), suggesting that they are not routed to the lysosome. The distribution of two of the retromer components Vps26, (part of the cargo-binding element of the complex) (Shi *et al.*, 2006), and SNX-1,

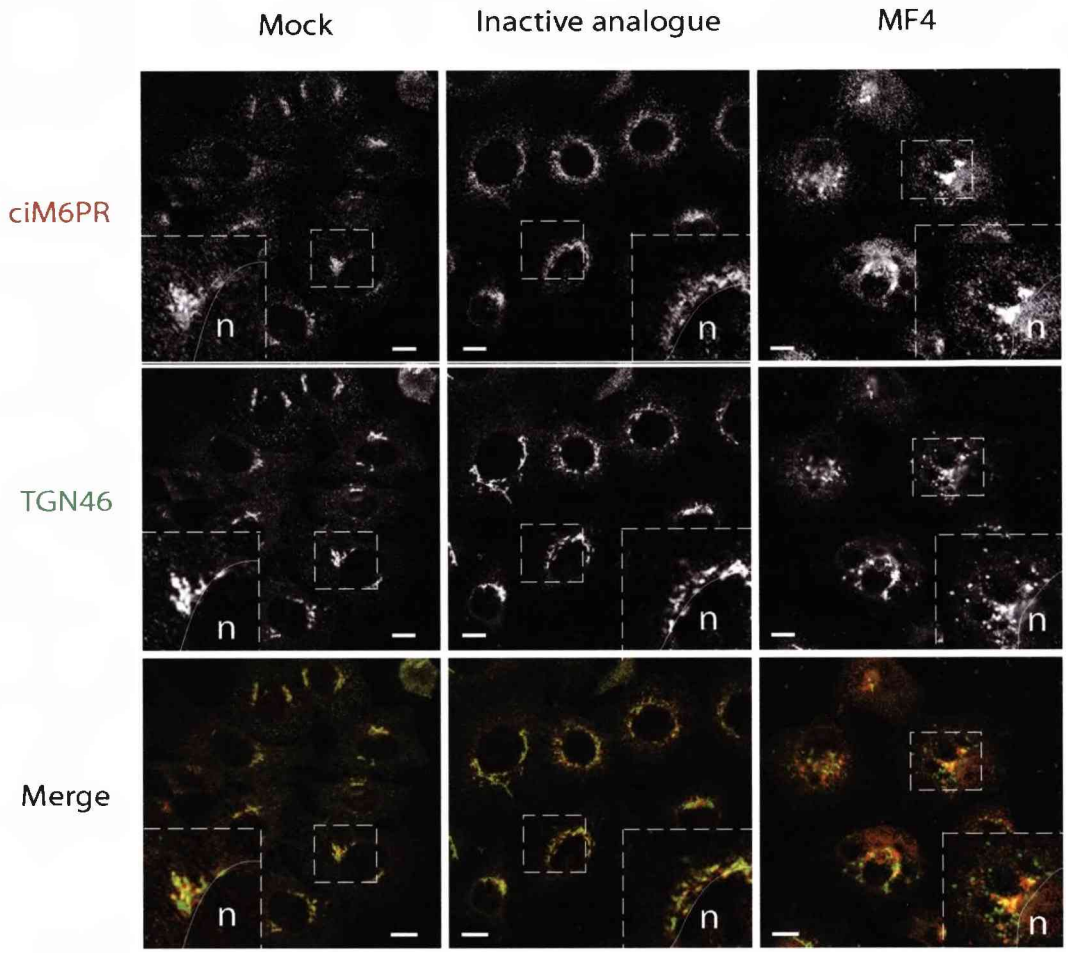

Figure 4.7. Acute inhibition of PIKfyve alters the distribution of ciM6PR and TGN46.

HeLa cells were treated with 800nM MF4 or inactive analogue for 4h prior to fixation in 3% PFA/PBS, permeabilisation in 0.2% TX-100 and staining with ciM6PR and TGN46 antibodies. Inhibition of PIKfyve altered the distribution of both markers, with the most severe disruption in cells with larger cytoplasmic vacuoles. Scale bars represent 20μm.

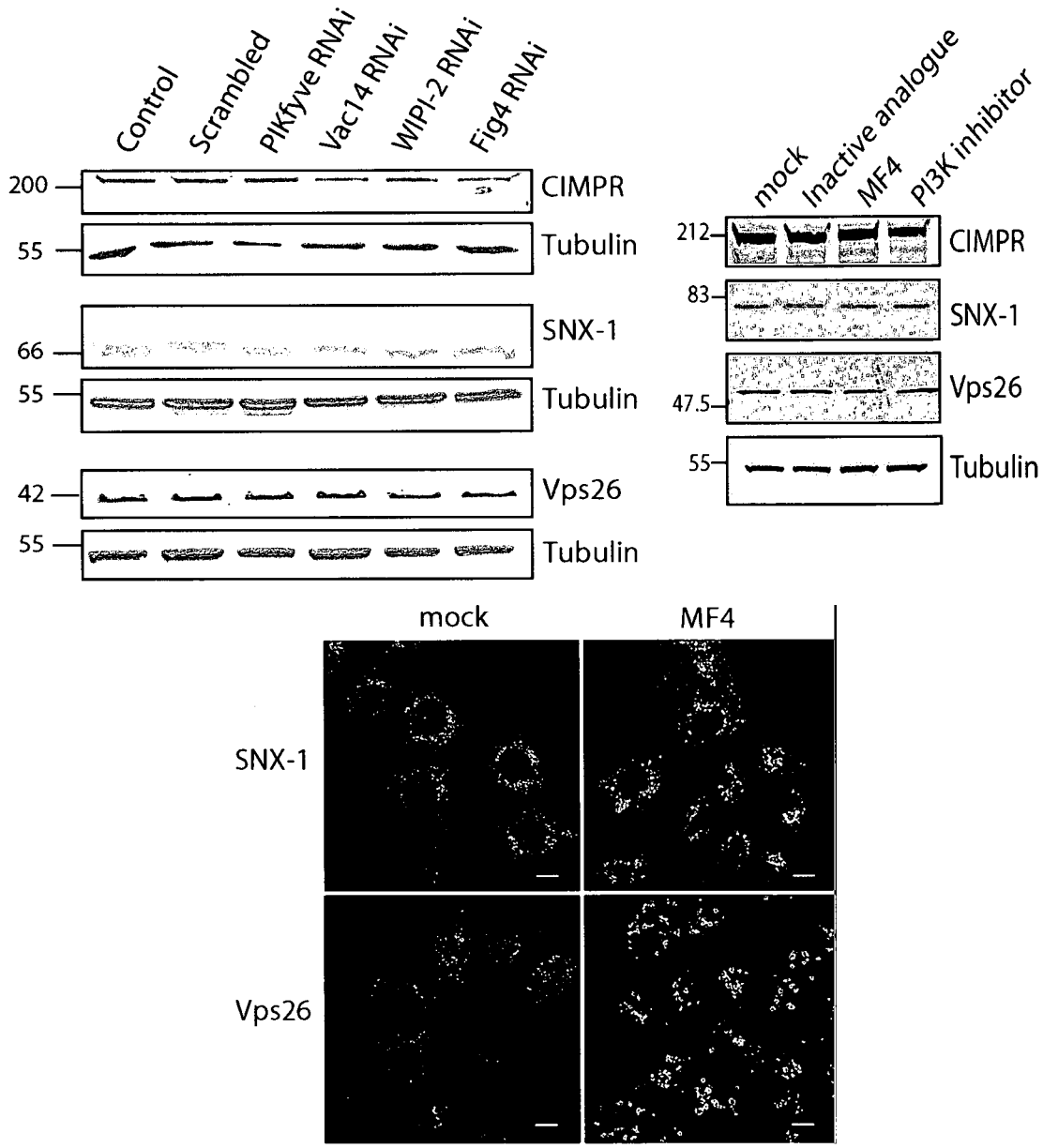

Figure 4.8. Cellular levels of ciM6PR and retromer components are unaffected.

HeLa cells were transfected with siRNA oligos against the indicated proteins for 72h or incubated with 800nM MF4 for 4h prior to lysis in NP40 lysis buffer and Western blotting, or fixation in 3% PFA/PBS and permeabilisation in 0.2% TX-100. Both fixed cells and Western blotting membranes were stained with antibodies against Vps26 and SNX-1, and Western blots were also probed with ciM6PR antibodies. α–Tubulin was used as a protein loading control, and scale bars represent 20μm. Although SNX-1 and Vps26 label a more swollen endosomal compartment, the cellular levels of these proteins, and of CIMPR are unaffected by loss of PIKfyve activity.

(plays a structural role) (Zhong *et al.*, 2002), were examined by immunofluorescence. These two proteins localised to swollen endosomal compartments upon loss of PIKfyve activity, suggesting that the localisation of these components of the retromer complex to the early endosome is unaffected.

4.2.5 Loss of PIKfyve activity disrupts TGN46 cycling

The TGN marker TGN46 was used to assess the levels of colocalisation of ciM6PR with the TGN, to determine if the cause of the redistribution was a failure of ciM6PR to retrieve to the TGN. However, the loss of PIKfyve activity also had a notable effect on the distribution of this TGN marker itself (Figures 4.6 and 4.7). In both PIKfyve knockdown and inhibitor treated cells, there was a marked change in TGN46 staining in approximately 20% of cells. This was judged by the blind quantitation of each siRNA treatment in 9 fields of cells per coverslip for three separate experiments (Figure 4.9). Two categories of TGN46 staining were established; tight perinuclear, ribbon-like staining typically observed in most control cells (catergory 1) and dispersed punctate staining that often surrounds swollen vacuoles (category 2). The proportion of cells not accounted for in the quantitation corresponds to an intermediate phenotype, where the Golgi staining was not as tight and perinuclear as usual, but did not display the vesicular staining. Cells treated with PIKfyve inhibitor also demonstrated altered TGN46 staining, in approximately 30% of cells. Notably, although PIKfyve inhibitor treatment did not cause category 1

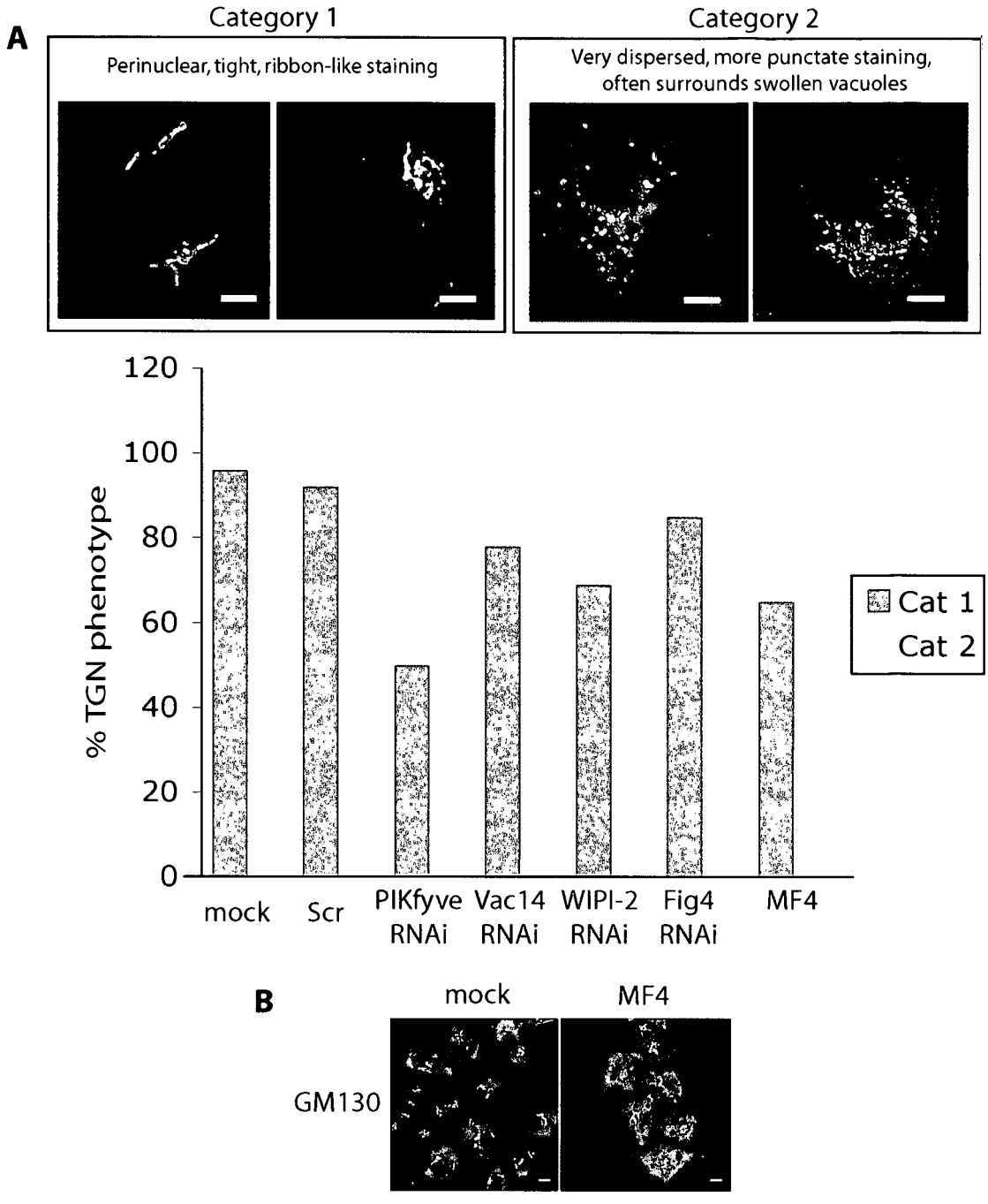

Figure 4.9. TGN46 cycling is disrupted upon loss of PIKfyve activity. HeLa cells were transfected with 40nM siRNA oligos against the indicated proteins, or a scrambled control, or incubated with MF4 for 4h prior to permeabilisation with 0.05% saponin and fixation in 3% PFA/PBS. Cells were stained with TGN46 antibodies and blind quantitation of the TGN phenotype in 9 fields of cells per coverslip for 3 independent experiments was performed for each condition (A). Loss of PIKfyve activity causes a general perturbation in TGN46 staining, and in some cells causes a severe redistribution into vesicular structures. cis-Golgi marker GM130 was unaffected (B). Scale bars represent 5μm (A) and 20μm (B).

staining in all cells, there was an increase in the percentage of cells displaying a general alteration to TGN46 staining.

As TGN46 itself has been shown to cycle between the TGN and plasma membrane, via the endosomal pathway (Ghosh *et al.*, 1998; Mallet and Maxfield, 1999), it is possible that loss of PIKfyve activity might also influence TGN46 cycling. In order to determine if this effect was due to a defect in TGN46 cycling, or a morphological disruption to the Golgi structure in general, the distribution of a *cis*-Golgi marker GM130, was also examined (Figure 4.9 B). Loss of PIKfyve activity did not significantly affect the distribution of this marker. In some cases it was less tightly perinuclear than in control cells, matching the third category of TGN46 staining, but this was more often associated with knockdown than treatment with the inhibitor, and there was no punctate, vesicular staining.

To further illustrate this point, colocalisation of TGN46 with a second trans-Golgi marker Golgin-245 that is not supposed to cycle, was examined (Figure 4.10). As with GM130 staining, there is mildly altered staining in some cells, this could reflect a slight effect of the presence of the large cytoplasmic vacuoles on Golgi morphology, as these occupy a significant portion of the cytoplasm in some cells. In cells displaying TGN46 vesiculation following loss of PIKfyve activity, there is a loss of colocalisation with Golgin-245. The cycling itinerary of TGN46 has been proposed to incorporate the early stages of the endosomal pathway, including recycling endosomes (Ghosh *et al.*, 1998). I examined the colocalisation of TGN46 with a marker of recycling endosomes, Tf receptor, and found that some of the vesicular structures were also positive for Tf receptor.

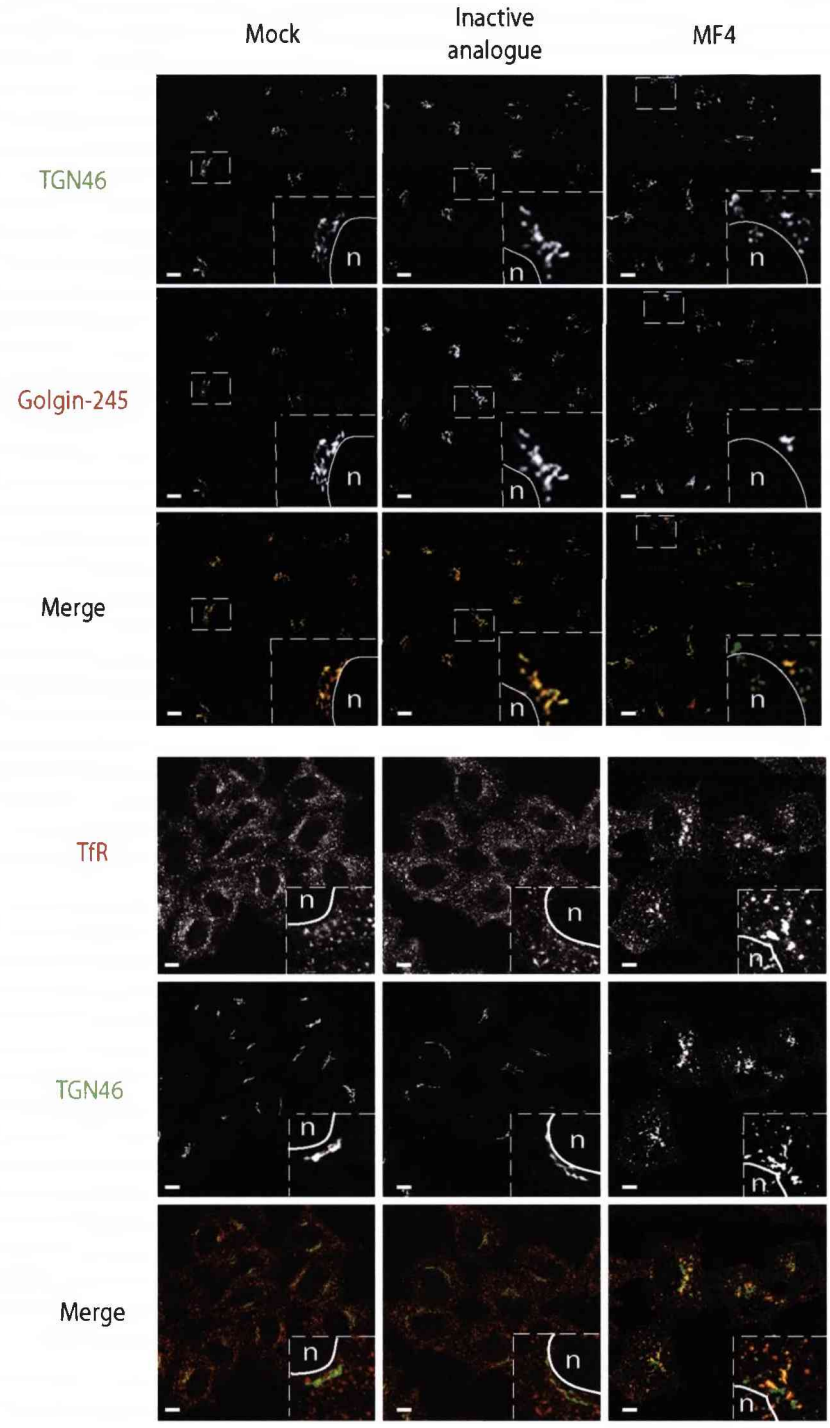

Figure 4.10. Following loss of PIKfyve activity TGN46 disperses from a golgi localisation to recycling/early endosomes.
HeLa cells were treated with 800nM MF4 prior to fixation. Cells were stained with antibodies to two classical trans-golgi markers TGN46 and Golgin-245, and antibodies to the Transferrin receptor. Following loss of PIKfyve activity, in cells where TGN46 is severely perturbed, there is less colocalisation with trans-golgi marker Golgin-245 and increased colocalisation with Transferrin receptor. Scale bars represent 20µm.

4.2.6 Loss of PIKfyve activity delays the retrieval proteins on both retromer-dependent and independent pathways

Both ciM6PR and TGN46 recycle to the TGN from early endosome or recycling compartments in a manner that is, at least in part, mediated by the retromer complex (Arighi *et al.*, 2004; Popoff *et al.*, 2007). A perturbation in retromer-mediated recycling to the TGN presents one potential explanation for the swollen early endosome compartments. However, the large cytoplasmic vacuoles do not label with early endosomal markers, and the swelling of this compartment must occur through other defects. ciM6PR is also retrieved from the late endosome in a manner dependent on Rab9, p40 and TIP47 (Diaz and Pfeffer, 1998; Carroll *et al.*, 2001), which could contribute to membrane swelling of this compartment. If both retromer-dependent and retromer-independent pathways are perturbed, this may indicate that PtdIns(3,5)P_2 plays a more general role in membrane retrieval from the endosomal pathway, contributing to the accumulation of swollen compartments. In order to investigate this, a HeLa cell line stably expressing the lumenal domain of CD8 fused to the cytosolic tail of ciM6PR and Furin was obtained. Furin is a subtilisin-like pro-protein convertase proposed to traffic to the TGN via late endosomes, in a retromer-independent manner (Mallet and Maxfield, 1999; Seaman, 2004). By following uptake of CD8 antibodies, the retrieval of cell surface CD8-ciM6PR and CD8-Furin to the TGN can be followed.

Following inhibition of PIKfyve, there is a delay in retrieval of both markers to the TGN (Figure 4.11). Although CD8-ciM6PR can ultimately reach the TGN (as judged by colocalisation with the perinuclear portion of

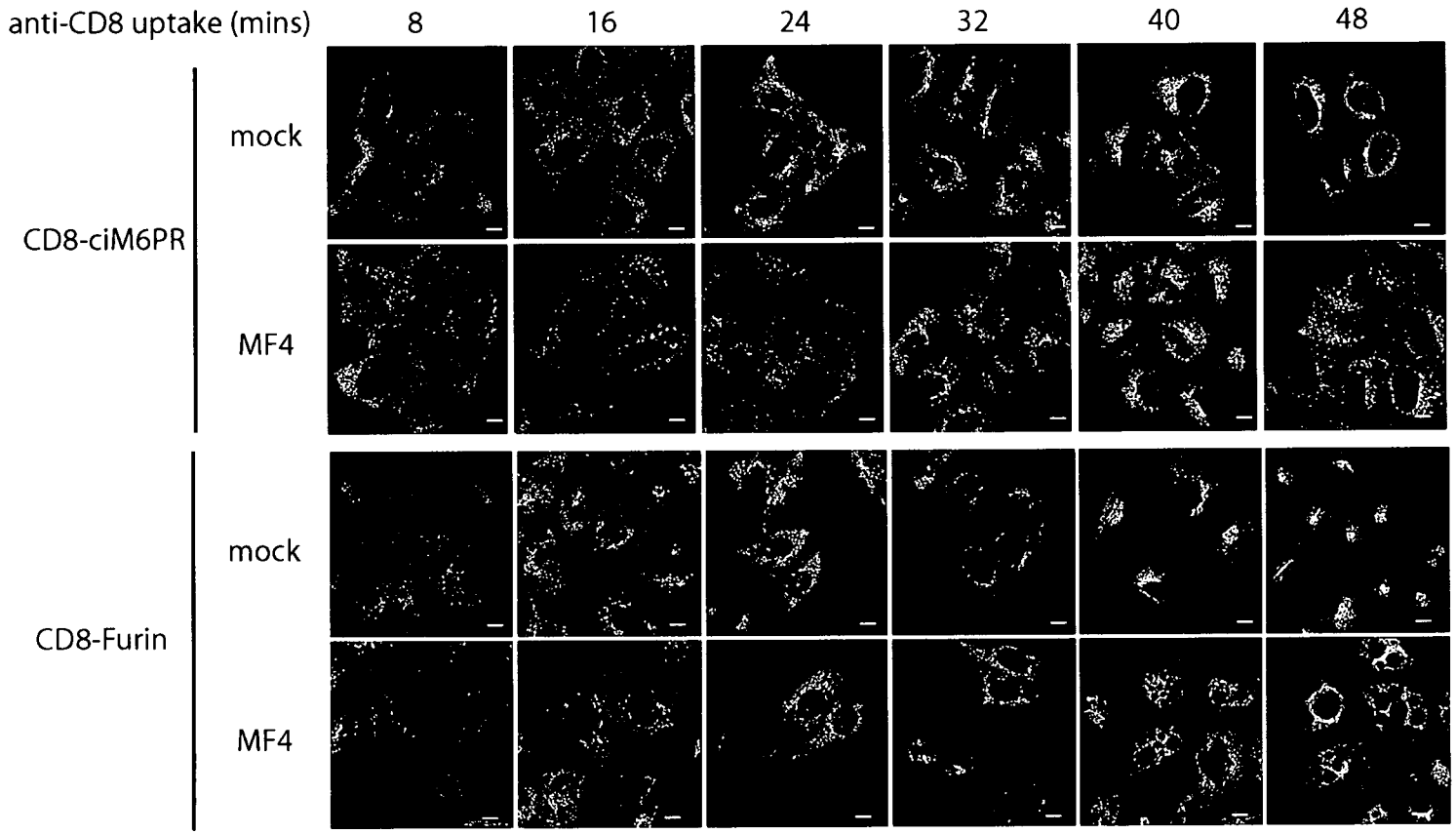

Figure 4.11. CD8-ciM6PR and Furin uptake is delayed following PIKfyve inhibition.
HeLa cells were treated with 800nM MF4 prior to staining with anti-CD8 antibodies and chase in HeLa medium for the indicated timepoints (see materials and methods for details). Loss of PIKfyve activity causes a delay in retrieval of both CD8-ciM6PR and Furin to a perinuclear distribution after 48mins. Scale bars represent 20μm.

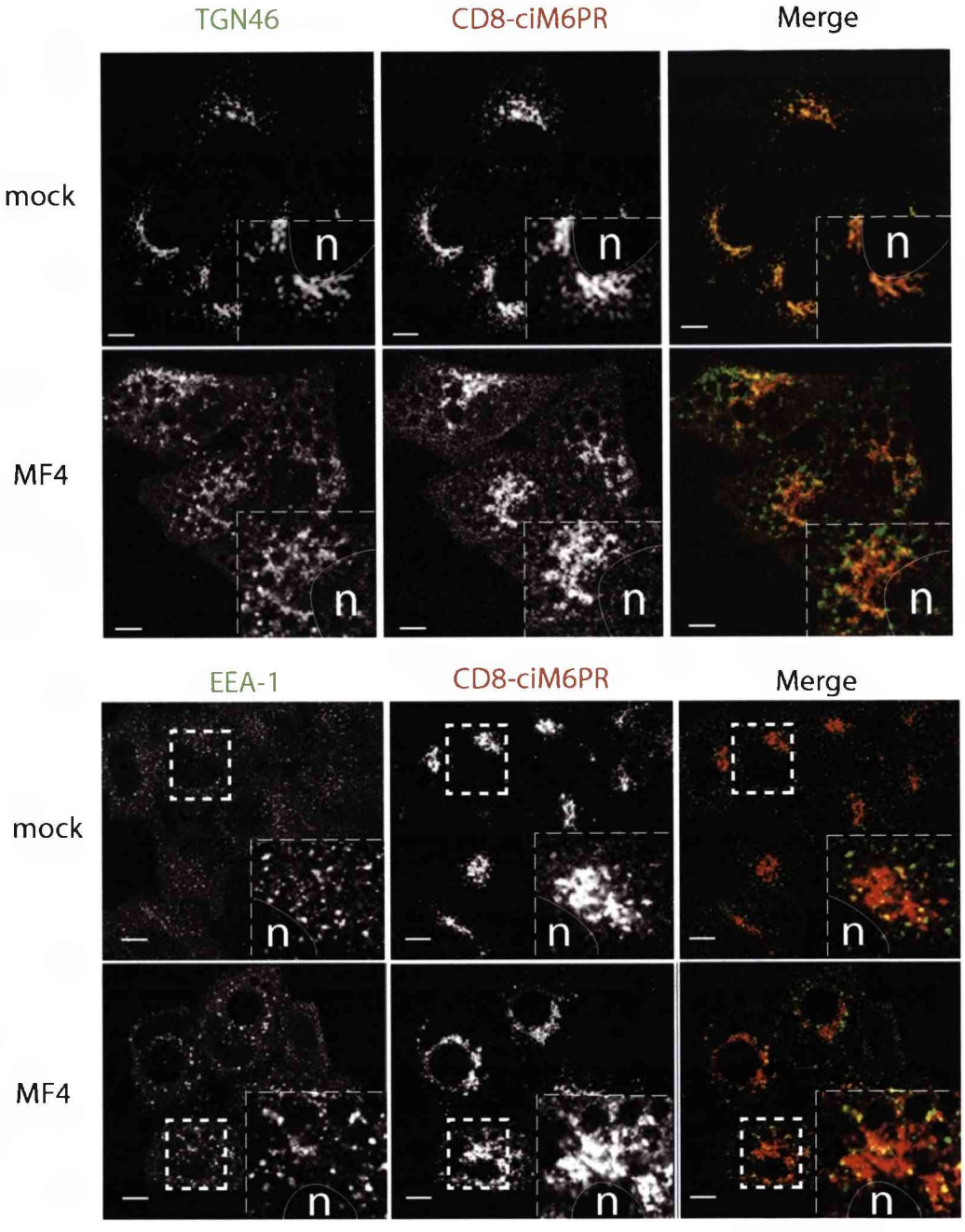

Figure 4.12. Dynamics of CD8-ciM6PR redistribution following loss of PIKfyve activity.

Colocalisation of the terminal timepoint of CD8-ciM6PR uptake (48mins) with golgi marker TGN46 and early endosomal marker (EEA-1). Following loss of PIKfyve activity, CD8-ciM6PR is found in both TGN46 and EEA-1 labelled compartments. In cells where TGN46 is severely perturbed there is no colocalisation between vesicular TGN46 and CD8-ciM6PR. Scale bars represent 20μm.

TGN46 at the final timepoint of CD8 uptake), it shows a slower rate of accumulation there. It also localises to swollen EEA-1 labelled compartments and around the larger cytoplasmic vacuoles, suggesting it may be trapped in both early and possibly late compartments (Figure 4.12). Due to technical difficulties I was unable to assess the colocalisation of CD8-Furin with these markers.

4.2.7 Loss of PIKfyve activity also affects the retrieval of Shiga toxin

The data presented thus far suggest that loss of PIKfyve affects both retromer-dependent and retromer-independent retrieval pathways to the TGN. In order to further reinforce this idea the retrieval of a final marker to the TGN was examined. The B subunit of the AB_5 type toxin, Shiga toxin, is reported to facilitate the entry of this toxin into the cell and its subsequent transport to the TGN via the early endocytic pathway (Mallard *et al.*, 1998; Bonifacino and Rojas, 2006). Given that this assay had not previously been examined in the context of knockdown of PIKfyve or any of the other proteins studied here, the effect of siRNA treatment was first examined. PIKfyve siRNA treatment leads to a delay in retrieval of Shiga toxin B subunit to the TGN, in a similar manner to that seen with the CD8 assay (Figure 4.13). Loss of Vac14, WIPI-2 or Fig4 has no effect on the Shiga toxin B subunit retrieval pathway (Figure 4.14). In addition, a combination of Vac14 and Fig4 knockdown had no effect. And, to ensure that WIPI-1 was not able to compensate for a loss of WIPI-2, a combination knockdown of both of these proteins was also examined, and was found to have no effect. Pharmacological inhibition of PIKfyve also affects this pathway in a similar

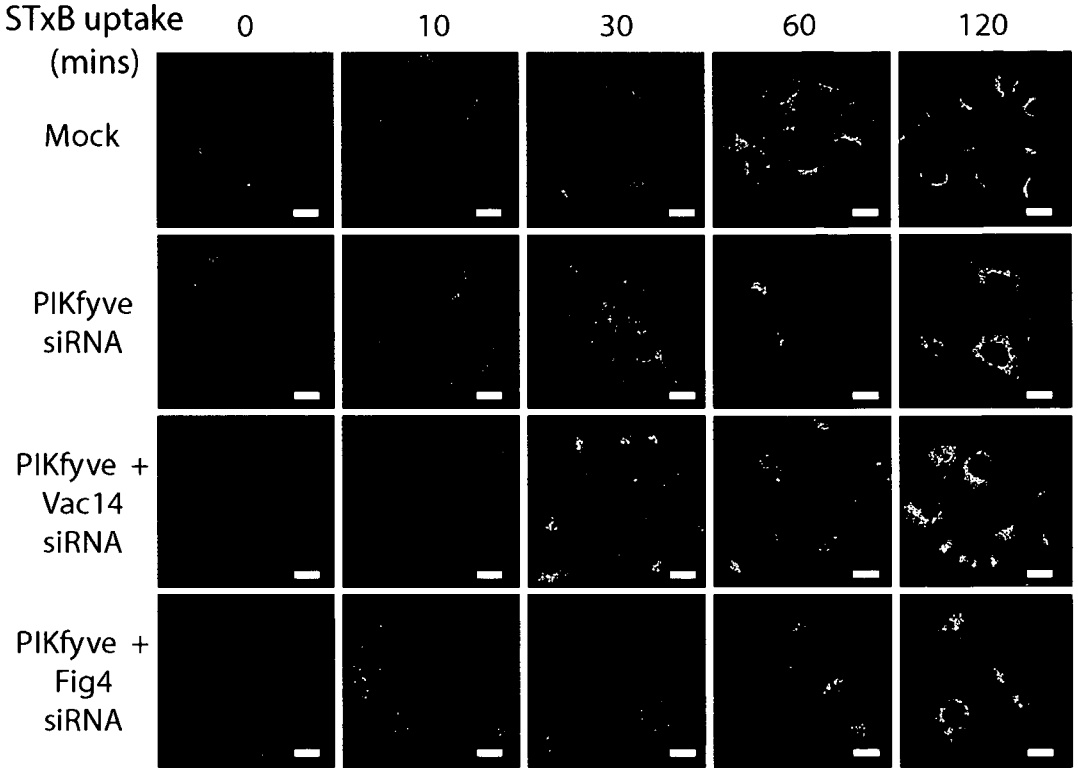

Figure 4.13. Shiga toxin retrieval is delayed following PIKfyve knockdown

HeLa cells were treated with 40nM of the indicated siRNA oligos for 72h prior to labelling with 2µg/ml Cy3-STxB as described in materials and methods and chase with fresh HeLa growth medium for the indicated timepoints. PIKfyve knockdown, and combination knockdowns including PIKfyve, caused a delay in retrieval of Shiga toxin to a perinuclear localisation at the 2h timepoint. Scale bars represent 20µm.

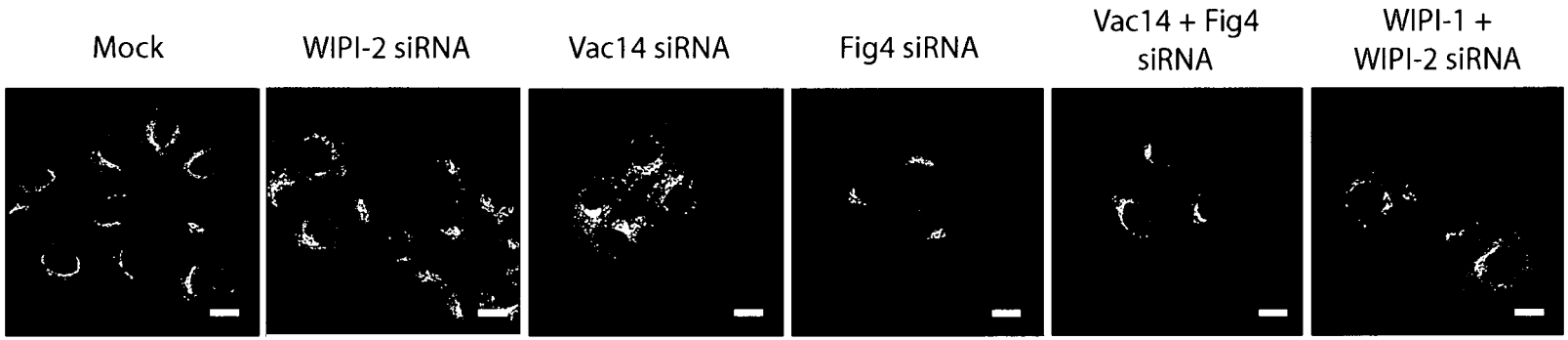

Figure 4.14. Knockdown of other proteins does not affect Shiga toxin retrieval.
HeLa cells were transfected twice with 40nM oligos against the indicated proteins over 72 hours, prior to labelling with 2μg/ml Cy3-STxB as described in materials and methods and chased with fresh HeLa growth medium for 120mins prior to fixation in 3% PFA/PBS. Depletion of these proteins had no effect on the retrieval of Shiga toxin. Scale bar represents 20μm.

manner to PIKfyve knockdown (Figure 4.15). This was further characterised (Figure 4.16) and the terminal timepoint of Cy3-STxB uptake was assessed for colocalisation with the TGN markers TGN46 and Golgin-245. As with CD8-ciM6PR and CD8-Furin, Cy3-STxB is able to reach a TGN compartment, illustrated by its colocalisation with Golgin-245. However, its accumulation there is impeded. Interestingly, in contrast to CD8-ciMPR and CD8-Furin there is significant colocalisation of Cy3-StxB with dispersed TGN46-labelled punctae.

4.3 Discussion

The work presented in this chapter serves to elaborate on the current literature regarding the proposed role of PtdIns(3,5)P_2 in regulating trafficking pathways between the endocytic pathway and the TGN. It is clearly demonstrated that a loss of kinase activity, and thus a loss of cellular PtdIns(3,5)P_2 is sufficient to disrupt a variety of retrieval pathways to the TGN.

4.3.1 Vacuole characterisation

In this study siRNA suppression of endogenous PIKfyve induces progressive accumulation of cytoplasmic vacuoles in approximately 30% of cells. This is in good agreement with other published work (Rutherford *et al.*, 2006). Vac14 suppression lead to the same phenotype in a very small minority of cells, again in agreement with published literature that suggests that knockdown of Vac14 does not induce vacuole formation, but instead make cells prone to develop cytoplasmic vacuoles following mild osmotic

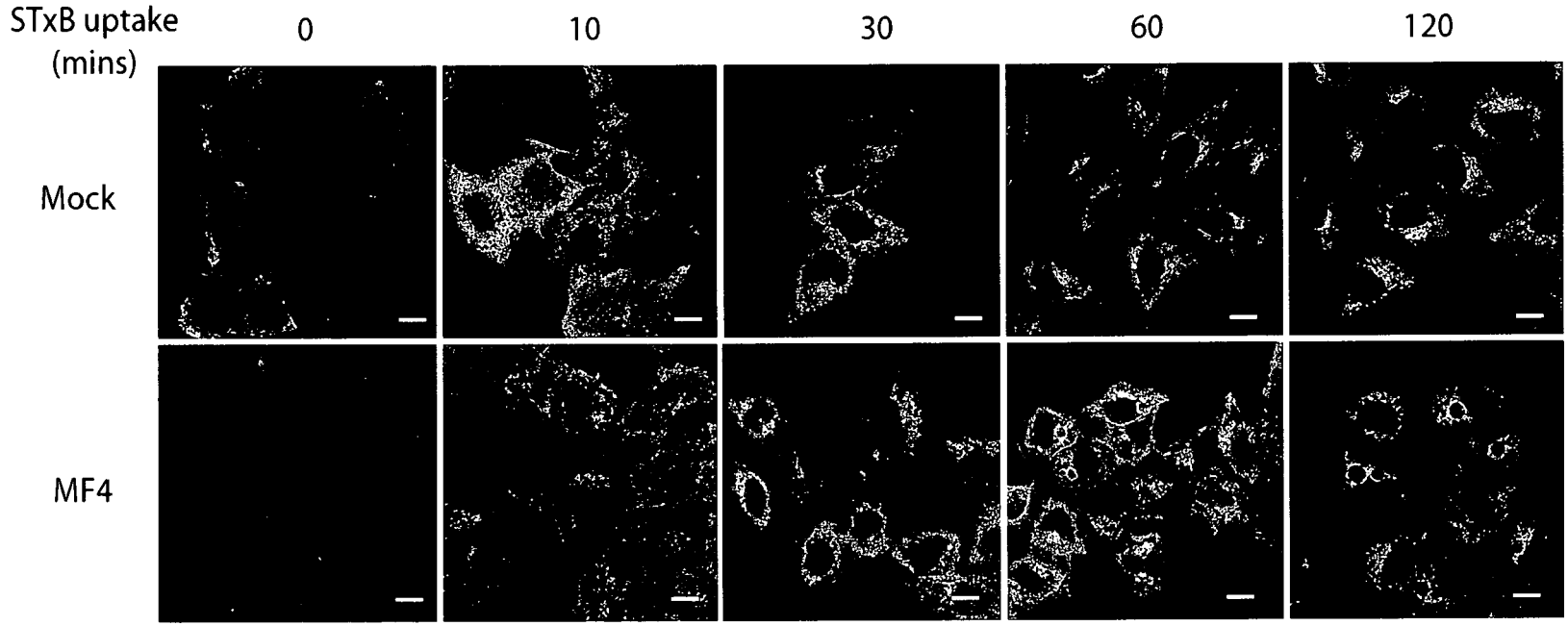

Figure 4.15. Inhibition of PIKfyve causes a delay in STxB retrieval.
HeLa cells were treated with 800nM MF4 prior to labelling with 2μg/ml Cy3-STxB and chase in HeLa growth medium for the indicated times. Inhibition of PIKfyve causes a delay in retrieval of Cy3-STxB to the TGN. Scale bars represent 20μm.

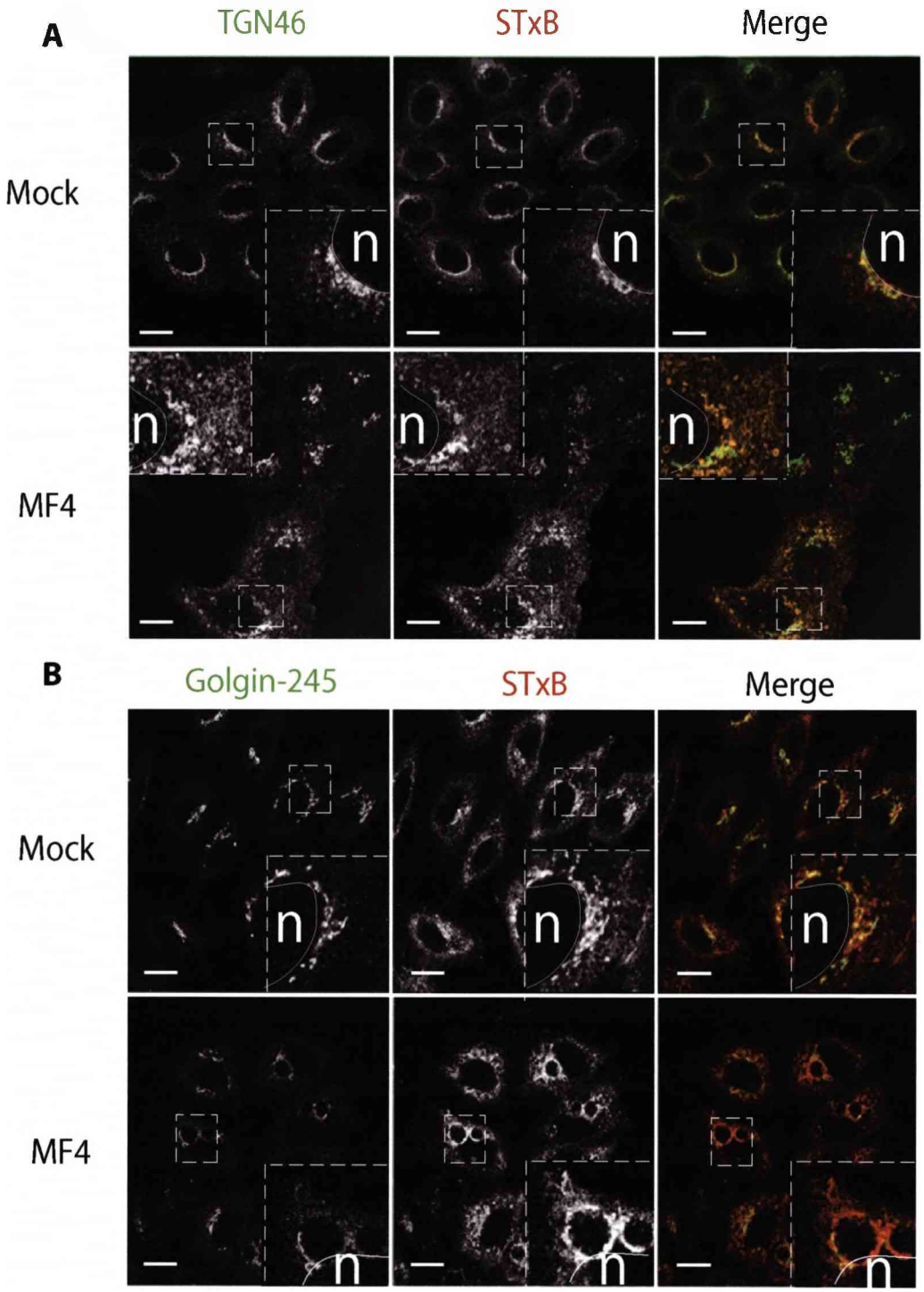

Figure 4.16. Loss of PIKfyve activity affects Shiga toxin and TGN46 retrieval in a similar manner.

The colocalisation of golgi markers with Cy3-STxB at the terminal timepoint of uptake (120mins) was examined in HeLa cells treated with 800nM MF4 for 4 hours. Following loss of PIKfyve activity, in cells where TGN46 is severely perturbed there is substantial colocalisation with Cy3-STxB (A). This is not the case for the more stable golgi marker Golgin-245 (B). Scale bars represent 20μm.

shock (Sbrissa *et al.*, 2004; this study). Furthermore, a combined knockdown of Vac14 and PIKfyve was found not to increase the number of cells displaying cytoplasmic vacuoles more than PIKfyve knockdown alone.

These findings suggest that PIKfyve is able to function in the absence of Vac14 activation, but that Vac14 may be required for optimal PtdIns(3,5)P_2 production under certain conditions. For example, where elevated levels of PtdIns(3,5)P_2 are observed, such as under certain cellular stresses, Vac14 may serve to further activate PIKfyve kinase activity beyond the basal level. This has been shown to be the case in yeast, where Vac14 is required for the elevation of PtdIns(3,5)P_2 in response to osmotic shock (Bonangelino *et al.*, 2002), however, in a number of mammalian cell lines (ie. Cos-7) PtdIns(3,5)P_2 levels do not increase in response to osmotic stress (Dove *et al.*, 1997).

An alternative explanation for this finding is that, given that Vac14 has been shown to interact with and stabilise the mammalian phosphatase Fig4 (Sbrissa *et al.*, 2007), a loss of Vac14 may result in reduced function of Fig4 and reduced turnover of PtdIns(3,5)P_2, effectively compensating for the reduced PIKfyve activity. In yeast, Vac14 has been shown to recruit Fig4 to membranes (Rudge *et al.*, 2004), although the exact purpose of the interaction between the mammalian proteins is not understood. In this study we were unable to detect any changes in localisation of the overexpressed proteins upon coexpression (Figure 3.11), but it has been demonstrated in the literature that overexpression of Vac14 increases punctate staining of Fig4 in Cos-7 cells (Sbrissa *et al.*, 2007).

Recently, it was demonstrated that cultured neurons and fibroblasts from Vac14 knockout mice have swollen cytoplasmic vacuoles (Zhang *et al.*, 2007). Thus, it is possible that the small amount of protein retained in cells following Vac14 knockdown is sufficient to carry out Vac14 function, and that vacuoles are only present when loss of Vac14 protein is complete as in the knockout mice. Alternatively, Vac14 may play an as yet unidentified tissue specific critical role. For example, in neurons it has been shown to bind neuronal nitric oxide synthase (Lemaire and McPherson, 2006).

Fig4 and WIPI-2 knockdown do not induce formation of cytoplasmic vacuoles. This is somewhat surprising for WIPI-2 given that the yeast homologue Atg18/Svp1 was initially identified from a screen for mutant proteins that produced the same **s**wollen **v**acuole **p**henotype (hence **Svp1**) as Fab1 mutants. However, as discussed in section 1.8 (see also figure 1.12) there are four members of the mammalian WIPI family, WIPI-1 is 53% identical to WIPI-2 and both are equally related to the yeast protein. Therefore, the question remains as to whether there may be functional redundancy between these two proteins, and when WIPI-2 is no longer present, WIPI-1 may be able to compensate functionally.

As far as Fig4 is concerned, although no effective protein knockdown was demonstrated, from RT-PCR data it is clear that messenger RNA levels were reduced, which most likely corresponds to a loss of protein. Mutant Fig4 cells in yeast do not display a swollen vacuole phenotype, and show no change in PtdIns(3,5)P_2 levels (Rudge *et al.*, 2004), suggesting that there may be other 5-phosphatases that can dephosphorylate PtdIns(3,5)P_2 and compensate for a loss of Fig4. In mammalian cells however, ablation of

mammalian Fig4 (also described as Sac3), has been shown to increase levels of PtdIns(3,5)P_2 *in vitro* but still did not lead to formation of cytoplasmic vacuoles. Instead, in a similar manner to Vac14, it renders them more prone to developing such vacuoles upon treatment with mild osmotic stress (Sbrissa *et al.*, 2007). A combined knockdown of PIKfyve and Fig4 did not affect the number of cells displaying the vacuole phenotype, suggesting that loss of Fig4 and reduced turnover of PtdIns(3,5)P_2 is insufficient to compensate for the PIKfyve knockdown phenotype.

It has previously been shown that the loss of endomembrane integrity and subsequent formation of vacuoles is dependent on the lipid kinase activity of PIKfyve and not its protein kinase activity or other functions (Ikonomov *et al.*, 2002a). The finding that vacuoles are displayed in cells treated with PIKfyve inhibitor further indicates that their formation is as a direct result of loss of PIKfyve activity, and most likely reduced levels of PtdIns(3,5)P_2. It could also be due to a reduction in PtdIns(5)P or an elevation of PtdIns(3)P levels. However, the latter seems unlikely, because the vacuoles appear to be of endosomal origin, and the swelling of endosomal compartments is similar to the swollen vacuole phenotype observed in *S. cerevisiae*, which have no detectable levels of PtdIns(5)P (McEwen *et al.*, 1999; Walker *et al.*, 2001). Also, mutations in myotubularins that are predicted to lower PtdIns(5)P levels do not display this phenotype (Schaletzky *et al.*, 2003; Tsujita *et al.*, 2004). Furthermore, it is unlikely to be due to an increase in PtdIns(3)P as knockdown of Vps34, the kinase that catalyses the formation of PtdIns(3)P, results in a loss of both PtdIns(3)P and PtdIns(3,5)P_2, and also displays swollen vacuoles (Johnson *et al.*, 2006).

However, in order to be certain that these results truly represent a specific loss of PtdIns(3,5)P_2 it would be necessary to examine the levels of phosphoinositide lipids following treatment with the inhibitor, something that is technically demanding and was not feasible in the time limitation of this study. This is a limitation that therefore needs to be taken into account.

Characterisation of the cytoplasmic vacuoles in this study revealed that they were endosomal in origin, and they most likely represent some form of late endosomal/MVB defect. The large vacuoles are surrounded by LAMP-2 vesicles, although it is unclear if this marker labels the limiting membrane or not. It could be that the LAMP-2 labels microdomains on the membrane of the vacuoles, or that the LAMP-2 staining represents LAMP-2 vesicles fused to the surface of the vacuoles. Immuno-EM studies would help to further clarify the nature of this staining and the origin of the vacuoles. It is clear however, that early endosomal compartments are also more elaborate and swollen, but early endosomal markers are excluded from the larger vacuoles, despite the finding that Rab5 positive vesicles fuse to the expanding vacuole membrane (Jefferies *et al.*, 2008). This suggests that maturation from early endosome to MVB/late endosome/MVB is most likely unaffected, but also that EEA-1 and PtdIns(3)*P* function is unaffected. And indeed localisation of PtdIns(3)*P*, as judged by examination of a biotinylated GST-tagged tandem FYVE domain, was also unaffected.

Electron microscopy studies reveal that large cytoplasmic vacuoles do not readily take up endocytosed HRP, in agreement with a recent study that found that they are also inaccessible to the fluid-phase marker Dextran (Zhang *et al.*, 2007). Large cytoplasmic vacuoles were often found to be

surrounded by smaller HRP labelled swollen compartments that most likely correspond to swollen endosomes, as the early endosomal marker displays a similar distribution by immunofluorescence.

Given that these large vacuoles contain fewer internal vesicles, and are predominantly empty, it has been suggested that they represent a failure in the formation of ILVs. The finding that a member of the ESCRT III complex, CHMP3, and other proteins involved in MVB formation, may be effectors of PtdIns(3,5)P_2, although the evidence for the specificity of these interactions is disputed, adds weight to this hypothesis. However, we observed ILVs in both the EEA-1 labelled compartments and also normal MVBs and lysosomes by EM following both knockdown and inhibition of PIKfyve, suggesting that if PtdIns(3,5)P_2 does function in formation of internal vesicles, this may only be in a subset of MVBs. It is widely believed that different populations of MVBs may exist with different functions (as discussed in section 1.2.4), thus PIKfyve function may be expendable for certain types of ILV formation.

Knockdown of the WIPI-2 and Fig4 was also examined by electron microscopy. Neither displayed any visible phenotype at neither the light microscope nor the electron microscope level, except that it was noted that WIPI-2 knockdown caused a substantial amount of cell death. Overexpression of WIPI-2 constructs also affected both HeLa and HEK293 cells in this manner, suggesting that changes in the levels of WIPI-2 is toxic to cells and its abundance may be tightly regulated.

4.3.2 Endosome to TGN trafficking

Previous characterisation of some of these proteins in both *S. cerevisiae* and mammalian cells, indicated that PtdIns(3,5)P_2 may be involved in the regulation of trafficking between endosomes and the TGN. I chose to revisit this hypothesis and examine the effect of siRNA suppression of each protein and inhibition of PIKfyve on a range of different pathways.

Over the past few years the existence of several distinct pathways from the endocytic pathway to the TGN has come to light. Each pathway seemingly transports different cargos using a range of different protein coats and complexes. One such pathway is the retromer-mediated pathway, which uses the retromer complex (described in section 1.2.7) to mediate recycling of the bulk of the ciM6PR back to the TGN once they have delivered their cargo onto the endosomal pathway.

By examining the effect of knockdowns and PIKfyve inhibition on the steady state distribution of ciM6PR, and subsequently on the retrieval of cell surface CD8-ciM6PR to the TGN, I found that a loss of PIKfyve activity, both long-term chronic loss and acute pharmacological inhibition, had the same effect. They caused redistribution of ciM6PR at steady state, and a delay in retrieval of the chimeric construct to the TGN, such that these markers did not display a typical perinuclear staining, but instead surrounded the cytoplasmic vacuoles, and labelled swollen endosomal compartments.

However, chimeric CD8-ciM6PR was able to reach a TGN compartment to some degree, and there was no alteration in cellular levels of ciM6PR, or of retromer proteins Vps26 and SNX-1 (interestingly, SNX-1, is proposed to bind PtdIns(3,5)P_2). This suggested that ciM6PR was eventually

able to retrieve to the TGN, albeit with altered dynamics, and was not rerouted to the lysosome, since the protein was not degraded. Alternatively, a second defect in lysosomal acidification in mammalian cells, similar to the improper acidification of the yeast vacuole, could also explain this finding.

It was also noted that the TGN marker TGN46 displayed a different distribution following loss of PIKfyve activity, redistributing into punctate, vesicular structures in some cells. TGN46 has been reported to cycle between the plasma membrane and the TGN via the endocytic pathway, albeit via a partially different route to ciM6PR; through early and recycling endosomes, bypassing the late endocytic pathway (Ghosh *et al.*, 1998; Mallet and Maxfield, 1999). My further investigation showed that the TGN46 punctae colocalised with Tf-labelled recycling endosomes, suggesting that TGN46 becomes trapped in early/recycling compartments to some degree. TGN46 did still display a partially perinuclear distribution and showed overlap with ciM6PR in this position. Taken together with an increased colocalisation between CD8-ciM6PR and EEA-1, these results imply that there is not a complete loss of cycling but more a delay in retrieval and therefore a shift in the steady state equilibrium of these proteins.

A second assay for examining the dynamics of retrieval from endosomes to the TGN also showed a delay following loss of PIKfyve activity. The Shiga toxin B subunit reportedly traffics on the same pathway as TGN46 to reach the TGN. Thus, the fact that not only was its retrieval perturbed, but that it also colocalised with TGN46 vesicular structures, further supports the hypothesis that multiple pathways are perturbed and that

recycling cargo becomes trapped to some degree in swollen endosomal compartments.

Loss of PIKfyve activity not only affected various trafficking itineraries from the endocytic pathway to the TGN, but also various retrieval mechanisms. There was also a delay in the retrieval of CD8-Furin to the TGN, a protein that is thought to utilise a retromer-independent mechanism to recycle to the TGN. Although not examined in the current study, previous work has determined that recycling of EGF to the plasma membrane is unaffected following PIKfyve knockdown (Rutherford *et al.*, 2006); this suggests that this recycling pathway, believed by many to represent a default pathway that does not require any specific sorting motifs, may be unaffected, and that PIKfyve may specifically coordinate the retrieval of TGN-directed membrane from endosomes.

A limitation of the work presented in this chapter is that morphological studies are not quantitative, and do not give any indication of the proportion of cells affected by the phenotypes observed, except in the case of TGN46. In order to increase the impact of the work presented, quantitative assessment using programs such as Image J could help to give an indication of the statistical significance of the results presented. This was not done due to time limitations of the current study.

4.3.3 Conclusion

In conclusion, this chapter establishes a role for PtdIns(3,5)P_2 in regulating the dynamics of endosome to TGN trafficking, and suggests that a defect in membrane retrieval from various stages of the endocytic pathway

could result in the swollen endocytic compartments and cytoplasmic vacuoles observed upon loss of this lipid. Current models for endocytic trafficking suggest that material is continually sorted throughout the progression of the pathway to the lysosome. Tubulation of early endosomes and MVBs permits membrane retrieval from this pathway to various intracellular destinations, whereas ILV formation segregates cargo for lysosomal degradation. As the pathway progresses the MVB matures or cargo is passed onto a more mature compartment that possesses less tubules and more ILVs and is capable of fusing with the lysosome. The fact that proteins that display delayed trafficking to the TGN are redistributed to the limiting membrane of the swollen endocytic compartments, and that these swollen compartments display fewer intralumenal vesicles, suggests that PtdIns(3,5)P_2 might be involved in coordinating the maturation of the MVB and the coordinated sorting of internalised cargo into the correct regions of the endosome for retrieval or for delivery to the lysosome.

Indeed PtdIns(3,5)P_2 and PIKfyve have been reported to interact with various proteins which coordinate these different functions. For example, PIKfyve interacts with p40 (Ikonomov *et al.*, 2003b), a Rab9 effector responsible for retrieval of ciM6PR from the late endosome, and PtdIns(3,5)P_2 interacts with SNX-1 (Carlton *et al.*, 2005), a component of the mammalian retromer complex. Fab1 has been reported to bind a range of different effector proteins from a variety of endosome to TGN pathways, including AP-1 components (Phelan *et al.*, 2006). Another reported PtdIns(3,5)P_2 effector is the Epsin-like protein Ent3p (Eugster *et al.*, 2004). Ent3 binds clathrin, AP-1 and the GGA proteins, suggesting it also promotes

vesicle formation at the endosomal membrane (Duncan *et al.*, 2003). On the other hand various components of MVB formation are also reported to bind PtdIns(3,5)P_2, such as Vps24/CHMP3 (Whitley *et al.*, 2003), a member of the ESCRTIII complex proposed to facilitate MVB formation. The reduced number of intralumenal vesicles in the swollen endocytic compartments observed with loss of PIKfyve activity, have lead some to conclude that the defect lies in internalisation of intralumenal vesicles. However, MVBs with many internal vesicles are present in *Drosophila* Fab1 mutant cells (Rusten *et al.*, 2006), and following siRNA and inhibition of PIKfyve (this study), suggesting that PIKfyve is dispensable for at least some types of inward veisculation. In support of this hypothesis, a recent study determined that in cells overexpressing kinase-deficient PIKfyve, intralumenal vesiculation of LBPA containing late endosomes was unaffected (Ikonomov *et al.*, 2006).

CHAPTER FIVE

The Role of PIKfyve in Regulating Tyrosine Kinase Receptor Downregulation

5.1 Introduction

Cells deficient in PtdIns(3,5)P_2 display massively dilated endocytic compartments, and perturbed uptake of fluid phase markers into MVBs/late endosomes, as characterised in this study and previous literature. A key question in PtdIns(3,5)P_2 biology is the origin of these swollen vacuoles. There are a number of potential reasons for their appearance. Findings from the previous chapter, in the context of the current literature, indicate that one contributing factor may be perturbed retrieval of membrane from various stages of the endocytic pathway to the TGN. However, the reduced number of ILVs in these compartments, observed by EM, also suggests that there might be a defect in invagination of membrane into the MVB/late endosome, which could further add to the membrane swelling.

Both of these findings could be consolidated by the hypothesis that PtdIns(3,5)P_2 acts to recruit a range of effector proteins that coordinate the progressive maturation of endosomes, by regulating the dynamics of partitioning of endosomes into tubular and vesicular membranes. At the early and late endosome PtdIns(3,5)P_2 effectors, such as SNX-1, and PIKfyve binding proteins, such as p40, may facilitate the inclusion of recycling cargo into tubular elements destined for retrieval to the TGN. However, at a later stage of the endocytic pathway, other PtdIns(3,5)P_2

effectors may help to coordinate the maturation of the vesicular MVB/late endosome, such that it is able to fuse with the lysosome.

If this were the case, one might expect to see perturbations in the trafficking of endocytosed material to the lysosome. In keeping with this hypothesis, *Drosophila* Fab1 mutants display perturbation in downregulation of internalised receptors (Rusten *et al.*, 2006) and in *S. cerevisiae* Fab1 mutants have an improperly acidified vacuole and a defect in trafficking biosynthetic material to the vacuole (Odorizzi *et al.*, 1998; Rudge *et al.*, 2004). However, conflicting evidence suggests that trafficking of endocytosed material in *S. cerevisiae* is unperturbed and the defects in trafficking of biosynthetic material can be overcome by irreversible ubiquitination. Furthermore, in mammalian cells, studies with both PIKfyve siRNA and overexpression of a kinase-dead mutant, have found no effect on the downregulation of EGFR (Ikonomov *et al.*, 2003a; Rutherford *et al.*, 2006), a well-characterised endocytic cargo, suggesting that endocytosed material is still able to reach a functional lysosome.

Given that PIKfyve knockdown is somewhat inefficient, and the caveats of analysing overexpressed proteins, I decided to re-examine EGFR downregulation in mammalian cells following acute inhibition of PIKfyve with MF4. Furthermore, the effects of loss of other proteins associated with PtdIns(3,5)P_2 metabolism has not been examined in this context. In particular, given that loss of WIPI-2 does not exhibit any effects on endosome to TGN trafficking pathways, this protein may instead act as an effector of PtdIns(3,5)P_2 in other cellular processes. The aim of this chapter was to consolidate the observations made in different organisms and

conclusively determine what effect loss of PIKfyve activity has on trafficking of endocytic cargo to the lysosome in mammalian cells. Furthermore, to determine whether knockdown of other PtdIns(3,5)P_2 associated proteins may exhibit an effect on this pathway.

5.2 Results

5.2.1 Effect of single knockdowns on EGFR downregulation

The effect of suppression of each protein on the rate of EGFR downregulation was examined (Figure 5.1). Following 72-hour transfection with siRNA oligos specific to each protein, ligand was added to culture medium at a saturating concentration (100ng/ml), following overnight serum starvation. Ligand binds to cell surface EGFR causing its internalisation and subsequent sorting to and degradation in the lysosome. Cells were lysed at various timepoints, and Western blotting used to assess the amount of EGFR remaining in the cell. Knockdown efficiency of the oligos used in these experiments is outlined in figure 4.1 (PIKfyve oligo 3, WIPI-2 and Vac14 oligo 4). There is no effect on the rate of EGFR downregulation following knockdown of each protein. A sample of control cell lysates was also loaded onto each gel (although not shown in the final figure) to serve as a loading standard and enable quantitation between blots.

5.2.2 Effect of combined knockdowns on EGFR downregulation

Our initial hypothesis was that knockdown of PIKfyve alone may not be sufficient to display an effect on EGFR downregulation, due to the residual levels of protein upon incomplete knockdown (see figure 4.1). As

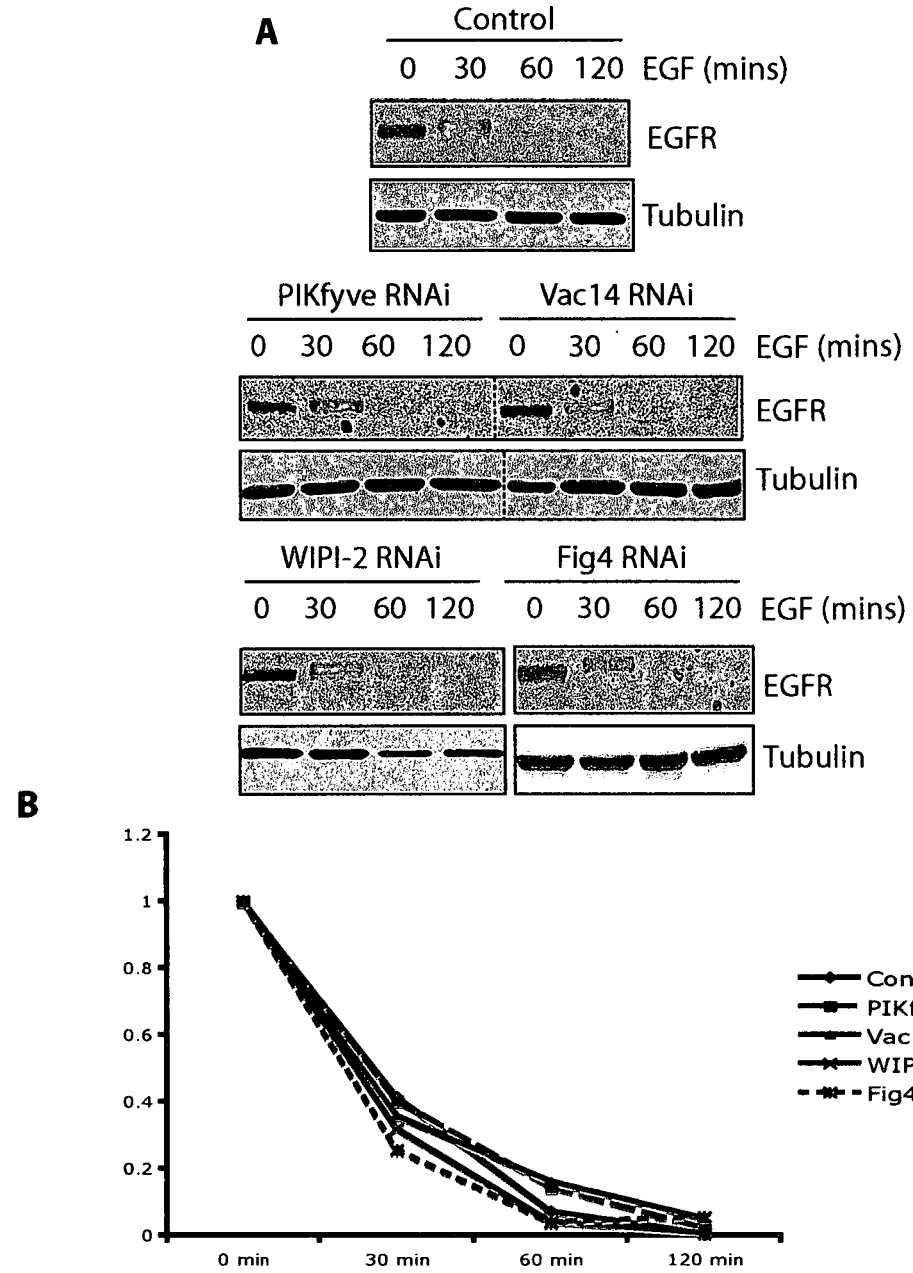

Figure 5.1. EGFR degradation is unaffected in single knockdown cells
HeLa cells were seeded onto 6-well plates and transfected twice with 40nM siRNA scrambled oligos and individual or pooled (Fig4) oligos specific for the indicated proteins over 72h. Cells were then serum starved overnight and the following day 100ng/ml mouse EGF added for the indicated time points, followed by lysis in NP40 lysis buffer. A) Proteins were resolved by SDS-PAGE, transferred to nitrocellulose and probed with a goat anti-EGFR antibody. Mouse anti-tubulin antibodies were used to probe tubulin levels and serve as a protein loading control. B) The amount of control EGFR remaining at each time point was quantified using Odyssey software, relative to control lysates loaded onto each separate gel. EGFR degradation is unperturbed following individual knockdown of each protein.

such, several proteins were suppressed simultaneously to examine their combined effects. Whilst knockdown of PIKfyve on its own had no significant effect on EGFR downregulation, combination with either Vac14 or Fig4 knockdown produced a subtle delay in its degradation (Figure 5.2 A). The percentage of EGFR remaining following 2 hours of EGF stimulation was quantified for each condition (Figure 5.2 B) using Odyssey software; levels of EGFR at 2 hours were assessed relative to EGFR levels at 0 hours, and were compared to the levels of a control protein lysate (not shown) to account for samples being run on separate gels.

5.2.3 Effect of PIKfyve inhibition on EGFR and c-Met downregulation

Given that residual PIKfyve protein remains following siRNA treatment, and that combined knockdowns incorporating PIKfyve produced a mild effect on EGFR downregulation, it was hypothesised that to see the effect of PIKfyve on this pathway may require a stronger suppression of PIKfyve activity, or a more dramatic acute loss of PtdIns(3,5)P_2. Indeed, acute pharmacological inhibition of PIKfyve activity with MF4 led to a much more pronounced delay in EGFR downregulation (Figure 5.3).

Initial experiments were performed with 3μM PIKfyve inhibitor (Figure 5.3 A). Upon observation of a strong effect, these experiments were repeated at a range of inhibitor concentrations, spanning the *in vitro* IC_{50} of the drug (23nM), in order to reduce the likelihood that MF4 could potentially be inhibiting other kinases. Severe effects on EGFR downregulation could be seen at concentrations beginning at approximately 1μM MF4 (Figure 5.3 B). Experiments were subsequently repeated at 800nM, to match the

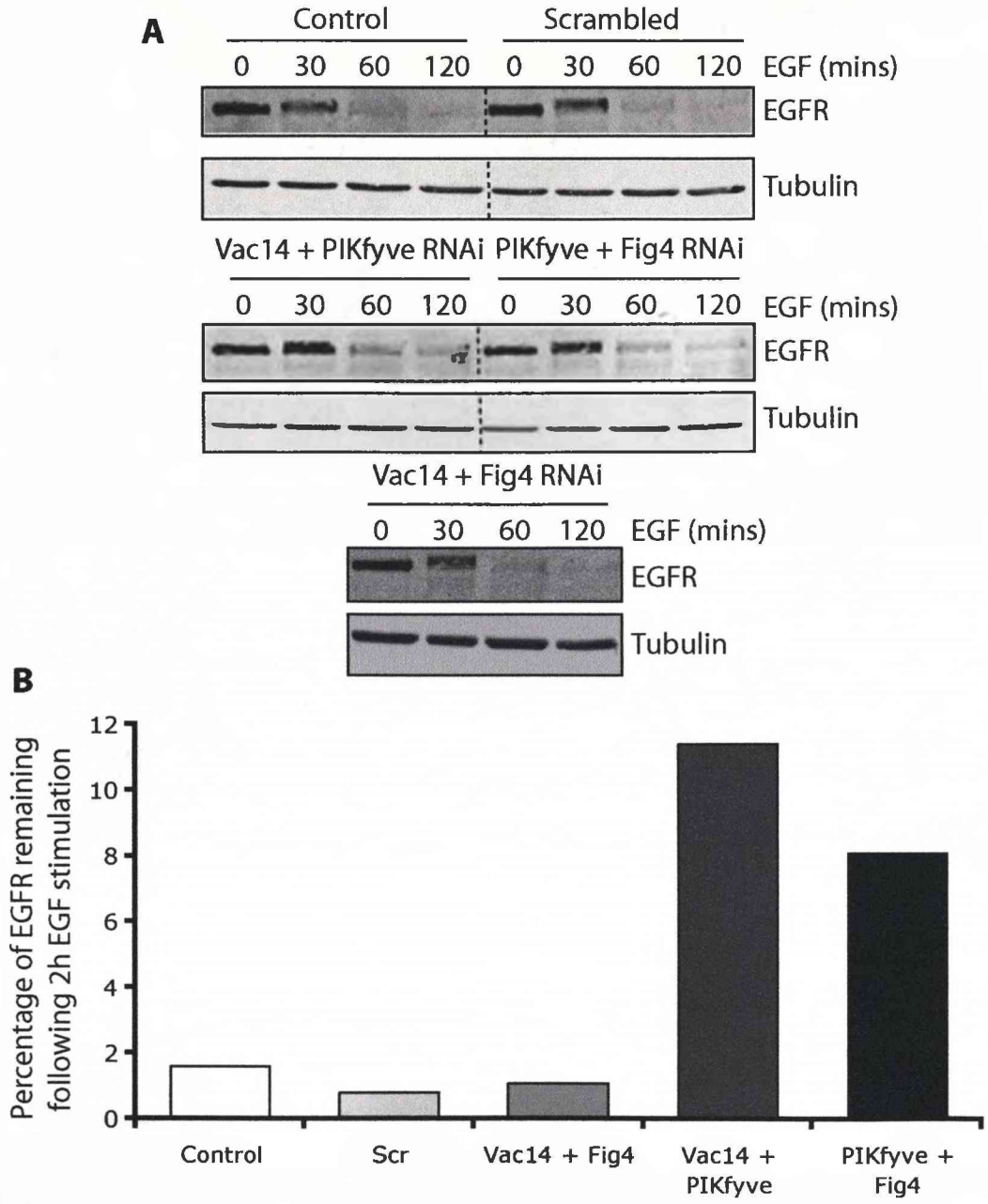

Figure 5.2. A delay in EGFR degradation is observed following combination knockdowns incorporating PIKfyve.

HeLa cells were seeded onto 6-well plates and transfected twice with scrambled or individual or pooled (Fig4) specific oligos as indicated over 72h. Subsequently cells were serum starved overnight and then 100ng/ml mouse EGF added for the indicated timepoints. Cells were lysed in NP40 lysis buffer and 50µg run on an SDS-PAGE gel. A) Proteins were transferred to nitrocellulose and probed with goat anti-EGFR antibodies. Mouse anti-α tubulin antibodies were used to probe for tubulin as a protein loading control. B) The percentage of EGFR remaining after 2h EGF stimulation was quantified. Combined knockdown of either Vac14 or FIg4 with PIKfyve causes a delay in EGFR downregulation.

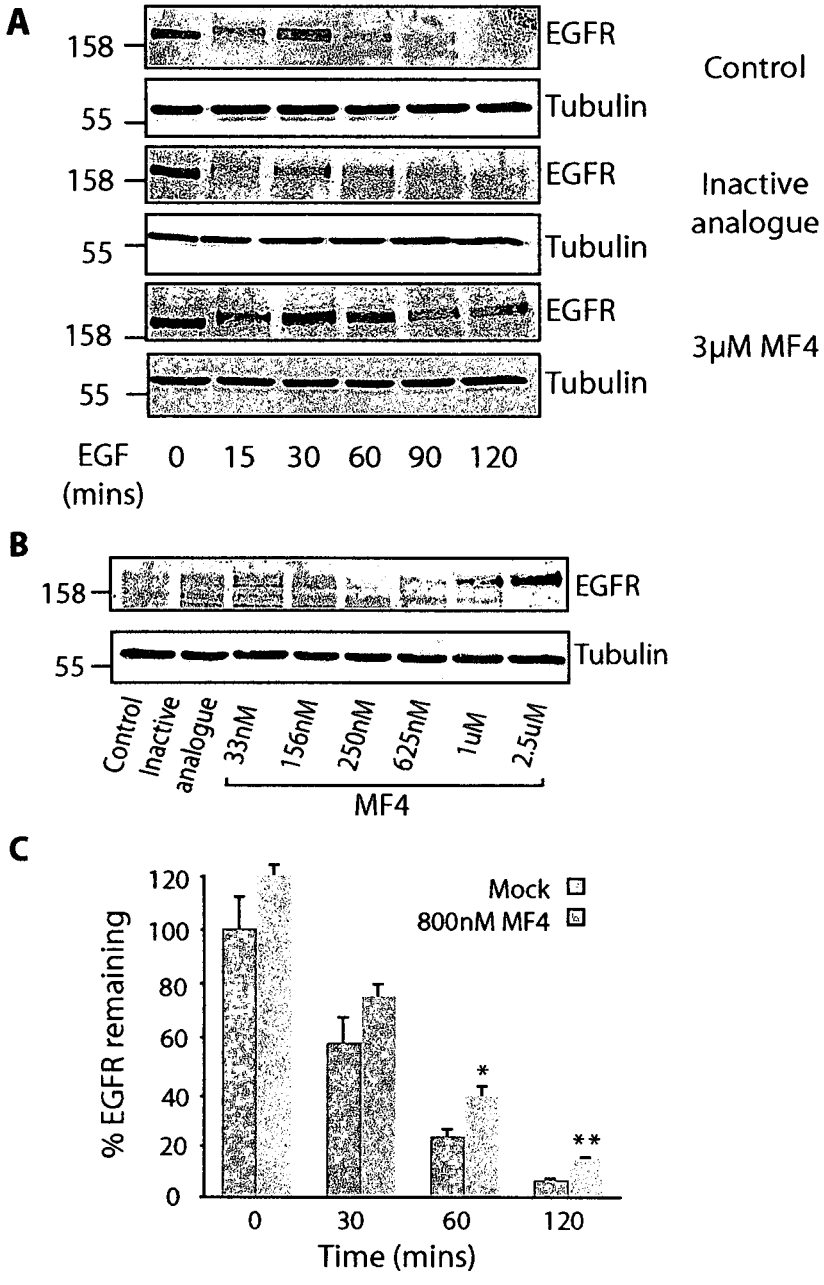

Figure 5.3. EGFR downregulation is severely delayed following inhibition of PIKfyve kinase activity.

HeLa cells were seeded onto 6-well plates. The following day cells were treated with A) 3μM MF4 B) a range of different concentrations or C) 800nM EGF for 4 hours. 100ng/ml EGF was then added to the cells for the indicated timepoints (A and C) or 120mins (B). Cells were lysed in NP40 lysis buffer and 50μg protein was resolved on an SDS-PAGE gel. Proteins were transferred to nitrocellulose and probed with goat anti-EGFR antibodies. Mouse anti-αtubulin antibodies were used to probe for tubulin as a protein loading control. C) The affect on downregulation was quantified using Odyssey software, N=3 +/- SEM, * $p<0.05$ ** $p<0.01$ (t-test). PIKfyve inhibition significantly delays the degradation of EGFR.

concentration used in previous experiments (Jefferies *et al.*, 2008). Although the effect was not as substantial at this lower dose, a statistically significant delay in EGFR downregulation was observed at later timepoints (Figure 5.3 C) (N=3, $p<0.05$, student's t-test).

In order to determine if this was a general effect on the degradative pathway, or specific to EGFR trafficking, I examined the downregulation of a second tyrosine kinase receptor. I found that downregulation of the hepatocyte growth factor receptor (c-Met) was also delayed in cells treated with 3μM PIKfyve inhibitor (Figure 5.4).

5.2.4 EGFR immunofluorescence following loss of PIKfyve activity

In order to dissect the mechanism by which the downregulation of tyrosine kinase receptors was perturbed in PIKfyve deficient cells, the immunofluorescence of EGFR was examined in siRNA and inhibitor treated cells. Individual oligos against WIPI-2 and pooled oligos against Fig4 were used and found to have no effect on cellular EGFR levels (Figure 5.5) as also observed by Western blotting (Figure 5.1). Interestingly, despite the observation that PIKfyve siRNA treatment on its own has no significant effect on EGFR degradation, as assessed by Western blotting (Figure 5.1), a residual amount of EGFR was detected in these cells by immunofluorescence after 4 hours of EGF stimulation, and a small amount remained following Vac14 knockdown also. This suggests that the effect of PIKfyve (and possibly Vac14) depletion is small and only detected by more sensitive methods.

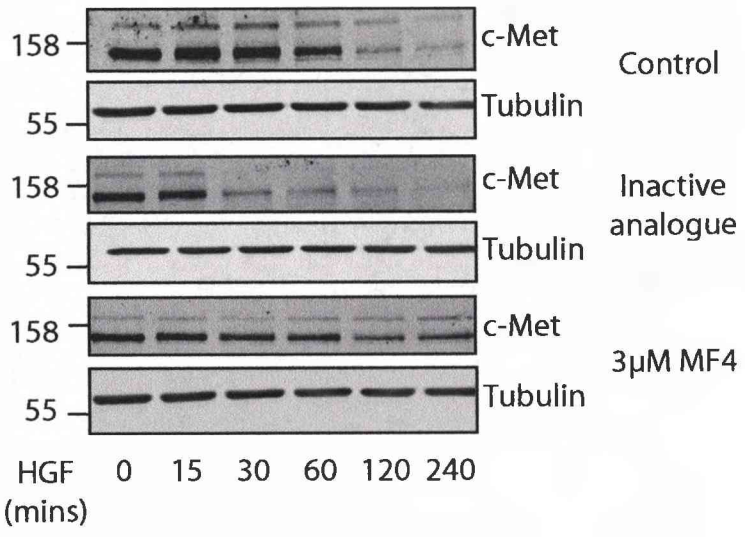

Figure 5.4. c-Met downregulation is also delayed in PIKfyve inhibitor treated cells

HeLa cells were seeded onto 6-well plates and the following day treated with 3μM MF4 or its inactive analogue for 4 hours. 100ng/ml HGF was then added to the medium for the indicated timepoints. Cells were then lysed in NP40 lysis buffer and 50μg protein was resolved on an SDS-PAGE gel. Proteins were transferred to nitrocellulose and probed with mouse anti-Met antibodies. Mouse anti-α tubulin antibodies were used as a protein loading control. The downregulation of Met receptor is perturbed following inhibition of PIKfyve.

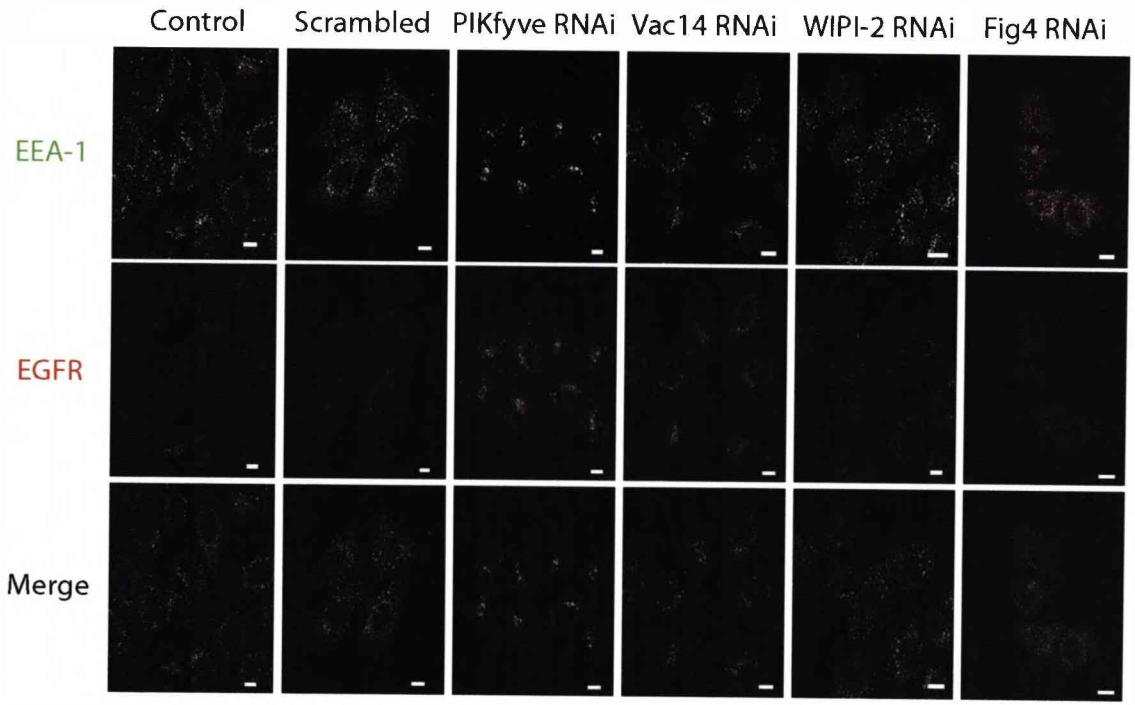

Figure 5.5. EGFR downregulation in single knockdown cells examined by immunofluorescence.
HeLa cells were seeded onto coverslips in 6-well plates. The following day cells were transfected with 40nM scrambled, pooled (Fig4) or individual (PIKfyve, Vac14 and WIPI-2) oligos. 24h later cells were split onto coverslips and a further 24h later transfected again with the same RNAi oligos. Cells were serum starved overnight on day 4, and on day 5 100ng/ml mouse EGF added for 4h. Cells were subsequently fixed in 3% PFA/PBS, permeabilised with 0.2% TX-100 and incubated with a mouse monoclonal EGFR antibody and a rabbit polyclonal EEA-1 antibody. Cells were visualised on a Leica confocal microscope. Scale bars represent 20μm. Despite observing no effect on EGFR degradation in PIKfyve knockdown cells, by a more sensitive IF assay residual EGFR was observed in these cells.

In accordance with the Western blotting data for combination knockdown treatments, when cells were treated with combinations of siRNA oligos directed at PIKfyve with those directed at either Vac14 or Fig4, or when treated with 800nM PIKfyve inhibitor (Figure 5.6), there was a substantial accumulation of EGFR after 4 hours of ligand-induced EGFR downregulation, when compared to control cells.

The question was then raised as to how EGFR downregulation is affected. It was unclear whether the delay in downregulation occurred because the EGFR was unable to reach the lysosome, or if the EGFR reaches the lysosome but is not degraded as this compartment is improperly acidified. Furthermore, if it is unable to reach the lysosome, is this the result of an internalisation defect at the MVB or due to a failure in maturation of the MVB/late endosome and its ultimate fusion with the lysosome? Evidence from *Drosophila*, that the downregulation of wingless receptors is delayed but their signalling output is not prolonged, would suggest that the former explanation is unlikely (Rusten *et al.*, 2006). In this study colocalisation of EGFR with an early endosomal marker EEA-1 revealed that a proportion of the EGFR appeared to have been internalised into the lumen of swollen early endosomes (Figure 5.6), suggesting that internalisation of EGFR was unaffected.

5.2.5 Effect of loss of PIKfyve on downstream signalling and internalisation

In order to further examine the question of the requirement for PIKfyve activity in EGFR degradation, the effect of loss of PIKfyve activity upon downstream signalling pathways was determined. The phosphorylation of

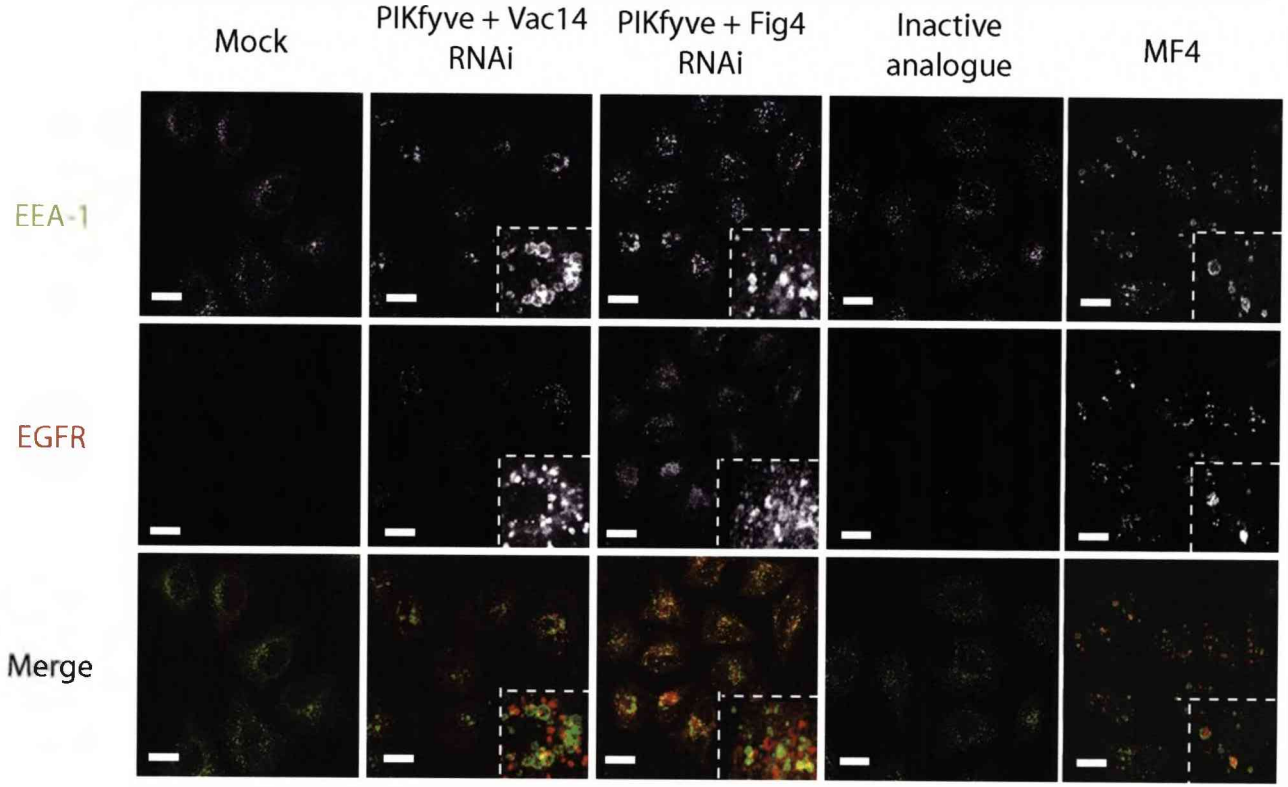

Figure 5.6. EGFR downregulation in combination knockdown and inhibitor treated cells examined by immunofluorescence.

HeLa cells were seeded onto coverslips and the following day treated with 800nM MF4 or its inactive analogue for 4 hours. 100ng/ml EGF was added to the medium for 4h. Cells were fixed in 3% PFA/PBS and permeabilised with 0.2% TX-100. EGFR and early endosomes were labelled with mouse anti-EGFR and rabbit anti-EEA-1 antibodies respectively. Residual EGFR can be seen in HeLa cells following double knockdowns incorporating PIKfyve, or treatment with PIKfyve inhibitor. A portion of this EGFR appears to be internalised into the lumen of swollen EEA-1 labelled compartments. Scale bars 20μm.

two downstream targets of activated EGFR was studied over the timecourse of EGF stimulation (Figure 5.7).

EGFR is activated by the binding of its ligands (ie. EGF), which triggers a series of events including dimerisation, autophosphorylation at several different intrinsic tyrosine residues, signal transduction by phosphorylation of downstream targets (Carpenter, 1987), and receptor internalisation onto the endocytic pathway (Dunn and Hubbard, 1984; Cohen and Fava, 1985; Carpentier *et al.*, 1987). Two key downstream signalling events are the phosphorylation of mitogen activated protein kinase (MAPK) via the Ras/Raf pathway (Rozakis-Adcock *et al.*, 1992; Avruch *et al.*, 1994; Batzer *et al.*, 1994; Robinson and Cobb, 1997), and phosphorylation of Akt/PKB by the PI(3)-kinase pathway (Meisner *et al.*, 1995; Fukazawa *et al.*, 1996).

Following internalisation, EGFR is targeted for degradation in the lysosome, but it has been shown to continue signalling from the surface of early endosomes prior to its internalisation into the MVB lumen where the signal is terminated (Kay *et al.*, 1986; Lai *et al.*, 1989; Sorkin and Carpenter, 1991; Di Guglielmo *et al.*, 1994; Vieira *et al.*, 1996). Thus, if there is a defect in EGFR internalisation, we might expect to find prolonged downstream signalling events. However, downregulation of pAKT/PKB and pMAPK was found to be similar to control cells. In fact, there appeared to be a more rapid downregulation of pAKT/PKB compared to control cells (Figure 5.7).

This suggests that the effects on EGFR downregulation occur at a point after internalisation into the MVB lumen. However, the question remains why there is a defect in EGFR downregulation. There are several

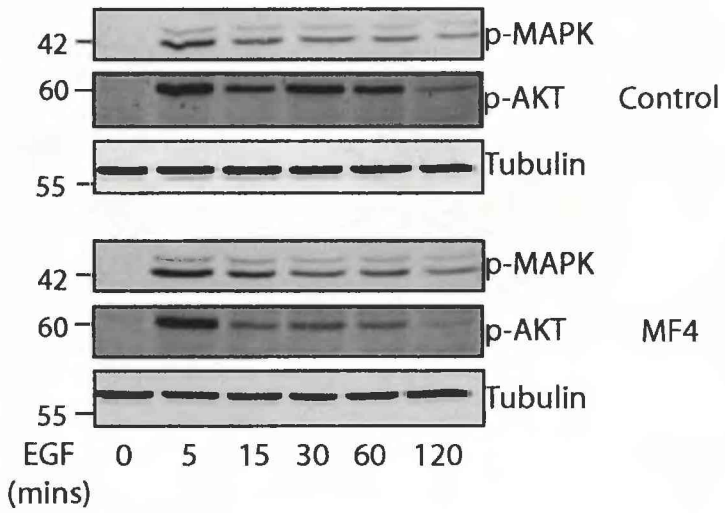

Figure 5.7. pAKT and pMAPK signalling is not prolonged following loss of PIKfyve activity

HeLa cells were seeded onto 6-well plates and the following day treated with 3μM MF4 for 4 hours. EGF was added to the medium for the indicated timepoints. Cells were then lysed in NP40 lysis buffer and 50μg protein was resolved on an SDS-PAGE gel. Proteins were transferred to nitrocellulose and probed with mouse anti-pMAPK and rabbit anti-pAKT. pAKT and pMAPK signalling was not prolonged by loss of PIKfyve activity.

possible explanations. Once internalised into the MVB efficient degradation of the receptor depends upon it reaching a correctly functioning lysosome. Thus, there could be a defect in the fusion of the MVB/late endosome with the lysosome. Alternatively, the EGFR could reach a lysosomal compartment that is unable to function correctly due to improper acidification. In support of the latter hypothesis, the yeast vacuole in Fab1 mutant cells is not properly acidified (Gary *et al.*, 1998). By immunofluorescence, a portion of the EGFR does not reside in the EEA-1 labelled compartments. I attempted to further identify the nature of the compartment to which this portion of the EGFR localised, and to determine the acidification of the endosomal compartments following loss of PIKfyve activity.

Using an acidotropic dye that accumulates in the lysosome, Lysotracker red, I determined that there is no defect in acidification of the endocytic compartments, and most likely this dye accumulates in lysosomes as in normal cells (figure 5.8). It labels swollen compartments that surround the large cytoplasmic vacuoles (most likely the EEA-1 labelled compartments), as well as non-swollen compartments throughout the cytoplasm (most likely the lysosomes observed by EM (see figure 4.3)). However, to be sure that the acidic compartments are lysosomes, it will be necessary to observe lysotracker colocalisation with endosomal markers. Due to the technical difficulty of fixing lysotracker dye in these cells, we were unable to perform these experiments. The lysotracker dye does not label the limiting membrane or the lumen of the large vacuoles. Although, this could be as a result of the large volume of these vacuoles and the fact that these are confocal slices, it seems likely that the large vacuoles are not acidic.

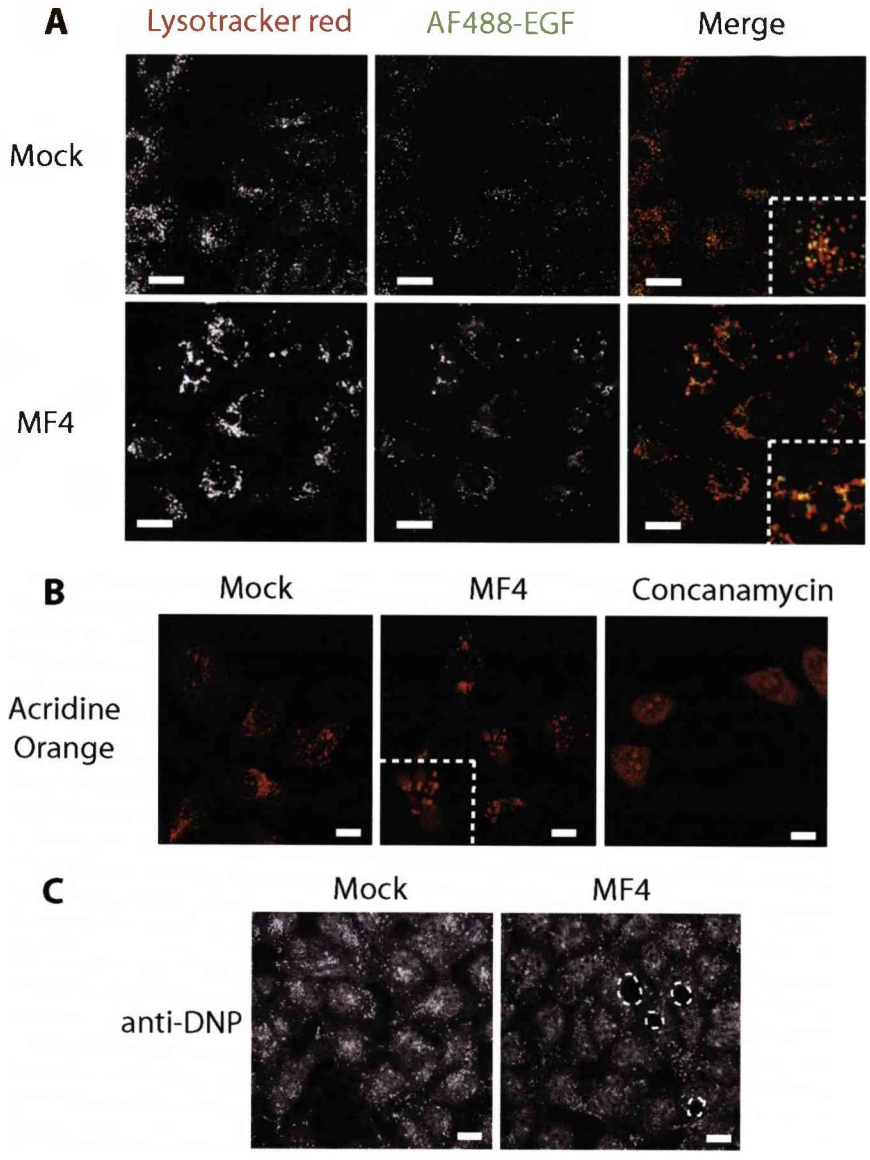

Figure 5.8. Internalised EGF reaches some acidic compartments but not the non-acidified vacuoles.

A) HeLa cells were seeded onto coverslips, serum starved overnight and the following day treated with 800nM MF4 for 4h. 100ng/ml AF488-EGF was then added to cells for 4h and lysotracker red for 2h. B) Alternatively cells were labelled with 5µg/ml Acridine orange for 10 mins. As a negative control cells were pre-treated with the vacuolar proton pump inhibitor Concanamycin (100nM) for 1h. Cells were washed in PBS, mounted onto slides and examined live by confocal microscopy at 37°C. C) For DAMP staining HEK293A cells were labelled with DAMP for 1h, fixed and permeabilised as normal and stained for monoclonal anti-DNP antibodies. Scale bars represent 20µm, dotted lines represent vacuoles. AF488-EGF is able to reach similar acidic compartments to control cells, but is not found in the large vacuoles that are poorly acidified.

In this experiment I also examined the degradation of a fluorescently tagged ligand (AF488-EGF). Although some EGF remains even in control cells, as some of the fluorescent tag may fail to get degraded along with the ligand, the same trend was observed that more EGF remained in cells treated with MF4. The remaining EGF in both control and MF4 treated cells partially overlaps with Lysotracker-labelled, acidic compartments. Thus, at least some of the EGF-EGFR complex is able to reach acidified compartments. However, the exact nature of these acidic compartments remains unclear, as does the nature of the compartments to which both EGF (Figure 5.8) and EGFR (Figure 5.6) localise that are not acidic or labelled with EEA-1. Of course these compartments are not necessarily one and the same, the EGFR and EGF could be in both an acidic lysosome and in a swollen EEA-1 compartment, but the fact that the acidic compartments, to which the majority of EGF localises are swollen, suggests that these are the EEA-1 labelled compartments observed by immunofluorescence. Both LAMP-2 staining and EM suggests that the lysosomes are not swollen in these cells.

I also examined a number of other markers of acidification, both Acridine Orange and DAMP (3-(2,4-dinitroanilino)-3_-amino-N-methyldipropylamine) staining, in cells treated with MF4 (Figure 5.8 B and C). DAMP is a basic congener of dinitrophenol (DNP) that readily diffuses into intact cells where its primary and tertiary amino groups allow it to accumulate in acidic organelles, and where it can be detected by anti-DNP antibodies. Acridine orange is a fluorescent dye that becomes protonated upon entry into acidic compartments, and trapped there. Both dyes show that although there

are acidic compartments within the cell, the large vacuoles have very low levels of acidification. In the case of the acridine orange experiment these pictures were taken on a fluorescence microscope, not a confocal microscope, and should reflect the total fluorescence of these compartments rather than a slice through them.

5.3 Discussion

In this chapter we set out to further dissect the involvement of PtdIns(3,5)P_2 in endocytic trafficking pathways. Conflicting evidence from the literature showed impaired trafficking of ubiquitinated cargo Carboxypeptidase S to the vacuole in *S. cerevisiae* Fab1 mutants (Odorizzi *et al.*, 1998), failure in degradation of Wingless and Notch receptors in *Drosophila* Fab1 mutants (Rusten *et al.*, 2006), and defective formation of terminal lysosomes in *C. elegans* Fab1 mutants (Nicot *et al.*, 2006), but in mammalian cells loss of PIKfyve activity had no effect on the downregulation of internalised receptors (Ikonomov *et al.*, 2003a; Rutherford *et al.*, 2006) despite causing a reduction in MVB/ECV formation (Sbrissa *et al.*, 2007). In addition to these findings, it has also been shown that degradation of the EGFR is significantly reduced in cells overexpressing the proposed PtdIns(3,5)P_2 binding domain of Vps24 (Yan *et al.*, 2005) and overexpressing the PtdIns(3,5)P_2 binding myotubularin MTM1 (Tsujita *et al.*, 2004), although the specificity of PtdIns(3,5)P_2 binding of these proteins is unclear.

In this chapter we present evidence that loss of PIKfyve leads to a delay in the downregulation of tyrosine kinase receptors. We were able to confirm the finding that siRNA oligos against PIKfyve had no effect on

receptor downregulation by Western blotting. However, a more sensitive immunofluorescence assay suggested that there was a minor effect on EGFR degradation. Given the residual protein left upon PIKfyve knockdown, it is possible that PtdIns(3,5)P_2 plays a role in this process, but with a relatively low threshold value. We therefore wondered if combined knockdown of PIKfyve with its allosteric activator Vac14 might have a synergistic effect on this pathway. Although a combined knockdown of Vac14 and PIKfyve does not increase the percentage of cells displaying the vacuolar phenotype, it does have a mild effect on the rate of EGFR degradation, suggesting that in cells where both PIKfyve and Vac14 are depleted, there is an additional suppression of PtdIns(3,5)P_2 production. Furthermore, it suggests that there is a role for PtdIns(3,5)P_2 in the trafficking of endocytosed receptors, but at a relatively low threshold value.

Interestingly, a combined knockdown of PIKfyve and the phosphatase Fig4 also showed a mild effect on EGFR depletion. We might expect that depletion of Fig4 would serve to counteract the effects of PIKfyve knockdown, particularly when we consider work from Shisheva and colleagues that suggests that knockdown of Sac3 (mammalian Fig4) causes an increase in cellular PtdIns(3,5)P_2 and in MVB formation (Sbrissa *et al.*, 2007), and thus we might expect to see an increase in EGFR downregulation. That we see the opposite effect is particularly interesting given recent data that suggests that the *S. cerevisiae* proteins Fab1, Vac14 and Fig4 form a lipid kinase-signalling complex, and that Vac14 and Fig4 are co-dependent for interaction with the chaperonin-related domain of Fab1 (Botelho *et al.*, 2008). Previous work has established that Vac14 and Fig4

form a complex in yeast that plays a dual role in both the synthesis and turnover of PtdIns(3,5)P_2 (Rudge *et al.*, 2004; Duex *et al.*, 2006b). Studies in mammalian cells presented in this study (Figures 3.19 and 3.21) and in the literature have shown that the interaction between Vac14 and Fig4 is conserved in higher organisms (Sbrissa *et al.*, 2007). An interaction between Vac14 and PIKfyve has also been demonstrated (Sbrissa *et al.*, 2004), and has lead to the suggestion that these three proteins also from a ternary complex in mammalian cells that tightly regulates the levels of PtdIns(3,5)P_2 (Sbrissa *et al.*, 2007). Thus the finding that a combined knockdown of PIKfyve with either Vac14 or Fig4 perturbs EGFR downregulation, suggests that these proteins may indeed be acting in a complex with PIKfyve to tightly regulate the levels of PtdIns(3,5)P_2. Indeed, the tight control of PtdIns(3,5)P_2 levels has been shown to be important for mammalian cell resistance to selected bacterial pathogens. Some pathogens, such as *Salmonella enterica,* have evolved mechanisms to overcome this response. They secrete a phosphatase, SopB, which uses PtdIns(3,5)P_2 as one of its substrates, and is thought the promote the survival of the pathogen by preventing transport to the lysosome (Marcus *et al.*, 2001; Hernandez *et al.*, 2004; Pizarro-Cerda and Cossart, 2004), providing further evidence that the tight regulation of PtdIns(3,5)P_2 levels is essential for this pathway.

There was no delay in EGFR downregulation following loss of Vac14 or Fig4 or a combination of the two, suggesting either that PIKfyve is able to produce sufficient PtdIns(3,5)P_2 in the absence of other components of the complex, or that knockdown of these proteins alone is insufficient to greatly perturb the levels of PtdIns(3,5)P_2 in the cell. Combined knockdown of

Vac14 and Fig4 does not produce the cytoplasmic vacuoles typically associated with PtdIns(3,5)P_2 depletion, suggesting that depletion of PtdIns(3,5)P_2 under these conditions must be minimal. I previously demonstrated that the PtdIns(3,5)P_2 threshold value for EGFR degradation must be relatively low as PIKfyve knockdown alone has only a small effect, therefore it is unsurprising that this combination of knockdowns has no effect on this pathway. It is also possible that regulation of the lipid kinase activity of PIKfyve by the Vac14/Fig4 complex is only necessary under certain conditions to stimulate increased production of PtdIns(3,5)P_2 and subsequently ensure that they do not stay elevated for longer than necessary, such as during hyperosmotic or other stresses. This is supported by the observation that knockdown of either protein renders certain mammalian cells more susceptible to cytoplasmic vacuolation following treatment with ammonium chloride and by the finding that PIKfyve and Vac14 are both involved in mediating the rise in PtdIns(3,5)P_2 levels during hyperosmotic stress in 3T3-L1 adipocytes (Sbrissa *et al.*, 2004; Sbrissa and Shisheva, 2005; Sbrissa *et al.*, 2007).

In accordance with a role for PtdIns(3,5)P_2 in tyrosine kinase receptor downregulation, an acute pharmacological inhibition of PIKfyve, at concentrations which do not produce any major perturbation in the levels of other 3-phosphoinositides (data supplied by Kevan Shokat, also shown for YM201636 (Jefferies *et al.*, 2008)), revealed a statistically significant delay in the degradation of EGFR and indicated that this delay was the same for other tyrosine kinase receptors such as c-Met, although this experiment was performed only once. This was further reinforced by immunofluorescence

studies, which demonstrated that following 4 hours of ligand-induced receptor internalisation, there was a large amount of residual EGFR in MF4 treated and combination knockdown cells. However, it must be taken into account that a limitation of any small molecule inhibitor is that its effects may not be as specific as predicted by *in vitro* studies. It is possible that this PIKfyve inhibitor may affect not only other PI(3)kinases, although the levels of PtdIns(3)*P* were assessed to some extent by immunofluorescence of the tandem FYVE domain probe, but also other phosphoinositide kinases such as PI(4)-kinases or even other non-phosphoinositide kinases. Any effect on the kinase PDK-1 for example, may explain the effects on pAKT and pMAPK that are observed. This must be taken into account when assessing the data in this chapter, although can be overcome to some extent with observations from multiple systems such as protein knockdown in parallel to inhibitor treatment.

The larger swollen vacuoles are surrounded by late endosomal markers (LAMP-2), and contain few intralumenal vesicles. One possible explanation for the effects on EGFR degradation, is a failure to internalise the receptor into the lumen of the MVB/late endosome. However, the appearance of a proportion of the EGFR in swollen endosomes labelled with EEA-1 suggests some internalisation is able to take place, and that this is not the major impediment in this case. This is further reinforced by Western blot analysis of the levels of phosphorylated MAPK and AKT/PKB, two downstream signalling targets of EGFR. A failure in internalisation of the EGFR into the lumen of the MVB, such as that observed in Hepatocyte growth factor regulated tyrosine kinase substrate (Hrs)-depleted cells,

prolongs receptor signalling (Lloyd *et al.*, 2002). The levels of pMAPK and pAKT are unaffected by loss of PIKfyve activity suggesting that the defect in receptor degradation occurs at a point after the receptor has been internalised into the MVB and signalling has been silenced. Thus we can reconcile the effects in mammalian cells with those observed in model organisms, suggesting that the downregulation of endocytosed receptors, such as *Drosophila* wingless, is affected but that their signalling output is not (Rusten *et al.*, 2006).

In the previous chapter I demonstrated a failure in retrieval of ciM6PR to the TGN. This defect may lead to a failure in the effective delivery of lysosomal hydrolases to these compartments, which might further contribute to a failure in degradation of lysosomally directed cargo. This hypothesis is supported by recent data that showed a defect in the processing of Cathepsin D in Vac14 knockout mice (Zhang *et al.*, 2007), suggesting that there is a failure in the delivery of this lysosomal enzyme. Normally pro-Cathepsin D is synthesised at the TGN and transported to endosomes where the propeptide is cleaved to give an intermediate form. In the lysosome, this intermediate form is further cleaved into two noncovalently linked fragments. It was shown that both the pro and intermediate forms of Cathepsin D accumulated in Vac14 knockout mice, suggesting that it is not correctly processed at the endocytic pathway. Alternatively other proteins may need to be retrieved from the MVB to allow its correct acidification, and given the demonstration that the retrieval of a number of proteins is perturbed, this may also contribute to improper acidification of this compartment following loss of PIKfyve activity.

In conclusion, reduced ILV formation, inefficient lysosomal enzyme delivery and improper acidification may all contribute to the failure in maturation of a subset of MVBs and the phenotype observed following loss of PIKfyve activity.

CHAPTER SIX

The Role of the WIPI Proteins in Mammalian Autophagy

6.1 Introduction

Thus far, the evidence presented has demonstrated a role for PtdIns(3,5)P_2 in retrieval to the TGN (chapter four) and lysosomal delivery of endocytosed material (chapter five). These findings could both be explained by a failure in endosomal maturation. As the endocytic pathway progresses, endocytosed material is sorted to either tubular retrieval pathways, or to vesicular degradative pathways. PtdIns(3,5)P_2 may function to coordinate these sorting events, such that following its depletion we observe a delayed retrieval to the TGN, and perturbed degradation of lysosomally targeted material. Interestingly, apart from PIKfyve, none of the other PtdIns(3,5)P_2 associated proteins displayed any visible aberrant knockdown phenotype, or had any effect on either membrane retrieval or lysosomal degradation, unless combined with PIKfyve knockdown in the case of Vac14 and Fig4.

WIPI-2 is a member of a family of proposed downstream effectors of PtdIns(3,5)P_2 function (Jeffries *et al.*, 2004; Proikas-Cezanne *et al.*, 2004). Another member of the WIPI family, WIPI-1 has been shown to play a role in membrane retrieval to the TGN, as has the yeast protein Atg18/Svp1 (Dove *et al.*, 2004; Jeffries *et al.*, 2004). Therefore, it is particular interesting that WIPI-2 had no effect on membrane retrieval pathways to the TGN. This suggests that, if it is indeed an effector of PtdIns(3,5)P_2, it does not function on these PtdIns(3,5)P_2-dependent pathways, and indeed members of the WIPI family may have different effector functions.

PtdIns(3)*P* has been shown to play an important role in autophagy, as discussed in section 1.9.3.2 (Herman and Emr, 1990; Kihara *et al.*, 2001; Byfield *et al.*, 2005). The finding that the yeast protein Atg18/Svp1 and the mammalian WIPI family, are also proposed to play a role in autophagy, has implicated PtdIns(3,5)P_2 in this process (Barth *et al.*, 2001; Guan *et al.*, 2001; Dove *et al.*, 2004; Stromhaug *et al.*, 2004; Proikas-Cezanne *et al.*, 2007). However, the precise role of these proteins and how this relates to their phosphoinositide binding capacity remains unclear.

In order to further examine the requirement of PtdIns(3,5)P_2 in autophagy, the role of the kinase, Fab1, has been examined to some extent. Consistent with its proposed role on the endocytic pathway, in *Drosophila* the kinase Fab1 was found to be necessary for the maturation of autolysosomes in autophagy, subsequent to the fusion of autophagosomes with the endosomal system (Rusten *et al.*, 2007). Loss of Atg18 in *S. cerevisiae* has also been shown to inhibit the fusion of autophagosomal structures with the endocytic pathway (Barth *et al.*, 2001). Atg18 is proposed to play a role in retrieval of the transmembrane protein Atg9 from the autophagosome prior to it's completion, the precise function of which is not known (Reggiori *et al.*, 2004). It has been also suggested that the function of Atg18/Svp1 in autophagy is independent of its binding to PtdIns(3,5)P_2 (Dove *et al.*, 2004). In mammalian studies WIPI-1 has been linked to autophagy in human tumour cells, dependent on its capacity to bind PtdIns(3)*P* (Proikas-Cezanne *et al.*, 2007) but the role of WIPI-2 in mammalian autophagy has yet to be investigated. The aim of this chapter was to begin to answer some of these questions.

1) To examine the role of PtdIns(3,5)P_2 in mammalian autophagy.

2) To assess the function of WIPI-2 in mammalian autophagy in general and in relation to its role as an effector of PtdIns(3,5)P_2.

6.2 Results

6.2.1 Autophagy assay

In order to examine the role of PtdIns(3,5)P_2 and WIPI-2 in autophagy, we made use of an established autophagy assay using a HEK293A cell line stably transfected with GFP-LC3, hereafter referred to as 2GL9 cells (Chan *et al.*, 2007). The autophagy protein LC3 is proposed to be a marker of autophagosome formation. As discussed in section 1.9.3.3, following induction of autophagy, LC3 is conjugated to a lipid, PE by means of a conserved ubiquitin-like conjugation system (Kabeya *et al.*, 2000; Ohsumi and Mizushima, 2004). Conjugated, membrane-associated LC3 protein (LC3 II) localises to punctate structures in the cell, whereas unconjugated LC3 (LC3 I) is distributed throughout the cytoplasm.

This can be expoited for monitoring mammalian autophagy in two ways. Firstly, by visualising the accumulation of GFP-LC3 II at autophagosomal membranes (GFP-LC3 II puncta formation) by immunofluorescence. Secondly, the conjugation corresponds to a shift in molecular weight on an SDS-PAGE gel. Thus the ratio of LC3 II to total LC3 (LC3 I + LC3 II) can also be examined (Mizushima, 2004).

6.2.2 Role of PIKfyve in autophagy

Although the role of the yeast protein in autophagy has been examined to some extent, the role of the mammalian protein PIKfyve has not. Therefore, I began by assessing the effect of PIKfyve siRNA treatment in the established autophagy assay. It caused a modest increase in the ratio of GFP-LC3 II to total GFP-LC3 (Figure 6.1 A and C). Three oligos were used to assess the robustness of this effect, two oligos that had previously been shown to suppress the levels of endogenous PIKfyve, and one that had exhibited no effect (as demonstrated in figure 4.1). However, reassessment of siRNA efficiency, demonstrated that all three oligos suppressed PIKfyve protein levels in this case (Figure 6.1 B). Only one of the three oligos was found to have a significant effect on GFP-LC3 ratios (Figure 6.1 C) ($N=3$, $p<0.01$).

Given the inefficiency of PIKfyve knockdown, and the residual protein remaining after 72 hours of transfection, the effects of the PIKfyve inhibitor were examined. Acute pharmacological inhibition of PIKfyve caused a significant increase in the ratio of GFP-LC3 II to total GFP-LC3 following starvation induction of autophagy (Figure 6.2 A and quantified in B) ($N=3$, $p<0.01$). There was no effect on the basal ratio (in fed cells), and an inactive analogue of the PIKfyve inhibitor had no effect. This accumulation could be as a result of either an increase in autophagosome formation, or a decrease in their degradation.

Treatment with the protease inhibitor Leupeptin following starvation induction of autophagy causes a further increase in the ratio of GFP-LC3 II to total GFP-LC3, as autophagosomes are no longer efficiently degraded. In

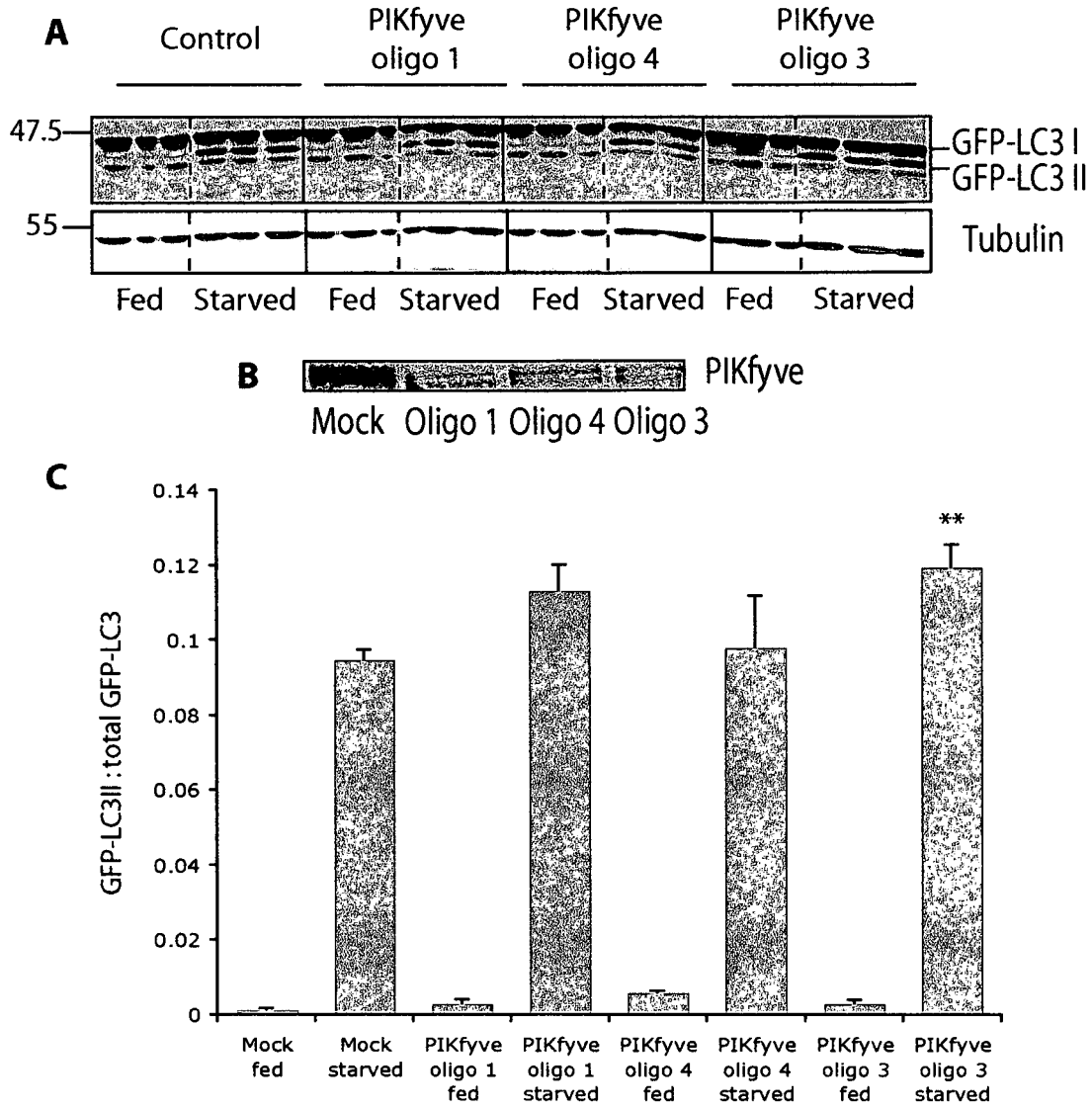

Figure 6.1. PIKfyve knockdown causes an accumulation of lipidated GFP-LC3 following starvation induction of autophagy.

2GL9 cells were seeded onto 12-well plates and transfected twice with 40nM PIKfyve oligos over 72h, then starved or fed for 2h.

A) Cells were lysed in 1X sample buffer containing 1mM DTT and 10µg protein resolved by SDS-PAGE. Protein was transferred to nitrocellulose and probed with polyclonal GFP antibodies.

B) 50µg NP40 lysates were resolved by SDS-PAGE and the resulting nitrocelluose probed with anti-PIKfyve antibodies.

C) The ratio of GFP-LC3II to total GFP-LC3 was quantified using LiCor Odyssey software (N=3, +/-SEM, ** $p<0.01$, Student's T-test).

PIKfyve knockdown causes a mild accumulation in GFP-LC3 lipidation following starvation induction of autophagy, but has no effect on basal levels of lipidation. All three oligos suppress the levels of endogenous PIKfyve, and two of the three oligos give a corresponding increase in GFP-LC3II.

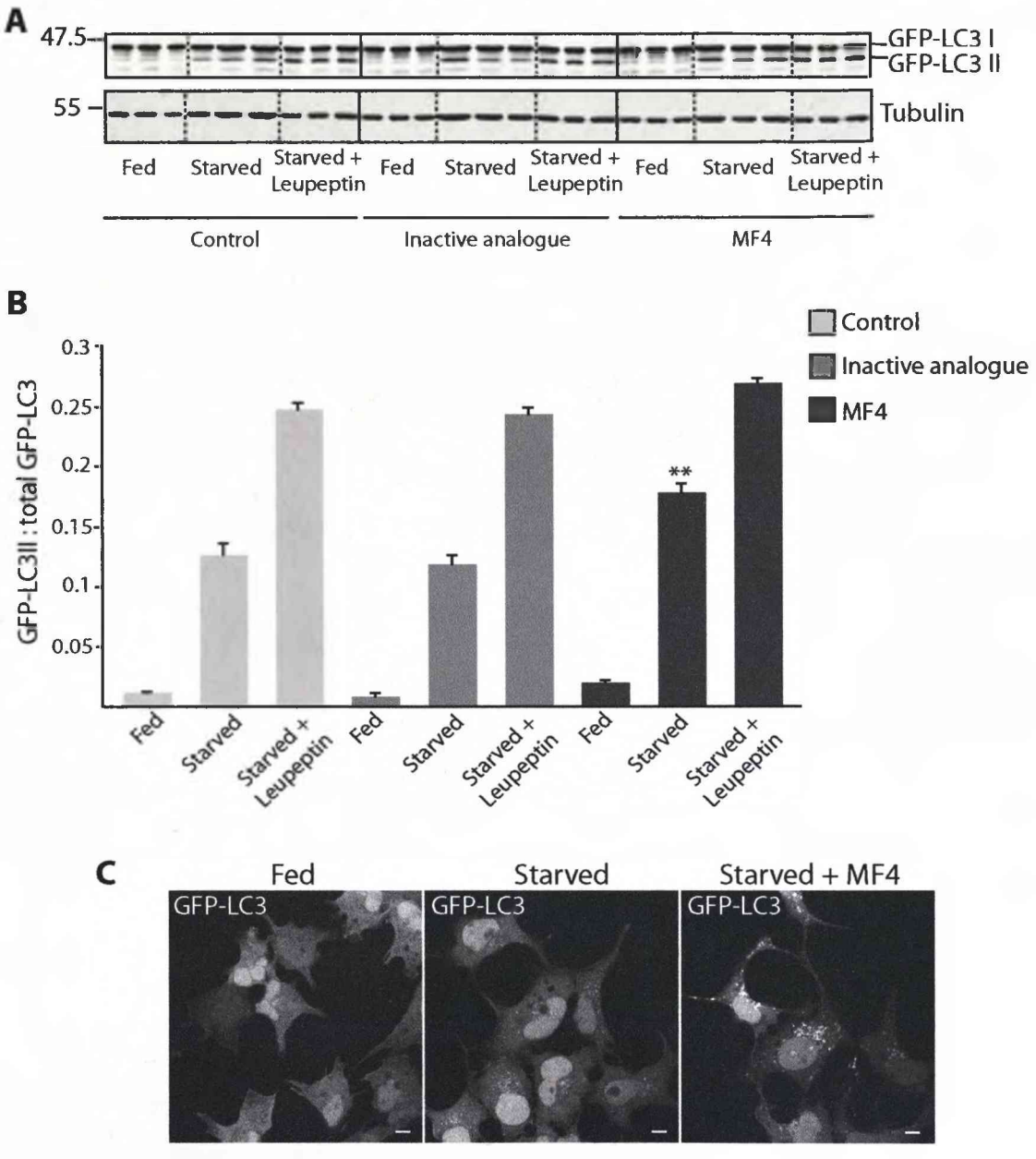

Figure 6.2. PIKfyve inhibition causes a significant accumulation of lipidated GFP-LC3 following starvation induction of autophagy.

2GL9 cells were seeded onto 12-well plates with coverslips for IF. Following treatment with 800nM MF4 for 4 hours cells were fed or starved 2h, with 0.25mg/ml Leupeptin where indicated.

A) Cells were lysed in 1X sample buffer containing 1mM DTT and 10µg lysates resolved by SDS-PAGE, transferred to nitrocellulose and probed with polyclonal anti-GFP antibodies.

B) The ratio of GFP-LC3II to total GFP-LC3 was quantified. N=3, +/- SEM, ** $p<0.01$, Students t-test.

C) Cells were fixed in 3% PFA/PBS and GFP-LC3II positive puncta formation examined.

control cells and those treated with an inactive analogue of the inhibitor, Leupeptin treatment caused a further 50% increase in lipidation. Whilst PIKfyve inhibitor treatment also caused a further increased in lipidation following Leupeptin treatment, the level of increase was not the same, which suggests that there is a defect in protein degradation rather than an increase in autophagosome formation. Therefore the effects of inhibiting PIKfyve (MF4 treatment) and lysosomal protease inhibition (Leupeptin treatment) most likely overlap, as the effect is not additive. The effect of inhibition of PIKfyve can also be seen by immunofluorescence. There is an accumulation of GFP-LC3 II positive punctae in PIKfyve inhibitor treated cells following starvation induction of autophagy (Figure 6.2 C).

6.2.3 Opposing roles of WIPI-2 and PIKfye

Next, the effects of of Vac14, WIPI-2, WIPI-1, Fig4 and PIKfyve knockdown were examined in parallel (Figure 6.3). Knockdown of Vac14, WIPI-1 and Fig4 had no significant effect on lipidated GFP-LC3 levels. The slight decrease observed with Vac14 was not reproducible but the increase following knockdown of PIKfyve is reiterated in this figure. Interestingly, knockdown of the PtdIns(3,5)P_2 effector WIPI-2 had the opposite effect to knockdown of PIKfyve, causing a decrease in the ratio of GFP-LC3 II to total GFP-LC3. Thus, PIKfyve and WIPI-2 were found to have the opposite effect on GFP-LC3 lipidation in this assay.

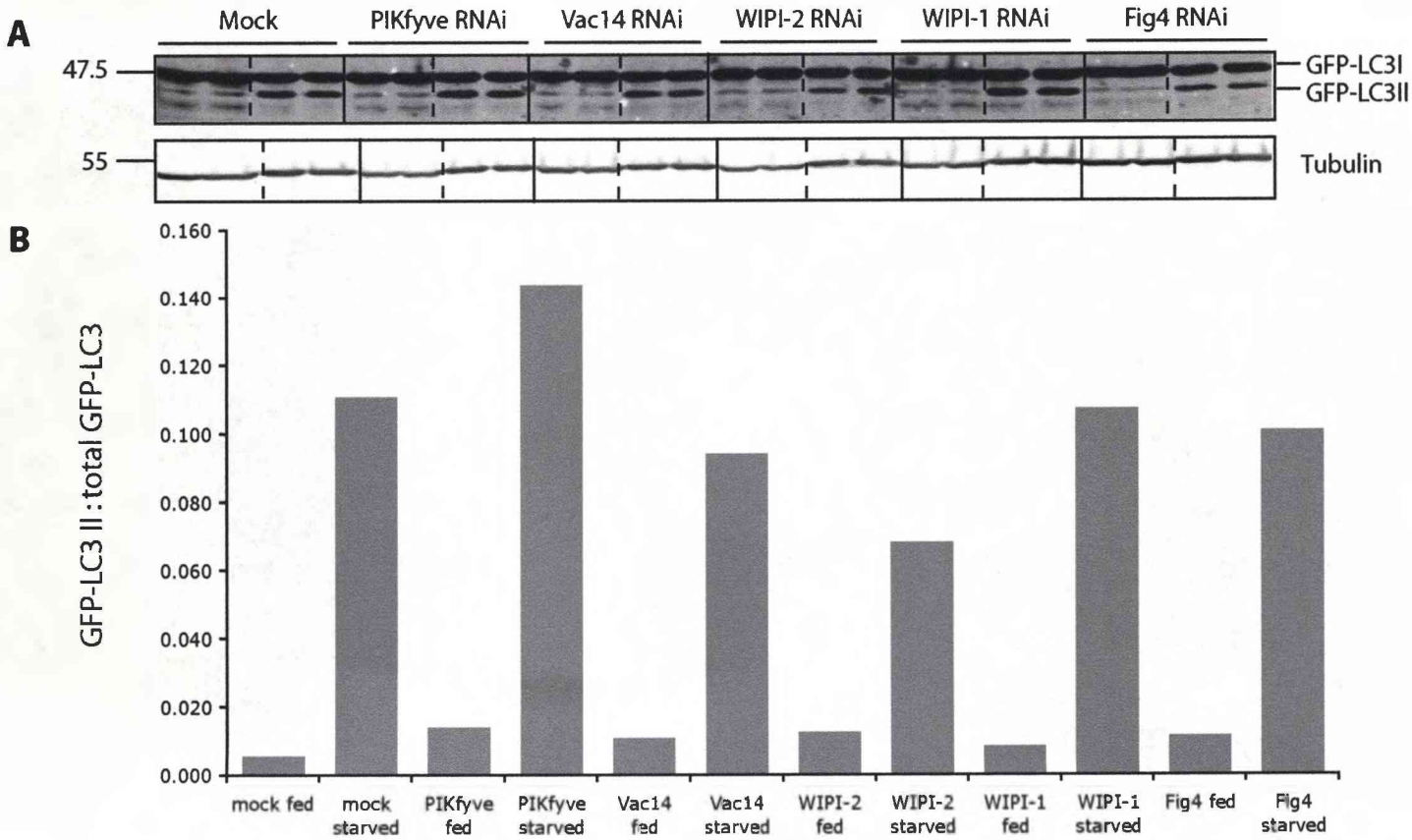

Figure 6.3. PIKfyve and WIPI-2 have different effects in autophagy.
2GL9 cells were seeded onto 12-well plates and transfected twice with 40nM indicated individual or pooled (Fig4 and WIPI-1) oligos over 72h. A) Cells were lysed in 1X sample buffer and lysate resolved by SDS-PAGE. Proteins were transferred to nitrocellulose and probed with anti-GFP antibodies. B) The ratio of GFP-LC3II to total GFP-LC3 was quantified using LiCor Odyssey software. PIKfyve and WIPI-2 have the opposite effect on GFP-LC3 lipidation following starvation induction of autophagy.

6.2.4 Dissecting the role of WIPI-2 in autophagy

The role of WIPI-2 in autophagy was subsequently examined in more detail. Using the WIPI-2 antibody characterised in Chapter three, we were able to show that starvation-induced autophagy causes a 5-fold increase in the number of WIPI-2 puncta (Figure 6.4), initially seen at a low level in fed cells for both endogenous and overexpressed protein (Figures 3.16 and 3.12 respectively). Punctae were quantified from a number of images taken with the same laser settings and subsequently thresholded using Image J software (Rasband, W.S., ImageJ, U. S. National Institutes of Health, Bethesda, _Maryland, USA, http://rsb.info.nih.gov/ij/, 1997-2008). Punctate and cytosolic staining was lost following WIPI-2 siRNA treatment, indicating that the punctae are specific to WIPI-2. It was subsequently shown that approximately 37% of the WIPI-2 punctae colocalise with the autophagosome marker GFP-LC3. Attempts were made to identify the nature of the non-autophagosomal pool of WIPI-2 (Figure 6.5). However, there was no colocalisation with any of the markers used.

WIPI-2 is a proposed downstream effector of PtdIns(3,5)P_2 function and yet loss of PtdIns(3,5)P_2 (as judged by inhibition or knockdown of PIKfyve) and loss of WIPI-2 have the opposite effect. Given that the function of Svp1/Atg18 in autophagy has been proposed to be independent of its binding of PtdIns(3,5)P_2 (Dove *et al.*, 2004), and that mammalian WIPI-1 punctae formation is dependent on PtdIns(3)*P* binding (Proikas-Cezanne *et al.*, 2007), I examined the effects of PIKfyve and PI(3)-kinase inhibitors on WIPI-2 punctae formation (Figure 6.6). Treatment with PIKfyve inhibitor causes a corresponding accumulation of WIPI-2 punctae, in addition to the

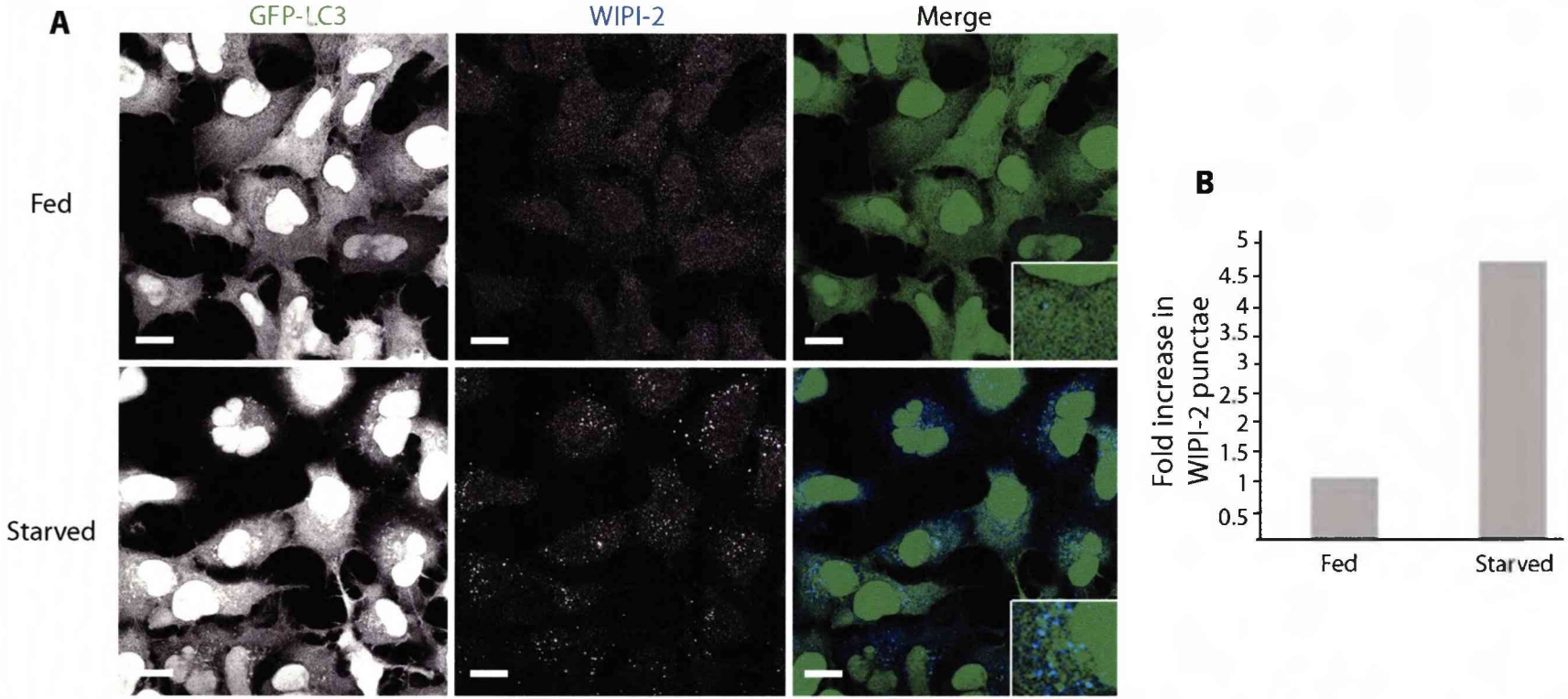

Figure 6.4. WIPI-2 redistributes to autophagic structures following starvation induction of autophagy.
2GL9 cells were seeded onto 12-well plates with coverslips. Cells were fed in DMEM or starved in EBSS for 2h prior to fixation in 3% PFA/PBS, permeabilisation with 0.2% TX-100 and staining with the WIPI-2 antibody characterised in chapter 3. Scale bars represent 20μm.
A) Inset in merged image clearly shows that both WIPI-2 and GFP-LC3 localise to punctate structures following starvation.
B) There is a 5-fold increase in WIPI-2 punctae and approximately 37% of WIPI-2 punctae colocalise with GFP-LC3 II punctae, as quantified using ImageJ.

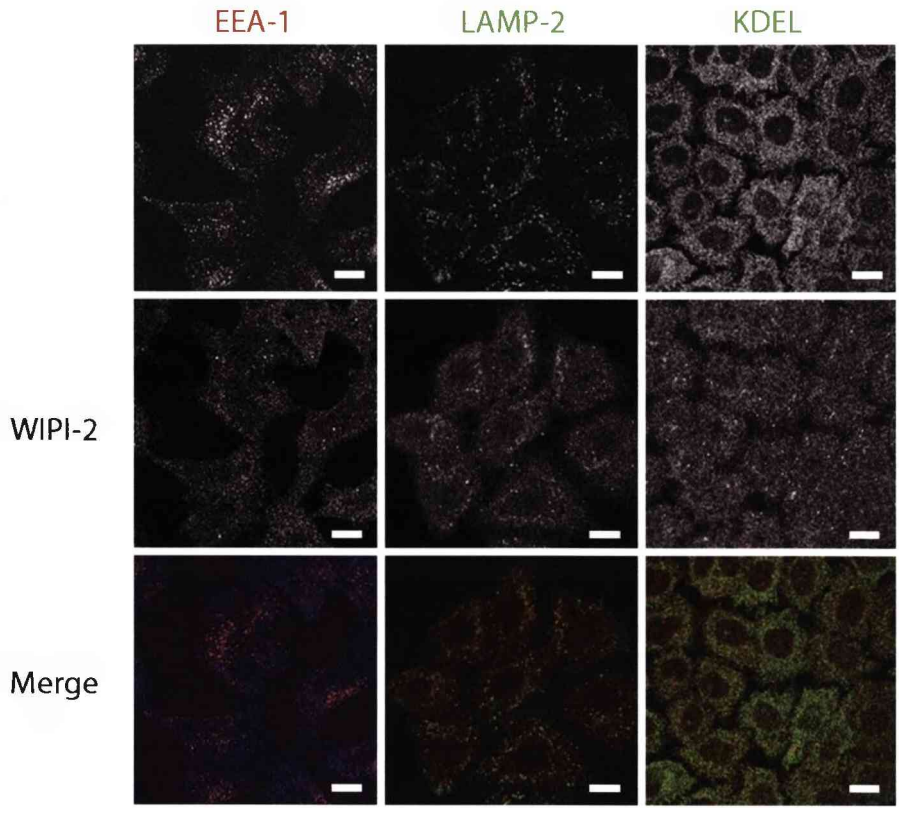

Figure 6.5. WIPI-2 puncta do not colocalise with endosomal or ER markers.
HeLa cells were seeded onto coverslips and fixed in 3% PFA/PBS, permeabilised in 0.2% TX100 and stained with WIPI-2, EEA-1 (early endosome), LAMP-2 (late endosome) and KDEL (ER) markers. Scale bars represent 20μm.

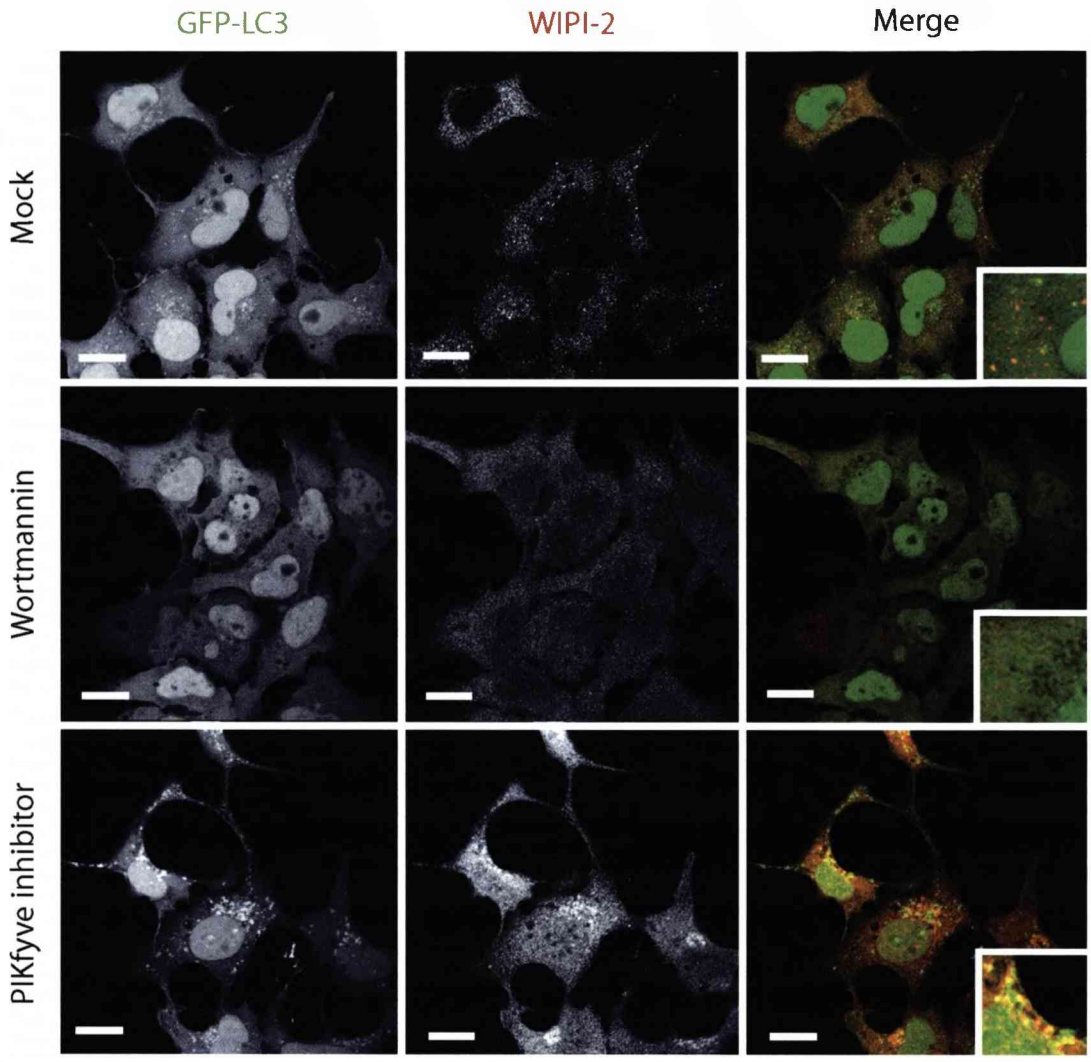

Figure 6.6. WIPI-2 and GFP-LC3 starvation-induced punctae formation is dependent on the activity of PtdIns(3)-kinase but not PIKfyve.
2GL9 cells were seeded onto 12-well plates with coverslips for IF. Following treatment with 800nM PIKfyve inhibitor for 4 hours cells were fed in full DMEM or starved in EBSS for 2h, with 100nM Wortmannin for the final 30 minutes where indicated. Cells were fixed in 3% PFA/PBS, permeabilised in 0.2% TX-100 and stained with WIPI-2 antibody. Wortmannin causes the ablation of both GFP-LC3 and WIPI-2 puncta, whereas PIKfyve inhibitor causes their accumulation. Scale bars represent 20μm.

accumulation of GFP-LC3 II punctae. Treatment with the PI(3)-kinase inhibitor Wortmannin, on the other hand, causes ablation of both forms of punctae.

Decrease in the ratio of GFP-LC3 II to total GFP-LC3 following WIPI-2 knockdown was found to be robust (Figure 6.7). This effect was also shown to be dependent on the level of WIPI-2 protein knockdown, the greater the level of WIPI-2 knockdown the greater the effect on GFP-LC3 lipidation (6.7 A and quantified in B) (N=3, $p<0.01$). An oligo that does not suppress WIPI-2 protein has no effect on GFP-LC3 II levels.

Given that a reduction in GFP-LC3 II could represent either a decreased formation of autophagosomes or an increase in turnover of autophagosomes at the lysosome, I assessed the additional effects of Leupeptin and MF4 treatment in combination with WIPI-2 siRNA (Figure 6.8). A significant decrease in lipidation is observed once again following WIPI-2 knockdown (N=3, $p<0.01$). Following Leupeptin treatment in WIPI-2 siRNA cells there is a typical level of increase in lipidation. MF4 treatment brings lipidation levels in WIPI-2 siRNA cells back to those seen in control cells, but not to a level comparable with Leupeptin treatment.

In order to further dissect the role of WIPI-2 in autophagy, its effect on GFP-LC3 lipidation was compared to other autophagy genes known to be involved in the initial stages of autophagosome formation. ULK-1 is a serine threonine kinase that is an integral part of the autophagy-inducing complex as discussed in section 1.9.3.1 (Chan *et al.*, 2007) whilst Beclin is part of the PI(3)-kinase complex involved in autophagy, as also discussed in section 1.9.3.2 (Liang *et al.*, 1999; Boya *et al.*, 2005; Zeng *et al.*, 2006).

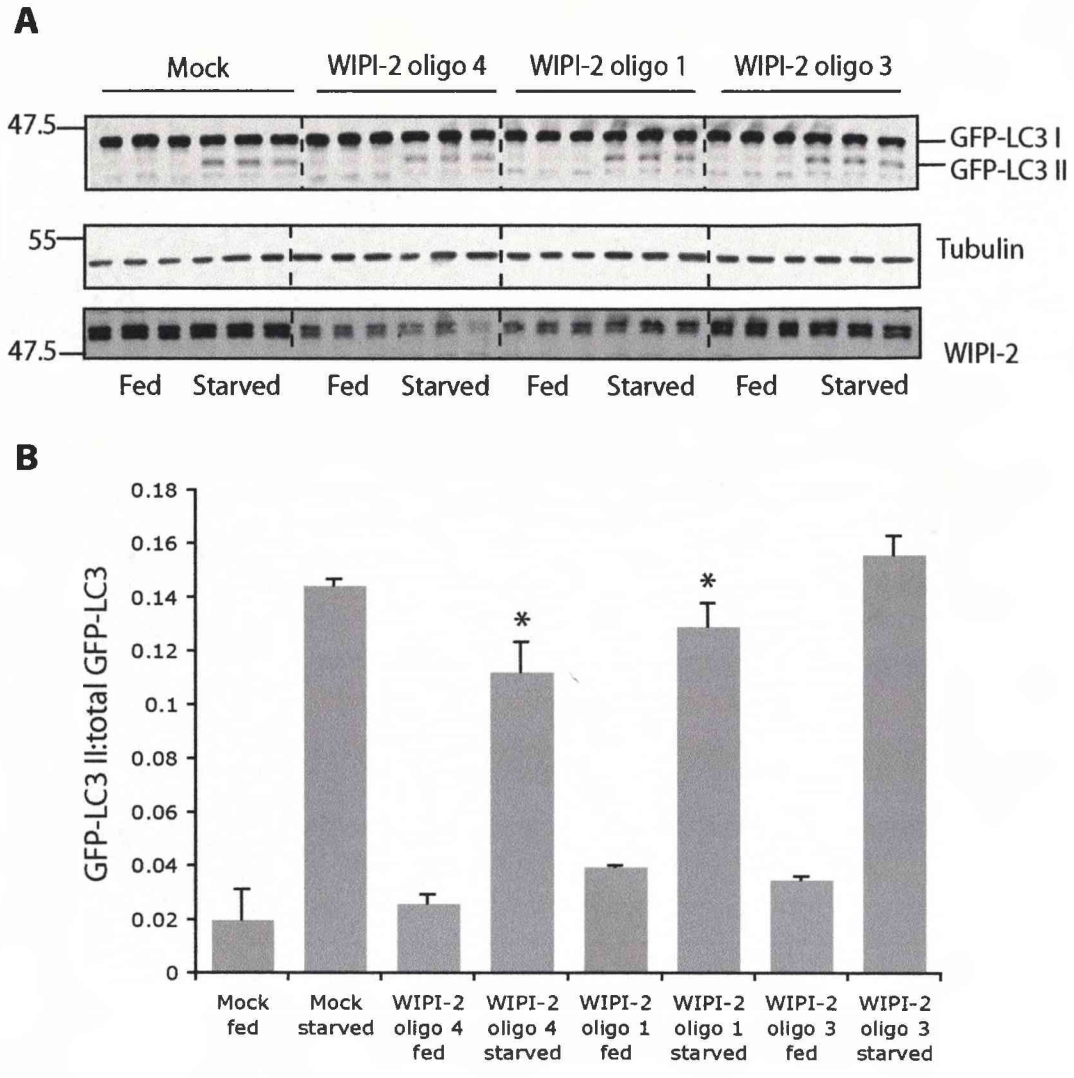

Figure 6.7. WIPI-2 knockdown causes a reduction in GFP-LC3 lipidation following starvation induction of autophagy.
2GL9 cells were seeded onto 12-well plates and transfected twice with 40nM individual WIPI-2 oligos over 72h. A) Cells were lysed in 1X sample buffer containing 1mM DTT and 10µg protein resolved by SDS-PAGE. Protein was transferred to nitrocellulose and probed with polyclonal GFP antibodies. B) The ratio of GFP-LC3II to total GFP-LC3 was quantified using LiCor Odyssey software (N=3, +/-SEM, * $p<0.05$, Student's T-test). WIPI-2 knockdown causes a reduction in GFP-LC3 lipidation following starvation induction of autophagy, but has no effect on basal levels of lipidation. The effect is knockdown efficiency dependent, such that the greatest level of protein knockdown gives the greatest effect on lipidation.

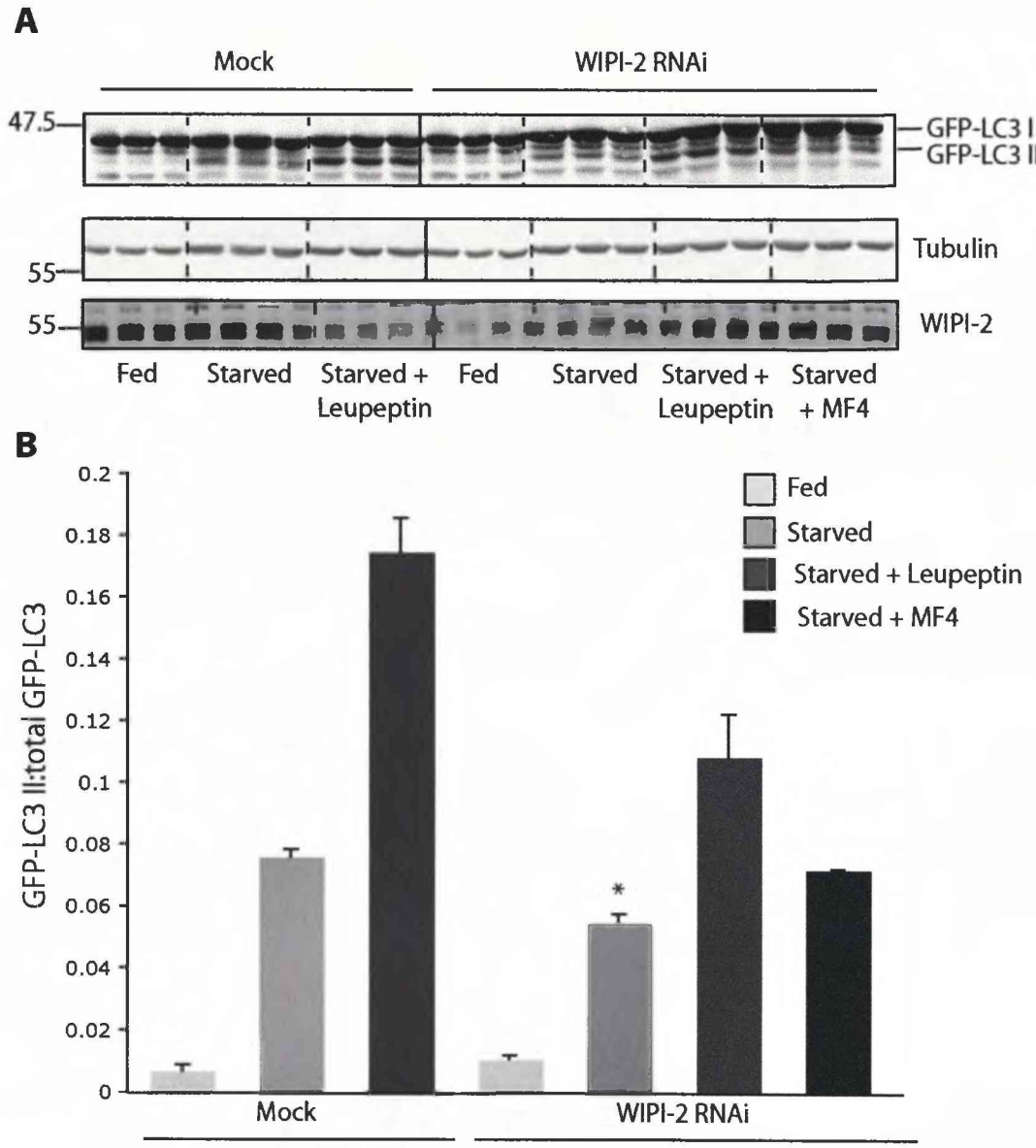

Figure 6.8. The effects of WIPI-2 knockdown are partially reversed following treatment with Leupeptin or MF4.

2GL9 cells were seeded onto 12-well plates and transfected twice with 40nM WIPI-2 oligos over 72h. 0.25mg/ml Leupeptin and 800nM MF4 were added where indicated. Cells were starved in EBSS for 2 hours.

A) Cells were lysed in 1X sample buffer containing 1mM DTT and 10µg protein resolved by SDS-PAGE. Protein was transferred to nitrocellulose and probed with polyclonal GFP antibodies.

B) The ratio of GFP-LC3II to total GFP-LC3 was quantified using LiCor Odyssey software (N=3, +/-SEM, * $p<0.05$, Student's T-test).

Treatment with Leupeptin or MF4 partially counteracts the effects of WIPI-2 knockdown, bringing LC3 lipidation back to the levels of control starved cells.

WIPI-2 produces a similar effect on GFP-LC3 lipidation as the key autophagy protein ULK-1 (Figure 6.9). Furthermore, a combined knockdown of both WIPI-2 and ULK-1 has an additive effect on GFP-LC3 lipidation. Efficient knockdown of Beclin could not be established, therefore I was unable to compare the effects of WIPI-2 knockdown to Beclin knockdown or examine the effects of their combined knockdown.

To further establish that the effects of WIPI-2 knockdown on lipidation are due directly to a loss of WIPI-2 protein, it was subsequently demonstrated that overexpression of siRNA resistant WIPI-2 could rescue these effects (Figure 6.10). This can also be observed by immunofluorescence (Figure 6.11). The number of GFP-LC3 II positive punctae was counted in all the cells in each of 5 fields for each condition. As before this was performed in images taken with the same laser settings that were subsequently thresholded and quantified in Image J. Where constructs were transfected into cells the counts were divided into those in cells expressing the construct of interest and those not transfected. In cells not expressing the siRNA resistant myc-WIPI-2, one would expect to see the same phenotype as the WIPI-2 siRNA treated cells.

As demonstrated using the SDS-PAGE shift assay, there was a reduction in GFP-LC3 II positive punctae in cells treated with WIPI-2 siRNA. Control cells had an average of 21 ± 1.3 GFP-LC3 II punctae, whereas those treated with WIPI-2 siRNA had 12.8 ± 1.18. In cells transfected with siRNA resistant myc-WIPI-2, the number of GFP-LC3 II punctae was similar to control cells (25.6 ± 2). In non-transfected cells in the same field there was also a slight increase compared to WIPI-2 siRNA treated cells, but still less

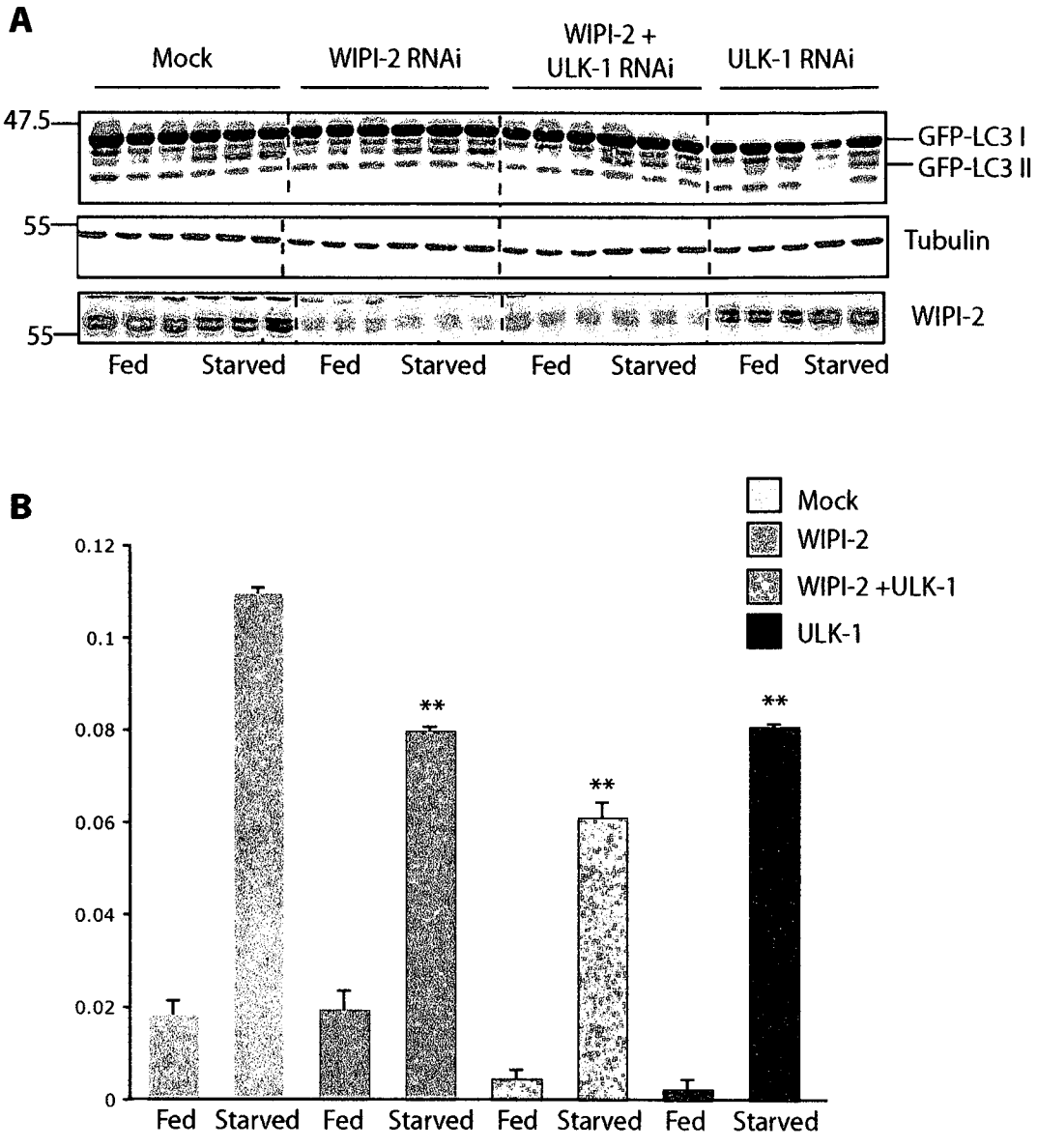

Figure 6.9. WIPI-2 and ULK-1 have comparable effects in autophagy, and their combined knockdown has an additive effect.

2GL9 cells were seeded onto 12-well plates and transfected twice with 40nM of the indicated individual oligos over 72h.

A) Cells were lysed in 1X sample buffer containing 1mM DTT and 10µg protein resolved by SDS-PAGE. Protein was transferred to nitrocellulose and probed with polyclonal GFP antibodies.

B) The ratio of GFP-LC3II to total GFP-LC3 was quantified using LiCor Odyssey software (N=3, +/-SEM,** $p<0.01$, Student's T-test).

Loss of WIPI-2 has a comparable effect to that of ULK-1. Combined knockdown of the two has an additive effect on GFP-LC3 lipidation.

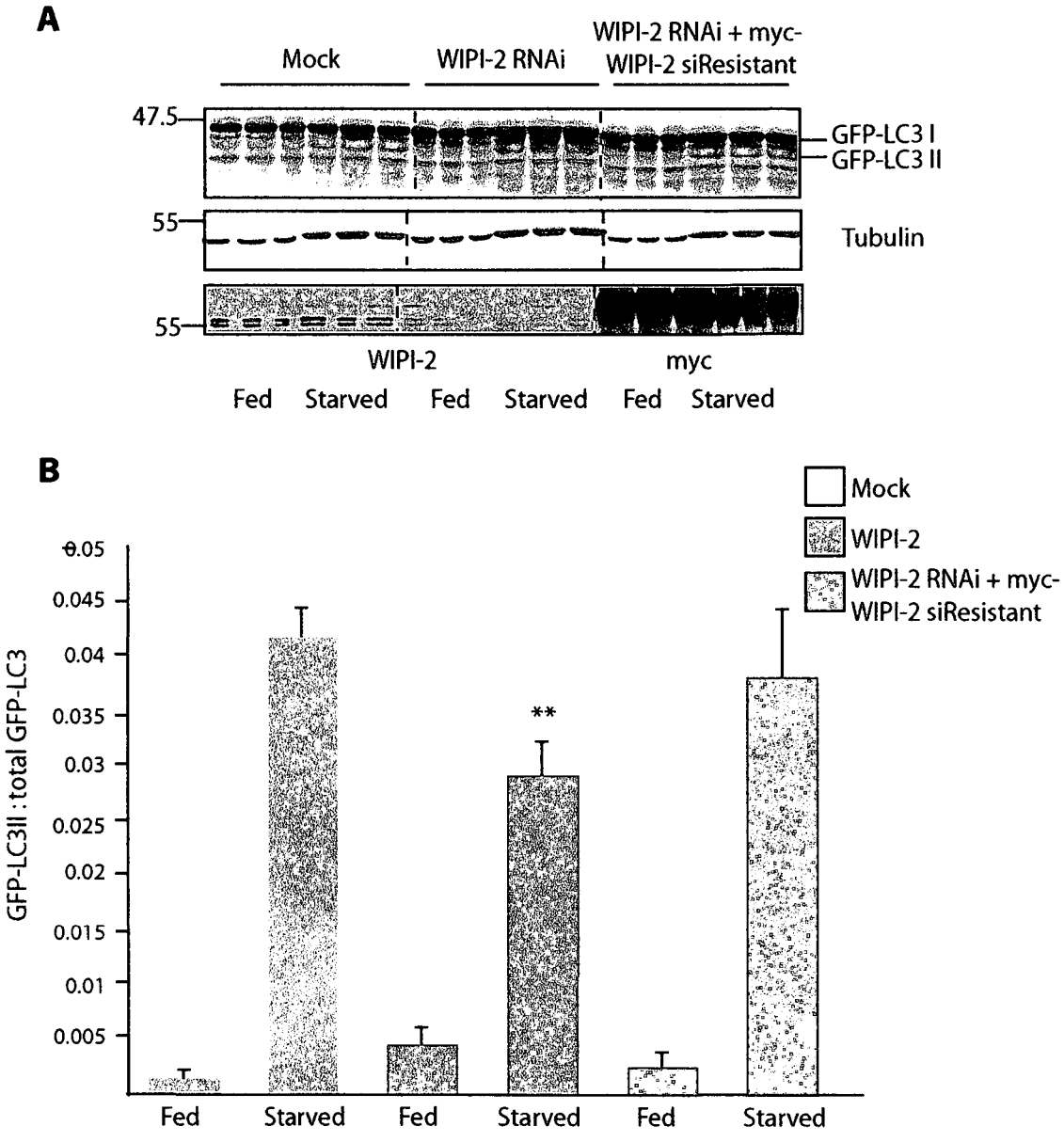

Figure 6.10. Overexpression of siRNA resistant WIPI-2 rescues the WIPI-2 knockdown phenotype.

2GL9 cells were seeded onto 12-well plates and transfected twice with 40nM individual WIPI-2 oligos over 72h and transfected with siRNA resistant WIPI-2 once for 24h.

A) Cells were lysed in 1X sample buffer containing 1mM DTT and 10µg protein resolved by SDS-PAGE. Protein was transferred to nitrocellulose and probed with polyclonal GFP antibodies.

B) The ratio of GFP-LC3II to total GFP-LC3 was quantified using LiCor Odyssey software (N=3, +/-SEM, * $p<0.05$ ** $p<0.01$, Student's T-test).

The effect of loss of WIPI-2 can be rescued by overexpression of a knockdown resistant construct.

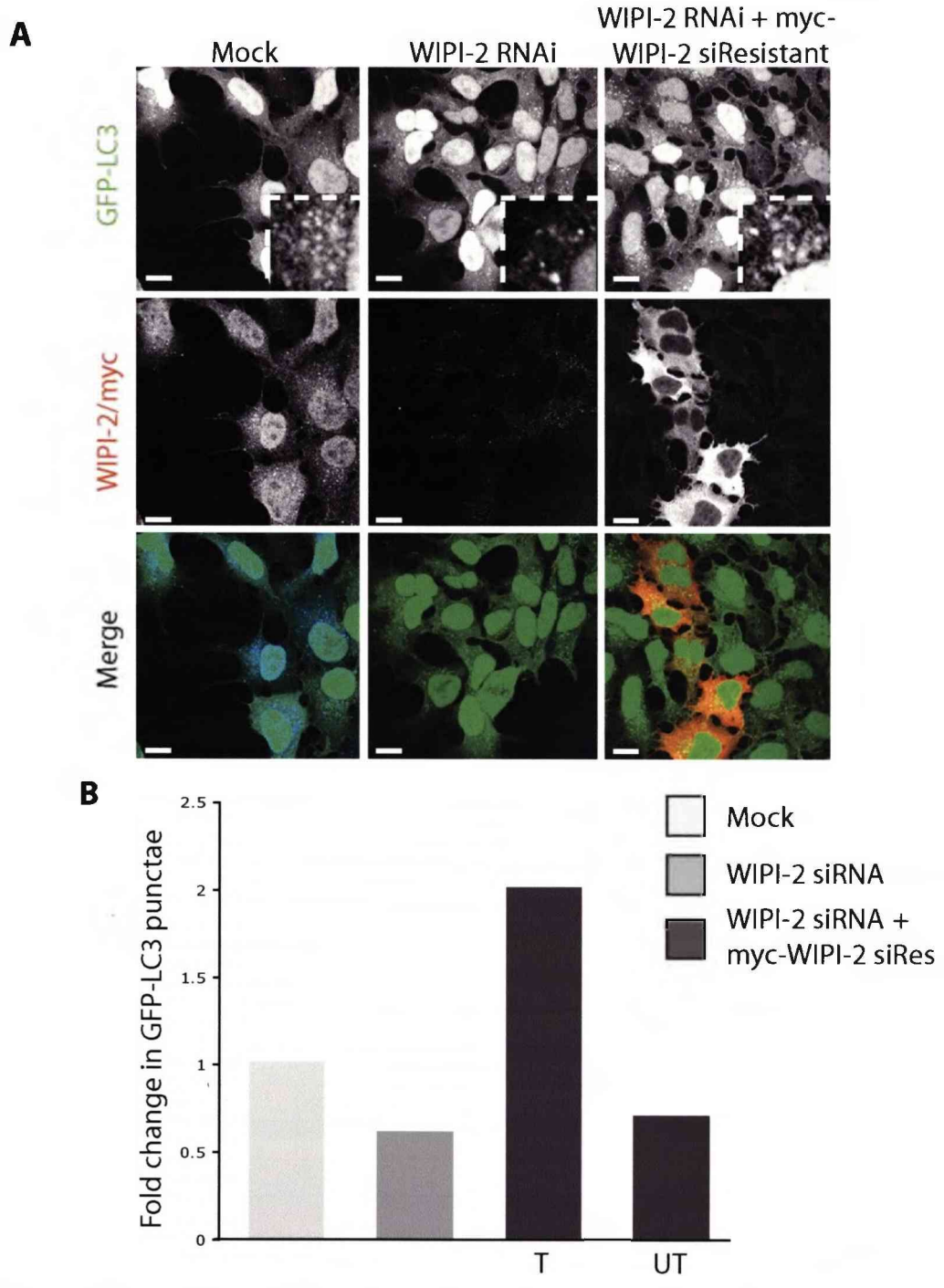

Figure 6.11. myc-WIPI-2 overexpression rescues the WIPI-2 siRNA phenotype as examined by immunofluorescence.

2GL9 cells were seeded onto coverslips and transfected twice with 40nM WIPI-2 siRNA oligos over 72h and with overexpression constructs for 24h.

A) Cells were fixed in 3% PFA/PBS, permeabilised in 0.2% TX100 and stained with WIPI-2 antibodies.

B) The number of GFP-LC3 II punctae in each cell in five fields were counted for each condition and quantified as fold change from control. Scale bars represent 20μm. T= transfected UT = untransfected.

than control. These cells could be transfected with the overexpression constructs but expressing the protein at levels below the detection threshold of the myc antibody by immunofluorescence.

6.2.5 A role for WIPI-1

WIPI-1 has previously been shown to redistribute to punctate structures following starvation induction of autophagy in human tumour cells (Proikas-Cezanne *et al.*, 2007). Overexpression of myc-WIPI-1 caused a reduction in the number of WIPI-2 punctae, suggesting the two are possibly competing for the same binding sites (Figure 6.12). However, we were unable to find any effect of WIPI-1 knockdown on autophagosome formation (Figure 6.3 and 6.13) and a combined knockdown of WIPI-1 and WIPI-2 had the same effect as knockdown of WIPI-2 alone (Figure 6.13). It was difficult to assess the levels of WIPI-1 knockdown, as WIPI-1 antibodies were unable to detect endogenous WIPI-1 in this cell line. Thus the lack of effect could have been due to ineffective suppression of WIPI-1 or because the levels of WIPI-1 are negligible in this cell line.

6.3 Discussion

The work presented in this chapter examined the role of PtdIns(3,5)P_2 and one of its proposed downstream effectors, WIPI-2, in mammalian autophagy. Previous work has established that the yeast proteins Atg18/Svp1 and the mammalian WIPI family member, WIPI-1, play a role in autophagy in both organisms (Barth *et al.*, 2001; Dove *et al.*, 2004; Jeffries *et al.*, 2004; Proikas-Cezanne *et al.*, 2004). Given that these proteins have

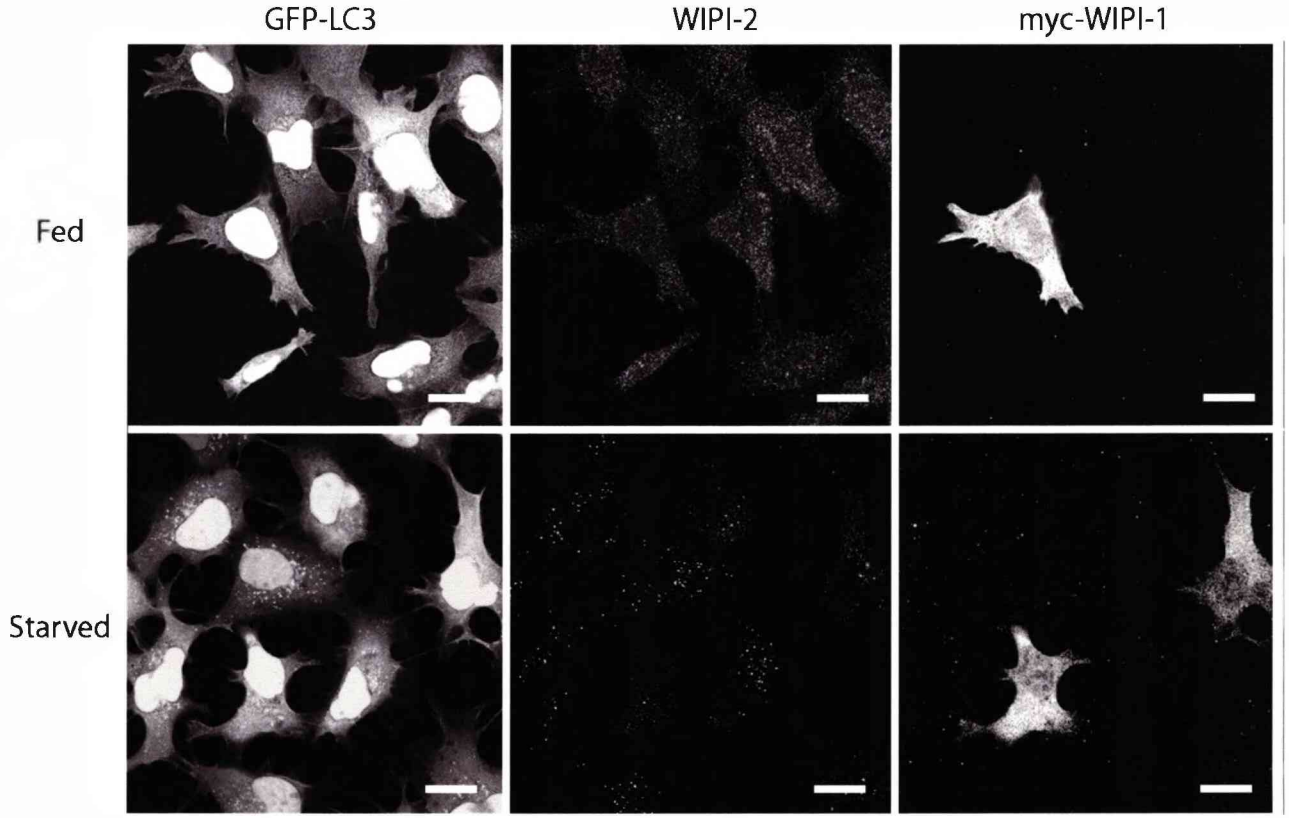

Figure 6.12. Overexpression of myc-WIPI-1 displaces endogenous WIPI-2 punctae.
2GL9 cells were seeded onto 12-well plates with coverslips and transfected with myc-WIPI-1 for 24h. Subsequently cells were fixed in 3% PFA/PBS, permeabilised with 0.2% TX-100 and stained with anti-myc and anti-WIPI-2 antibodies. In cells expressing myc-WIPI-1 there are fewer endogenous WIPI-2 puncta. Scale bars represent 20μm.

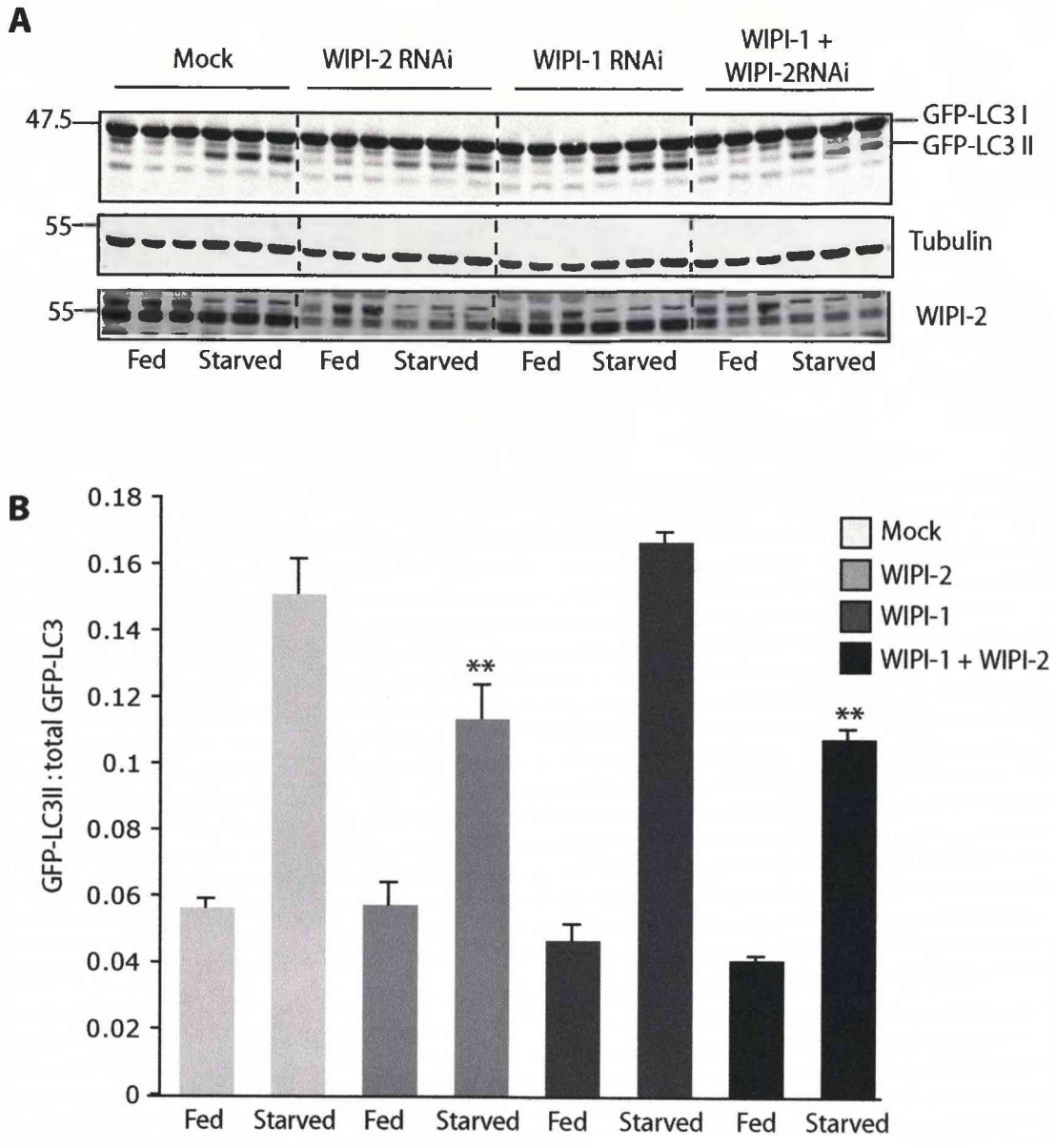

Figure 6.13. WIPI-1 has no effect on GFP-LC3 lipidation following starvation induced autophagy.

2GL9 cells were seeded onto 12-well plates and transfected twice with 40nM of the indicated individual (WIPI-2) or pooled (WIPI-1) oligos over 72h. Cells were fed in DMEM or starved in EBSS for 2h.

A) Cells were lysed in 1X sample buffer containing 1mM DTT and 10µg protein resolved by SDS-PAGE. Protein was transferred to nitrocellulose and probed with polyclonal GFP antibodies.

B) The ratio of GFP-LC3II to total GFP-LC3 was quantified using LiCor Odyssey software (N=3, +/-SEM, * $p<0.05$, Student's T-test). WIPI-1 has no effect on GFP-LC3 lipidation, although the protein may not be suppressed effectively.

been shown to bind both PtdIns(3)*P* and PtdIns(3,5)P_2, this lead to the suggestion of a role for PtdIns(3,5)P_2 in autophagy. In *S. cerevisiae*, however, the role of Svp1 is thought to be independent of its PtdIns(3,5)P_2 binding capacity (Dove *et al.*, 2004). In this chapter I set out to examine the potential roles of PtdIns(3,5)P_2 and the WIPI proteins in mammalian autophagy.

6.3.1 The role of PtdIns(3,5)P_2 in mammalian autophagy

Autophagy occurs at a basal level in most cells and contributes to turnover of cytoplasmic components. However, in response to starvation or cellular insults, autophagic activity is increased to ensure cellular survival (Schworer and Mortimore, 1979; Mortimore and Poso, 1987). Portions of the cytoplasm are engulfed by a double membrane bound autophagosome that then fuses with the endolysosomal system, where its contents are degraded in the lysosome (Arstila and Trump, 1968; Gordon and Seglen, 1988; Stromhaug and Seglen, 1993). Induction of autophagosome formation requires PtdIns(3)*P* (Petiot *et al.*, 2000), isolation membranes of unknown origin, and two ubiquitin-like modification systems (Ohsumi and Mizushima, 2004). One of these modifications is the conjugation of Atg8/LC3 to PE, which was used to assay autophagosome formation in this study.

By examining the knockdown of PIKfyve protein and inhibition of its activity, we clearly demonstrate that loss of PIKfyve activity causes a significant increase in GFP-LC3 lipidation, and a large accumulation of GFP-LC3 II positive punctae by immunofluorescence. This suggests that loss of PIKfyve either causes an increase in autophagosome formation, or a

reduction in their degradation. The protease inhibitor Leupeptin causes an increase in GFP-LC3 lipidation for the latter reason. Therefore, comparing the effects of Leupeptin on control cells and those treated with PIKfyve inhibitor should give an idea of what effect loss of PIKfyve activity is having. If it is causing an increase in autophagosome formation, then treatment with both Leupeptin and PIKfyve inhibitor should have an additive effect on GFP-LC3 lipidation. However, following Leupeptin treatment, there is only a very slight further increase in GFP-LC3 lipidation (Figure 6.2). This suggests that the two effects must overlap with one another and that PIKfyve inhibition is exerting a similar effect to Leupeptin on autophagy. This finding complements the existing literature in *Drosophila*, which showed that Fab1 mutants displayed an accumulation of amphisomes subsequent to fusion with the endocytic pathway, rather than autophagosomes (Rusten *et al.*, 2007). Furthermore, PIKfyve inhibition was found to cause a decrease in protein degradation (Jefferies *et al.*, 2008). Taken together these data, and the defect in EGFR degradation demonstrated in chapter five, indicate that PtdIns(3,5)P_2 most likely has an indirect effect on the autophagy pathway. Autophagosomes are able to fuse with the endocytic pathway to form amphisomes, but defects in maturation of the MVB/late endosome mean that subsequent degradation of the autophagosome is not achieved, just as EGFR is not effectively degraded. It would be interesting to examine the acidification of GFP-LC3 labelled compartments in these cells to further elucidate the specific effect on degradation; due to technical difficulties I was unable to do these experiments in this study.

6.3.2 The role of WIPI-2 in mammalian autophagy

PtdIns(3,5)P_2 was first linked to autophagy through the identification of its downstream effectors Atg18/Svp1 and Atg21 in yeast, and the mammalian WIPI family, which play a role in this cellular process, as described in section 1.9.3.4. Atg18/Svp1 has been shown to bind the transmembrane protein Atg9, an autophagy protein that localises to the forming autophagosome and other unknown punctate structures, and is not present on the completed autophagosome, suggesting that it is recycled from the forming autophagosome membrane at some point. Atg18/Svp1 is proposed to be involved in the cycling of Atg9 as it binds both Atg9 and the Atg1-Atg13 complex that governs Atg9 cycling (Reggiori *et al.*, 2004). Evidence suggests that this function may be independent of its binding of PtdIns(3,5)P_2 in yeast, but the mammalian proteins have not yet been examined in any detail. One member of this family, WIPI-1 has been proposed to be involved in retrograde transport to the TGN and has also been shown to play a role in autophagy in human tumour cells (Jeffries *et al.*, 2004; Proikas-Cezanne *et al.*, 2004). WIPI-1 has also been shown to bind both PtdIns(3)P and PtdIns(3,5)P_2 *in vitro*, but any parallel role in mammalian Atg9 cycling has yet to be clearly established, nor in fact has any clear understanding of their precise function in autophagy.

In this study we find that knockdown of WIPI-2 causes a significant and reproducible decrease in GFP-LC3 lipidation, which is confirmed by the use of several siRNA oligos that suppress WIPI-2 protein levels. The specificity of this effect is further demonstrated by the fact that an oligo that does not suppress WIPI-2 protein levels does not affect GFP-LC3 lipidation,

and that overexpression of siRNA resistant WIPI-2 is able to rescue the phenotype. Loss of WIPI-2 could be causing either a decrease in autophagosome formation or an increase in lysosomal degradation but the finding that there is the same degree of response to Leupeptin treatment. The fact that PIKfyve inhibition also reverses the WIPI-2 phenotype again reinforces the idea that PIKfyve functions at a later stage of the autophagy pathway in regulating degradation.

In a manner similar to LC3, WIPI-2 is recruited to membrane bound structures during starvation induced autophagy. There was a basal level of WIPI-2 punctae, most likely representing the basal level of autophagy occurring in these cells. Over a third of WIPI-2 punctae colocalised with the autophagosome marker GFP-LC3 II, suggesting that WIPI-2 is recruited to the autophagosome to perform its autophagic function. I was unable to characterise the punctae that did not colocalise with GFP-LC3 in starved cells. It has been suggested that GFP-LC3 may be quenched once the autophagosome fuses with acidic compartments, thus these WIPI-2 punctae could represent a later pool of amphisomes or acidic autophagosomes. In order to assess this, I attempted to examine the colocalisation of each set of punctae with both endogenous LC3 and Lysotracker markers, however for technical reasons I was unable to make the required observations. It is clear however that these punctae do not colocalise with early or late endosomal markers suggesting that WIPI-2 does not localise to these endosomal compartments. Colocalisation with an ER marker was also examined, given that one of the proposed origins of the autophagosomal membranes is the

ER (Dunn, 1994; Kovacs *et al.*, 2000), but again no significant colocalisation was observed.

WIPI-2 and PIKfyve produce opposite effects on autophagy assays. The role of Atg18 has been shown to be independent of its binding to PtdInd(3,5)P_2 in yeast and my data suggest that this may also the case with the mammalian proteins. This hypothesis was confirmed by treating cells with the PI(3)-kinase inhibitor wortmannin, which was found to ablate the formation of both WIPI-2 and GFP-LC3 II punctae. Although it is possible that this is an indirect effect of reducing the levels of PtdIns(3,5)P_2 due to loss of its precursor PtdIns(3)P, it was subsequently shown that treatment with PIKfyve inhibitor had the opposite effect, causing an accumulation of WIPI-2 and GFP-LC3 II punctae. This suggests that WIPI-2 is recruited to autophagic membranes through its binding of PtdIns(3)P and not PtdIns(3,5)P_2, although this does not rule out subsequent binding to PtdIns(3,5)P_2 and further autophagic functions.

Through further experiments I began to dissect the role of WIPI-2 in autophagy in more detail. By comparison with known autophagy protein ULK-1 it was demonstrated that these proteins have a comparable effect on autophagosome formation. ULK-1 is a serine threonine protein kinase and the mammalian homologue of the yeast protein Atg1, which is thought to form an essential part of the autophagy-inducing complex downstream of TOR signalling. Knockdown of ULK-1 has previously been shown to cause a reduction in GFP-LC3 lipidation (Chan *et al.*, 2007). That WIPI-2 and ULK-1 exert similar effects on lipidation, suggests that they may have equally important roles in autophagy. However, as WIPI-2 is recruited to the

autophagic membrane in a PtdIns(3)*P* dependent manner, then it would most likely be involved in a different part of the autophagic pathway to ULK-1, as PtdIns(3)*P* is formed by the action of the Vp34/Beclin complex that is recruited to the forming autophagosome membrane after autophagy has been induced by the autophagy inducing complex incorporating ULK-1. To test this hypothesis a combined knockdown of ULK-1 and WIPI-2 were examined. If WIPI-2 and ULK-1 exert their effects on different parts of the autophagy machinery (induction and autophagosome formation) then a combined knockdown should produce an additive effect on GFP-LC3 lipidation, which it did. However, it must also be taken into account that in yeast, the Atg1-Atg13 complex is also proposed to regulate Atg9 cycling along with Atg18/Svp1 (Reggiori *et al.*, 2004), a function that may also be conserved for the mammalian protein ULK-1 (Young *et al.*, 2006). Therefore, the conclusion that WIPI-2 and ULK-1 knockdown affect two independent parts of the autophagy pathway is not absolutely clear, as knockdown of ULK-1 could be having an indirect effect on WIPI-2 if the interactions for the yeast proteins hold true for their mammalian counterparts. Interestingly, WIPI-2 has the opposite phenotype to Atg18 in autophagy, suggesting that perhaps the WIPI family may have a more complex role in autophagy that the yeast proteins.

6.3.3 A role for WIPI-1

Finally, I reexamined the potential role of WIPI-1 in autophagy. It has previously been shown that WIPI-1 is recruited to autophagic structures following starvation (Proikas-Cezanne *et al.*, 2007), as demonstrated in this

study with WIPI-2, suggesting that the two proteins may have similar functions, and may display some functional redundancy. In accordance with this, I found that overexpression of WIPI-1 caused a reduction in the recruitment of endogenous WIPI-2 to autophagic structures. However, I was unable to demonstrate an effect of WIPI-1 knockdown on GFP-LC3 lipidation. Furthermore, a combined knockdown of WIPI-1 and WIPI-2 had only the same effect as WIPI-2 knockdown alone. This suggested either that the expression of this protein is negligible in this cell line, given that an effect for WIPI-1 was demonstrated in a different cell line, or that the knockdown of WIPI-1 was inefficient. Indeed, detection of endogenous WIPI-1 in these cells was difficult, and the knockdown efficiency could not be effectively determined. WIPI-1 antibodies were obtained through the course of collaborative work. As such, they had previously been tested in other cell lines and shown to specifically detect both overexpressed and endogenous WIPI-1 (personal communication Dr Hannah Polson).

6.3.4 Conclusions

In conclusion, the work presented in this chapter, summarised in figure 6.14, demonstrates that the main role of PtdIns(3,5)P_2 in mammalian autophagy is most likely indirect. In combination with data outlined in chapters four and five it suggests that PtdIns(3,5)P_2 functions primarily in coordinating the maturation of the MVB/late endosome such that it is capable of fusing with a degradative compartment or acquiring a degradative capacity. Thus, cargo targeted for lysosomal degradation, such as EGFR or the contents of the autophagosome, fails to be properly degraded.

Despite its capacity to bind PtdIns(3,5)P_2, the function of WIPI-2 in autophagy appears to be at an earlier stage in autophagosome formation, where it is most likely recruited to autophagic membranes through its binding of PtdIns(3)*P*. The function of WIPI-2 as a PtdIns(3,5)P_2 effector, either at a later stage in autophagy or in a different cellular process remains to be determined.

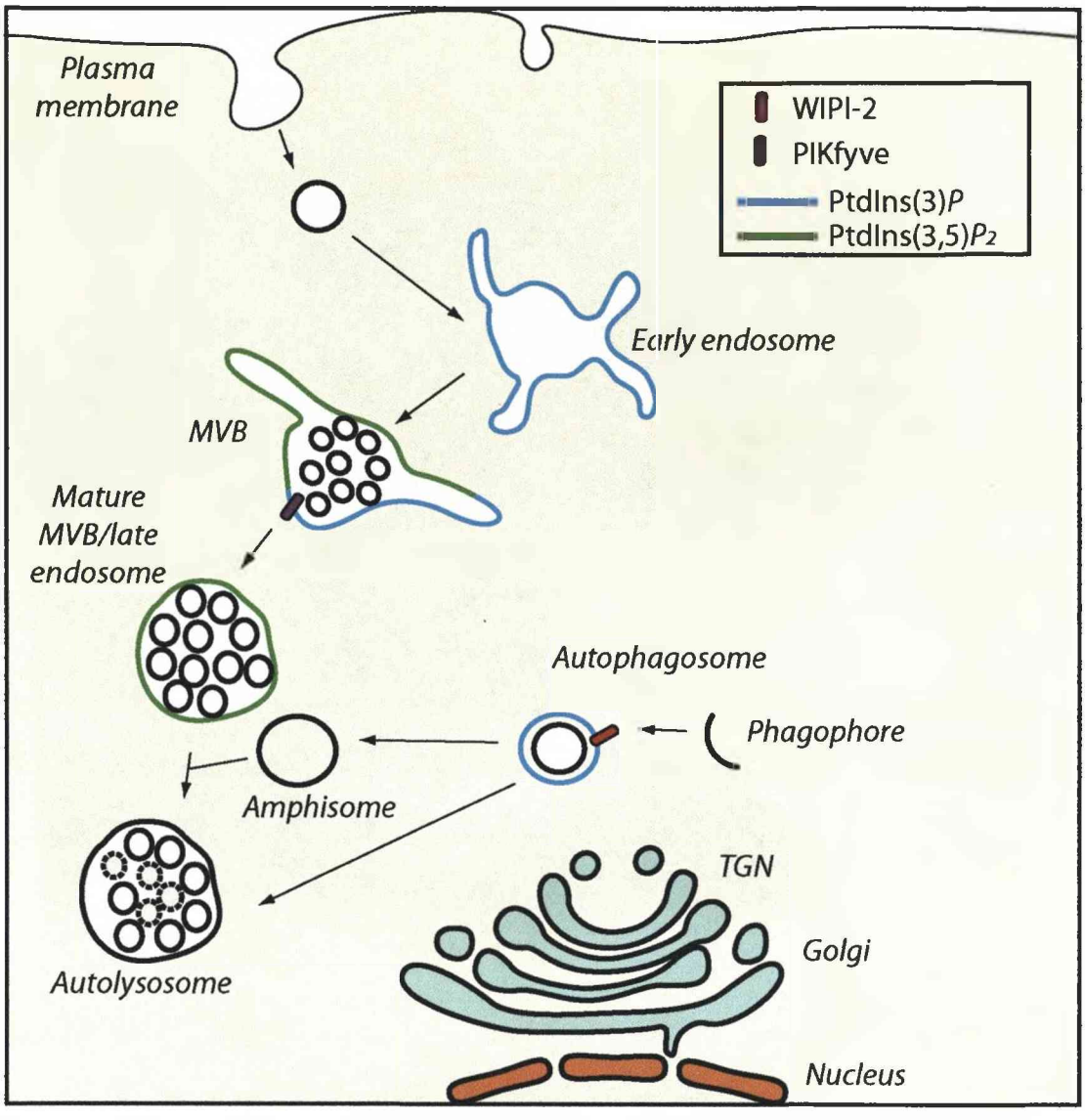

Figure 6.14. PIKfyve and WIPI-2 play opposing roles in mammalian autophagy.

WIPI-2 is recruited to the autophagosome following PtdIns(3)*P* production by the Beclin-Vps34 complex. Here it is proposed to be involved in recruiting membrane to the expanding autophagosome. Supporting this hypothesis a loss of WIPI-2 leads to a reduction in lipidated LC3, suggesting that autophagosome formation is reduced. PIKfyve on the other hand causes an increase in lipidated LC3. Its localisation to early endosomes, combined with the finding that loss of its activity does not affect WIPI-2 localisation and reduces long-lived protein degradation suggest that it may affect autophagy indirectly. Once autophagosomes have fused to the endocytic pathway their subsequent fate is partially dependent on PtdIns(3,5)P_2. Loss of PIKfyve causes a failure in degradation of the contents of autophagosomes in a similar manner to its effects on internalised EGFR.

CHAPTER SEVEN

Conclusion

This chapter will summarise the key findings of the work presented in this thesis, in the context of the current literature, whilst highlighting the key questions arising from this and the work of others that remain to be addressed. My work has focussed on the characterisation of four proteins associated with the metabolism of the phosphoinositide lipid PtdIns(3,5)P_2. The main aim of this work was to dissect the roles of these proteins in mammalian cells in relation to a variety of membrane trafficking pathways on which PtdIns(3,5)P_2 is proposed to play a role. An interest in this lipid stems from previous work in the lab characterising the roles of a group of phosphoinositide 3-phosphatases, the Myotubularins, and the aim to further characterise the putative mammalian 5-phosphatase Fig4, as at the time this protein had not been examined in any detail. However, the main body of the work has, over the course of my studies, been redirected to focus on the further characterisation of PIKfyve, as explained in more detail in this concluding chapter.

7.1 Summary and context of the current findings

7.1.1 Generation and use of key reagants

A key outcome of this work is the production and characterisation of invaluable tools and resources, such as antibodies, expression constructs, and purified protein, to permit continuation of research in this area. Furthermore, this assisted in the characterisation of three relatively poorly

examined PtdIns(3,5)P_2 associated mammalian proteins in unison, in a range of different cellular contexts. In addition to this, characterisation of the effects of a small molecule inhibitor of PIKfyve complements the pre-existing body of literature on this protein in mammalian cells.

In chapter three, the production and initial uses of these tools and reagents was outlined. Antibodies against Vac14 and WIPI-2 were found to be effective in detecting both overexpressed and endogenous protein in mammalian cells. These antibodies were subsequently used to validate protein knockdown for siRNA studies, and to assess the role of WIPI-2 in mammalian autophagy, as discussed later. A direct interaction between Vac14 and Fig4 was demonstrated by two independent methods, confirming the yeast literature, and at the time elucidating a novel interaction for the mammalian proteins, though this has since been demonstrated by another group (Sbrissa *et al.*, 2007). A small amount of Vac14 protein was purified from bacterial cells. The key purpose of protein purification was to obtain both Vac14 and Fig4, and to assess the substrate specificity of Fig4 and the nature of its interaction with Vac14, thus this was not pursued further due to the limited success of Fig4 protein production.

My biochemical data intriguingly indicated that Vac14 stabilises Fig4 in mammalian cells. In yeast the vacuole association of Fig4 is dependent on the presence of Vac14 (Rudge *et al.*, 2004), and more recently in mammalian cells, a loss of Vac14 has been shown to affect the immunofluorescent localisation of Fig4 to punctate structures (Sbrissa *et al.*, 2007). Recently, phosphatase activity has been established for mammalian Fig4, demonstrating that this protein hydrolyses PtdIns(3,5)P_2 *in vitro*, and that

ablation of Fig4 leads to a slight but significant increase in PtdIns(3,5)P_2 in intact cells. It was also found that Fig4 coimmunoprecipitates with both Vac14 and PIKfyve, and that ablation of Fig4 leads to an unexpected increase in PtdIns(3)*P* levels (Sbrissa *et al.*, 2007). These data suggest that the Vac14/Fig4 complex observed in yeast is conserved in higher organisms. Whilst Fig4 is clearly able to turnover PtdIns(3,5)P_2 in mammalian cells, as in yeast, it may also play a more complex role in regulating the activation of PIKfyve kinase activity through its interaction with Vac14, and potentially in a ternary complex between all three proteins. Purification of Fig4 protein therefore remains an important objective, such that the nature of the interaction between Vac14 and Fig4 may be assessed in more detail.

7.1.2 PIKfyve knockdown vs acute inhibition

Another key aim of this thesis was to examine the knockdown phenotypes associated with each protein. However, apart from PIKfyve, the proteins examined had no effect on these pathways. Previously, Vac14 and Fig4 depletion in other mammalian cell lines have not demonstrated the cytoplasmic vacuolation associated with PIKfyve knockdown, but instead rendered cells prone to vacuolation following osmotic stress (Sbrissa *et al.*, 2004; Sbrissa *et al.*, 2007). Only in cells taken from knockdown animals or patients with neurodegenerative diseases involving mutations of Fig4, were cytoplasmic vacuoles observed (Chow *et al.*, 2007; Zhang *et al.*, 2007). Interestingly, my work showed that combined knockdowns of Vac14 and Fig4 with PIKfyve, although not increasing the percentage of cells with cytoplasmic vacuolation increased the effect on several endosomal pathways

examined, possibly because these three proteins act in a common complex to tightly regulate the levels of the lipid.

A source of the recently identified small molecule inhibitor of PIKfyve was also obtained. PIKfyve knockdown studies have the following drawbacks: i) PIKfyve has proven hard to completely deplete, such that residual enzymatic activity could produce sufficient PtdIns(3,5)P_2 ii) it is unclear if the phenotypes observed are due to a loss of enzymatic activity or some other function of the protein iii) depletion is gradual and therefore any effect may be an indirect result of a loss of protein over a prolonged time period, and any compensatory mechanisms employed by the cell as a result. The small molecule inhibitor of PIKfyve has recently been characterised in the literature (Jefferies *et al.*, 2008), but has not been directly compared against PIKfyve siRNA to examine the role of PIKfyve on endosomal trafficking pathways. Therefore, the work presented in chapters four and five reassessed common membrane trafficking phenotypes attributed to loss of PIKfyve through siRNA treatment and overexpression studies, and made a direct comparison with the effects of acute inhibition of this protein. A summary of the key phenotypes associated with loss of PIKfyve in the context of other findings from yeast and higher eukaryotes is shown in table 7.1.

7.1.3 Endosomal maturation

PtdIns(3,5)P_2 was first linked to the endosomal system by the observation that yeast Fab1 deletion mutants display markedly swollen vacuoles (Gary *et al.*, 1998; Odorizzi *et al.*, 1998). This is also true in

mammals, where PIKfyve siRNA treatment or overexpression of a kinase-deficient mutant leads to the dilation of endosomal compartments and formation of cytoplasmic vacuoles (Sbrissa *et al.*, 1999; Rutherford *et al.*, 2006). I therefore chose to re-examine the characteristics of these swollen vacuoles in cells treated with PIKfyve inhibitor and to assess the possible mechanisms that lead to their formation. The large cytoplasmic are surrounded by swollen early and late endosomes and its limiting membrane is closely associated with LAMP-2. They have few ILVs and are poorly accessible to markers of fluid phase endocytosis. A number of lines of evidence have attributed this phenotype to a role of PtdIns(3,5)P_2 in membrane retrieval pathways, endosomal membrane homeostasis and terminal maturation of lysosomes (Nicot *et al.*, 2006; Rusten *et al.*, 2006; Rutherford *et al.*, 2006), therefore I compared the effects of PIKfyve knockdown and acute pharmalogical inhibition on these cellular processes.

Both PIKfyve knockdown and inhibition affected the distribution of a number of different proteins that cycle between endosomes and the TGN, that utilise both retromer-dependent and independent sorting mechanisms, including the trans-Golgi resident protein TGN46 and ciM6PR, responsible for transport of newly synthesised lysosomal enzymes. As well as the steady state distribution, the kinetics of transport from the cell surface, via the endosome, to the TGN are also perturbed for a range of proteins, including the Shiga toxin B subunit, and CD8-ciM6PR and Furin reporter constructs. These results confirm previous observations that PIKfyve plays a role on this pathway (Rutherford *et al.*, 2006), and furthermore suggests that PIKfyve

enzymatic activity and generation of PtdIns(3,5)P_2 is important for the general retrieval of membrane from various stages of the endocytic pathway.

Conflicting evidence from the literature suggests that PtdIns(3,5)P_2 may also be involved in ILV formation, sorting of endocytosed receptors into the lumen of the MVB or lysosomal degradation. Therefore, I examined the effects of pharmacological inhibition of PIKfyve on tyrosine kinase receptor degradation. Knockdown of PIKfyve alone had no effect on EGFR degradation, as previously shown in other studies (Rutherford *et al.*, 2006), however combined knockdown of PIKfyve and its activator Vac14 caused a delay in EGFR downregulation. Consistent with these observations, pharmacological inhibition of PIKfyve, at concentrations which do not produce any major perturbation in the levels of 3-phosphoinositides, revealed a strong block to EGFR and a second tyrosine kinase receptor, c-Met, downregulation. This data suggests that loss of PIKfyve enzymatic activity causes a defect in the lysosomal degradation of endocytosed receptors, but with a relatively low threshold value. Despite the possibility that components of the ESCRT complex may bind to PtdIns(3,5)P_2 (Whitley *et al.*, 2003), and that cytoplasmic vacuoles appear to be endosomal compartments with few ILVs (Ikonomov *et al.*, 2003a), the observed effect on EGFR degradation was shown to occur subsequent to its translocation into the lumen of the MVB. This finding is in agreement with previous work in *Drosophila*, which found a delay in the degradation but not internalisation of Wingless and Notch receptors (Rusten *et al.*, 2006).

These data suggest that PtdIns(3,5)P_2 may coordinate the maturation of at least a subset of MVBs. Cargo is delivered to the endocytic pathway

but is unable to recycle back to the TGN, therefore disrupting the balance of membrane delivery and retrieval and leading to a swelling of endosomal compartments. Furthermore, a defect in ciM6PR recycling perturbs the delivery of lysosomal enzymes and possibly the retrieval of certain proteins necessary for correct acidification of the MVB. Each of these defects may lead to a failure in the correct maturation of the MVB such that it is rendered refractory to fusion with the lysosome.

Further work is needed to clarify the role of PtdIns(3,5)P_2 in endosomal progression. Other groups have suggested that PIKfyve negatively regulates early to late endosomal fusion, thus leading to the formation of enlarged late endosomes (Ikonomov *et al.*, 2006). They also showed that other undefined fusion events may be regulated by PIKfyve, such as ILV fusion with the MVB limiting membrane, thereby explaining the reduced number of ILVs observed by EM. Perhaps PIKfyve mediated conversion of PtdIns(3)*P* to PtdIns(3,5)P_2 switches the balance from early-late endosome fusion to late endosome-lysosome fusion, a model that would consolidate my findings with these. Immuno-EM studies examining the distribution of markers previously examined by IF following loss of PIKfyve may help to build a clearer picture of the precise point of the block in these trafficking pathways. It may also prove interesting to examine the distribution of Rab proteins and to further examine fusion rates following loss of PIKfyve enzymatic activity. A recent paper described the combination of live-cell imaging techniques with new software to analyse the conversion of Rab5 to Rab7 in early to late endosome transport (Rink *et al.*, 2005). Although the steady-state localisation of Rab5 and Rab7 has been examined (Ikonomov *et*

al., 2006), such techniques could potentially be applied to examine early to late endosome dynamics following PIKfyve knockdown.

7.1.4 Autophagy

Another proposed cellular function of PtdIns(3,5)P_2 is in autophagy. Although a role for PtdIns(3)*P* has been established, the precise function of PtdIns(3,5)P_2 remains elusive. It has been suggested to act through the downstream effector Svp1/Atg18, however, at least in yeast the role of Svp1 is thought to be independent of its binding to PtdIns(3,5)P_2 (Dove *et al.*, 2004). Groups working on the mammalian protein WIPI-1 have also identified a potential role for this protein in autophagy (Proikas-Cezanne *et al.*, 2004; Proikas-Cezanne *et al.*, 2007). I therefore chose to examine the role of each of the four PtdIns(3,5)P_2 associated proteins in mammalian autophagy for a number of reasons: 1) to attempt to assess the contribution of PIKfyve enzymatic activity, and therefore PtdIns(3,5)P_2 in autophagy, through the use of PIKfyve inhibitor 2) to examine the role of WIPI-2 in autophagy (given that only WIPI-1 has been assessed in this context, and that WIPI-2 had no effect on other endosomal trafficking pathways) and 3) to determine how the role of WIPI-2 relates to its role as an effector of PtdIns(3,5)P_2.

The work described in chapter six determined that loss of PIKfyve enzymatic activity lead to an accumulation of the autophagosomal marker GFP-LC3 II, whereas loss of WIPI-2 had the opposite effect, causing a decrease in GFP-LC3 II. WIPI-2 was shown to be recruited to autophagosomal structures following starvation-induction of autophagy, an

effect that was subsequently shown to be ablated by wortmannin but not PIKfyve inhibitor treatment, suggesting that WIPI-2 recruitment to autophagosomes is independent of its potential capacity to bind PtdIns(3,5)P_2. Further analysis suggested that loss of WIPI-2 gave a similar phenotype to loss of the integral autophagy protein ULK-1, part of the autophagy-inducing complex in yeast. Furthermore, combined knockdown of the two proteins lead to an even more dramatic loss of GFP-LC3 II. The evidence suggests that PIKfyve and WIPI-2 have different roles in autophagy. Interestingly, WIPI-2 also has the opposite effect to the yeast Fab1 mutant, suggesting that the relationship between the yeast and mammalian proteins may be more complicated than originally suspected. PIKfyve most likely exerts an indirect effect on the autophagy pathway, by affecting the progression of autophagosomal content to the lysosome in a similar manner to its role in EGFR degradation. However, WIPI-2 appears to be a more integral part of the autophagy machinery, potentially mimicking its role in Atg9 cycling in yeast, although its precise role remains to be dissected in detail.

Further work is needed to determine the lipid binding capacity of WIPI-2, as this has only been assessed for WIPI-1, and it seems that it may preferentially bind to PtdIns(3)P (Jeffries *et al.*, 2004). If WIPI-2 does bind to both PtdIns(3)P and PtdIns(3,5)P_2 in a cellular context, then its role as a PtdIns(3,5)P_2 effector and how its lipid-binding capacity relates to its effect in autophagy, remain to be determined. Currently, work is being undertaken to determine if the ability of overexpression of WIPI-2 to rescue the WIPI-2 knockdown phenotype is dependent on its lipid binding capacity, by

production of a lipid-binding mutant. Furthermore, a yeast-two hybrid screen to identify novel binding partners of the WIPI proteins is underway to determine other potential functions of these proteins.

7.2 Limitations of the study

The data presented in the current study have been assessed in the context of the current literature, but the limitations of the various techniques used must also be taken into consideration. Although treatment with a specific inhibitor of PIKfyve allows us to overcome some of the caveats of overexpression and siRNA studies, it has limitations of its own. In this study the levels of phosphoinositide levels following treatment with either siRNA suppression of PIKfyve or Fig4 enzymes, or inhibition of PIKfyve, were not assessed due to the technical demands of the techniques involved. The levels of lipids have been examined for the structurally similar YM201636, but this does not mean that the two compounds have the same effects. MF4 appears to have a more substantial effect on PI(3)-kinases than YM201636, and although this could be explained by the use of different ATP concentrations when measuring IC50 values, this could mean that MF4 is affecting other phosphoinositide kinases. The levels of PtdIns(3)*P* were assessed by immunofluorescence to address this issue to some extent and results were compared directly with PIKfyve siRNA treatment to help us to draw general trends in loss of PIKfyve phenotypes, but in order to be certain that this inhibitor is specific for PIKfyve and affects only PtdIns(3,5)P_2 levels the phosphoinositide levels need to be measured. Therefore, we must bear

in mind that where PIKfyve inhibitor is used we make the assumption that the observed results are as a direct result of loss of PIKfyve activity alone.

A key limitation of the work presented in chapter four is that data presented are morphological studies and do not give any quantitative assessment of these phenotypes. In order to reinforce this data, it would be prudent to assess these phenotypes using image analysis software. The key phenotype of PIKfyve deficient cells is the formation of swollen cytoplasmic vacuoles, and the very presence of these vacuoles may cause morphological disruption to cells, such that retrieval of cargo to the TGN is perturbed for this reason rather than effects on the trafficking machinery. The assessment of TGN46 in comparison to other golgi proteins suggests that golgi structure at least remains intact.

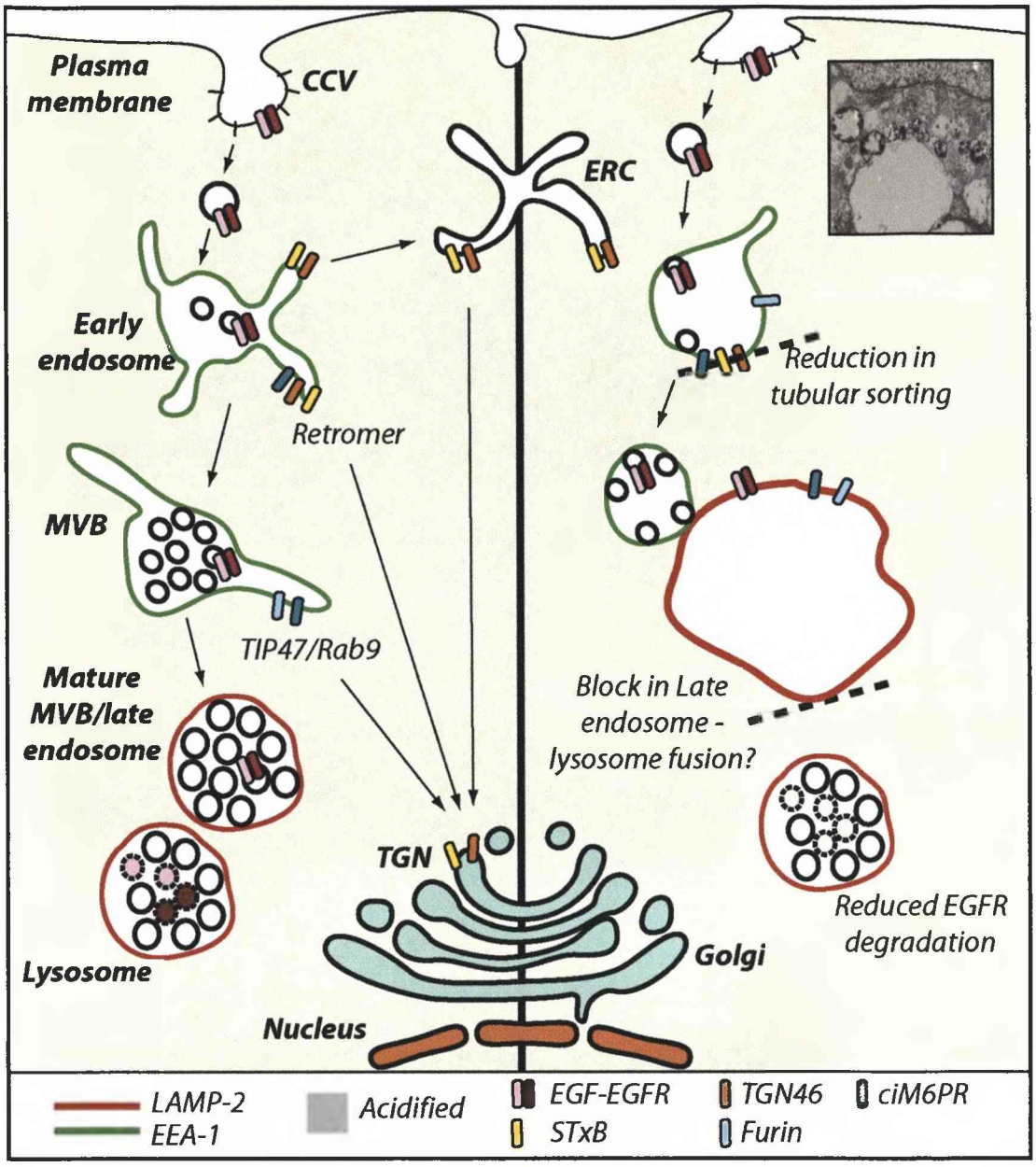

Figure 7.1. PtdIns(3,5)P_2 regulates endosomal membrane dynamics. In a normal cell (left) endocytosed material passes through the compartments of the endocytic pathway where it is gradually sorted into tubular or vacuolar partitions of endosomes. Cargo sorted into tubules is transported to various cellular localisations, whereas vacuoles accumulate in the maturing MVB, sorting cargo for lysosomal degradation. Loss of PIKfyve activity (right) produces swollen early and MVB/late endosomes with fewer intralumenal vesicles (EM inset). EGFR is internalised into MVBs where signalling is terminated, but a proportion of the receptor fails to get degraded. EGFR is able to reach acidified compartments, but fails to get degraded as the MVB is refractory to fusion with the lysosome. A variety of retromer-dependent and independent TGN retrieval pathways are perturbed as formation of recycling tubules is affected.

Table 7.1. Intracellular trafficking events affected by loss of Fab1/PIKfyve activity in *S. cerevisiae* and higher eukaryotes

Nd – Not determined, DN – dominant negative, RNAi – protein knockdown, INH – PIKfyve inhibitor, 1 – (Odorizzi *et al.*, 1998; Onishi *et al.*, 2003), 2 - (Yamamoto *et al.*, 1995), 3 - (Bryant *et al.*, 1998; Dove *et al.*, 2004), 4 - (Nicot *et al.*, 2006), 5 - (Rusten *et al.*, 2006), 6 - (Ikonomov *et al.*, 2003a; Ikonomov *et al.*, 2006), 7 – This study, 8 - (Rutherford *et al.*, 2006), 9 - (Jefferies *et al.*, 2008).

Organism/ Event	*S. cerevisiae*	*C. elegans (4)*	*D. melanogaster (5)*	Mammals		
				DN (6)	RNAi	INH
MVB sorting/receptor internalisation	Some cargos affected (1)	Functional	Functional	Functional	Functional (7)	Functional (7)
Acidification	Vacuole not acidified (2)	Defective	Defective	Nd	Functional, large vacuoles not acidified (7)	Functional, large vacuoles not acidified (7)
Fusion	Nd	Increase (lysosomes)	Nd	Increase (early endosomes)	Nd	Nd
Fission	Nd	Nd	Nd	Decrease (early endosomes)	Nd	Nd
Lysosomal degradation	Defective (1)	Functional (maturation defective)	Defective	Functional	Functional/defective if combined with Vac14 RNAi (7/8)	Defective (7)
Fluid phase endocytosis	Nd	Functional	Retarded	Retarded	Retarded (7)	Retarded (7)
Endosome to TGN transport	Defective (Vac7 and Svp1Δ) (3)	Nd	Nd	Nd	Delayed (7/8)	Delayed (7)
Autophagy pathway	Defective (Svp1Δ) (3)	Accumulation of autophagosomal marker	Accumulation of amphisomes	Nd	Accumulation of autophagosomal marker (7)	Accumulation of autophagosomal marker (7) /reduction in long-lived protein degradation (9)

Bibliography

Abdel-Latif, A.A., Akhtar, R.A., and Hawthorne, J.N. (1977). Acetylcholine increases the breakdown of triphosphoinositide of rabbit iris muscle prelabelled with [32P] phosphate. Biochem J *162*, 61-73.

Agranoff, B.W., Bradley, R.M., and Brady, R.O. (1958). The enzymatic synthesis of inositol phosphatide. J Biol Chem *233*, 1077-1083.

Apodaca, G. (2001). Endocytic traffic in polarized epithelial cells: role of the actin and microtubule cytoskeleton. Traffic *2*, 149-159.

Arico, S., Petiot, A., Bauvy, C., Dubbelhuis, P.F., Meijer, A.J., Codogno, P., and Ogier-Denis, E. (2001). The tumor suppressor PTEN positively regulates macroautophagy by inhibiting the phosphatidylinositol 3-kinase/protein kinase B pathway. J Biol Chem *276*, 35243-35246.

Arighi, C.N., Hartnell, L.M., Aguilar, R.C., Haft, C.R., and Bonifacino, J.S. (2004). Role of the mammalian retromer in sorting of the cation-independent mannose 6-phosphate receptor. J Cell Biol *165*, 123-133.

Arstila, A.U., and Trump, B.F. (1968). Studies on cellular autophagocytosis. The formation of autophagic vacuoles in the liver after glucagon administration. Am J Pathol *53*, 687-733.

Auger, K.R., Serunian, L.A., Soltoff, S.P., Libby, P., and Cantley, L.C. (1989). PDGF-dependent tyrosine phosphorylation stimulates production of novel polyphosphoinositides in intact cells. Cell *57*, 167-175.

Augsten, M., Hubner, C., Nguyen, M., Kunkel, W., Hartl, A., and Eck, R. (2002). Defective Hyphal induction of a Candida albicans phosphatidylinositol 3-phosphate 5-kinase null mutant on solid media does not lead to decreased virulence. Infect Immun *70*, 4462-4470.

Avruch, J., Zhang, X.F., and Kyriakis, J.M. (1994). Raf meets Ras: completing the framework of a signal transduction pathway. Trends Biochem Sci *19*, 279-283.

Babst, M. (2005). A protein's final ESCRT. Traffic *6*, 2-9.

Babst, M., Sato, T.K., Banta, L.M., and Emr, S.D. (1997). Endosomal transport function in yeast requires a novel AAA-type ATPase, Vps4p. Embo J *16*, 1820-1831.

Banfic, H., Downes, C.P., and Rittenhouse, S.E. (1998). Biphasic activation of PKBalpha/Akt in platelets. Evidence for stimulation both by phosphatidylinositol 3,4-bisphosphate, produced via a novel pathway, and by phosphatidylinositol 3,4,5-trisphosphate. J Biol Chem *273*, 11630-11637.

Banta, L.M., Robinson, J.S., Klionsky, D.J., and Emr, S.D. (1988). Organelle assembly in yeast: characterization of yeast mutants defective in vacuolar biogenesis and protein sorting. J Cell Biol *107*, 1369-1383.

Barth, H., Meiling-Wesse, K., Epple, U.D., and Thumm, M. (2001). Autophagy and the cytoplasm to vacuole targeting pathway both require Aut10p. FEBS Lett *508*, 23-28.

Batzer, A.G., Rotin, D., Urena, J.M., Skolnik, E.Y., and Schlessinger, J. (1994). Hierarchy of binding sites for Grb2 and Shc on the epidermal growth factor receptor. Mol Cell Biol *14*, 5192-5201.

Baudhuin, P., Beaufay, H., and De Duve, C. (1965). Combined biochemical and morphological study of particulate fractions from rat liver. Analysis of preparations enriched in lysosomes or in particles containing urate oxidase, D-amino acid oxidase, and catalase. J Cell Biol *26*, 219-243.

Bell, R.M. (1986). Protein kinase C activation by diacylglycerol second messengers. Cell *45*, 631-632.

Berger, P., Schaffitzel, C., Berger, I., Ban, N., and Suter, U. (2003). Membrane association of myotubularin-related protein 2 is mediated by a pleckstrin homology-GRAM domain and a coiled-coil dimerization module. Proc Natl Acad Sci U S A *100*, 12177-12182.

Berridge, M.J. (1983). Rapid accumulation of inositol trisphosphate reveals that agonists hydrolyse polyphosphoinositides instead of phosphatidylinositol. Biochem J *212*, 849-858.

Berridge, M.J., and Irvine, R.F. (1989). Inositol phosphates and cell signalling. Nature *341*, 197-205.

Besterman, J.M., Airhart, J.A., Woodworth, R.C., and Low, R.B. (1981). Exocytosis of pinocytosed fluid in cultured cells: kinetic evidence for rapid turnover and compartmentation. J Cell Biol *91*, 716-727.

Bidlingmaier, S., and Snyder, M. (2002). Large-scale identification of genes important for apical growth in Saccharomyces cerevisiae by directed allele replacement technology (DART) screening. Funct Integr Genomics *1*, 345-356.

Blott, E.J., and Griffiths, G.M. (2002). Secretory lysosomes. Nat Rev Mol Cell Biol *3*, 122-131.

Bonangelino, C.J., Catlett, N.L., and Weisman, L.S. (1997). Vac7p, a novel vacuolar protein, is required for normal vacuole inheritance and morphology. Mol Cell Biol *17*, 6847-6858.

Bonangelino, C.J., Nau, J.J., Duex, J.E., Brinkman, M., Wurmser, A.E., Gary, J.D., Emr, S.D., and Weisman, L.S. (2002). Osmotic stress-induced increase of phosphatidylinositol 3,5-bisphosphate requires Vac14p, an activator of the lipid kinase Fab1p. J Cell Biol *156*, 1015-1028.

Bonifacino, J.S., and Rojas, R. (2006). Retrograde transport from endosomes to the trans-Golgi network. Nat Rev Mol Cell Biol *7*, 568-579.

Botelho, R.J., Efe, J.A., Teis, D., and Emr, S.D. (2008). Assembly of a Fab1 Phosphoinositide Kinase Signaling Complex Requires the Fig4 Phosphoinositide Phosphatase. Mol Biol Cell.

Boya, P., Gonzalez-Polo, R.A., Casares, N., Perfettini, J.L., Dessen, P., Larochette, N., Metivier, D., Meley, D., Souquere, S., Yoshimori, T., Pierron, G., Codogno, P., and Kroemer, G. (2005). Inhibition of macroautophagy triggers apoptosis. Mol Cell Biol *25*, 1025-1040.

Brian, P.W. (1957). The effects of some microbial metabolic products on plant growth. Symp Soc Exp Biol *54*, 166-182.

Briza, P., Bogengruber, E., Thur, A., Rutzler, M., Munsterkotter, M., Dawes, I.W., and Breitenbach, M. (2002). Systematic analysis of sporulation phenotypes in 624 non-lethal homozygous deletion strains of Saccharomyces cerevisiae. Yeast *19*, 403-422.

Bryant, N.J., Piper, R.C., Weisman, L.S., and Stevens, T.H. (1998). Retrograde traffic out of the yeast vacuole to the TGN occurs via the prevacuolar/endosomal compartment. J Cell Biol *142*, 651-663.

Burd, C.G., and Emr, S.D. (1998). Phosphatidylinositol(3)-phosphate signaling mediated by specific binding to RING FYVE domains. Mol Cell *2*, 157-162.

Byfield, M.P., Murray, J.T., and Backer, J.M. (2005). hVps34 is a nutrient-regulated lipid kinase required for activation of p70 S6 kinase. J Biol Chem *280*, 33076-33082.

Cabezas, A., Pattni, K., and Stenmark, H. (2006). Cloning and subcellular localization of a human phosphatidylinositol 3-phosphate 5-kinase, PIKfyve/Fab1. Gene *371*, 34-41.

Carlton, J.G., Bujny, M.V., Peter, B.J., Oorschot, V.M., Rutherford, A., Arkell, R.S., Klumperman, J., McMahon, H.T., and Cullen, P.J. (2005). Sorting nexin-2 is associated with tubular elements of the early endosome, but is not essential for retromer-mediated endosome-to-TGN transport. J Cell Sci *118*, 4527-4539.

Carpenter, G. (1987). Receptors for epidermal growth factor and other polypeptide mitogens. Annu Rev Biochem *56*, 881-914.

Carpentier, J.L., White, M.F., Orci, L., and Kahn, R.C. (1987). Direct visualization of the phosphorylated epidermal growth factor receptor during its internalization in A-431 cells. J Cell Biol *105*, 2751-2762.

Carroll, K.S., Hanna, J., Simon, I., Krise, J., Barbero, P., and Pfeffer, S.R. (2001). Role of Rab9 GTPase in facilitating receptor recruitment by TIP47. Science *292*, 1373-1376.

Chan, E.Y., Kir, S., and Tooze, S.A. (2007). siRNA screening of the kinome identifies ULK1 as a multidomain modulator of autophagy. J Biol Chem *282*, 25464-25474.

Chavrier, P., Parton, R.G., Hauri, H.P., Simons, K., and Zerial, M. (1990). Localization of low molecular weight GTP binding proteins to exocytic and endocytic compartments. Cell *62*, 317-329.

Cheever, M.L., Sato, T.K., de Beer, T., Kutateladze, T.G., Emr, S.D., and Overduin, M. (2001). Phox domain interaction with PtdIns(3)P targets the Vam7 t-SNARE to vacuole membranes. Nat Cell Biol *3*, 613-618.

Chow, C.Y., Zhang, Y., Dowling, J.J., Jin, N., Adamska, M., Shiga, K., Szigeti, K., Shy, M.E., Li, J., Zhang, X., Lupski, J.R., Weisman, L.S., and Meisler, M.H. (2007). Mutation of FIG4 causes neurodegeneration in the pale tremor mouse and patients with CMT4J. Nature *448*, 68-72.

Cohen, S., and Fava, R.A. (1985). Internalization of functional epidermal growth factor:receptor/kinase complexes in A-431 cells. J Biol Chem *260*, 12351-12358.

Cooke, F.T. (2002). Phosphatidylinositol 3,5-bisphosphate: metabolism and function. Arch Biochem Biophys *407*, 143-151.

Cooke, F.T., Dove, S.K., McEwen, R.K., Painter, G., Holmes, A.B., Hall, M.N., Michell, R.H., and Parker, P.J. (1998). The stress-activated phosphatidylinositol 3-phosphate 5-kinase Fab1p is essential for vacuole function in S. cerevisiae. Curr Biol *8*, 1219-1222.

Corvera, S., D'Arrigo, A., and Stenmark, H. (1999). Phosphoinositides in membrane traffic. Curr Opin Cell Biol *11*, 460-465.

Cozier, G.E., Carlton, J., McGregor, A.H., Gleeson, P.A., Teasdale, R.D., Mellor, H., and Cullen, P.J. (2002). The phox homology (PX) domain-dependent, 3-phosphoinositide-mediated association of sorting nexin-1 with an early sorting endosomal compartment is required for its ability to regulate epidermal growth factor receptor degradation. J Biol Chem *277*, 48730-48736.

Dalton, A.J., and Felix, M.D. (1954). Cytologic and cytochemical characteristics of the Golgi substance of epithelial cells of the epididymis in situ, in homogenates and after isolation. Am J Anat *94*, 171-207.

Davletov, B.A., and Sudhof, T.C. (1993). A single C2 domain from synaptotagmin I is sufficient for high affinity Ca2+/phospholipid binding. J Biol Chem *268*, 26386-26390.

Dawson, R.M. (1954). The measurement of 32P labelling of individual kephalins and lecithin in a small sample of tissue. Biochim Biophys Acta *14*, 374-379.

De Duve, C. (1965). The separation and characterization of subcellular particles. Harvey Lect *59*, 49-87.

de Duve, C. (1983). Lysosomes revisited. Eur J Biochem *137*, 391-397.

Dell'Angelica, E.C., Puertollano, R., Mullins, C., Aguilar, R.C., Vargas, J.D., Hartnell, L.M., and Bonifacino, J.S. (2000). GGAs: a family of ADP ribosylation factor-binding proteins related to adaptors and associated with the Golgi complex. J Cell Biol *149*, 81-94.

Di Guglielmo, G.M., Baass, P.C., Ou, W.J., Posner, B.I., and Bergeron, J.J. (1994). Compartmentalization of SHC, GRB2 and mSOS, and hyperphosphorylation of Raf-1 by EGF but not insulin in liver parenchyma. Embo J *13*, 4269-4277.

Diaz, E., and Pfeffer, S.R. (1998). TIP47: a cargo selection device for mannose 6-phosphate receptor trafficking. Cell *93*, 433-443.

Doray, B., Ghosh, P., Griffith, J., Geuze, H.J., and Kornfeld, S. (2002). Cooperation of GGAs and AP-1 in packaging MPRs at the trans-Golgi network. Science *297*, 1700-1703.

Dove, S.K., Cooke, F.T., Douglas, M.R., Sayers, L.G., Parker, P.J., and Michell, R.H. (1997). Osmotic stress activates phosphatidylinositol-3,5-bisphosphate synthesis. Nature *390*, 187-192.

Dove, S.K., McEwen, R.K., Mayes, A., Hughes, D.C., Beggs, J.D., and Michell, R.H. (2002). Vac14 controls PtdIns(3,5)P(2) synthesis and Fab1-dependent protein trafficking to the multivesicular body. Curr Biol *12*, 885-893.

Dove, S.K., Piper, R.C., McEwen, R.K., Yu, J.W., King, M.C., Hughes, D.C., Thuring, J., Holmes, A.B., Cooke, F.T., Michell, R.H., Parker, P.J., and Lemmon, M.A. (2004). Svp1p defines a family of phosphatidylinositol 3,5-bisphosphate effectors. Embo J *23*, 1922-1933.

Duex, J.E., Nau, J.J., Kauffman, E.J., and Weisman, L.S. (2006a). Phosphoinositide 5-phosphatase Fig 4p is required for both acute rise and subsequent fall in stress-induced phosphatidylinositol 3,5-bisphosphate levels. Eukaryot Cell *5*, 723-731.

Duex, J.E., Tang, F., and Weisman, L.S. (2006b). The Vac14p-Fig4p complex acts independently of Vac7p and couples PI3,5P2 synthesis and turnover. J Cell Biol *172*, 693-704.

Duncan, M.C., Costaguta, G., and Payne, G.S. (2003). Yeast epsin-related proteins required for Golgi-endosome traffic define a gamma-adaptin ear-binding motif. Nat Cell Biol *5*, 77-81.

Dunn, K.W., and Maxfield, F.R. (1992). Delivery of ligands from sorting endosomes to late endosomes occurs by maturation of sorting endosomes. J Cell Biol *117*, 301-310.

Dunn, W.A., and Hubbard, A.L. (1984). Receptor-mediated endocytosis of epidermal growth factor by hepatocytes in the perfused rat liver: ligand and receptor dynamics. J Cell Biol *98*, 2148-2159.

Dunn, W.A., Jr. (1994). Autophagy and related mechanisms of lysosome-mediated protein degradation. Trends Cell Biol *4*, 139-143.

Dunphy, W.G., and Rothman, J.E. (1985). Compartmental organization of the Golgi stack. Cell *42*, 13-21.

Efe, J.A., Botelho, R.J., and Emr, S.D. (2005). The Fab1 phosphatidylinositol kinase pathway in the regulation of vacuole morphology. Curr Opin Cell Biol *17*, 402-408.

Erdman, S., Lin, L., Malczynski, M., and Snyder, M. (1998). Pheromone-regulated genes required for yeast mating differentiation. J Cell Biol *140*, 461-483.

Eugster, A., Pecheur, E.I., Michel, F., Winsor, B., Letourneur, F., and Friant, S. (2004). Ent5p is required with Ent3p and Vps27p for ubiquitin-dependent protein sorting into the multivesicular body. Mol Biol Cell *15*, 3031-3041.

Fernandez-Borja, M., Wubbolts, R., Calafat, J., Janssen, H., Divecha, N., Dusseljee, S., and Neefjes, J. (1999). Multivesicular body morphogenesis requires phosphatidyl-inositol 3-kinase activity. Curr Biol *9*, 55-58.

Folch, J. (1949). Complete fractionation of brain cephalin; isolation from it of phosphatidyl serine, phosphatidyl ethanolamine, and diphosphoinositide. J Biol Chem *177*, 497-504.

Fong, H.K., Hurley, J.B., Hopkins, R.S., Miake-Lye, R., Johnson, M.S., Doolittle, R.F., and Simon, M.I. (1986). Repetitive segmental structure of the transducin beta subunit: homology with the CDC4 gene and identification of related mRNAs. Proc Natl Acad Sci U S A *83*, 2162-2166.

Friant, S., Pecheur, E.I., Eugster, A., Michel, F., Lefkir, Y., Nourrisson, D., and Letourneur, F. (2003). Ent3p Is a PtdIns(3,5)P2 effector required for protein sorting to the multivesicular body. Dev Cell *5*, 499-511.

Fruman, D.A., Meyers, R.E., and Cantley, L.C. (1998). Phosphoinositide kinases. Annu Rev Biochem *67*, 481-507.

Fry, M.J. (1994). Structure, regulation and function of phosphoinositide 3-kinases. Biochim Biophys Acta *1226*, 237-268.

Fukazawa, T., Miyake, S., Band, V., and Band, H. (1996). Tyrosine phosphorylation of Cbl upon epidermal growth factor (EGF) stimulation and its association with EGF receptor and downstream signaling proteins. J Biol Chem *271*, 14554-14559.

Futter, C.E., Collinson, L.M., Backer, J.M., and Hopkins, C.R. (2001). Human VPS34 is required for internal vesicle formation within multivesicular endosomes. J Cell Biol *155*, 1251-1264.

Gallusser, A., and Kirchhausen, T. (1993). The beta 1 and beta 2 subunits of the AP complexes are the clathrin coat assembly components. Embo J *12*, 5237-5244.

Garcia-Higuera, I., Fenoglio, J., Li, Y., Lewis, C., Panchenko, M.P., Reiner, O., Smith, T.F., and Neer, E.J. (1996). Folding of proteins with WD-repeats: comparison of six members of the WD-repeat superfamily to the G protein beta subunit. Biochemistry *35*, 13985-13994.

Gary, J.D., Sato, T.K., Stefan, C.J., Bonangelino, C.J., Weisman, L.S., and Emr, S.D. (2002). Regulation of Fab1 phosphatidylinositol 3-phosphate 5-kinase pathway by Vac7 protein and Fig4, a polyphosphoinositide phosphatase family member. Mol Biol Cell *13*, 1238-1251.

Gary, J.D., Wurmser, A.E., Bonangelino, C.J., Weisman, L.S., and Emr, S.D. (1998). Fab1p is essential for PtdIns(3)P 5-kinase activity and the maintenance of vacuolar size and membrane homeostasis. J Cell Biol *143*, 65-79.

Gaullier, J.M., Simonsen, A., D'Arrigo, A., Bremnes, B., Stenmark, H., and Aasland, R. (1998). FYVE fingers bind PtdIns(3)P. Nature *394*, 432-433.

Gavin, A.C., Aloy, P., Grandi, P., Krause, R., Boesche, M., Marzioch, M., Rau, C., Jensen, L.J., Bastuck, S., Dumpelfeld, B., Edelmann, A., Heurtier, M.A., Hoffman, V., Hoefert, C., Klein, K., Hudak, M., Michon, A.M., Schelder, M., Schirle, M., Remor, M., Rudi, T., Hooper, S., Bauer, A., Bouwmeester, T., Casari, G., Drewes, G., Neubauer, G., Rick, J.M., Kuster, B., Bork, P., Russell, R.B., and Superti-Furga, G. (2006). Proteome survey reveals modularity of the yeast cell machinery. Nature *440*, 631-636.

Georgakopoulos, T., Koutroubas, G., Vakonakis, I., Tzermia, M., Prokova, V., Voutsina, A., and Alexandraki, D. (2001). Functional analysis of the Saccharomyces cerevisiae YFR021w/YGR223c/YPL100w ORF family suggests relations to mitochondrial/peroxisomal functions and amino acid signalling pathways. Yeast *18*, 1155-1171.

Geuze, H.J., Slot, J.W., Strous, G.J., Lodish, H.F., and Schwartz, A.L. (1983). Intracellular site of asialoglycoprotein receptor-ligand uncoupling: double-label immunoelectron microscopy during receptor-mediated endocytosis. Cell *32*, 277-287.

Ghosh, R.N., Mallet, W.G., Soe, T.T., McGraw, T.E., and Maxfield, F.R. (1998). An endocytosed TGN38 chimeric protein is delivered to the TGN after trafficking through the endocytic recycling compartment in CHO cells. J Cell Biol *142*, 923-936.

Gillooly, D.J., Morrow, I.C., Lindsay, M., Gould, R., Bryant, N.J., Gaullier, J.M., Parton, R.G., and Stenmark, H. (2000). Localization of phosphatidylinositol 3-phosphate in yeast and mammalian cells. Embo J *19*, 4577-4588.

Godi, A., Di Campli, A., Konstantakopoulos, A., Di Tullio, G., Alessi, D.R., Kular, G.S., Daniele, T., Marra, P., Lucocq, J.M., and De Matteis, M.A. (2004). FAPPs control Golgi-to-cell-surface membrane traffic by binding to ARF and PtdIns(4)P. Nat Cell Biol *6*, 393-404.

Gomes de Mesquita, D.S., van den Hazel, H.B., Bouwman, J., and Woldringh, C.L. (1996). Characterization of new vacuolar segregation mutants, isolated by screening for loss of proteinase B self-activation. Eur J Cell Biol *71*, 237-247.

Gorden, P., Carpentier, J.L., Cohen, S., and Orci, L. (1978). [Interaction of epidermal growth factor with human fibroblasts in culture: an autoradiographic study at the ultrastructural level]. C R Acad Sci Hebd Seances Acad Sci D *286*, 1471-1474.

Gordon, P.B., and Seglen, P.O. (1988). Prelysosomal convergence of autophagic and endocytic pathways. Biochem Biophys Res Commun *151*, 40-47.

Gozuacik, D., and Kimchi, A. (2004). Autophagy as a cell death and tumor suppressor mechanism. Oncogene *23*, 2891-2906.

Gray, A., Van Der Kaay, J., and Downes, C.P. (1999). The pleckstrin homology domains of protein kinase B and GRP1 (general receptor for phosphoinositides-1) are sensitive and selective probes for the cellular detection of phosphatidylinositol 3,4-bisphosphate and/or phosphatidylinositol 3,4,5-trisphosphate in vivo. Biochem J *344 Pt 3*, 929-936.

Griffiths, G., Back, R., and Marsh, M. (1989). A quantitative analysis of the endocytic pathway in baby hamster kidney cells. J Cell Biol *109*, 2703-2720.

Griffiths, G., and Gruenberg, J. (1991). The arguments for pre-existing early and late endosomes. Trends Cell Biol *1*, 5-9.

Griffiths, G., and Simons, K. (1986). The trans Golgi network: sorting at the exit site of the Golgi complex. Science *234*, 438-443.

Guan, J., Stromhaug, P.E., George, M.D., Habibzadegah-Tari, P., Bevan, A., Dunn, W.A., Jr., and Klionsky, D.J. (2001). Cvt18/Gsa12 is required for cytoplasm-to-vacuole transport, pexophagy, and autophagy in Saccharomyces cerevisiae and Pichia pastoris. Mol Biol Cell *12*, 3821-3838.

Guo, S., Stolz, L.E., Lemrow, S.M., and York, J.D. (1999). SAC1-like domains of yeast SAC1, INP52, and INP53 and of human synaptojanin encode polyphosphoinositide phosphatases. J Biol Chem *274*, 12990-12995.

Haft, C.R., de la Luz Sierra, M., Bafford, R., Lesniak, M.A., Barr, V.A., and Taylor, S.I. (2000). Human orthologs of yeast vacuolar protein sorting proteins Vps26, 29, and 35: assembly into multimeric complexes. Mol Biol Cell *11*, 4105-4116.

Haigler, H.T., McKanna, J.A., and Cohen, S. (1979). Direct visualization of the binding and internalization of a ferritin conjugate of epidermal growth factor in human carcinoma cells A-431. J Cell Biol *81*, 382-395.

Hanson, P.I., Roth, R., Lin, Y., and Heuser, J.E. (2008). Plasma membrane deformation by circular arrays of ESCRT-III protein filaments. J Cell Biol *180*, 389-402.

Harlan, J.E., Hajduk, P.J., Yoon, H.S., and Fesik, S.W. (1994). Pleckstrin homology domains bind to phosphatidylinositol-4,5-bisphosphate. Nature *371*, 168-170.

Hawthorne, J.N. (1960). The inositol phospholipids. J Lipid Res *1*, 255-280.

Hawthorne, J.N., and White, D.A. (1975). Myo-inositol lipids. Vitam Horm *33*, 529-573.

Hayakawa, M., Kaizawa, H., Moritomo, H., Koizumi, T., Ohishi, T., Okada, M., Ohta, M., Tsukamoto, S., Parker, P., Workman, P., and Waterfield, M. (2006). Synthesis and biological evaluation of 4-morpholino-2-phenylquinazolines and related derivatives as novel PI3 kinase p110alpha inhibitors. Bioorg Med Chem *14*, 6847-6858.

Herman, P.K., and Emr, S.D. (1990). Characterization of VPS34, a gene required for vacuolar protein sorting and vacuole segregation in Saccharomyces cerevisiae. Mol Cell Biol *10*, 6742-6754.

Hernandez, L.D., Hueffer, K., Wenk, M.R., and Galan, J.E. (2004). Salmonella modulates vesicular traffic by altering phosphoinositide metabolism. Science *304*, 1805-1807.

Hershko, A., and Ciechanover, A. (1992). The ubiquitin system for protein degradation. Annu Rev Biochem *61*, 761-807.

Hiles, I.D., Otsu, M., Volinia, S., Fry, M.J., Gout, I., Dhand, R., Panayotou, G., Ruiz-Larrea, F., Thompson, A., Totty, N.F., and et al. (1992). Phosphatidylinositol 3-kinase: structure and expression of the 110 kd catalytic subunit. Cell *70*, 419-429.

Hirao, M., Sato, N., Kondo, T., Yonemura, S., Monden, M., Sasaki, T., Takai, Y., Tsukita, S., and Tsukita, S. (1996). Regulation mechanism of ERM (ezrin/radixin/moesin) protein/plasma membrane association: possible

involvement of phosphatidylinositol turnover and Rho-dependent signaling pathway. J Cell Biol *135*, 37-51.

Hirst, J., Lui, W.W., Bright, N.A., Totty, N., Seaman, M.N., and Robinson, M.S. (2000). A family of proteins with gamma-adaptin and VHS domains that facilitate trafficking between the trans-Golgi network and the vacuole/lysosome. J Cell Biol *149*, 67-80.

Hirst, J., Seaman, M.N., Buschow, S.I., and Robinson, M.S. (2007). The role of cargo proteins in GGA recruitment. Traffic *8*, 594-604.

Hokin, L.E., and Hokin, M.R. (1955). Effects of acetylcholine on phosphate turnover in phospholipides of brain cortex in vitro. Biochim Biophys Acta *16*, 229-237.

Hokin, L.E., and Hokin, M.R. (1958). Phosphoinositides and protein secretion in pancreas slices. J Biol Chem *233*, 805-810.

Hokin, L.E., and Hokin, M.R. (1964a). The Incorporation of 32p from Triphosphate into Polyphosphoinositides (Gamma-32p)Adenosine and Phosphatidic Acid in Erythrocyte Membranes. Biochim Biophys Acta *84*, 563-575.

Hokin, M.R., and Hokin, L.E. (1964b). The Synthesis of Phosphatidic Acid and Protein-Bound Phosphorylserine in Salt Gland Homogenates. J Biol Chem *239*, 2116-2122.

Honing, S., Sosa, M., Hille-Rehfeld, A., and von Figura, K. (1997). The 46-kDa mannose 6-phosphate receptor contains multiple binding sites for clathrin adaptors. J Biol Chem *272*, 19884-19890.

Hopkins, C.R. (1983). The importance of the endosome in intracellular traffic. Nature *304*, 684-685.

Huber, L.A., Fialka, I., Paiha, K., Hunziker, W., Sacks, D.B., Bahler, M., Way, M., Gagescu, R., and Gruenberg, J. (2000). Both calmodulin and the unconventional myosin Myr4 regulate membrane trafficking along the recycling pathway of MDCK cells. Traffic *1*, 494-503.

Hughes, W.E., Cooke, F.T., and Parker, P.J. (2000). Sac phosphatase domain proteins. Biochem J *350 Pt 2*, 337-352.

Ikonomov, O.C., Sbrissa, D., Foti, M., Carpentier, J.L., and Shisheva, A. (2003a). PIKfyve controls fluid phase endocytosis but not recycling/degradation of endocytosed receptors or sorting of procathepsin D by regulating multivesicular body morphogenesis. Mol Biol Cell *14*, 4581-4591.

Ikonomov, O.C., Sbrissa, D., Mlak, K., Deeb, R., Fligger, J., Soans, A., Finley, R.L., Jr., and Shisheva, A. (2003b). Active PIKfyve associates with and promotes the membrane attachment of the late endosome-to-trans-Golgi network transport factor Rab9 effector p40. J Biol Chem *278*, 50863-50871.

Ikonomov, O.C., Sbrissa, D., Mlak, K., Kanzaki, M., Pessin, J., and Shisheva, A. (2002a). Functional dissection of lipid and protein kinase signals of PIKfyve reveals the role of PtdIns 3,5-P2 production for endomembrane integrity. J Biol Chem *277*, 9206-9211.

Ikonomov, O.C., Sbrissa, D., and Shisheva, A. (2001). Mammalian cell morphology and endocytic membrane homeostasis require enzymatically active phosphoinositide 5-kinase PIKfyve. J Biol Chem *276*, 26141-26147.

Ikonomov, O.C., Sbrissa, D., and Shisheva, A. (2006). Localized PtdIns 3,5-P2 synthesis to regulate early endosome dynamics and fusion. Am J Physiol Cell Physiol *291*, C393-404.

Ikonomov, O.C., Sbrissa, D., Yoshimori, T., Cover, T.L., and Shisheva, A. (2002b). PIKfyve Kinase and SKD1 AAA ATPase define distinct endocytic compartments. Only PIKfyve expression inhibits the cell-vacoulating activity of Helicobacter pylori VacA toxin. J Biol Chem *277*, 46785-46790.

Itoh, T., Koshiba, S., Kigawa, T., Kikuchi, A., Yokoyama, S., and Takenawa, T. (2001). Role of the ENTH domain in phosphatidylinositol-4,5-bisphosphate binding and endocytosis. Science *291*, 1047-1051.

Jamieson, J.D., and Palade, G.E. (1967). Intracellular transport of secretory proteins in the pancreatic exocrine cell. II. Transport to condensing vacuoles and zymogen granules. J Cell Biol *34*, 597-615.

Jefferies, H.B., Cooke, F.T., Jat, P., Boucheron, C., Koizumi, T., Hayakawa, M., Kaizawa, H., Ohishi, T., Workman, P., Waterfield, M.D., and Parker, P.J. (2008). A selective PIKfyve inhibitor blocks PtdIns(3,5)P(2) production and disrupts endomembrane transport and retroviral budding. EMBO Rep *9*, 164-170.

Jeffries, T.R., Dove, S.K., Michell, R.H., and Parker, P.J. (2004). PtdIns-specific MPR pathway association of a novel WD40 repeat protein, WIPI49. Mol Biol Cell *15*, 2652-2663.

Jentsch, S. (1992). The ubiquitin-conjugation system. Annu Rev Genet *26*, 179-207.

Johnson, E.E., Overmeyer, J.H., Gunning, W.T., and Maltese, W.A. (2006). Gene silencing reveals a specific function of hVps34 phosphatidylinositol 3-kinase in late versus early endosomes. J Cell Sci *119*, 1219-1232.

Jones, A.T., and Clague, M.J. (1995). Phosphatidylinositol 3-kinase activity is required for early endosome fusion. Biochem J *311 (Pt 1)*, 31-34.

Jones, D.R., Gonzalez-Garcia, A., Diez, E., Martinez, A.C., Carrera, A.C., and Merida, I. (1999). The identification of phosphatidylinositol 3,5-bisphosphate in T-lymphocytes and its regulation by interleukin-2. J Biol Chem *274*, 18407-18413.

Jones, S.M., and Howell, K.E. (1997). Phosphatidylinositol 3-kinase is required for the formation of constitutive transport vesicles from the TGN. J Cell Biol *139*, 339-349.

Jost, M., Simpson, F., Kavran, J.M., Lemmon, M.A., and Schmid, S.L. (1998). Phosphatidylinositol-4,5-bisphosphate is required for endocytic coated vesicle formation. Curr Biol *8*, 1399-1402.

Kabeya, Y., Mizushima, N., Ueno, T., Yamamoto, A., Kirisako, T., Noda, T., Kominami, E., Ohsumi, Y., and Yoshimori, T. (2000). LC3, a mammalian homologue of yeast Apg8p, is localized in autophagosome membranes after processing. Embo J *19*, 5720-5728.

Kamada, Y., Funakoshi, T., Shintani, T., Nagano, K., Ohsumi, M., and Ohsumi, Y. (2000). Tor-mediated induction of autophagy via an Apg1 protein kinase complex. J Cell Biol *150*, 1507-1513.

Kametaka, S., Okano, T., Ohsumi, M., and Ohsumi, Y. (1998). Apg14p and Apg6/Vps30p form a protein complex essential for autophagy in the yeast, Saccharomyces cerevisiae. J Biol Chem *273*, 22284-22291.

Kanai, F., Liu, H., Field, S.J., Akbary, H., Matsuo, T., Brown, G.E., Cantley, L.C., and Yaffe, M.B. (2001). The PX domains of p47phox and p40phox bind to lipid products of PI(3)K. Nat Cell Biol *3*, 675-678.

Katzmann, D.J., Sarkar, S., Chu, T., Audhya, A., and Emr, S.D. (2004). Multivesicular body sorting: ubiquitin ligase Rsp5 is required for the modification and sorting of carboxypeptidase S. Mol Biol Cell *15*, 468-480.

Kay, D.G., Lai, W.H., Uchihashi, M., Khan, M.N., Posner, B.I., and Bergeron, J.J. (1986). Epidermal growth factor receptor kinase translocation and activation in vivo. J Biol Chem *261*, 8473-8480.

Kearns, M.A., Monks, D.E., Fang, M., Rivas, M.P., Courtney, P.D., Chen, J., Prestwich, G.D., Theibert, A.B., Dewey, R.E., and Bankaitis, V.A. (1998). Novel developmentally regulated phosphoinositide binding proteins from soybean whose expression bypasses the requirement for an essential phosphatidylinositol transfer protein in yeast. Embo J *17*, 4004-4017.

Kihara, A., Noda, T., Ishihara, N., and Ohsumi, Y. (2001). Two distinct Vps34 phosphatidylinositol 3-kinase complexes function in autophagy and carboxypeptidase Y sorting in Saccharomyces cerevisiae. J Cell Biol *152*, 519-530.

Kim, J., Huang, W.P., Stromhaug, P.E., and Klionsky, D.J. (2002). Convergence of multiple autophagy and cytoplasm to vacuole targeting components to a perivacuolar membrane compartment prior to de novo vesicle formation. J Biol Chem *277*, 763-773.

Kirk, C.J., Creba, J.A., Downes, C.P., and Michell, R.H. (1981). Hormone-stimulated metabolism of inositol lipids and its relationship to hepatic receptor function. Biochem Soc Trans *9*, 377-379.

Klionsky, D.J. (2005). The molecular machinery of autophagy: unanswered questions. J Cell Sci *118*, 7-18.

Klionsky, D.J. (2007). Autophagy: from phenomenology to molecular understanding in less than a decade. Nat Rev Mol Cell Biol *8*, 931-937.

Knight, Z.A., Gonzalez, B., Feldman, M.E., Zunder, E.R., Goldenberg, D.D., Williams, O., Loewith, R., Stokoe, D., Balla, A., Toth, B., Balla, T., Weiss, W.A., Williams, R.L., and Shokat, K.M. (2006). A pharmacological map of the PI3-K family defines a role for p110alpha in insulin signaling. Cell *125*, 733-747.

Kobayashi, T., Beuchat, M.H., Lindsay, M., Frias, S., Palmiter, R.D., Sakuraba, H., Parton, R.G., and Gruenberg, J. (1999). Late endosomal membranes rich in lysobisphosphatidic acid regulate cholesterol transport. Nat Cell Biol *1*, 113-118.

Kobayashi, T., Vischer, U.M., Rosnoblet, C., Lebrand, C., Lindsay, M., Parton, R.G., Kruithof, E.K., and Gruenberg, J. (2000). The tetraspanin CD63/lamp3 cycles between endocytic and secretory compartments in human endothelial cells. Mol Biol Cell *11*, 1829-1843.

Kornfeld, S. (1992). Structure and function of the mannose 6-phosphate/insulinlike growth factor II receptors. Annu Rev Biochem *61*, 307-330.

Kornfeld, S., and Mellman, I. (1989). The biogenesis of lysosomes. Annu Rev Cell Biol *5*, 483-525.

Kovacs, A.L., Rez, G., Palfia, Z., and Kovacs, J. (2000). Autophagy in the epithelial cells of murine seminal vesicle in vitro. Formation of large sheets of nascent isolation membranes, sequestration of the nucleus and inhibition by wortmannin and 3-ethyladenine. Cell Tissue Res *302*, 253-261.

Krugmann, S., Anderson, K.E., Ridley, S.H., Risso, N., McGregor, A., Coadwell, J., Davidson, K., Eguinoa, A., Ellson, C.D., Lipp, P., Manifava, M., Ktistakis, N., Painter, G., Thuring, J.W., Cooper, M.A., Lim, Z.Y., Holmes, A.B., Dove, S.K., Michell, R.H., Grewal, A., Nazarian, A., Erdjument-Bromage, H., Tempst, P., Stephens, L.R., and Hawkins, P.T. (2002). Identification of ARAP3, a novel PI3K effector regulating both Arf and Rho GTPases, by selective capture on phosphoinositide affinity matrices. Mol Cell *9*, 95-108.

Kunz, J.B., Schwarz, H., and Mayer, A. (2004). Determination of four sequential stages during microautophagy in vitro. J Biol Chem *279*, 9987-9996.

Kyle, J.W., Nolan, C.M., Oshima, A., and Sly, W.S. (1988). Expression of human cation-independent mannose 6-phosphate receptor cDNA in receptor-negative mouse P388D1 cells following gene transfer. J Biol Chem *263*, 16230-16235.

Laemmli, U.K. (1970). Cleavage of structural proteins during the assembly of the head of bacteriophage T4. Nature *227*, 680-685.

Lai, W.H., Cameron, P.H., Doherty, J.J., 2nd, Posner, B.I., and Bergeron, J.J. (1989). Ligand-mediated autophosphorylation activity of the epidermal growth factor receptor during internalization. J Cell Biol *109*, 2751-2760.

Lakadamyali, M., Rust, M.J., and Zhuang, X. (2006). Ligands for clathrin-mediated endocytosis are differentially sorted into distinct populations of early endosomes. Cell *124*, 997-1009.

Lazar, T., Scheglmann, D., and Gallwitz, D. (2002). A novel phospholipid-binding protein from the yeast Saccharomyces cerevisiae with dual binding specificities for the transport GTPase Ypt7p and the Sec1-related Vps33p. Eur J Cell Biol *81*, 635-646.

Lemaire, J.F., and McPherson, P.S. (2006). Binding of Vac14 to neuronal nitric oxide synthase: Characterisation of a new internal PDZ-recognition motif. FEBS Lett *580*, 6948-6954.

Lemmon, M.A., and Ferguson, K.M. (2000). Signal-dependent membrane targeting by pleckstrin homology (PH) domains. Biochem J *350 Pt 1*, 1-18.

Leondaritis, G., Tiedtke, A., and Galanopoulou, D. (2005). D-3 phosphoinositides of the ciliate Tetrahymena: characterization and study of their regulatory role in lysosomal enzyme secretion. Biochim Biophys Acta *1745*, 330-341.

Li, G., D'Souza-Schorey, C., Barbieri, M.A., Roberts, R.L., Klippel, A., Williams, L.T., and Stahl, P.D. (1995). Evidence for phosphatidylinositol 3-kinase as a regulator of endocytosis via activation of Rab5. Proc Natl Acad Sci U S A *92*, 10207-10211.

Li, S., Tiab, L., Jiao, X., Munier, F.L., Zografos, L., Frueh, B.E., Sergeev, Y., Smith, J., Rubin, B., Meallet, M.A., Forster, R.K., Hejtmancik, J.F., and Schorderet, D.F. (2005). Mutations in PIP5K3 are associated with Francois-Neetens mouchetee fleck corneal dystrophy. Am J Hum Genet *77*, 54-63.

Liang, X.H., Jackson, S., Seaman, M., Brown, K., Kempkes, B., Hibshoosh, H., and Levine, B. (1999). Induction of autophagy and inhibition of tumorigenesis by beclin 1. Nature *402*, 672-676.

Liang, X.H., Kleeman, L.K., Jiang, H.H., Gordon, G., Goldman, J.E., Berry, G., Herman, B., and Levine, B. (1998). Protection against fatal Sindbis virus encephalitis by beclin, a novel Bcl-2-interacting protein. J Virol *72*, 8586-8596.

Lloyd, T.E., Atkinson, R., Wu, M.N., Zhou, Y., Pennetta, G., and Bellen, H.J. (2002). Hrs regulates endosome membrane invagination and tyrosine kinase receptor signaling in Drosophila. Cell *108*, 261-269.

Lobel, P., Fujimoto, K., Ye, R.D., Griffiths, G., and Kornfeld, S. (1989). Mutations in the cytoplasmic domain of the 275 kd mannose 6-phosphate receptor differentially alter lysosomal enzyme sorting and endocytosis. Cell *57*, 787-796.

Luzio, J.P., Poupon, V., Lindsay, M.R., Mullock, B.M., Piper, R.C., and Pryor, P.R. (2003). Membrane dynamics and the biogenesis of lysosomes. Mol Membr Biol *20*, 141-154.

Luzio, J.P., Rous, B.A., Bright, N.A., Pryor, P.R., Mullock, B.M., and Piper, R.C. (2000). Lysosome-endosome fusion and lysosome biogenesis. J Cell Sci *113 (Pt 9)*, 1515-1524.

MacDougall, L.K., Domin, J., and Waterfield, M.D. (1995). A family of phosphoinositide 3-kinases in Drosophila identifies a new mediator of signal transduction. Curr Biol *5*, 1404-1415.

Majeski, A.E., and Dice, J.F. (2004). Mechanisms of chaperone-mediated autophagy. Int J Biochem Cell Biol *36*, 2435-2444.

Mallard, F., Antony, C., Tenza, D., Salamero, J., Goud, B., and Johannes, L. (1998). Direct pathway from early/recycling endosomes to the Golgi apparatus revealed through the study of shiga toxin B-fragment transport. J Cell Biol *143*, 973-990.

Mallet, W.G., and Maxfield, F.R. (1999). Chimeric forms of furin and TGN38 are transported with the plasma membrane in the trans-Golgi network via distinct endosomal pathways. J Cell Biol *146*, 345-359.

Marcus, S.L., Wenk, M.R., Steele-Mortimer, O., and Finlay, B.B. (2001). A synaptojanin-homologous region of Salmonella typhimurium SigD is essential for inositol phosphatase activity and Akt activation. FEBS Lett *494*, 201-207.

Mari, M., Bujny, M.V., Zeuschner, D., Geerts, W.J., Griffith, J., Petersen, C.M., Cullen, P.J., Klumperman, J., and Geuze, H.J. (2008). SNX1 defines an early endosomal recycling exit for sortilin and mannose 6-phosphate receptors. Traffic *9*, 380-393.

Martin, T.F. (1998). Phosphoinositide lipids as signaling molecules: common themes for signal transduction, cytoskeletal regulation, and membrane trafficking. Annu Rev Cell Dev Biol *14*, 231-264.

Martys, J.L., Wjasow, C., Gangi, D.M., Kielian, M.C., McGraw, T.E., and Backer, J.M. (1996). Wortmannin-sensitive trafficking pathways in Chinese hamster ovary cells. Differential effects on endocytosis and lysosomal sorting. J Biol Chem *271*, 10953-10962.

Mayor, S., Presley, J.F., and Maxfield, F.R. (1993). Sorting of membrane components from endosomes and subsequent recycling to the cell surface occurs by a bulk flow process. J Cell Biol *121*, 1257-1269.

McEwen, R.K., Dove, S.K., Cooke, F.T., Painter, G.F., Holmes, A.B., Shisheva, A., Ohya, Y., Parker, P.J., and Michell, R.H. (1999). Complementation analysis in PtdInsP kinase-deficient yeast mutants demonstrates that Schizosaccharomyces pombe and murine Fab1p homologues are phosphatidylinositol 3-phosphate 5-kinases. J Biol Chem *274*, 33905-33912.

McPherson, P.S., Garcia, E.P., Slepnev, V.I., David, C., Zhang, X., Grabs, D., Sossin, W.S., Bauerfeind, R., Nemoto, Y., and De Camilli, P. (1996). A presynaptic inositol-5-phosphatase. Nature *379*, 353-357.

Meiling-Wesse, K., Barth, H., Voss, C., Eskelinen, E.L., Epple, U.D., and Thumm, M. (2004). Atg21 is required for effective recruitment of Atg8 to the preautophagosomal structure during the Cvt pathway. J Biol Chem *279*, 37741-37750.

Meisner, H., Conway, B.R., Hartley, D., and Czech, M.P. (1995). Interactions of Cbl with Grb2 and phosphatidylinositol 3'-kinase in activated Jurkat cells. Mol Cell Biol *15*, 3571-3578.

Mellman, I., Fuchs, R., and Helenius, A. (1986). Acidification of the endocytic and exocytic pathways. Annu Rev Biochem *55*, 663-700.

Mellman, I., and Simons, K. (1992). The Golgi complex: in vitro veritas? Cell *68*, 829-840.

Michell, R.H., Heath, V.L., Lemmon, M.A., and Dove, S.K. (2006). Phosphatidylinositol 3,5-bisphosphate: metabolism and cellular functions. Trends Biochem Sci *31*, 52-63.

Mills, I.G., Jones, A.T., and Clague, M.J. (1998). Involvement of the endosomal autoantigen EEA1 in homotypic fusion of early endosomes. Curr Biol *8*, 881-884.

Mizushima, N. (2004). Methods for monitoring autophagy. Int J Biochem Cell Biol *36*, 2491-2502.

Morishita, M., Morimoto, F., Kitamura, K., Koga, T., Fukui, Y., Maekawa, H., Yamashita, I., and Shimoda, C. (2002). Phosphatidylinositol 3-phosphate 5-kinase is required for the cellular response to nutritional starvation and mating pheromone signals in Schizosaccharomyces pombe. Genes Cells *7*, 199-215.

Mortimore, G.E., and Poso, A.R. (1987). Intracellular protein catabolism and its control during nutrient deprivation and supply. Annu Rev Nutr *7*, 539-564.

Mukherjee, S., Ghosh, R.N., and Maxfield, F.R. (1997). Endocytosis. Physiol Rev *77*, 759-803.

Mullins, C., and Bonifacino, J.S. (2001). The molecular machinery for lysosome biogenesis. Bioessays *23*, 333-343.

Murphy, R.F. (1991). Maturation models for endosome and lysosome biogenesis. Trends Cell Biol *1*, 77-82.

Murray, J.L., Mavrakis, M., McDonald, N.J., Yilla, M., Sheng, J., Bellini, W.J., Zhao, L., Le Doux, J.M., Shaw, M.W., Luo, C.C., Lippincott-Schwartz, J., Sanchez, A., Rubin, D.H., and Hodge, T.W. (2005). Rab9 GTPase is required for replication of human immunodeficiency virus type 1, filoviruses, and measles virus. J Virol *79*, 11742-11751.

Murray, J.T., Panaretou, C., Stenmark, H., Miaczynska, M., and Backer, J.M. (2002). Role of Rab5 in the recruitment of hVps34/p150 to the early endosome. Traffic *3*, 416-427.

Muziol, T., Pineda-Molina, E., Ravelli, R.B., Zamborlini, A., Usami, Y., Gottlinger, H., and Weissenhorn, W. (2006). Structural basis for budding by the ESCRT-III factor CHMP3. Dev Cell *10*, 821-830.

Neer, E.J., Schmidt, C.J., Nambudripad, R., and Smith, T.F. (1994). The ancient regulatory-protein family of WD-repeat proteins. Nature *371*, 297-300.

Nicot, A.S., Fares, H., Payrastre, B., Chisholm, A.D., Labouesse, M., and Laporte, J. (2006). The phosphoinositide kinase PIKfyve/Fab1p regulates terminal lysosome maturation in Caenorhabditis elegans. Mol Biol Cell *17*, 3062-3074.

Niggli, V., Andreoli, C., Roy, C., and Mangeat, P. (1995). Identification of a phosphatidylinositol-4,5-bisphosphate-binding domain in the N-terminal region of ezrin. FEBS Lett *376*, 172-176.

Noda, T., Kim, J., Huang, W.P., Baba, M., Tokunaga, C., Ohsumi, Y., and Klionsky, D.J. (2000). Apg9p/Cvt7p is an integral membrane protein required for transport vesicle formation in the Cvt and autophagy pathways. J Cell Biol *148*, 465-480.

O'Reilly, K.E., Rojo, F., She, Q.B., Solit, D., Mills, G.B., Smith, D., Lane, H., Hofmann, F., Hicklin, D.J., Ludwig, D.L., Baselga, J., and Rosen, N. (2006). mTOR inhibition induces upstream receptor tyrosine kinase signaling and activates Akt. Cancer Res *66*, 1500-1508.

Odorizzi, G., Babst, M., and Emr, S.D. (1998). Fab1p PtdIns(3)P 5-kinase function essential for protein sorting in the multivesicular body. Cell *95*, 847-858.

Odorizzi, G., Babst, M., and Emr, S.D. (2000). Phosphoinositide signaling and the regulation of membrane trafficking in yeast. Trends Biochem Sci *25*, 229-235.

Ohsumi, Y., and Mizushima, N. (2004). Two ubiquitin-like conjugation systems essential for autophagy. Semin Cell Dev Biol *15*, 231-236.

Onishi, M., Nakamura, Y., Koga, T., Takegawa, K., and Fukui, Y. (2003). Isolation of suppressor mutants of phosphatidylinositol 3-phosphate 5-kinase deficient cells in Schizosaccharomyces pombe. Biosci Biotechnol Biochem *67*, 1772-1779.

Osborne, S.L., Wen, P.J., Boucheron, C., Nguyen, H.N., Hayakawa, M., Kaizawa, H., Parker, P.J., Vitale, N., and Meunier, F.A. (2008). PIKfyve negatively regulates exocytosis in neurosecretory cells. J Biol Chem *283*, 2804-2813.

Palade, G. (1975). Intracellular Aspects of the Process of Protein Synthesis. Science *189*, 867.

Patki, V., Lawe, D.C., Corvera, S., Virbasius, J.V., and Chawla, A. (1998). A functional PtdIns(3)P-binding motif. Nature *394*, 433-434.

Paulus, H., and Kennedy, E.P. (1960). The enzymatic synthesis of inositol monophosphatide. J Biol Chem *235*, 1303-1311.

Peden, A.A., Oorschot, V., Hesser, B.A., Austin, C.D., Scheller, R.H., and Klumperman, J. (2004). Localization of the AP-3 adaptor complex defines a novel endosomal exit site for lysosomal membrane proteins. J Cell Biol *164*, 1065-1076.

Pendaries, C., Tronchere, H., Plantavid, M., and Payrastre, B. (2003). Phosphoinositide signaling disorders in human diseases. FEBS Lett *546*, 25-31.

Petiot, A., Faure, J., Stenmark, H., and Gruenberg, J. (2003). PI3P signaling regulates receptor sorting but not transport in the endosomal pathway. J Cell Biol *162*, 971-979.

Petiot, A., Ogier-Denis, E., Blommaart, E.F., Meijer, A.J., and Codogno, P. (2000). Distinct classes of phosphatidylinositol 3'-kinases are involved in signaling pathways that control macroautophagy in HT-29 cells. J Biol Chem *275*, 992-998.

Phelan, J.P., Millson, S.H., Parker, P.J., Piper, P.W., and Cooke, F.T. (2006). Fab1p and AP-1 are required for trafficking of endogenously ubiquitylated cargoes to the vacuole lumen in S. cerevisiae. J Cell Sci *119*, 4225-4234.

Pizarro-Cerda, J., and Cossart, P. (2004). Subversion of phosphoinositide metabolism by intracellular bacterial pathogens. Nat Cell Biol *6*, 1026-1033.

Ponting, C.P., and Bork, P. (1996). Pleckstrin's repeat performance: a novel domain in G-protein signaling? Trends Biochem Sci *21*, 245-246.

Popoff, V., Mardones, G.A., Tenza, D., Rojas, R., Lamaze, C., Bonifacino, J.S., Raposo, G., and Johannes, L. (2007). The retromer complex and clathrin define an early endosomal retrograde exit site. J Cell Sci *120*, 2022-2031.

Prescott, A.R., Lucocq, J.M., James, J., Lister, J.M., and Ponnambalam, S. (1997). Distinct compartmentalization of TGN46 and beta 1,4-galactosyltransferase in HeLa cells. Eur J Cell Biol *72*, 238-246.

Presley, J.F., Mayor, S., McGraw, T.E., Dunn, K.W., and Maxfield, F.R. (1997). Bafilomycin A1 treatment retards transferrin receptor recycling more than bulk membrane recycling. J Biol Chem *272*, 13929-13936.

Proikas-Cezanne, T., Ruckerbauer, S., Stierhof, Y.D., Berg, C., and Nordheim, A. (2007). Human WIPI-1 puncta-formation: a novel assay to assess mammalian autophagy. FEBS Lett *581*, 3396-3404.

Proikas-Cezanne, T., Waddell, S., Gaugel, A., Frickey, T., Lupas, A., and Nordheim, A. (2004). WIPI-1alpha (WIPI49), a member of the novel 7-bladed WIPI protein family, is aberrantly expressed in human cancer and is linked to starvation-induced autophagy. Oncogene *23*, 9314-9325.

Rabitsch, K.P., Toth, A., Galova, M., Schleiffer, A., Schaffner, G., Aigner, E., Rupp, C., Penkner, A.M., Moreno-Borchart, A.C., Primig, M., Esposito, R.E., Klein, F., Knop, M., and Nasmyth, K. (2001). A screen for genes required for meiosis and spore formation based on whole-genome expression. Curr Biol *11*, 1001-1009.

Raiborg, C., Bache, K.G., Gillooly, D.J., Madshus, I.H., Stang, E., and Stenmark, H. (2002). Hrs sorts ubiquitinated proteins into clathrin-coated microdomains of early endosomes. Nat Cell Biol *4*, 394-398.

Raiborg, C., Bremnes, B., Mehlum, A., Gillooly, D.J., D'Arrigo, A., Stang, E., and Stenmark, H. (2001). FYVE and coiled-coil domains determine the specific localisation of Hrs to early endosomes. J Cell Sci *114*, 2255-2263.

Rajawat, Y.S., and Bossis, I. (2008). Autophagy in aging and in neurodegenerative disorders. Hormones (Athens) *7*, 46-61.

Rambourg, A., and Clermont, Y. (1990). Three-dimensional electron microscopy: structure of the Golgi apparatus. Eur J Cell Biol *51*, 189-200.

Rameh, L.E., Tolias, K.F., Duckworth, B.C., and Cantley, L.C. (1997). A new pathway for synthesis of phosphatidylinositol-4,5-bisphosphate. Nature *390*, 192-196.

Raymond, C.K., Howald-Stevenson, I., Vater, C.A., and Stevens, T.H. (1992). Morphological classification of the yeast vacuolar protein sorting mutants: evidence for a prevacuolar compartment in class E vps mutants. Mol Biol Cell *3*, 1389-1402.

Reggiori, F., Tucker, K.A., Stromhaug, P.E., and Klionsky, D.J. (2004). The Atg1-Atg13 complex regulates Atg9 and Atg23 retrieval transport from the pre-autophagosomal structure. Dev Cell *6*, 79-90.

Rieder, S.E., Banta, L.M., Kohrer, K., McCaffery, J.M., and Emr, S.D. (1996). Multilamellar endosome-like compartment accumulates in the yeast vps28 vacuolar protein sorting mutant. Mol Biol Cell *7*, 985-999.

Riederer, M.A., Soldati, T., Shapiro, A.D., Lin, J., and Pfeffer, S.R. (1994). Lysosome biogenesis requires Rab9 function and receptor recycling from endosomes to the trans-Golgi network. J Cell Biol *125*, 573-582.

Rink, J., Ghigo, E., Kalaidzidis, Y., and Zerial, M. (2005). Rab conversion as a mechanism of progression from early to late endosomes. Cell *122*, 735-749.

Robinson, M.J., and Cobb, M.H. (1997). Mitogen-activated protein kinase pathways. Curr Opin Cell Biol *9*, 180-186.

Rozakis-Adcock, M., McGlade, J., Mbamalu, G., Pelicci, G., Daly, R., Li, W., Batzer, A., Thomas, S., Brugge, J., Pelicci, P.G., and et al. (1992). Association of the Shc and Grb2/Sem5 SH2-containing proteins is implicated in activation of the Ras pathway by tyrosine kinases. Nature *360*, 689-692.

Rudge, S.A., Anderson, D.M., and Emr, S.D. (2004). Vacuole size control: regulation of PtdIns(3,5)P2 levels by the vacuole-associated Vac14-Fig4 complex, a PtdIns(3,5)P2-specific phosphatase. Mol Biol Cell *15*, 24-36.

Rusten, T.E., Rodahl, L.M., Pattni, K., Englund, C., Samakovlis, C., Dove, S., Brech, A., and Stenmark, H. (2006). Fab1 phosphatidylinositol 3-phosphate 5-kinase controls trafficking but not silencing of endocytosed receptors. Mol Biol Cell *17*, 3989-4001.

Rusten, T.E., Vaccari, T., Lindmo, K., Rodahl, L.M., Nezis, I.P., Sem-Jacobsen, C., Wendler, F., Vincent, J.P., Brech, A., Bilder, D., and Stenmark, H. (2007). ESCRTs and Fab1 regulate distinct steps of autophagy. Curr Biol *17*, 1817-1825.

Rutherford, A.C., Traer, C., Wassmer, T., Pattni, K., Bujny, M.V., Carlton, J.G., Stenmark, H., and Cullen, P.J. (2006). The mammalian phosphatidylinositol 3-phosphate 5-kinase (PIKfyve) regulates endosome-to-TGN retrograde transport. J Cell Sci *119*, 3944-3957.

Sachse, M., Urbe, S., Oorschot, V., Strous, G.J., and Klumperman, J. (2002). Bilayered clathrin coats on endosomal vacuoles are involved in protein sorting toward lysosomes. Mol Biol Cell *13*, 1313-1328.

Sbrissa, D., Ikonomov, O.C., Deeb, R., and Shisheva, A. (2002a). Phosphatidylinositol 5-phosphate biosynthesis is linked to PIKfyve and is involved in osmotic response pathway in mammalian cells. J Biol Chem *277*, 47276-47284.

Sbrissa, D., Ikonomov, O.C., Fu, Z., Ijuin, T., Gruenberg, J., Takenawa, T., and Shisheva, A. (2007). Core protein machinery for mammalian phosphatidylinositol 3,5-bisphosphate synthesis and turnover that regulates the progression of endosomal transport. Novel Sac phosphatase joins the ArPIKfyve-PIKfyve complex. J Biol Chem *282*, 23878-23891.

Sbrissa, D., Ikonomov, O.C., and Shisheva, A. (1999). PIKfyve, a mammalian ortholog of yeast Fab1p lipid kinase, synthesizes 5-phosphoinositides. Effect of insulin. J Biol Chem *274*, 21589-21597.

Sbrissa, D., Ikonomov, O.C., and Shisheva, A. (2000). PIKfyve lipid kinase is a protein kinase: downregulation of 5'-phosphoinositide product formation by autophosphorylation. Biochemistry *39*, 15980-15989.

Sbrissa, D., Ikonomov, O.C., and Shisheva, A. (2002b). Phosphatidylinositol 3-phosphate-interacting domains in PIKfyve. Binding specificity and role in PIKfyve. Endomenbrane localization. J Biol Chem *277*, 6073-6079.

Sbrissa, D., Ikonomov, O.C., and Shisheva, A. (2005). Analysis of potential binding of the recombinant Rab9 effector p40 to phosphoinositide-enriched synthetic liposomes. Methods Enzymol *403*, 696-705.

Sbrissa, D., Ikonomov, O.C., Strakova, J., Dondapati, R., Mlak, K., Deeb, R., Silver, R., and Shisheva, A. (2004). A mammalian ortholog of Saccharomyces cerevisiae Vac14 that associates with and up-regulates PIKfyve phosphoinositide 5-kinase activity. Mol Cell Biol *24*, 10437-10447.

Sbrissa, D., and Shisheva, A. (2005). Acquisition of unprecedented phosphatidylinositol 3,5-bisphosphate rise in hyperosmotically stressed 3T3-L1 adipocytes, mediated by ArPIKfyve-PIKfyve pathway. J Biol Chem *280*, 7883-7889.

Schaletzky, J., Dove, S.K., Short, B., Lorenzo, O., Clague, M.J., and Barr, F.A. (2003). Phosphatidylinositol-5-phosphate activation and conserved

substrate specificity of the myotubularin phosphatidylinositol 3-phosphatases. Curr Biol *13*, 504-509.

Schu, P.V., Takegawa, K., Fry, M.J., Stack, J.H., Waterfield, M.D., and Emr, S.D. (1993). Phosphatidylinositol 3-kinase encoded by yeast VPS34 gene essential for protein sorting. Science *260*, 88-91.

Schweichel, J.U., and Merker, H.J. (1973). The morphology of various types of cell death in prenatal tissues. Teratology *7*, 253-266.

Schworer, C.M., and Mortimore, G.E. (1979). Glucagon-induced autophagy and proteolysis in rat liver: mediation by selective deprivation of intracellular amino acids. Proc Natl Acad Sci U S A *76*, 3169-3173.

Seaman, M.N. (2004). Cargo-selective endosomal sorting for retrieval to the Golgi requires retromer. J Cell Biol *165*, 111-122.

Seaman, M.N. (2007). Identification of a novel conserved sorting motif required for retromer-mediated endosome-to-TGN retrieval. J Cell Sci *120*, 2378-2389.

Seaman, M.N., Marcusson, E.G., Cereghino, J.L., and Emr, S.D. (1997). Endosome to Golgi retrieval of the vacuolar protein sorting receptor, Vps10p, requires the function of the VPS29, VPS30, and VPS35 gene products. J Cell Biol *137*, 79-92.

Seay, M.D., and Dinesh-Kumar, S.P. (2007). Autophagy takes its TOLL on innate immunity. Cell Host Microbe *2*, 69-70.

Serunian, L.A., Auger, K.R., Roberts, T.M., and Cantley, L.C. (1990). Production of novel polyphosphoinositides in vivo is linked to cell transformation by polyomavirus middle T antigen. J Virol *64*, 4718-4725.

Shaw, J.D., Hama, H., Sohrabi, F., DeWald, D.B., and Wendland, B. (2003). PtdIns(3,5)P2 is required for delivery of endocytic cargo into the multivesicular body. Traffic *4*, 479-490.

Sheff, D.R., Daro, E.A., Hull, M., and Mellman, I. (1999). The receptor recycling pathway contains two distinct populations of early endosomes with different sorting functions. J Cell Biol *145*, 123-139.

Shi, H., Rojas, R., Bonifacino, J.S., and Hurley, J.H. (2006). The retromer subunit Vps26 has an arrestin fold and binds Vps35 through its C-terminal domain. Nat Struct Mol Biol *13*, 540-548.

Shim, S., Kimpler, L.A., and Hanson, P.I. (2007). Structure/function analysis of four core ESCRT-III proteins reveals common regulatory role for extreme C-terminal domain. Traffic *8*, 1068-1079.

Shisheva, A. (2001). PIKfyve: the road to PtdIns 5-P and PtdIns 3,5-P(2). Cell Biol Int *25*, 1201-1206.

Shisheva, A., Rusin, B., Ikonomov, O.C., DeMarco, C., and Sbrissa, D. (2001). Localization and insulin-regulated relocation of phosphoinositide 5-kinase PIKfyve in 3T3-L1 adipocytes. J Biol Chem *276*, 11859-11869.

Shisheva, A., Sbrissa, D., and Ikonomov, O. (1999). Cloning, characterization, and expression of a novel Zn2+-binding FYVE finger-containing phosphoinositide kinase in insulin-sensitive cells. Mol Cell Biol *19*, 623-634.

Shpetner, H., Joly, M., Hartley, D., and Corvera, S. (1996). Potential sites of PI-3 kinase function in the endocytic pathway revealed by the PI-3 kinase inhibitor, wortmannin. J Cell Biol *132*, 595-605.

Simonsen, A., Lippe, R., Christoforidis, S., Gaullier, J.M., Brech, A., Callaghan, J., Toh, B.H., Murphy, C., Zerial, M., and Stenmark, H. (1998). EEA1 links PI(3)K function to Rab5 regulation of endosome fusion. Nature *394*, 494-498.

Sonnichsen, B., De Renzis, S., Nielsen, E., Rietdorf, J., and Zerial, M. (2000). Distinct membrane domains on endosomes in the recycling pathway visualized by multicolor imaging of Rab4, Rab5, and Rab11. J Cell Biol *149*, 901-914.

Sorkin, A., and Carpenter, G. (1991). Dimerization of internalized epidermal growth factor receptors. J Biol Chem *266*, 23453-23460.

Spiro, D.J., Boll, W., Kirchhausen, T., and Wessling-Resnick, M. (1996). Wortmannin alters the transferrin receptor endocytic pathway in vivo and in vitro. Mol Biol Cell *7*, 355-367.

Srinivasan, S., Seaman, M., Nemoto, Y., Daniell, L., Suchy, S.F., Emr, S., De Camilli, P., and Nussbaum, R. (1997). Disruption of three phosphatidylinositol-polyphosphate 5-phosphatase genes from Saccharomyces cerevisiae results in pleiotropic abnormalities of vacuole morphology, cell shape, and osmohomeostasis. Eur J Cell Biol *74*, 350-360.

Stack, J.H., DeWald, D.B., Takegawa, K., and Emr, S.D. (1995). Vesicle-mediated protein transport: regulatory interactions between the Vps15 protein kinase and the Vps34 PtdIns 3-kinase essential for protein sorting to the vacuole in yeast. J Cell Biol *129*, 321-334.

Stack, J.H., and Emr, S.D. (1994). Vps34p required for yeast vacuolar protein sorting is a multiple specificity kinase that exhibits both protein kinase and phosphatidylinositol-specific PI 3-kinase activities. J Biol Chem *269*, 31552-31562.

Stack, J.H., Herman, P.K., Schu, P.V., and Emr, S.D. (1993). A membrane-associated complex containing the Vps15 protein kinase and the Vps34 PI 3-kinase is essential for protein sorting to the yeast lysosome-like vacuole. Embo J *12*, 2195-2204.

Stein, M.P., Cao, C., Tessema, M., Feng, Y., Romero, E., Welford, A., and Wandinger-Ness, A. (2005). Interaction and functional analyses of human VPS34/p150 phosphatidylinositol 3-kinase complex with Rab7. Methods Enzymol *403*, 628-649.

Stenmark, H., Aasland, R., Toh, B.H., and D'Arrigo, A. (1996). Endosomal localization of the autoantigen EEA1 is mediated by a zinc-binding FYVE finger. J Biol Chem *271*, 24048-24054.

Stolz, L.E., Huynh, C.V., Thorner, J., and York, J.D. (1998). Identification and characterization of an essential family of inositol polyphosphate 5-phosphatases (INP51, INP52 and INP53 gene products) in the yeast Saccharomyces cerevisiae. Genetics *148*, 1715-1729.

Storrie, B., and Desjardins, M. (1996). The biogenesis of lysosomes: is it a kiss and run, continuous fusion and fission process? Bioessays *18*, 895-903.

Stromhaug, P.E., Reggiori, F., Guan, J., Wang, C.W., and Klionsky, D.J. (2004). Atg21 is a phosphoinositide binding protein required for efficient lipidation and localization of Atg8 during uptake of aminopeptidase I by selective autophagy. Mol Biol Cell *15*, 3553-3566.

Stromhaug, P.E., and Seglen, P.O. (1993). Evidence for acidity of prelysosomal autophagic/endocytic vacuoles (amphisomes). Biochem J *291 (Pt 1)*, 115-121.

Suzuki, K., Kirisako, T., Kamada, Y., Mizushima, N., Noda, T., and Ohsumi, Y. (2001). The pre-autophagosomal structure organized by concerted functions of APG genes is essential for autophagosome formation. Embo J *20*, 5971-5981.

Tarassov, K., Messier, V., Landry, C.R., Radinovic, S., Molina, M.M., Shames, I., Malitskaya, Y., Vogel, J., Bussey, H., and Michnick, S.W. (2008). An in vivo map of the yeast protein interactome. Science *320*, 1465-1470.

Traer, C.J., Rutherford, A.C., Palmer, K.J., Wassmer, T., Oakley, J., Attar, N., Carlton, J.G., Kremerskothen, J., Stephens, D.J., and Cullen, P.J. (2007). SNX4 coordinates endosomal sorting of TfnR with dynein-mediated transport into the endocytic recycling compartment. Nat Cell Biol *9*, 1370-1380.

Traub, L.M., Kornfeld, S., and Ungewickell, E. (1995). Different domains of the AP-1 adaptor complex are required for Golgi membrane binding and clathrin recruitment. J Biol Chem *270*, 4933-4942.

Tsujita, K., Itoh, T., Ijuin, T., Yamamoto, A., Shisheva, A., Laporte, J., and Takenawa, T. (2004). Myotubularin regulates the function of the late endosome through the gram domain-phosphatidylinositol 3,5-bisphosphate interaction. J Biol Chem *279*, 13817-13824.

Ueno, T., Sato, W., Horie, Y., Komatsu, M., Tanida, I., Yoshida, M., Ohshima, S., Mak, T.W., Watanabe, S., and Kominami, E. (2008). Loss of Pten, a tumor suppressor, causes the strong inhibition of autophagy without affecting LC3 lipidation. Autophagy *4*, 692-700.

Urbe, S., Mills, I.G., Stenmark, H., Kitamura, N., and Clague, M.J. (2000). Endosomal localization and receptor dynamics determine tyrosine phosphorylation of hepatocyte growth factor-regulated tyrosine kinase substrate. Mol Cell Biol *20*, 7685-7692.

van Meel, E., and Klumperman, J. (2008). Imaging and imagination: understanding the endo-lysosomal system. Histochem Cell Biol *129*, 253-266.

Vanhaesebroeck, B., and Waterfield, M.D. (1999). Signaling by distinct classes of phosphoinositide 3-kinases. Exp Cell Res *253*, 239-254.

Varshavsky, A. (1992). The N-end rule. Cell *69*, 725-735.

Vieira, A.V., Lamaze, C., and Schmid, S.L. (1996). Control of EGF receptor signaling by clathrin-mediated endocytosis. Science *274*, 2086-2089.

Wagner, M. (2005). Growth factor control of autophagy. Nat Cell Biol *7*, 212.

Walker, D.M., Urbe, S., Dove, S.K., Tenza, D., Raposo, G., and Clague, M.J. (2001). Characterization of MTMR3. an inositol lipid 3-phosphatase with novel substrate specificity. Curr Biol *11*, 1600-1605.

Wang, Y.X., Zhao, H., Harding, T.M., Gomes de Mesquita, D.S., Woldringh, C.L., Klionsky, D.J., Munn, A.L., and Weisman, L.S. (1996). Multiple classes of yeast mutants are defective in vacuole partitioning yet target vacuole proteins correctly. Mol Biol Cell *7*, 1375-1389.

Watt, S.A., Kular, G., Fleming, I.N., Downes, C.P., and Lucocq, J.M. (2002). Subcellular localization of phosphatidylinositol 4,5-bisphosphate using the pleckstrin homology domain of phospholipase C delta1. Biochem J *363*, 657-666.

White, I.J., Bailey, L.M., Aghakhani, M.R., Moss, S.E., and Futter, C.E. (2006). EGF stimulates annexin 1-dependent inward vesiculation in a multivesicular endosome subpopulation. Embo J *25*, 1-12.

Whiteford, C.C., Brearley, C.A., and Ulug, E.T. (1997). Phosphatidylinositol 3,5-bisphosphate defines a novel PI 3-kinase pathway in resting mouse fibroblasts. Biochem J *323 (Pt 3)*, 597-601.

Whitley, P., Reaves, B.J., Hashimoto, M., Riley, A.M., Potter, B.V., and Holman, G.D. (2003). Identification of mammalian Vps24p as an effector of phosphatidylinositol 3,5-bisphosphate-dependent endosome compartmentalization. J Biol Chem *278*, 38786-38795.

Winter, V., and Hauser, M.T. (2006). Exploring the ESCRTing machinery in eukaryotes. Trends Plant Sci *11*, 115-123.

Wishart, M.J., and Dixon, J.E. (2002). PTEN and myotubularin phosphatases: from 3-phosphoinositide dephosphorylation to disease. Trends Cell Biol *12*, 579-585.

Wong, H.C., Mao, J., Nguyen, J.T., Srinivas, S., Zhang, W., Liu, B., Li, L., Wu, D., and Zheng, J. (2000). Structural basis of the recognition of the dishevelled DEP domain in the Wnt signaling pathway. Nat Struct Biol *7*, 1178-1184.

Woodman, P.G., and Futter, C.E. (2008). Multivesicular bodies: co-ordinated progression to maturity. Curr Opin Cell Biol *20*, 408-414.

Xie, Z., Nair, U., and Klionsky, D.J. (2008). Atg8 Controls Phagophore Expansion during Autophagosome Formation. Mol Biol Cell.

Xu, Y., Hortsman, H., Seet, L., Wong, S.H., and Hong, W. (2001). SNX3 regulates endosomal function through its PX-domain-mediated interaction with PtdIns(3)P. Nat Cell Biol *3*, 658-666.

Xu, Y., Jagannath, C., Liu, X.D., Sharafkhaneh, A., Kolodziejska, K.E., and Eissa, N.T. (2007). Toll-like receptor 4 is a sensor for autophagy associated with innate immunity. Immunity *27*, 135-144.

Yamamoto, A., DeWald, D.B., Boronenkov, I.V., Anderson, R.A., Emr, S.D., and Koshland, D. (1995). Novel PI(4)P 5-kinase homologue, Fab1p, essential for normal vacuole function and morphology in yeast. Mol Biol Cell *6*, 525-539.

Yan, Q., Hunt, P.R., Frelin, L., Vida, T.A., Pevsner, J., and Bean, A.J. (2005). mVps24p functions in EGF receptor sorting/trafficking from the early endosome. Exp Cell Res *304*, 265-273.

Yin, J., and Buchwald, S.L. (2002). Pd-catalyzed intermolecular amidation of aryl halides: the discovery that xantphos can be trans-chelating in a palladium complex. J Am Chem Soc *124*, 6043-6048.

Yorimitsu, T., and Klionsky, D.J. (2005). Autophagy: molecular machinery for self-eating. Cell Death Differ *12 Suppl 2*, 1542-1552.

Young, A.R., Chan, E.Y., Hu, X.W., Kochl, R., Crawshaw, S.G., High, S., Hailey, D.W., Lippincott-Schwartz, J., and Tooze, S.A. (2006). Starvation and ULK1-dependent cycling of mammalian Atg9 between the TGN and endosomes. J Cell Sci *119*, 3888-3900.

Yu, L., Gaitatzes, C., Neer, E., and Smith, T.F. (2000). Thirty-plus functional families from a single motif. Protein Sci *9*, 2470-2476.

Zeng, X., Overmeyer, J.H., and Maltese, W.A. (2006). Functional specificity of the mammalian Beclin-Vps34 PI 3-kinase complex in macroautophagy versus endocytosis and lysosomal enzyme trafficking. J Cell Sci *119*, 259-270.

Zhang, B., and Zelhof, A.C. (2002). Amphiphysins: raising the BAR for synaptic vesicle recycling and membrane dynamics. Bin-Amphiphysin-Rvsp. Traffic *3*, 452-460.

Zhang, Y., Zolov, S.N., Chow, C.Y., Slutsky, S.G., Richardson, S.C., Piper, R.C., Yang, B., Nau, J.J., Westrick, R.J., Morrison, S.J., Meisler, M.H., and Weisman, L.S. (2007). Loss of Vac14, a regulator of the signaling lipid phosphatidylinositol 3,5-bisphosphate, results in neurodegeneration in mice. Proc Natl Acad Sci U S A *104*, 17518-17523.

Zheng, B., Wu, J.N., Schober, W., Lewis, D.E., and Vida, T. (1998). Isolation of yeast mutants defective for localization of vacuolar vital dyes. Proc Natl Acad Sci U S A *95*, 11721-11726.

Zhong, Q., Lazar, C.S., Tronchere, H., Sato, T., Meerloo, T., Yeo, M., Songyang, Z., Emr, S.D., and Gill, G.N. (2002). Endosomal localization and function of sorting nexin 1. Proc Natl Acad Sci U S A *99*, 6767-6772.

Zhu, Y., Doray, B., Poussu, A., Lehto, V.P., and Kornfeld, S. (2001). Binding of GGA2 to the lysosomal enzyme sorting motif of the mannose 6-phosphate receptor. Science *292*, 1716-1718.

Zvelebil, M.J., MacDougall, L., Leevers, S., Volinia, S., Vanhaesebroeck, B., Gout, I., Panayotou, G., Domin, J., Stein, R., Pages, F., and et al. (1996). Structural and functional diversity of phosphoinositide 3-kinases. Philos Trans R Soc Lond B Biol Sci *351*, 217-223.